ANALYSIS AND SYNTHESIS OF NONLINEAR DYNAMIC SYSTEMS BASED ON FUZZY MODEL AND FREQUENCY DOMAIN METHOD

LI JINGYING

PhD

The Hong Kong Polytechnic University

This programme is jointly offered by The Hong Kong Polytechnic University and Harbin Institute of Technology

2021

The Hong Kong Polytechnic University

Department of Mechanical Engineering

Harbin Institute of Technology

Department of Control Science and Engineering

Analysis and Synthesis of Nonlinear Dynamic Systems Based on Fuzzy Model and Frequency Domain Method

LI JINGYING

A thesis submitted in partial fulfilment of the requirements

for the degree of Doctor of Philosophy

August 2019

CERTIFICATE OF ORIGINALITY

CERTIFICATE OF ORIGINALITY

I hereby declare that this thesis is my own work and that, to the best of my knowledge and belief, it reproduces no material previously published or written, nor material that has been accepted for the award of any other degree or diploma, except where due acknowledgement has been made in the text.

________________________ (Signed)

LI Jingying (Name of student)

Publications Arising from the Thesis

Journal Papers

1. **Jingying Li**, Xingjian Jing, Zhengchao Li and Xianlin Huang. A Novel Parametric Characteristic Function for Hybrid Linear and Nonlinear Parameters Analysis and Design of Nonlinear Systems.(**To be submitted**)
2. **Jingying Li**, Xingjian Jing, Zhengchao Li and Xianlin Huang. Optimization of Membership Functions for Fuzzy-Model-Based Controllers Using Frequency Domain Analysis Method.(**To be submitted to IEEE Transactions on Cybernetics**)
3. **Jingying Li**, Xingjian Jing, Zhengchao Li and Xianlin Huang. Fuzzy Adaptive Control for Nonlinear Suspension Systems Based on a Bio-inspired Reference Model with Deliberately Designed Nonlinear Damping. ***IEEE Transactions on Industrial Electronics***. 2018. (IF: 7.503)
4. **Jingying Li**, Xianlin Huang and Zhengchao Li. Exponential stabilization for fuzzy sampled-data system based on a unified framework and its application. ***Journal of the Franklin Institute***. 2017. (IF: 3.576)
5. **Jingying Li**, Xianlin Huang and Zhengchao Li. Extended dissipative filtering of fuzzy systems with time-varying delay under imperfect premise matching.***International Journal of Systems Science***. 2017. (IF: 2.185)
6. Zhengchao Li, **Jingying Li**, Jinyong Yu. Robust filter design for a class of uncertain systems with D stability constraints under a unified framework. ***Journal of the Franklin Institute***. 2016. (IF: 3.576)

Conference Papers

1. **Jingying Li**, Xingjian Jing, Zhengchao Li, and Xianlin Huang. Optimization of Fuzzy Membership Function based on the NCOS function method. **IECON2020, the 46th Annual Conference of the IEEE Industrial Electronics Society (IES).**

2. **Jingying Li**, Xingjian Jing, Zhengchao Li, and Xianlin Huang.A Novel Linear and Nonlinear Characteristic Parameter Approach for Analysis and Design of Nonlinear Systems. **2020 IEEE International Conference on Industrial Cyber-Physical Systems.**

3. **Jingying Li**, Zhengchao Li, Xingjian Jing and Xianlin Huang. Fuzzy adaptive tracking control for nonlinear suspension systems based on a bio-inspired reference model. **2018 13th World Congress on Intelligent Control and Automation (WCICA). IEEE**. 2018.

4. **Jingying Li**, Xianlin Huang. A switched event-triggered H_∞ control approach to nonlinear network control system. **2017 36th Chinese Control Conference (CCC). IEEE**. 2017.

5. **Jingying Li**, Xianlin Huang. New results on variable sampling stabilization of nonlinear system via fuzzy control approach. **2015 34th Chinese Control Conference (CCC). IEEE**. 2015.

Abstract

In aerospace, astronautics and industrial process, it is usually difficult to model and analyze the dynamics of controlled object exactly due to strong nonlinearities, internal/external disturbances, variation of loads, system uncertainties, etc. Classical time and frequency domain theories and methods are not applicable to analyze and control such nonlinear dynamic systems. Thus control and analysis of such complicated nonlinear systems are becoming more and more challengeable. Fuzzy control system, due to its capability of approximating any smooth nonlinear systems on a compact set with arbitrary accuracy, provides an appealing and efficient approach to facilitate analysis and synthesis of nonlinear systems. Nonlinear Characteristic Output Spectrum (nCOS) function has been well developed for analysis and design of nonlinear systems in frequency domain. Although there have been researches on control and analysis of nonlinear dynamic systems based on fuzzy model and frequency domain nCOS function, there are still some technical problems to be solved: explore stability analysis conditions of fuzzy system with lower conservativeness and new frequency domain methods to analyze and optimize nonlinear dynamic systems, etc. Objective of this thesis is to propose new control and frequency domain analysis methods to analyze, synthesize and optimize nonlinear dynamic systems with sampled-data behavior, time delay and imperfect premise matching based on fuzzy model and nCOS function. Some of the obtained results are applied to control and analysis of nonlinear vehicle suspension systems.

First, fuzzy adaptive control for nonlinear active suspension system based on a bio-inspired reference model is studied. Fuzzy logic systems are used to approximate unknown nonlinear terms. A general bio-inspired nonlinear structure, which can present ideal nonlinear quasi-zero-stiffness for vibration isolation, is adopted as tracking reference model. Particularly, a nonlinear damping is designed to improve damping characteristics of the bio-inspired reference model. With beneficial

nonlinear stiffness and improved nonlinear damping of the bio-inspired reference model, the proposed fuzzy adaptive controller can effectively suppress vibration of suspension systems with less actuator force and much improved ride comfort, thus energy saving performance can be achieved.

Then fuzzy sampled-data control problems for nonlinear dynamic systems under aperiodic sampling are studied. A sampling period dependent Lyapunov-Krasovskii functional together with a novel efficient integral inequality, which has the advantages of reducing conservativeness, is adopted. On the basis of stability conditions, a sampled-data controller that cannot only exponentially stabilize the system but also guarantee the extended$-$dissipativity performance is then designed. Simulation results of a quarter-vehicle suspension system with considering payload uncertainties and aperiodic sampling are provided to verify effectiveness and advantages of the designed controller.

The problems of imperfect premise matching fuzzy filtering design for continuous-time nonlinear systems with time-varying delays are investigated. Based on the extended dissipative performance index, a new delay-dependent filter design approach in terms of linear matrix inequalities (LMIs) is obtained by employing Lyapunov-Krasovskii functional method together with a novel efficient integral inequality. The designed filter can guarantee the filtering error system satisfy H_∞, $L_2 - L_\infty$, passive and dissipative performance by tuning the weighting matrices in the conditions. Moreover, the fuzzy filter does not need to share the same membership function with fuzzy model, which can enhance design flexibility and robust property of the fuzzy filter system.

An advantageous optimization method developed based on the nCOS function is introduced to optimize mismatched fuzzy controller membership function parameters. Compared to traditional search-based optimization approach, which can only obtain optimal results and parameters, more analytical results can be obtained with less time consuming via this optimization method. This provides an in-depth understanding of nonlinear parameters' influence on system output spectrum. Simulation results demonstrate that with the frequency domain optimization method, disturbance suppression capability of the fuzzy-model-based controller over a concerned frequency band is further enhanced.

A novel parametric characteristic function approach for hybrid linear and nonlinear parameters analysis and design of nonlinear systems is proposed based on the nCOS function. Thus influence of linear and nonlinear parameters on system output spectrum can be simultaneously considered. The results of a specific case demonstrate that the proposed hybrid approach can provide a more comprehensive solution for nonlinear system analysis and design. Then the proposed hybrid parameter analysis approach, together with an n-th order output spectrum calculation method is used to identify and locate plant and controller faults of closed-loop control systems, which provides an in-depth insight of fault characteristics analysis and identification of closed-loop control systems.

Acknowledgments

This work was done during my PhD. study at the Hong Kong Polytechnic University (PolyU) and at the Harbin Institute of Technology (HIT) under the joint PhD. programmes leading to dual awards. I would like to express my most sincere gratitude to Dr. JING Xingjian, my chief supervisor at PolyU, for his constructive suggestion, persistent guidance and support. I also appreciate his profound knowledge and deep insight into the research topics and his assistance on completion of this thesis. I am also deeply indebted to Prof. HUANG Xianlin, my co-supervisor at HIT, for his continuous support and guidance of my PhD. study and related research.

I would like to thank Dr. QIU Jianbin from HIT for his valuable discussions and enthusiastic supports. I would like to extend my thanks to all my wonderful friends and colleagues from research groups at PolyU and HIT. Their generous friendship and encouragement have always accompanied me and made my life more colorful, I wish them all the best.

Finally, I would like to thank my beloved husband, parents, brothers, sister, nephew and niece for their understanding, endless support and love.

Hung Hom, August 2019 LI, Jingying

Table of Contents

List of Notations

Abbreviation

Abbreviation	Expansion
T-S	Takagi-Sugeno
PDC	Parallel Distributed Compensation
NCSs	Networked Control Systems
LMIs	Linear Matrix Inequalities
MSD	Mass-Spring-Damper
QZS	Quasi-Zero-Stiffness
RMS	Root-Mean-Square
GA	Genetic Algorithm
nOS	nonlinear Output Spectrum
GFRFs	General Frequency Response Functions
nCOS	nonlinear Characteristic Output Spectrum
pCOS	parametric Characteristic Output Spectrum
FFT	Fast Fourier Transform

Notations

Notation	Description
$\mathbb{R}^n$	$n-$dimensional Euclidean space
$\forall$	for all
$\in$	belong to
$\approx$	approximately equal

s.t.	subject to
$\rightarrow$	approach
P^T	transport of P
P^{-1}	inverse of P
$P^{\perp}$	complement of P
$[A]_s$	$A + A^T$
$diag\{...\}$	a block-diagonal matrix
$\|\cdot\|$	Euclidean norm or spectral norm
$P > 0$	matrix P is real symmetric and positive-definite
$\star$	a term in a block matrix induced by symmetry
$\mathcal{L}_2[0, \infty)$	square-integrable vector functions over $[0, \infty)$

Chapter 1

Introduction

1.1 Background and motivation

Objective of control on dynamic systems is to provide the principles and methods used to design engineering systems that maintain desirable performance by automatically adapting to changes in the environment [1]. Practical industrial systems inherently exhibit nonlinear behaviors and frequently encounter many complex characteristics, such as, uncertainties, time-delay, internal/external disturbances and actuator saturation, etc. For most model based control approaches, model for nonlinear plant dynamics plays a fundamental role in the whole controller design procedure. However, a comprehensive mathematical model of a nonlinear industrial plant is generally difficult to obtain due to the complexity of physical, chemical or other inexplicit behaviors. Fortunately, there are some well-known control-oriented modeling approaches for nonlinear dynamics, such as the fuzzy modelling approach, etc.

Fuzzy control system, especially Takagi-Sugeno (T-S) fuzzy model system, has received a great deal of attention from both theoretical analysis and industrial application in recent years [2–10] due to its generalized modeling capability for nonlinear systems, for example, air-breathing hypersonic vehicles (AHVs), direct current-direct current (DC-DC) converters and mechanical systems [2,4,9,11–13]. Essentially, T-S fuzzy model combines the known linear system theory with the flexible fuzzy linguistic theory, which can provide a systematic and powerful way to handle nonlinear system. Tremendous significant results have been achieved based on T-S fuzzy model approach (see [5–10, 12, 14–23]).

The nonlinear characteristic output spectrum (nCOS) function, which is developed with a parametric characteristic approach based on the generalized frequency response function (GFRF) concept [112], has been widely used in nonlinear analysis and design [24–27], nonlinear system identification, fault detection, fault diagnosis [28–30], etc. One significant advantage of nCOS function is that the nonlinear output spectrum can be expressed in the form of a polynomial function with respect to the nonlinear system model parameters, which provides an explicit and analytical relationship between the nonlinear output spectrum and the nonlinear model parameters of interest.

Even though analysis and synthesis of nonlinear dynamic systems have been well investigated, yet for some more demanding situations, there remain many interesting and challenging issues to be addressed. Following are some issues worth further studying.

1.1.1 Fuzzy control for nonlinear suspension systems

Suspension systems, which are of great importance in improving vehicle ride comfort, maneuverability and passengers' safety, have gained significant attention in the literatures [31–37]. Generally, suspension systems can be classified as: passive suspension, semi-active suspension and active suspension [38–43]. Active suspension system, which uses actuator components, can provide desired force for both adding and dissipating energy. This mechanism can effectively reduce road roughness impact and increase ride comfort. However, to ensure handling capability and ride comfort, both semi-active and active suspension control systems cost a great deal of energy, which may be constrained in practical systems. It is also known that vehicle suspension systems always have some inherent nonlinearities. Sometimes, beneficial nonlinearities may lead to even better performance in practical implementation. As shown in [44–49], nonlinear stiffness and damping characteristics can achieve excellent vibration isolation performance. With a systematic frequency domain approach referred to as the output frequency response function or nonlinear characteristic output spectrum based method [48–50], it is theoretically shown that nonlinear damping has very good advantage over linear damping [51].

Although these results present an effective characteristic parametric approach to the analysis and design of nonlinear systems, most existing results for active suspension control just simply cancel nonlinearities to achieve vibration suppression performance [52], which leads to consumption of extra energy. Therefore, how to employ beneficial nonlinearities in vibration control would be of high relevance to engineering practice, since nonlinearity always exists. To address this issue, a more general and systematic bio-inspired dynamics based fuzzy adaptive control method, which makes proper use of favorable nonlinearities is studied in this thesis.

It is noticed that biologically inspired methods have wide applications in engineering, such as mechanical structure design, robot locomotion [53–56]. Recently, a bio-inspired limb-like nonlinear structure (also called X-shaped structure), which takes inspiration from limb legs of animals, has been successfully applied to some practical engineering systems, like the quasi-zero-stiffness vibration isolator [57–59]. This bio-inspired structure has very beneficial equivalent nonlinear stiffness and damping, which are generated through the specially geometric nonlinearities of the limb-like structure. It has been proven that this bio-inspired model can always provide a very excellent quasi-zero-stiffness characteristic with high loading capacity, low natural frequency and broad frequency range of vibration isolation [57–59]. And therefore is much better than traditional linear vibration systems. One of the targets in this thesis is to take advantages of the beneficial nonlinear properties of this bio-inspired reference model in active suspension control.

A general way to suppress resonant peak is to adopt high level damping. Increasing damping can effectively reduce resonant peak but also degrade vibration isolation performance of non-resonant frequency region. To overcome this dilemma, a novel nonlinear damping is deliberately designed and integrated into the bio-inspired reference model in our study. This dynamic nonlinear damping is expected to suppress resonant peak without deteriorating vibration transmissibility at high frequencies, which has never been reported before. Note that the model studied in previous work [60] is only the simplest case without nonlinear damping and only one layer is considered there, which might lead to higher resonant peak of the suspension system. Since a more general bio-inspired nonlinear dynamics model of more layers in the bio-inspired structure is adopted in our study, which can further strengthen the vibration isolation performance with a much milder nonlinear response. Thus the bio-inspired reference model used in this thesis is more generic for both nonlinear stiffness and damping design which are needed to produce superior vibration isolation performance and better for practical implementation.

In order to follow the nonlinear dynamic characteristics of the bio-inspired reference model, fuzzy adaptive controller will be considered for the tracking control of suspension systems. In suspension systems, the sprung mass varies due to the change of payload, if the controller is designed without considering the uncertainties of these parameters the vehicle suspension system performance will be degraded. Therefore, adaptive control would be more preferred in practical applications [61–64]. In this thesis, an adaptive backstepping controller based on fuzzy logic system is developed to attenuate the effect of parameter uncertainties and external disturbances.

To the best of our knowledge, no attempt has been made towards solving fuzzy adaptive tracking problems based on the above mentioned bio-inspired reference model, which motivates the present study.

1.1.2 Fuzzy sampled-data control

The past decades have witnessed a boom of high speed digital devices, such as computers and microelectronics, which drastically lower the cost, improve the reliability and flexibility of digital control. Hence, more and more digital computers and microprocessors are utilized to control the continuous-time systems in very large number of practical applications [65–67]. Such control systems, in which both continuous and discrete dynamic behavior coexist, are called sampled-data systems [68]. Up to now, approaches applied to analysis and synthesis of sampled-data systems are mainly divided into the following three categories:

(1) *Discrete-time model*: transforming the sampled-data system into an approximately equivalent discrete-time system (e.g. delta operator) [69].

(2) *Impulsive model*: representing the sampled-data system as the form of impulsive model [70].

(3) *Input delay approach*: modelling the sampled-data system as a continuous-time system with control-input delay induced by sampler and holder [71].

where discrete-time approach is generally applicable for constant sampling intervals, impulsive model still suffers from several critical limitations (e.g., conservativeness problem, and the dimension of the impulsive system) when dealing with sampled-data systems with complex nonlinearities/ uncertainties. Thus, time-delay approach, where the sampling-and-holding behaviour is transformed as an input-delay term, gives a flexible and effective way to handle nonlinear sampled-data systems. Also, by resorting to the input-delay approach, conducting performance analysis (e.g. disturbance attenuation level, exponential stability analysis) for original closed-loop system is viable.

Analysis and synthesis problems for T-S fuzzy sampled-data system based input-delay approach have received more and more research attentions (see [72–83]).

Among these references, the problem of performance analysis with disturbance attenuation level has been extensively investigated. To mention a few, the problem of H_∞ state-feedback stabilization for fuzzy systems with aperiodic sampled-data was investigated in [74, 75], and H_∞ state and output feedback control problems for sampled-data fuzzy system and their applications to active suspension vehicle system were proposed in [77]. In [78, 79], the H_∞ tracking problems of nonlinear networked systems via fuzzy control approach under variable sampling were investigated. L_2-L_∞ filtering for multirate nonlinear sampled-data systems using T-S fuzzy model approach was proposed in [80]. The robust passive controller design problem for a class of nonlinear networked systems with variable sampling intervals, network-induced delay, and randomly occurring uncertainties was investigated through T-S fuzzy modeling method in [82]. Dissipativity-based sampled-data stabilization problems for T-S fuzzy system and its application to truck-trailer system were reported in [83].

It is especially worth pointing out that the (Q,S,R)-dissipative sysnthesis problem covers the H_∞ and passivity synthesis problem, except for the L_2-L_∞ synthesis issue. So, how to handle the L_2-L_∞ synthesis problem and the (Q,S,R)-dissipative issue for fuzzy sampled-data system with a unified performance index is an interesting topic worth further studying. In recently published literatures [84, 85] , a unified performance index, which can guarantee the H_∞, L_2-L_∞, passive and dissipative performance by changing the weighting matrices in extended dissipative inequalities gives answer to this question. This new unified performance index is called extended dissipativity. To the best of the authors' knowledge, until present there has been no attempt to solve the problems of stability and stabilization for fuzzy sampled-data systems under this unified frame, which motivates the present study.

From the viewpoint of input-delay model, the sawtooth delay induced by sampling-and-holding behavior inevitably leads to the inherent loss of information, which will affect the dynamic performance of closed-loop sampled-data system. Especially for the asynchronous sampling, this effect is fraught with more uncertainties. In this thesis, in order to obtain expected dynamic performance, exponential stability is imposed to guarantee that the resulting closed-loop sampled-data system satisfies the exponential stability with an exponential decay rate for arbitrary sampling period lying a bounded interval.

Considering the aforementioned observations, the extended dissipative and exponential stabilization problems for T-S fuzzy sampled-data systems will be investigated in this thesis.

1.1.3 Imperfect premise matching fuzzy filtering of nonlinear systems with time-varying delay

State variables of industrial systems are usually difficult to obtain directly. Thus it is necessary to estimate system states or part of system states via system measurement output. Classical Kalman filter is a very effective and widely used signal estimator [86,87]. However, when using classical Kalman filter, statistical properties of the system's dynamics and noise are required, which cannot always be guaranteed in practical industrial systems. In this case, performance of the Kalman filter cannot be maintained. H_∞ filter can estimate state for systems with unknown bounded noises. Time delays commonly occur in many engineering applications, such as chemical systems, metallurgical processing systems and network systems [88, 89]. Since the existence of delay often degrades system performance, sometimes even leads to instability, research on T-S fuzzy system with time delay is of great practical significance. Recently, some important results about nonlinear filtering for T-S fuzzy systems with time-delay, which is one of the fundamental problems in signal processing, communication and control applications, have been reported, such as H_∞ filter design [7,90–95], L_2-L_∞ filter design [96–101], passive filter design [102–104], and dissipative filter design [105–108].

In this thesis, instead of addressing the H_∞, $L_2 - L_\infty$, passive and dissipative filtering problems in a separate way, we study these filtering problems for T-S fuzzy time-delay systems under a unified framework by using the extended dissipativity performance index (see [84,109]), which can guarantee the H_∞, $L_2 - L_\infty$, passive and dissipative performance by tuning the weighting matrices in extended dissipative inequalities. However, it should be noted that some useful information about the time-derivative of Lyapunov-Krasovskii functional, such as the term $-\int_{-\bar{\tau}}^{0}\int_{t+\theta}^{t}\dot{\xi}^T(s)R_3\dot{\xi}(s)dsd\theta$ was neglected in [84] for convenient design, the filter design approach obtained in [84] inevitably suffers the conservativeness problem. In addition, to the best of the author's knowledge, so far no attempt has been made towards solving filtering problems for T-S fuzzy systems under such a unified framework, either with or without time-delay. Thus, the problem of extended dissipative filtering for T-S fuzzy time-delay system is still an open and challenging issue, which motivates the present study.

Moreover, in order to retain design flexibility and robust property of extended dissipative filter, the idea that fuzzy filter shares different premise variables with the T-S fuzzy model, which is referred to as imperfect premise matching (see [110, 111]), is further introduced in this thesis. Under imperfect premise matching, implementation cost of the fuzzy filtering can be reduced by employing some relatively simple membership functions different from those complex membership functions of the fuzzy model. In recent years, the study of fuzzy control with imperfect premise variables has made some achievements [110–112]. Unfortunately, few research has been pursued on the problem of fuzzy filter with imperfect premise variables, besides [113,114]. [113] investigated the filtering problem of Type-II fuzzy system subjected to D stability constraints with imperfect matching premise variables. [114] studied the decentralised H_∞ fuzzy filter problem for non-linear large-scale systems under imperfect premise matching. However, none of these research results is applicable to the filtering problem for fuzzy system with time-varying delay, which is the second motivation of our current research work.

Motivated by the observations above, the extended dissipative filtering problem for fuzzy system with time-varying delay under imperfect premise matching will be considered in this thesis.

1.1.4 Analysis and optimization of nonlinear system parameters with frequency domain method

Under imperfect premise matching, arbitrary slack matrices can be introduced to alleviate conservativeness. In recent years, the study of fuzzy control with imperfect premise variables has made some achievements [111, 112, 115]. To design mismatched fuzzy controller, the mismatched membership function only needs to satisfy certain design condition. However, some parameters associated with mismatched controller membership functions are determined in an ad hoc or arbitrary manner in the design process of mismatched fuzzy controller. These subjectively decided parameters play a role in achieving high quality control performance. Until present, systematic and comprehensive analysis on how mismatched membership functions' parameters affect the closed-loop system performance has not yet been considered in the existing design process. It is also worth noting that a large number of existing research work on fuzzy-model-based control or filtering under imperfect premise matching adopt Gaussian shape functions as mismatched membership functions for its smoothness and concise notation [23, 116–118]. So research on optimization of the mismatched membership functions' parameters, especially for Gaussian type membership functions, is of great theoretical and practical importance.

Conventional method to determine the optimal parameters of mismatched membership functions is adopting some optimization techniques via direct measurement of the closed-loop system performance, like genetic algorithm (GA) [119–121] and swarm optimization algorithm [122, 123]. However, almost all intelligent optimization methods are based on global searching in the available parameter space, which means that the larger parameter space, the longer time it takes to find optimal values. For systems with complicated dynamics and higher dimensions, computational complexity will increase to a very high level, which is not convenient for analysis and design. Moreover, intelligent optimization method can only give final optimal values of the concern parameters instead of explicit relationship between the parameters and system performance. Once the parameter space changes, the whole optimization process needs to be re-executed, which is extremely time inefficient.

To overcome this deficiency in optimization problem, nCOS function [49,124,125] is adopted to analyze the parameters' influence on system output frequency response. The nCOS function developed based on the Volterra series expansion theory [126] extends the transfer function concept to nonlinear systems, which provides a powerful insight into the parameters' influence on system response. Some significant results about the applications of nCOS function-based method have been obtained, including the analysis and design of nonlinear vehicle suspensions and fault diagnosis of bolt loosening in satellite structures [29, 30, 127]. Compared to search-based optimization method, nCOS function-based method can exactly demonstrate how the membership functions' parameters would affect the closed-loop system performance. This method provides powerful guidance in choosing parameters of controller membership functions in mismatched control. Subjectivity and blindness in the process of optimizing membership function parameters can be effectively avoided by using this method. Benefited from the analytical and explicit expression of the relationship between nonlinear output spectrum and mismatched membership functions' parameters, the time consumption using nCOS function-based optimization method is much less than search-based intelligent optimization methods, even for larger parameter space.

One of the critical issues in mechanical system is vibration suppression. In practice, vibration is usually induced at certain frequencies or only performance over a certain frequency band that we are interested in, for instance, the vehicle suspensions, we focus on the vertical vibration performance at 4 Hz-8 Hz, to which human body is much sensitive. In this regard, controller designed over a certain frequency region can achieve better disturbance attenuation performance, compared with the over-design generated by entire frequency approach. There have been lots of research on finite frequency H_∞ control and filter, see references [128–133] and therein. However, the problem of fuzzy finite frequency control under imperfect premise matching design has not been studied yet, which is an interesting topic worth further study. Motivated by the afore discussions, H_∞ controller over concerned frequency band is first designed under imperfect premise matching. Then the disturbance suppression capability of the fuzzy controller is further enhanced by combining the finite frequency H_∞ control with the nCOS function-based frequency domain optimization method.

1.1.5 Hybrid linear and nonlinear parameters analysis for nonlinear systems

The nonlinear analysis method using recursive algorithm [24–27] for calculations of GFRFs coefficients involves the issue of computational efficiency [49]. For systems with complicated dynamics, the computational complexity of high-order GFRFs induced by recursive algorithm will increase to a very high level, which is not convenient for analysis and design. In addition, the recursive algorithm based method cannot give an explicit expression about relationship between the output spectrum and system parameters of interest. To improve computational efficiency and analytically reveal the parameters' influence on system output, the nCOS functions has been well developed for nonlinear analysis and design [48, 49, 124, 125]. Explicit structure and expression of output spectrum in terms to system parameters are presented in a clear and concise manner, which provides an in-depth insight into the parameters' influence on system response.

The nonlinear system output spectrum is jointly determined by system characteristic parameters, such as linear and nonlinear parameters, excitation amplitude and frequency variables. Most of existing results about nCOS function based method mainly focus on nonlinear model parameters' influence on system output spectrum. Linear model parameters' influence on nonlinear systems output spectrum was investigated in [134]. It is worth pointing out that analysis of linear and nonlinear parameters' influence on system output spectrum in a separated manner is not comprehensive enough for in-depth understanding of the system characteristics.

Motivated by above observations, a hybrid linear and nonlinear model parameters analysis approach for nonlinear systems based on the nCOS function will be systematically investigated. Linear and nonlinear model parameters' influence on system output spectrum is simultaneously considered. Relationship between the system output spectrum and system parameters (both linear and nonlinear) is explicitly revealed. This result extends the nCOS function based method from the analysis and design of linear and nonlinear parameters in a separated manner to that of hybrid linear and nonlinear parameters, which provides a more comprehensive solution to in-depth analysis and design of nonlinear systems.

1.2 Objective of the thesis

Motivated by the above background and discussions, this thesis aims to control and analyze nonlinear systems based on fuzzy control and frequency domain analysis method and their applications to mechanical system. Objectives of this thesis are listed as follows:

- Propose new fuzzy control scheme for nonlinear mechanical systems.

  First, construct a new fuzzy adaptive controller, which uses a bio-inspired limb-like structure with quasi-zero-stiffness and elaborately designed nonlinear damping as reference model, to suppress vibration of suspension system.

Design a new fuzzy sampled-data controller for nonlinear system is under a unified framework to achieve better performance for suspension systems with considering payload changes and disturbances.

- Explore fuzzy filter problems and membership fucntion parameters optimizations problems under imperfect premise matching.

  Design an advantageous fuzzy filter for nonlinear system with time-delay under imperfect premise matching.

  Optimize mismatched fuzzy membership function parameters via a frequency domain method.

- Develop a novel parametric characteristic output spectrum function for analysis and design linear and nonlinear parameters simultaneously in nonlinear systems.

1.3 Contribution of the thesis

The main contributions of this thesis are summarized as follows:

(1) A more general bio-inspired structure with multilayers is adopted as the reference model for fuzzy adaptive control of nonlinear suspension system. This multilayered bio-inspired model can provide better vibration isolation performance than existing systems. A beneficial nonlinear damping is designed and integrated into bio-inspired nonlinear dynamic reference model. This innovative nonlinear damping is for the first time proposed for attenuating resonance peak and improving vibration isolation performance of nonresonant frequency region. Compared to standard fuzzy adaptive control, the controller designed with this generic bio-inspired nonlinear reference model can ensure the same or even better performance with less energy cost, which provides an alternative and effective way to active control of suspension systems.

(2) New stability conditions consisting of both exponential stability and extended dissipativity criterion for fuzzy sampled-data system have been established. A sampled-data controller that not only can exponentially stabilize the system but also guarantee the prescribed extended-dissipativity performance has been designed.

(3) A systematic and novel filter design method for fuzzy systems with time-varying delay under imperfect premise matching is proposed. Based on extended dissipative performance index, the H_∞, $L_2 - L_\infty$, passive and dissipative filter problems have been investigated. New delay-dependent conditions for performance analysis and filter design have been established in terms of LMIs by employing an efficient integral inequality.

(4) A novel nCOS function based optimization method, which aims to optimize the Gaussian membership functions' parameters, has been proposed in this thesis. Compared to traditional search-based optimization approaches only providing final optimal results, the nCOS function-based frequency domain optimization approach can provide analytical relationship between system output spectrum and fuzzy membership function parameters and is time efficient. This provides an in-depth understanding of nonlinear parameters' influence on system output spectrum. System performance over a concerned frequency band has been further enhanced by combining the finite frequency H_∞ controller with the nCOS function based frequency domain optimization method.

(5) A novel parametric characteristic output spectrum (pCOS) function is proposed based on nCOS function, to jointly analyze and design linear and nonlinear parameters of nonlinear systems. [49, 124, 125] developed a systematic method to express the nonlinear output spectrum function as an explicit polynomial function of nonlinear characteristic parameters and the new nCOS function proposed in [134], only investigated the relationship between nonlinear output spectrum and system linear parameters. The novel pCOS function proposed in this thesis is a strong complement to the nCOS function-based method in [49,124,125,134].

The proposed method can be applied to design and analyze both linear and nonlinear parameters of suspension system. Then the proposed hybrid parameter analysis approach, together with an n-th order output spectrum calculation method can be used to identify and locate plant and controller faults in closed-loop control systems, which provide an in-depth insight of fault characteristics analysis and identification of closed-loop nonlinear control systems.

1.4 Outline of the thesis

The organization structure of this thesis is shown in Fig.1.1 is structure. Outline of thesis is given as follows:

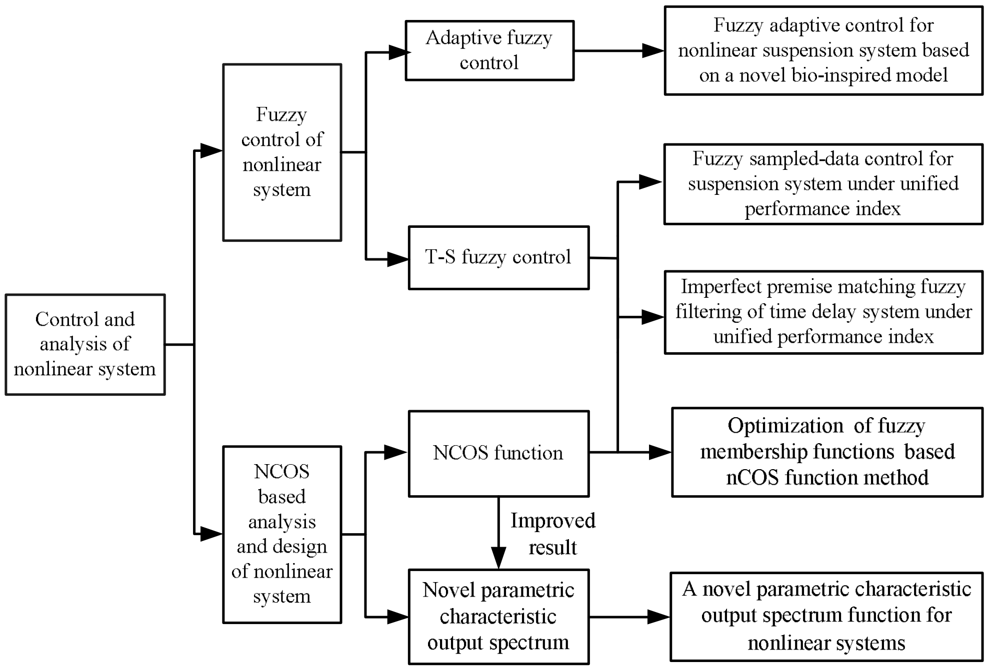

Fig. 1.1: Structure of the thesis

Chapter 2 investigates the problem of fuzzy adaptive tracking control for active suspension systems based on a bio-inspired reference model.

Chapter 3 investigates the exponential stabilization problems of T-S fuzzy aperiodic sampled-data system under a unified performance index.

The problems of imperfect premise matching fuzzy filter design for continuous-time nonlinear systems with time-varying delays based on a unified performance index−extended dissipative index are addressed in Chapter 4.

Chapter 5 studies the membership function parameters optimization issue for suspension system with mismatched finite frequency H_∞ controller based on frequency domain method.

A novel parametric characteristic output spectrum function based linear and nonlinear parameters analysis and design method is studied in Chapter 6.

Chapter 7 concludes this thesis.

Chapter 2

Fuzzy control of suspension systems based on bio-inspired nonlinear dynamics

This chapter proposes a bio-inspired reference model based fuzzy adaptive tracking control for active suspension systems. Fuzzy logic systems are used to approximate unknown nonlinear terms in nonlinear suspension systems. Particularly, a nonlinear damping is designed to improve damping characteristics of the bio-inspired reference model. With beneficial nonlinear stiffness and improved nonlinear damping of the bio-inspired reference model, the proposed fuzzy adaptive controller can effectively suppress vibration of suspension systems with less actuator force and much improved ride comfort, thus energy saving performance can be achieved. Finally, a quarter-vehicle active suspension system with considering payload uncertainties, general disturbance and actuator saturation is provided for evaluating the validity and superiority of the bio-inspired nonlinear dynamics based fuzzy adaptive control approach proposed in this chapter.

The main contributions of this chapter are summarized as follows:

1) A more general bio-inspired structure with multi-layers is adopted as the reference model for fuzzy adaptive control of nonlinear suspension systems. This multi-layer bio-inspired model can provide better vibration isolation performance than existing systems as discussed.

2) A beneficial nonlinear damping is designed and integrated into bio-inspired nonlinear dynamic reference models. This innovative nonlinear damping is for the first time proposed for attenuating resonance peak and improving vibration isolation performance of non-resonant frequency region.

3) With this generic bio-inspired nonlinear reference model, and compared to standard fuzzy adaptive control, the designed controller can ensure the same or even better performance with less energy cost, which provides an alternative and useful way to active control of suspension systems.

The rest of this chapter is organized as follows: Nonlinear suspension system is given in Section 2.1. The bio-inspired reference model and nonlinear damping design are presented in Section 2.2. Bio-inspired reference model based fuzzy adaptive controller is designed in Section 2.3. An example of the nonlinear quarter suspension is provided in Section 2.4 to demonstrate the applicability and effectiveness of the proposed method. Conclusion is drawn in Section 2.5.

2.1 System description and problem formulation

Fig.2.1 shows nonlinear quarter vehicle suspension system with bio-inspired reference model. m_s and m_u are sprung and unsprung mass, z_s, z_u and z_r are the

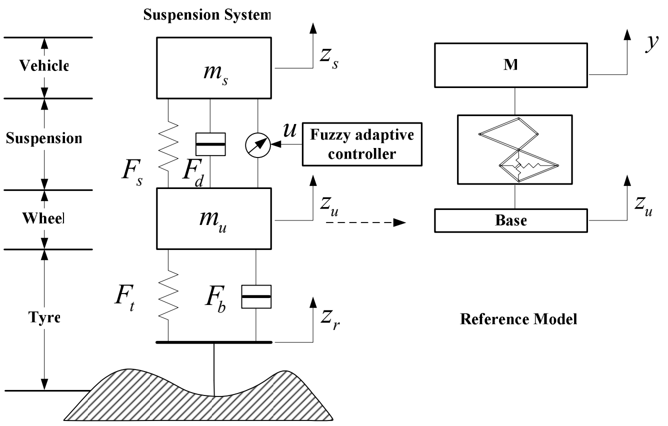

Fig. 2.1: Nonlinear suspension system with bio-inspired reference model vertical displacements of sprung mass, unsprung mass and road input, u is the control force applied on the suspension system. According to Newton's second law, nonlinear dynamic equation of the system is built as follows:

$$\begin{aligned} m_s\ddot{z}_s &= -F_s - F_d + u \\ m_u\ddot{z}_u &= F_s + F_d - F_t - F_b - u \end{aligned} \tag{2.1.1}$$

where F_s, F_d, F_t are the forces produced by the nonlinear spring, nonlinear damper and the tire, which are represented as follows

$$\begin{aligned} &F_s = k_{s1}(z_s - z_u) + k_{s2}(z_s - z_u)^2 + k_{s3}(z_s - z_u)^3 \\ &F_d = c_{s1}(\dot{z}_s - \dot{z}_u) + c_{s2}(\dot{z}_s - \dot{z}_u)^2, F_t = k_t(z_u - z_r), \quad F_b = c_t(\dot{z}_u - \dot{z}_r) \end{aligned}$$

k_{s1}, k_{s2} and k_{s3} are nonlinear stiffness coefficients, c_{s1} and c_{s2} are damping coefficients, k_t and c_t are stiffness and damping coefficients of the tire. The main purpose of this chapter is to construct a bio-inspired reference model with excellent vibration suppression performance (Fig.2.1 right), then a fuzzy adaptive controller is designed to make suspension state $z_s - z_u$ track the bio-inspired dynamics of reference model y_r.

Remark 2.1 *Due to the change of payload, the vehicle mass cannot remain constant. Thus, the quarter vehicle suspension model is an uncertain system that contains uncertain parameters $m_s(t)$. The uncertain parameter is supposed to vary in a given range $m_s(t) \in [m_{smin},\ m_{smax}]$.*

The following two indexes are commonly used to evaluate suspension system performance: root mean square (RMS) values of body acceleration $\ddot{z}_s$ and power consumption of actuator, which are calculated as:

$$\mathrm{RMS}_x = \sqrt{\frac{1}{T}\int_0^T x^T(t)x(t)dt}\ , \mathrm{RMS}_P = \sqrt{\frac{1}{T}\int_0^T (P_+(t))^2 dt}$$

where

$$\mathrm{P}_{+}(t) = \begin{cases} u(t)(\dot{z}_s - \dot{z}_u), & \text{If}\, u(t)(\dot{z}_s - \dot{z}_u) > 0 \\ 0, & \text{else} \end{cases}$$

2.2 Nonlinear damping design for the bio-inspired nonlinear reference model

In this section, a novel nonlinear damping system will be introduced for the bio-inspired reference model to create beneficial nonlinear characteristics for the active control of suspension systems. A brief analysis of the bio-inspired reference model is given below. Detailed analysis can be referred to [57, 60].

2.2.1 Modeling and analysis of bio-inspired system

As shown in Fig.2.2, a multi-layer asymmetrical bio-inspired structure consists of connecting rods, rotating joints and springs. This structure is inspired by the

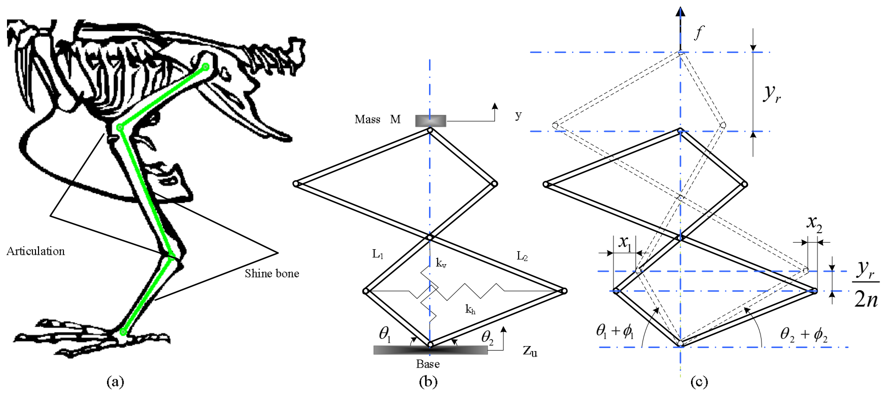

Fig. 2.2: (a) Bird's leg and its structure (b) Mechanical diagrams of the bio-inspired structure (c) Deformation analysis (layer number $n = 2$)

limb structure of animals in motion vibration control. The bird's leg shown in Fig.2.2(a) is a X-shaped structure. With this X-shaped structure, the bird can maintain super stability when running or landing, even with a very high speed, which indicates that this structure has the potential to suppress vibration. In Fig.2.2(b), M is the mass of the isolated object, L_1 and L_2 denote the length of the connection rods. θ_1 and θ_2 are initial angles with respect to the horizon line and the geometric relationship $L_1 \sin(\theta_1) = L_2 \sin(\theta_2)$ holds, k_v and k_h are stiffness of the two linear springs used as passive muscles in vertical and horizontal direction, respectively. y is the absolute motion of the mass, z_u is base excitation. ϕ_1 and ϕ_2 are rotational motions of the connection rods, horizontal motions are denoted by x_1 and x_2, $y_r = y - z_u$ is relative motion between the isolated object M and the base. And according to the geometrical relationship presented in Fig.2.2(b) and (c), the rotational and horizontal motions can be given as

$$\begin{aligned} x_i &= L_i\cos\theta_i - \sqrt{L_i^2 - (L_i\sin\theta_i + y_r/2n)^2} \\ \phi_i &= \text{acrtan}\left(\frac{L_i\sin\theta_i + y_r/2n}{L_i\cos\theta_i - x_i}\right) - \theta_i, i = 1, 2. \\ x &= x_1 + x_2, \phi = \phi_1 + \phi_2 \end{aligned} \tag{2.2.1}$$

The kinetic and potential energy of the bio-inspired structure can be given by

$$T = \frac{1}{2}M\dot{y}^2, U = \frac{1}{2}k_h x^2 + \frac{1}{2}k_v(y_r/n)^2 \tag{2.2.2}$$

Then the Lagrangian function is $L = T - U$. Different from some existing results, a nonlinear damper achieving better performance on specific frequency region will be designed. Then the non-conservative force can be calculated as

$$Q = -c_1\dot{y}_r - c_2 n_x \dot{\phi}\frac{\partial \phi}{\partial y} - F_n \tag{2.2.3}$$

where c_1 and c_2 are air damping and rotation friction coefficient, $\dot{\phi} = \frac{d\phi}{dy_r} \cdot \frac{dy_r}{dt}$, $n_x = 3n + 1$ is the number of joints, F_n is the force produced by desired nonlinear damper, which will be designed in the next subsection.

Then the Lagrange equation for the bio-inspired structure can be given as follows:

$$\frac{d}{dt}\left(\frac{\partial L}{\partial \dot{y}}\right) - \frac{\partial L}{\partial y} = Q \tag{2.2.4}$$

Substitute L and Q into (2.2.4), we can obtain the nonlinear dynamic equation of the bio-inspired reference model

$$M\ddot{y} + k_h x \frac{dx}{dy_r} \cdot \frac{dy_r}{dy} + k_v y_r/n^2 = -c_1\dot{y}_r - c_2 n_x \dot{\phi}\frac{\partial \phi}{\partial y} - F_n \tag{2.2.5}$$

Substitute $y_r = y - z_u$ into (2.2.5), the reference dynamic model can be rewritten as

$$M\ddot{y}_r + f_1(y_r) + k_v y_r/n^2 + c_1\dot{y}_r + c_2 n_x f_2(y_r)\dot{y}_r + F_n = -M\ddot{z}_u \tag{2.2.6}$$

where $f_1(y_r) = k_h x \frac{dx}{dy_r} \cdot \frac{dy_r}{dy}$, $f_2(y_r) = \left(\frac{d\phi}{dy_r}\right)^2$.

Define $v(y_r) = L_1\sin\theta_1 + y_r/2n$, and according to the rotational and horizontal motion, $f_1(y_r)$ and $f_2(y_r)$ can be further deduced as

$$\begin{aligned} f_1(y_r) =& \frac{k_h}{2n}\left(L_1\cos\theta_1 + L_2\cos\theta_2 - \sqrt{L_1^2 - v^2(y_r)} - \sqrt{L_2^2 - v^2(y_r)}\right) \\ &\times \left(\frac{v(y_r)}{\sqrt{L_1^2 - v^2(y_r)}} + \frac{v(y_r)}{\sqrt{L_2^2 - v^2(y_r)}}\right) \\ f_2(y_r) =& \left(\frac{1}{2n\sqrt{L_1^2 - v^2(y_r)}} + \frac{1}{2n\sqrt{L_2^2 - v^2(y_r)}}\right)^2 \end{aligned}$$

Define $y_1 = y_r$, $y_2 = \dot{y}_r$, the state space equation of the bio-inspired nonlinear model is

$$\begin{cases} \dot{y}_1 = y_2 \\ \dot{y}_2 = -\dfrac{1}{M}\left[h_1(y_1) + h_2(y_1, y_2) + F_n\right] - \ddot{z}_u \end{cases} \tag{2.2.7}$$

where $h_1(y_1) = f_1(y_1) + k_v \frac{y_r}{n^2}$, $h_2(y_1, y_2) = c_2 n_x f_2(y_1) y_2 + c_1 y_2$. $\ddot{z}_u$ is the unsprung mass acceleration of the suspension system. Until present, the multi-layer bio-inspired reference model has been established. The following subsection will present detailed nonlinear damping design procedure.

2.2.2 Nonlinear damping design

Displacement transmissibility of the bio-inspired reference model under different linear damping is illustrated in Fig.2.3. The higher the damping, the better performance in the resonant region and the worse transmissibility in non-resonant frequency region. The ideal damping should be high around resonance frequency but low at others [45–48]. To this aim, a novel nonlinear damping is proposed in this study to overcome the inherent trade-off in the choice of damping.

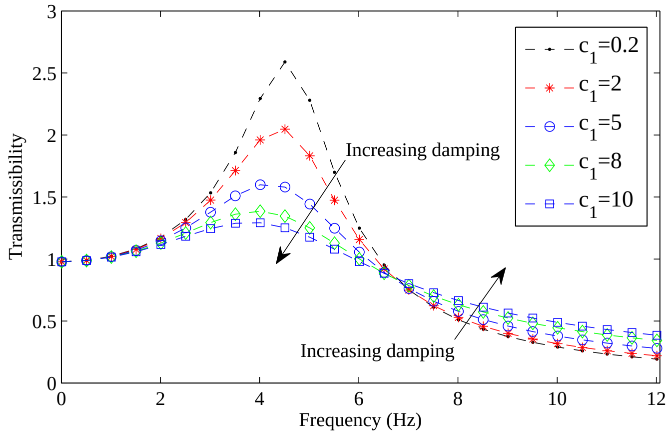

Fig. 2.3: Displacement transmissibility under different damping (The bio-inspired reference model parameters are $M = 0.5$ kg, $L_1 = 0.1$ m, $L_2=0.2$ m, $k_h=500$ N/m, $k_v=350$ N/m, $c_2=0.02$ N/sm, $\theta_1 = \frac{\pi}{6}$ rad).

A filter-based nonlinear damping in the following form $F_n(s) = C(s)U(s)$ is considered, s is Laplace operator, $U(s)$ is the Laplace transform of relative velocity $\dot{y}_r$, $C(s)$ is a linear dynamic filter to be designed, the frequency response of which has a peak around the natural frequency of the bio-inspired reference model and decays very quickly to a small value in the high frequency region. The key idea of designing the nonlinear damping is that using high level damping to suppress the resonant peak and adopting low level damping to improve the isolation performance of non-resonant frequency region. This nonlinear damping can be regarded as a frequency-dependent and/or displacement-dependent damping. The damping force is adjusted according to the frequency of $\dot{y}_r$. The frequency-dependent nonlinear damping can be designed in the frequency domain. So this linear filter can be chosen as the following second-order quasi band-pass filter. It is worth pointing out that the filter in the form of (2.2.8) is not unique.

$$C(s) = K\frac{s^2 + 2\,k_l\,\xi_l\,w_l s + a_l\,w_l^2}{s^2 + 2\,\xi_l\,w_l\,s + w_l^2} \tag{2.2.8}$$

Parameter K is the gain of nonlinear damping, $1 < k_l$, ξ_l and w_l are band-pass gain, damping ratio, and center frequency of the quasi band-pass filter, a_l determines the filter gain at low frequency region.

Especially when $k_l = 1$ and $a_l = 1$ hold, the nonlinear damping is reduced to linear damping with coefficient K. Assume that the band-pass gain k_l is far larger than a_l. The peak-gain can be approximated as $\lim_{s\to j\cdot w_l}\|C(s)\| \approx K\cdot k_l$. The low frequency gain and the high frequency gain can be respectively approximated as $\lim_{s\to j\cdot 0}\|C(s)\| \approx K\cdot a_l$ and $\lim_{s\to j\cdot\infty}\|C(s)\| \approx K$. For a given system, we can know the exact damping level. According to the desired damping, the peak-gain, low frequency gain and high frequency gain can be designed. The damping ratio ξ_l will be determined by the bandwidth of high damping. One way to implement the second order filter is to adopt analogue circuit.

Through inverse Laplace transform of (2.2.8), the time domain model of the nonlinear damping force is obtained

$$\begin{cases} \dfrac{dF_1}{dt} = F_2 \\ \dfrac{dF_2}{dt} = -w_l^2 F_1 - 2\xi_l w_l F_2 + u_F \end{cases} \tag{2.2.9}$$

where $F_1 = F_n$, $F_2 = \dot{F}_n$, u_F is the input consisting of relative velocity and its high order derivatives $u_F = K(a_l w_l^2\, y_2 + 2k_l\xi_l w_l\, y_3 + y_4)$, $y_2 = \dot{y}_r$, $y_3 = \dot{y}_2$, $y_4 = \dot{y}_3$. By utilizing relative velocity and its high order derivatives, the nonlinear damping force can also be implemented according to the model (2.2.9). y_r is the relative displacement between unsprung mass and sprung mass which can be measured by using potentiometer or other linear displacement sensors. Relative velocity

$\dot{y}_r$ can be obtained by differentiating y_r or integrating acceleration $\ddot{y}_r$. $\ddot{y}_r$ is the relative acceleration which can be obtained by measuring absolute acceleration of sprung mass and unsprung mass using two accelerometers. $\frac{d\ddot{y}_r}{dt}$ (called jerk) can be obtained by measuring absolute jerk of sprung mass and unsprung mass using jerk sensor.

The parameter selection of this filter requires considerations of both the natural frequency of the bio-inspired reference model and the specific isolation performance. Through Taylor series expansion of nonlinear stiffness term $f_1(y_r)$ at zero equilibrium, the natural frequency of the bio-inspired reference model is approximated as [57]

$$w_n = \sqrt{\frac{k_h}{M}} \sqrt{\frac{\gamma^2}{4n^2} \frac{(\sqrt{1-\gamma^2}+\sqrt{\beta^2-\gamma^2})^2}{(1-\gamma^2)(\beta^2-\gamma^2)} + \frac{\alpha}{n^2}} \tag{2.2.10}$$

where $\alpha = k_v/k_h, \beta = L_2/L_1, \gamma = \sin\theta_1$. For the bio-inspired reference model with parameters $M = 4.0$ kg, $L_1 = 0.1$ m, $L_2 = 0.2$ m, $k_h = 500$ N/m, $k_v = 350$ N/m, $\theta_1 = \frac{\pi}{6}$ rad, the natural frequency obtained by (2.2.10) is about $w_n = 5.22$ rad/s. In order to sufficiently suppress the resonant region and simultaneously guarantee the vibration isolation performance at high frequency, the center frequency of the quasi band-pass filter should be close to the natural frequency of reference model. The parameters of quasi band-pass filter are chosen as $K = 1$, $k_l = 20$, $\xi_l = 0.6$, $w_l = 4.22$ rad/s and $a_l = 2$.

In addition, (2.2.8) is a stable filter. Thus F_n can be approximately regarded as a bounded positive damping.

To demonstrate advantage of the designed nonlinear damping, comparison of vibration isolation performance of bio-inspired reference model between the original damping and the designed nonlinear damping is conducted. The original damping and the designed nonlinear damping are respectively selected as $c_1 = 2$, $c_2 = 0.01$, $F_n = 0$ and $c_1 = 0$, $c_2 = 0.01$, $F_n(s) = C(s)U(s)$. Assuming that excitation in the base of the bio-inspired reference model is harmonic in nature represented as

z_u. y is the motion transmitted to the top. The transmissibility is defined as the ratio of the magnitudes of the displacements $T_d = |\frac{y}{z_u}|$. By resorting to the harmonic balance method, the displacement transmissibility of the bio-inspired reference model with different damping is shown in Fig.2.4.

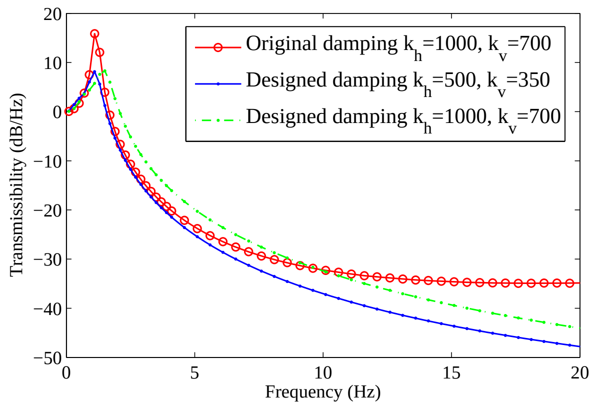

Fig. 2.4: Displacement transmissibility under different damping

The transmissibility around the resonant peak is significantly reduced as analyzed before due to the effect of peak damping around the natural frequency region. As the frequency increases, the nonlinear damping decays quickly to a small level and the transmissibility over the effective isolation region is almost unaffected. Furthermore, the transmissibility of higher frequency region can even be reduced owing to this small level damping. In Fig.2.4, red line and green line are displacement transmissibility under different damping with same stiffness. It is noted that there is slight shift of damped resonance frequency due to changes of damping. By tuning stiffness of the structure, the shift can be removed. In Fig.2.4, blue line is the transmissibility with modified stiffness.

Then, a random excitation is applied to the base of the bio-inspired reference model. The acceleration response and its power spectral density (PSD) are given in Fig.2.5(a) and Fig.2.5(b). From the acceleration response, it can be seen that the bio-inspired structure with designed nonlinear damping can achieve better vibration isolation performance than that with original damping since magnitude of platform acceleration is greatly reduced.

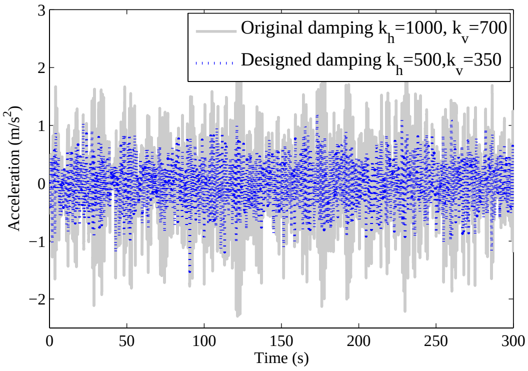

(a)

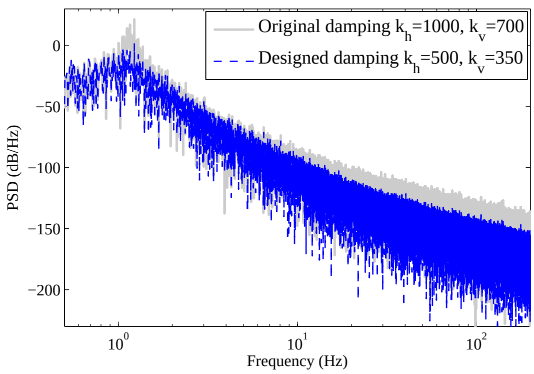

(b)

Fig. 2.5: Acceleration and power spectral density under original damping and designed damping

It should be emphasized that the attenuation of resonance peak at low frequency is not at the expense of isolation performance in higher frequency region, which can be validated from the PSD of acceleration. All these results indicate that both the attenuation of resonance peak and vibration isolation performance of non-resonant frequency region can be simultaneously guaranteed through designing the nonlinear damping force in (2.2.8). Next, a novel reference model with combination of the bio-inspired vibration structure and this nonlinear damping will be applied to the active control of vehicle suspension system.

Remark 2.2 *Although the nonlinear damping proposed in this chapter is applied to construct the reference model. Actually, the general active vibration control systems can also benefit from this nonlinear damping design method. A feasible method to implement the vibration isolation system with such nonlinear damping characteristic is to adopt magneto-rheological damper [38]. The damping force is adjusted according to the output of filter (2.2.8). For practical application, filter (2.2.8) can be constructed by using analogue circuits. The filter input is the velocity $\dot{y}_r$, which can be measured by DC tachogenerator.*

2.3 Fuzzy adaptive controller synthesis

Based on the bio-inspired reference model and nonlinear damping, the fuzzy adaptive backstepping controller design is presented in this section. First denote $z_1 = z_s - z_u$ and $z_2 = \dot{z}_s - \dot{z}_u$, thus the dynamic equations (2.1.1) can be rewritten in the following state space form.

$$\begin{cases} \dot{z}_1 = z_2 \\ \dot{z}_2 = \ddot{z}_s - \ddot{z}_u = \Theta_2^T \psi + b_2 u - \ddot{z}_u \end{cases} \tag{2.3.1}$$

$\Theta_2 = [-\frac{k_{s1}}{m_s}, -\frac{k_{s2}}{m_s}, -\frac{k_{s3}}{m_s}, -\frac{c_{s1}}{m_s}, -\frac{c_{s2}}{m_s}]^T$ and $b_2 = \frac{1}{m_s}$ are uncertain parameters and $\psi = [z_1, z_1^2, z_1^3, z_2, z_2^2]^T$ is the known nonlinear function vector.

A fuzzy logic system consists of knowledge base, fuzzifier, fuzzy inference engine and defuzzifier. The knowledge is a set of fuzzy IF-THEN rules which takes the following form:

Rule j : IF z_1 is F_1^j and $\cdots$ and z_n is F_n^j,

THEN y is B^j, $j = 1, 2, \cdots, N$.

Through singleton fuzzifier, center average defuzzification and product inference, the output of fuzzy logic system is

$$y(z) = \frac{\sum_{j=1}^{N} \theta_j \prod_{i=1}^{n} \mu_i^j(z_i)}{\sum_{j=1}^{N} \prod_{i=1}^{n} \mu_i^j(z_i)} \tag{2.3.2}$$

where $z = [z_1, \cdots, z_n]^T$, $\mu_i^j(z_i)$ is membership function, $\theta_j = \max\limits_{y \in R} B^j(y)$. Define fuzzy basis functions as

$$\xi(z) = \frac{\prod_{i=1}^{n} \mu_i^j(z_i)}{\sum_{j=1}^{N} \left[\prod_{i=1}^{n} \mu_i^j(z_i)\right]} \tag{2.3.3}$$

Denote $\xi(z) = [\xi_1(z), \xi_2(z), \cdots, \xi_N(z)]$, $\theta(z) = [\theta_1(z), \theta_2(z), \cdots, \theta_N(z)]$, then

$$y(z) = \theta^T \xi(z) \tag{2.3.4}$$

The following lemma is adopted to set relationship between the unknown nonlinear function and the fuzzy logic system.

Lemma 2.1 *[135] For any given continuous function $f(z)$, which is defined on the compact set Ω, there exists a constant $\varepsilon > 0$ and an optimal parameter vector $\theta^\star$ such that*

$$\sup_{z\in\Omega}|f(z) - y(z)| \leq \varepsilon \tag{2.3.5}$$

Then an adaptive fuzzy tracking controller can be designed by making the following change of coordinates $e_1 = z_1 - y_r$, $e_2 = z_2 - \alpha_1$, where y_r is the relative displacement of the bio-inspired reference model, which is bounded, so its derivative $\dot{y}_r$, α_1 is virtual control signal. Then the intermediate control signal and adaptive laws can be designed as follows:

$$\alpha_1 = -\lambda_1 e_1 + \dot{y}_r, \lambda_1 > 0 \tag{2.3.6}$$

$$u = -\lambda_2 e_2 - e_1 - \varphi_2, \lambda_2 > 0 \tag{2.3.7}$$

$$\dot{\theta} = re_2\xi(z) - 2k\theta, r > 0, k > 0 \tag{2.3.8}$$

where $\varphi_2 = \xi^T(z)\theta$, λ_1, λ_2, r and k are parameters to be designed.

Theorem 2.1 *For the nonlinear suspension system (2.3.1), the controller (2.3.7) with the intermediate control signal and parameter law (2.3.6) and (2.3.8) guarantees that all the signals involved are ultimately uniformly bounded, tracking errors converge to a small neighborhood around zero, the closed-loop system is globally stable.*

Proof: Lyapunov function is chosen as

$$V(t) = \frac{1}{2}e_1^2 + \frac{1}{2}e_2^2 + \frac{1}{2r}\tilde{\theta}^T\tilde{\theta}$$

where $\tilde{\theta} = \theta^\star - \theta$. Derivative of $V(t)$ can be written as:

$$\dot{V}(t) = e_1\dot{e}_1 + e_2\dot{e}_2 - \frac{1}{r}\tilde{\theta}^T\dot{\theta} = -\lambda_1 e_1^2 - \lambda_2 e_2^2 + e_2[f(z) - \varphi] - \frac{1}{r}\tilde{\theta}^T\dot{\theta} - \frac{e_2\ddot{z}_u}{b_2}$$

where $f(z) = (\Theta_2^T\psi - \dot{\alpha}_1)/b_2$, $\varphi = \xi^T(z)\theta$ is the fuzzy logic system used to approximate $f(z)$. Then $\dot{V}(t)$ can be rewritten as

$$\begin{aligned}\dot{V}(t) =& -\lambda_1 e_1^2 - \lambda_2 e_2^2 + e_2[f(z) - \xi^T(z)\theta^\star + \xi^T(z)\theta^\star - \xi^T(z)\theta] - \frac{\tilde{\theta}^T\dot{\theta}}{r} - \frac{e_2\ddot{z}_u}{b_2}\\ \le& -\lambda_1 e_1^2 - \lambda_2 e_2^2 + e_2\varepsilon + \tilde{\theta}^T(e_2\xi(z) - \frac{1}{r}\dot{\theta}) - \frac{e_2\ddot{z}_u}{b_2}\\ =& -\lambda_1 e_1^2 - \lambda_2 e_2^2 + e_2\varepsilon + \frac{k}{r}(2\theta^{\star T}\theta - 2\theta^T\theta) - \frac{e_2\ddot{z}_u}{b_2}\end{aligned}$$

Since $2\theta^{\star T}\theta - 2\theta^T\theta \le \theta^{\star T}\theta^\star - \theta^T\theta$. Then $\dot{V}(t)$ can be formulated as

$$\begin{aligned}\dot{V}(t) \le& -\lambda_1 e_1^2 - \lambda_2 e_2^2 + e_2\varepsilon + \frac{k}{r}(\theta^{\star T}\theta^\star - \theta^T\theta) - \frac{e_2\ddot{z}_u}{b_2}\\ =& -\lambda_1 e_1^2 - \lambda_2 e_2^2 + e_2\varepsilon + \frac{k}{r}(-\theta^T\theta - \theta^{\star T}\theta^\star) + \frac{2k}{r}\theta^{\star T}\theta^\star - \frac{e_2\ddot{z}_u}{b_2}\end{aligned}$$

According to the following inequalities $e_2\varepsilon \le \frac{1}{2}e_2^2 + \frac{1}{2}\varepsilon^2$, $\tilde{\theta}^T\tilde{\theta} = (\theta^\star - \theta)(\theta^\star - \theta)^T = \theta^{\star T}\theta^\star - 2\theta^{\star T}\theta + \theta^T\theta \le 2\theta^{\star T}\theta^\star + 2\theta^T\theta$, we have $-\frac{1}{2}\tilde{\theta}^T\tilde{\theta} \ge -\theta^{\star T}\theta^\star - \theta^T\theta$. Define $\lambda_2 = a + \frac{1}{2b_2^2}$, since $-\frac{e_2^2}{2b_2^2} - \frac{e_2\ddot{z}_u}{b_2} \le \frac{\ddot{z}_u^2}{2}$, $\ddot{z}_u^2 \le a_1$, a_1 is a positive constant. Then one can have

$$\begin{aligned}\dot{V}(t) \le& -\lambda_1 e_1^2 - (a - \frac{1}{2})e_2^2 + \frac{1}{2}\varepsilon^2 - \frac{k}{2r}\tilde{\theta}^T\tilde{\theta} + \frac{2k}{r}\theta^{\star T}\theta^\star + \frac{a_1}{2}\\ \le& -C(\frac{1}{2}e_1^2 + \frac{1}{2}e_2^2 + \frac{1}{2r}\tilde{\theta}^T\tilde{\theta}) + D\\ =& -CV + D\end{aligned} \tag{2.3.9}$$

where $C = \min\{2\lambda_1, 2a - 1, k\}$, $D = \frac{1}{2}\varepsilon^2 + \frac{2k}{r}\theta^{\star T}\theta^\star + \frac{a_1}{2}$. From (2.3.9), it is easy to conclude that

$$V(t) \le V(t_0)e^{-C(t-t_0)} + D/C \tag{2.3.10}$$

Therefore, signals $z(t)$, $e_1(t)$, $e_2(t)$, $\theta(t)$ and $u(t)$ are globally uniformly ultimately bounded and tracking error is bounded $e_1(t) \le \sqrt{2V(t_0)e^{-C(t-t_0)}} + \sqrt{2\frac{D}{C}}$. If the parameters C and D are appropriately chosen, then $\sqrt{2\frac{D}{C}}$ can be as small as possible. As $t \to \infty$, $e^{-C(t-t_0)/2} \to 0$, then there exists T, when $t \ge T$,

$|z_1(t) - y_r(t)| \leq \sqrt{2\frac{D}{C}}$. This completes the proof.

Remark 2.3 *For the proposed adaptive tracking controller, satisfactory closed-loop tracking performance can be achieved by properly adjusting design parameters λ_1, λ_2, r and k. Larger control gains bring about higher bandwidth of the closed-loop system, which can achieve fast transient response but also introduce high-frequency disturbances. The tracking performance may be degraded by the high-frequency disturbances. Thus, for choosing appropriate controller parameters, minor values are tested until the desired tracking performance is obtained. According to the adaptive law (2.3.6)–(2.3.8), the computational complexities of the controller is mainly determined by the number of fuzzy rule, the type of membership function and the dimension of adaptive law.*

Remark 2.4 *Generally speaking, the ideal tracking signal y_r is always chosen as zero in fuzzy adaptive tracking control. Instead of setting the tracking trajectory as zero, the dynamics output of the bio-inspired structure y_r and $\dot{y}_r$ are used as reference signals, which avoid cancellations of nonlinearities of the suspension system. In addition, a particularly designed nonlinear damping is applied on the bio-inspired reference model. Thus better ride comfort can be achieved. Furthermore, with this reference model, less actuator force is required, which means that the adaptive control method proposed in this chapter is energy efficient.*

Remark 2.5 *Actuator saturation, which is due to physical limitation of actuator, may lead to degraded performance, or even instability of the entire system. As stated in Remark 2.4, the bio-inspired reference model based fuzzy adaptive controller designed in this chapter requires less actuator force. Hence the method in this chapter can also find application in active suspension control system subject to actuator saturation. Detailed comparison discussion will be given later. For practical application, this fuzzy adaptive controller can be implemented through measuring the relative displacement $z_s - z_u$ and relative velocity $\dot{z}_s - \dot{z}_u$, which can* *be easily achieved by installing a linear displacement sensor between the vehicle body and suspension [39].*

2.4 Simulation results and analysis

Here, an example of quarter-vehicle active suspension system, the Hyundai Elantra suspension model with considering payload changes is considered. This example is provided to evaluate the validity and superiority of the designed bio-inspired structure based fuzzy adaptive controller.

Suspension model initial states are zeros. For the fuzzy adaptive controller, we assume that the sprung mass varies in a range of $[0.9m_s, 1.1m_s]$. The corresponding controller parameters are determined as $\lambda_1 = 51.5, \lambda_2 = 23.7, k = 1.5andr = 1$, fuzzy membership functions are chosen as

$$\mu_i^j(z_i) = e^{-0.5[z_i+0.5(5-j)]^2}, i = 1, 2, j = 1. \cdots, 9.$$

Parameters of the vehicle system and the bio-inspired reference model are listed in Table 2.1 and Table 2.2.

Table 2.1: Parameters of quarter vehicle suspension model

Parameter	Value	Parameter	Value
m_s	240 kg	m_u	23.61 kg
k_{s1}	15394 N/m	c_{s1}	1385.4 Ns/m
k_{s2}	-73696 N/m^2	c_{s2}	524.28 Ns^2/m^2
k_{s3}	3170400 N/m^3	c_t	13.8 Ns/m
k_t	181818.88 N/m		

Then the designed bio-inspired reference model based fuzzy adaptive controller is implemented on the quarter vehicle model. Comparison results are mainly conducted from the aspects of vibration suppression and energy consumption among

Table 2.2: Parameters of the bio-inspired reference model

Parameter	Value	Parameter	Value
M	80 kg	θ_1	$\pi/6\ rad$
L_1	0.1 m	c_1	5 Ns/m
L_2	0.2 m	c_2	0.15 Ns/m
k_v	350 N/m	k_h	500 N/m

the passive suspension system and the following three different active control methods:

1. Controller1: Active control using standard fuzzy adaptive backstepping controller in [136].
2. Controller2: Active control using fuzzy adaptive backstepping controller based on the multi-layer bio-inspired reference model in [57].
3. Controller3: Active control using fuzzy adaptive backstepping controller based on the multi-layer bio-inspired reference model with deliberately designed nonlinear damping proposed in this chapter.

In simulation, filtered white noise borrowed from [137] with road roughness class C is adopted. The equation of road excitation is expressed as

$$\dot{q}(t) = -2\pi n_q u q(t) + 2\pi n_0 \sqrt{G_q(n_0) u} w(t) \tag{2.4.1}$$

where $n_q = 0.0001 m^{-1}$ is the lowest frequency, $w(t)$ is standard Gaussian white noise with 0 mean and unit variance, $G_q(n_0) = 256 \times 10^{-6} m^2/m^{-1}$(class C), u is the vehicle forward velocity. In this chapter, three different vehicle forward velocities $V_1 = 10$ km/h, $V_2 = 20$ km/h and $V_3 = 35$ km/h are used to test the performance of the proposed control approach.

Comparisons of energy consumption and acceleration of the sprung mass $\ddot{z}_s$ for different vehicle forward velocities with different control methods in terms of the aforementioned RMS values are given in Table 2.3 and 2.4. In this chapter, we use simulation time $T = 50s$ to calculate the RMS values of the sprung mass acceleration and the consumed energy for different cases.

Table 2.3: RMS of energy consumption for different vehicle forward velocities (W)

V	Controller1	Controller2	Controller3
V_1=10 km/h	49.2455	20.0761 ($\downarrow$ 58.76%)	22.6746 ($\downarrow$ 53.43%)
V_2=20 km/h	98.8268	40.2628 ($\downarrow$ 58.79%)	45.4782 ($\downarrow$ 53.46%)
V_3=35 km/h	173.9919	70.7589 ($\downarrow$ 58.87%)	79.9422 ($\downarrow$ 53.53%)

Table 2.4: RMS of suspension acceleration for different vehicle forward velocities (m/s^2)

V	Passive	Controller1	Controller2	Controller3
V_1=10 km/h	0.0822	0.0082 ($\uparrow$ 86.74%)	0.0079 ($\uparrow$ 90.39%)	0.0070 ($\uparrow$ 91.48%)
V_2=20 km/h	0.1162	0.0117 ($\uparrow$ 86.75%)	0.0113 ($\uparrow$ 90.28%)	0.0099 ($\uparrow$ 91.48%)
V_3=35 km/h	0.1538	0.0155 ($\uparrow$ 86.67%)	0.01498 ($\uparrow$ 90.31%)	0.0132 ($\uparrow$ 91.42%)

From these tables, one can clearly observe that, compared to standard fuzzy adaptive Controller1, the bio-inspired reference model based tracking Controller2 and Controller3 can improve ride comfort for different forward velocities and meanwhile save more than 50% energy.

The time and frequency domain responses of the vehicle body acceleration are given in Fig.2.6 where $V_3 = 35$ km/h. It is obvious that the active suspension response outperforms the passive one, since magnitudes of vehicle body accelerations are greatly reduced with active Controller1-3 both in time and frequency domains. Moreover control forces required by Controller1 and Controller3 are shown in Fig.2.7(a). The control force of Controller3 is much smaller than that of standard fuzzy adaptive Controller1. The frequency comparison of control force is depicted in Fig.2.7(b), from which one can observe that Controller1 contains more components in high-frequency region and is more likely to occur actuator saturation. It is also well known that high bandwidth controllers are more sensitive to high frequency noise. Moreover, high bandwidth of actuator requires high speed sensor and actuator, which will lead to low tolerance of delay and increase cost of the entire control system. The simulation results show that, compared to standard fuzzy adaptive Controller1, Controller3 proposed in this chapter requires less energy and low bandwidth actuator while guarantees similar ride comfort with Controller1. It can also be verified from Table 2.3 and 2.4 ($V_3 = 35$ km/h), all active controllers improve ride comfort significantly compared to passive suspension system, since the RMS value of the sprung mass acceleration decreases about 86.67%(Controller1), 90.39%(Controller2), 91.48%(Controller3), while less energy, 70.7589W (Controller2) and 79.9422W (Controller3) are consumed, which is much better than the standard fuzzy adaptive controller(about 173.9919W).

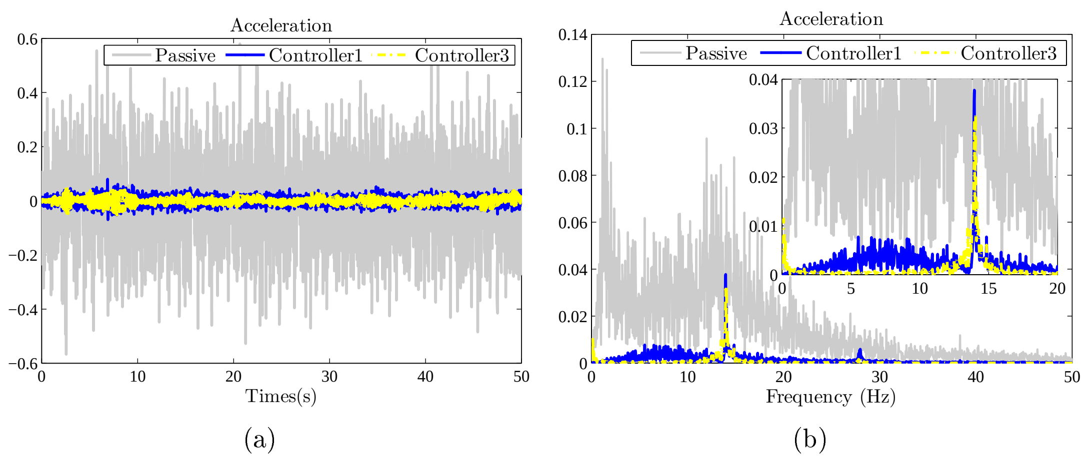

Fig. 2.6: Vehicle body acceleration and its frequency component

Additionally, constraint of suspension space and dynamic tyre load are also taken into account. Suspension deflection $z_s - z_u$ is given in Fig.2.8(b). It is clear that the controlled suspension spaces all fall into the acceptable ranges. Thus, this physical constraint can be guaranteed. The dynamic tire load is illustrated in Fig.2.8(b), which demonstrates that the dynamic tire load constraint $\frac{F_t+F_b}{(m_s+m_u)g} < 1$ is satisfied. In a word, Fig.2.8(a) and 2.8(b) validate that road holding capability and suspension deflection constraint can be guaranteed with improved ride

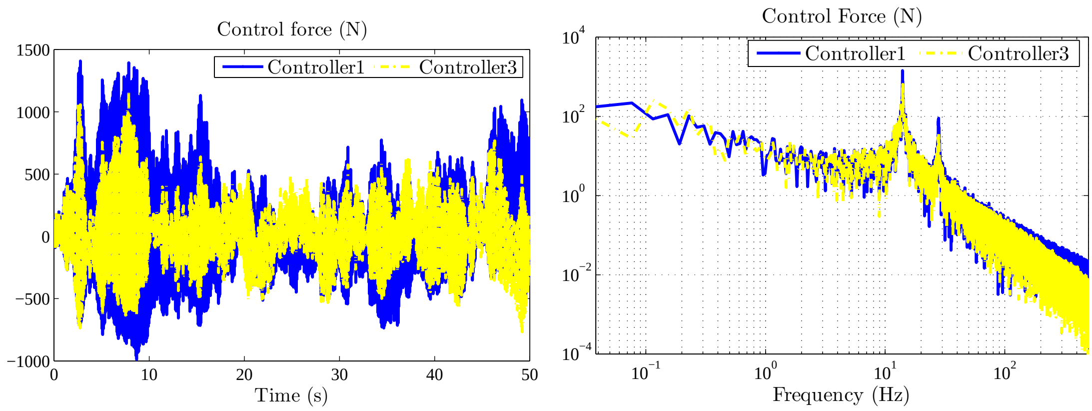

(a) (b)

Fig. 2.7: Control force and its frequency component

comfort.

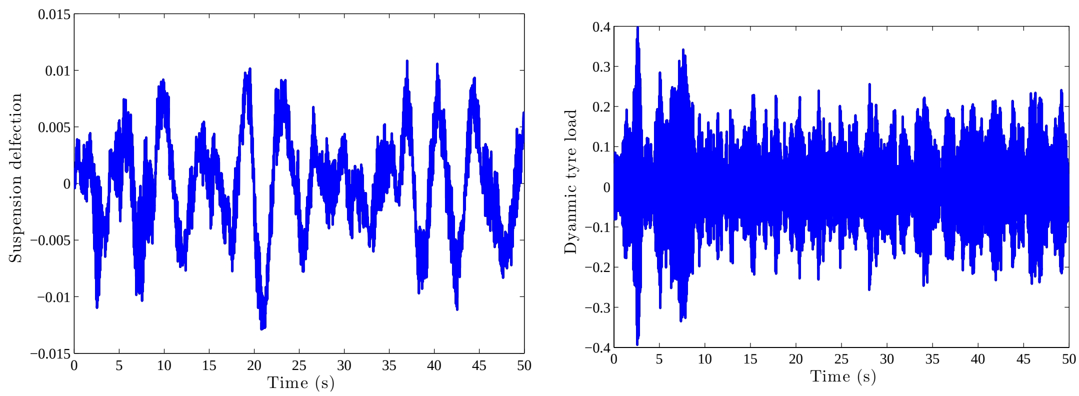

(a) (b)

Fig. 2.8: Suspension deflection and dynamic tyre load of the suspension system with a bio-inspired reference model

Then, to evaluate the robustness of the designed fuzzy adaptive controller, a general disturbance $F_d = \sin(3\pi t) + 0.2\sin(30\pi t)$ is added to the sprung mass. The disturbance contains components at 1.5 and 15 Hz, respectively. Comparisons are conducted when vehicle forward velocity is $V_3 = 35$km/h. Following the same analysis procedure, Table 2.5 and 2.6 show comparisons of RMS values using different controllers. Table 2.5 shows the energy consumed by different controllers. Bio-inspired based controllers consume 60% less energy than standard controller, which validate that the bio-inspired reference model based controllers are more

Table 2.5: RMS of energy consumption for different vehicle forward velocities when subject to disturbance (W)

V	Controller1	Controller2	Controller3
V_1=10 km/h	179.1717	54.6823 (↓ 69.48%)	57.5802 (↓ 67.86%)
V_2=20 km/h	237.7704	75.3530 (↓ 68.31%)	80.8523 (↓ 66.00%)
V_3=35 km/h	322.5624	105.8484 (↓ 67.18%)	115.2958 (↓ 64.26%)

Table 2.6: RMS of suspension acceleration for different vehicle forward velocities when subject to disturbance (m/s^2)

V	Passive	Controller1	Controller2	Controller3
V_1=10 km/h	1.2240	0.0130 (↑ 98.94%)	0.01243 (↑ 98.98%)	0.0104 (↑ 99.15%)
V_2=20 km/h	1.2272	0.0156 (↑ 98.72%)	0.0148 (↑ 98.79%)	0.0126 (↑ 98.97%)
V_3=35 km/h	1.2318	0.0189 (↑ 98.46%)	0.0178 (↑ 98.55%)	0.0153 (↑ 98.76%)

energy efficient when subject to disturbance. As for vibration isolation performance, from Table 2.6, we can see that the general disturbance has great impact on passive suspension system, while Controller1-3 reduce the values of vehicle body acceleration significantly for about 98% compared to passive system. This again verifies the results when there is no disturbance. Fig.2.9(a)–(b) are comparisons of the vehicle body acceleration in time domain and frequency domain. From these figures, compared to passive suspension, we can see that ride comfort are significantly improved with Controller1 and Controller3. Although the vehicle body accelerations with Controller1 and Controller3 are almost the same, the control force of Controller1 in Fig.2.10(a) is much larger than that of Controller3 and the control signal bandwidth of Controller1 in Fig.2.10(b) is much higher than that of Controller3, which means that Controller3 is more energy efficient and economic.

Fig.2.11(a) shows comparison of vehicle body acceleration between Controller2 and Controller3 subject to disturbance F_d. To further demonstrate the advantages

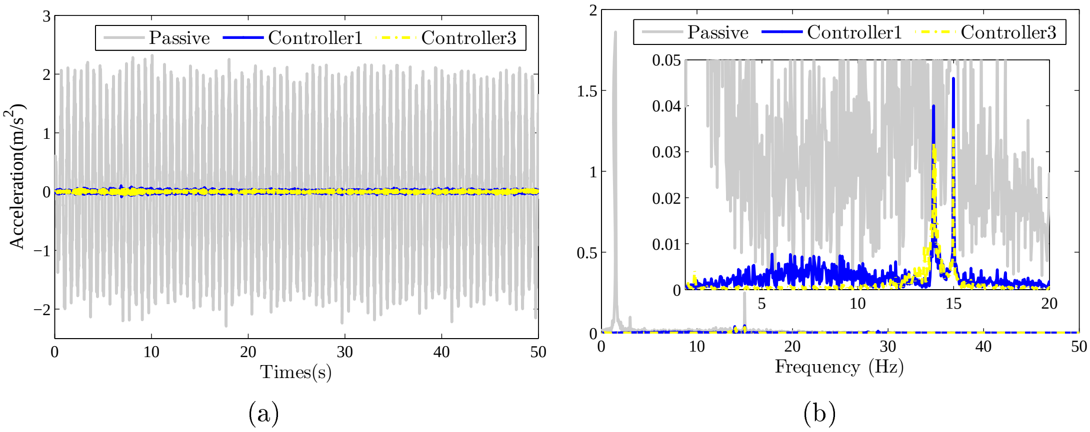

Fig. 2.9: Vehicle body acceleration and its frequency component when subject to disturbance

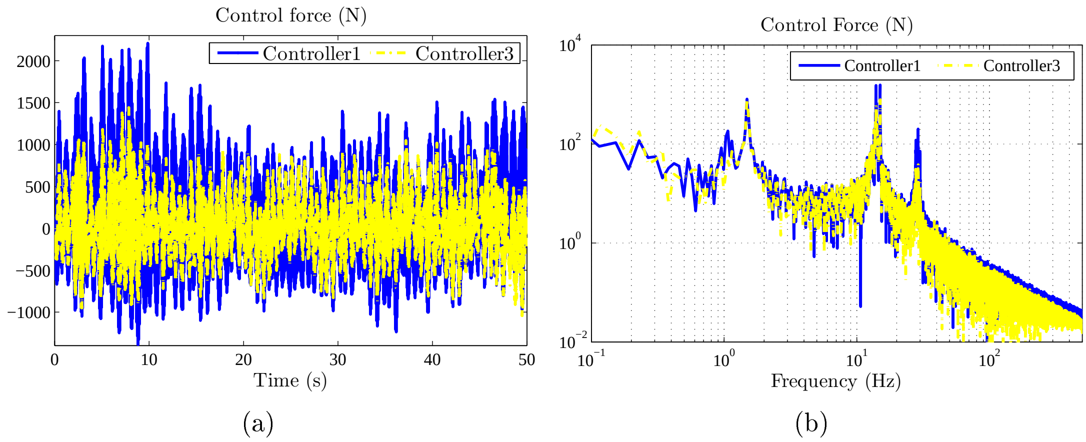

Fig. 2.10: Control force and its frequency component when subject to disturbance

of Controller3, a stronger disturbance with larger amplitude $F_d' = \sin(3\pi t) + \sin(30\pi t)$ is applied to suspension system. Fig.2.11(b) is comparison of vehicle body acceleration between Controller2 and Controller3 subject to disturbance F_d', from which it can be observed that the improvement of ride comfort over controller2 is more obvious when disturbance is stronger. The comparison results between the method proposed in Ref. [60] and Controller3 are also depicted in Fig.2.12, where the external disturbance and road input are selected as F_d' and C level, respectively. From Fig.2.12, one can observe that ride comfort at both low- and high-frequency can be simultaneously improved.

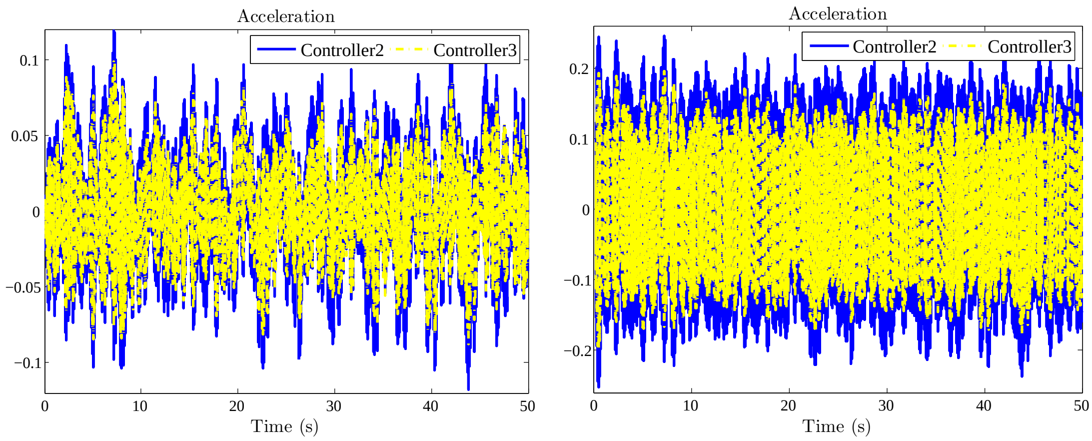

(a) (b)

Fig. 2.11: Vehicle body acceleration under different disturbance

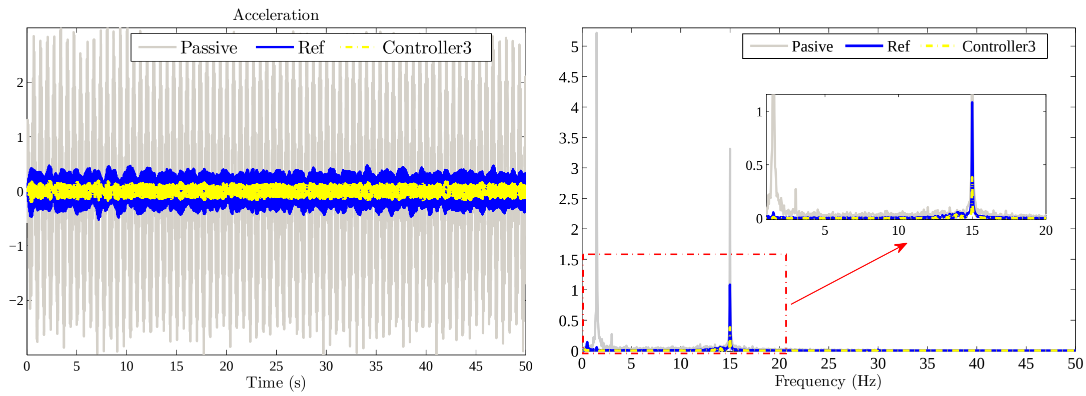

(a) (b)

Fig. 2.12: Vehicle body acceleration and its frequency component

Remark 2.6 *The bio-inspired model used in Ref. [60] was only single-layer, a more general model with multi-layer is adopted in this chapter. Moreover, in this chapter, a novel nonlinear damping is designed for the bio-inspired reference model. According to the analysis in Section 2.2, the novel nonlinear damping in the context of bio-inspired structure dynamics and more layers of bio-inspired structure can jointly contribute to the less vibration transmissibility. So Controller3 can achieve better vibration suppression performance which has been verified by the comparison results in Fig.2.11 and 2.12.*

Finally, the ability to address actuator saturation issues for different controllers is tested when vehicle forward velocity is $V_3 = 35$ km/h when subject to actuation saturation $u_{\max} = 1000$ N and 1300 N, respectively. Generally speaking, system performance will be degraded more or less in presence of actuator saturation. However, simulation results in Table 2.7, 2.8 and Fig.2.13(a), Fig.2.13(b) demonstrate that compared to standard Controller1, the bio-inspired reference model based Controller3 suffers much smaller performance degradations in terms of ride comfort and energy consumption. All simulation results verify the effectiveness of the bio-inspired reference model based control method proposed in this chapter.

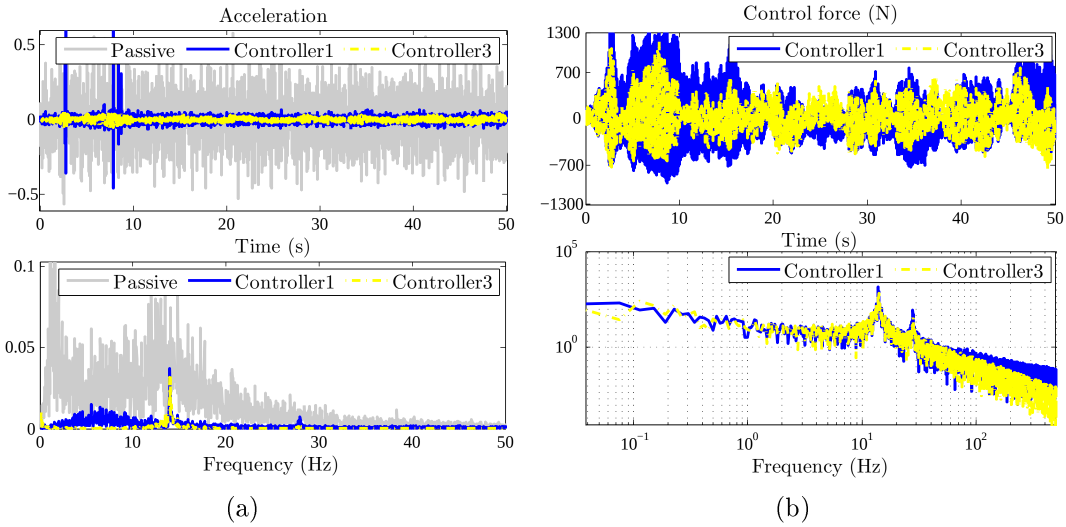

Fig. 2.13: Acceleration and control force (saturation is 1300)

Table 2.7: RMS of Energy consumption subject to actuator saturations for $V = 35$ km/h (W)

Saturation	Controller1	Controller2	Controller3
$u_{\max} = 1000$	126.9264	70.8401	80.1407
$u_{\max} = 1300$	172.0001	70.7589	79.9422

Table 2.8: RMS of suspension acceleration subject to actuator saturations for $V = 35$ km/h (m/s^2)

Saturation	Passive	Controller1	Controller2	Controller3
$u_{\max} = 1000$	0.1538	0.0694	0.0188	0.0167
$u_{\max} = 1300$	0.1538	0.0223	0.0149	0.0132

2.5 Conclusion

In the chapter, a novel bio-inspired reference model based fuzzy adaptive control method, which aims to simultaneously achieve vibration suppression and energy-saving in active suspension systems is presented. A beneficial nonlinear damping is deliberately designed to improve the overall vibration suppression performance. Then by taking full advantage of nonlinear dynamics of the bio-inspired reference model, vibration suppression and energy efficiency as well as robustness and actuator saturations issues are guaranteed. It should be emphasized that the generic bio-inspired nonlinear model with its associated nonlinear stiffness and nonlinear damping is for the first time fully employed in active tracking control as a reference model.

Chapter 3

Fuzzy sampled-data control for nonlinear systems

This chapter investigates the sampled-data control for fuzzy systems. First, extended dissipative and exponential stabilization problems for T-S fuzzy sampled-data systems is investigated in this chapter. The most important distinction between the work being undertaken and the existing literatures is that H_∞, $L_2 - L_\infty$, passive and dissipative control problems for T-S fuzzy sampled-data systems can be solved successfully under the unified framework of extended dissipative control, instead of addressing these control problems in a separate way. This can allow us to choose a suitable control strategy by adjusting the weighting matrices in the new performance index according to the practical applications or noise levels. What is more, the desired dynamic performance of closed-loop sampled-data system is guaranteed through setting an exponential decay rate in advance for arbitrary admissible sampling period.

The rest of this chapter is organized as follows. Firstly, a simple introduction of T-S fuzzy sampled-data system and the corresponding parallel distributed compensation (PDC) controller are presented. Then the unified performance index, which covers H_∞, $L_2 - L_\infty$, passive and dissipative performances as special cases is introduced. Furthermore, under variable sampling, stability conditions consisting of both exponential stability and extended dissipativity criterion for T-S fuzzy system are established through applying the Lyapunov-Krasovskii functional method together with an efficient integral inequality. It has been verified in [109] that this novel integral inequality has the potential capability of reducing conservatism.

Based on the stability conditions, a sampled-data controller that cannot only exponentially stabilize the system with an exponential decay rate but also guarantee the prescribed extended−dissipativity performance is then designed. Finally, a quarter-vehicle active suspension system with considering uncertain payload and aperiodic sampling is given for evaluating the effectiveness and advantages of the extended dissipative and exponential controller design approach proposed in this chapter over some ones of the existing literatures.

3.1 Problem formulation and preliminaries

Consider the T-S fuzzy model with r IF-THEN plant rules:

♦ Plant Rule i: IF $\theta_1(t)$ is μ_{i1} and $\theta_2(t)$ is μ_{i2} and $\cdots$ and $\theta_p(t)$ is μ_{ip}, THEN

$$\begin{cases} \dot{x}(t) = A_i x(t) + B_i u(t) + B_{wi}\omega(t) \\ z(t) = C_i x(t) + D_i u(t) + D_{wi}\omega(t) \end{cases} \tag{3.1.1}$$

where μ_{ij} is the fuzzy set, $x(t) \in \mathbb{R}^n$ represents the state vector, $z(t) \in \mathbb{R}^v$ denotes the measurement output; and $\omega(t) \in \mathbb{R}^q$ is the disturbance signal; A_i, B_i, B_{wi}, C_i, D_i, D_{wi} are known constant matrices with appropriate dimensions; $\theta_1(t), \theta_2(t), \cdots, \theta_p(t)$ are premise variables, which are functions of state variables, and r is the number of fuzzy IF-THEN rules. Denote $h_i(\theta(t)) = \vartheta_i(\theta(t))/\sum_{i=1}^{r}\vartheta_i(\theta(t))$, $\vartheta_i(\theta(t)) = \prod_{j=1}^{r}\mu_{ij}(\theta_j(t))$, where $\mu_{ij}(\theta_j(t))$ represents the grade of membership of $\theta_j(t)$ in μ_{ij}. Since $\vartheta_i(\theta(t)) \geq 0$, $i = 1, 2, \cdots, r$, then $h_i(\theta(t)) \geq 0$, $\sum_{i=1}^{r} h_i(\theta(t)) = 1$. Thus the overall fuzzy system can be obtained as follows:

$$\begin{cases} \dot{x}(t) = \sum_{i=1}^{r} h_i(\theta(t)) \left[A_i x(t) + B_i u(t) + B_{wi}\omega(t)\right] \\ z(t) = \sum_{i=1}^{r} h_i(\theta(t)) \left[C_i x(t) + D_i u(t) + D_{wi}\omega(t)\right] \end{cases} \tag{3.1.2}$$

Taking the sampled-data behavior into consideration, the state feedback signal can be transmitted to the controller only at discrete instants, which satisfy

$$0 < t_1 < \cdots < t_k < \cdots < \lim_{k\to\infty} t_k = \infty \tag{3.1.3}$$

In this chapter, we aim to design a parallel distributed compensation (PDC) technique based sampled-data controller, which takes the following form, to stabilize system (3.1.2) :

♦ Controller Rule j: IF $\theta_1(t_k)$ is μ_{j1} and $\theta_2(t_k)$ is μ_{j2} and $\cdots$ and $\theta_p(t_k)$ is μ_{jp}, THEN

$$u(t) = K_j x(t_k), t_k \leq t \leq t_{k+1}, \tag{3.1.4}$$

where K_j is the sub-controller gain, $x(t_k)$ is the sampled-data signal of state at t_k. Thus we can rewrite the fuzzy controller as :

$$u(t) = \sum\nolimits_{j=1}^{r} h_j(\theta(t_k))K_j x(t_k) \tag{3.1.5}$$

Then the closed-loop fuzzy sampled-data system is obtained as:

$$\begin{cases} \dot{x}(t) = \sum\nolimits_{i=1}^{r}\sum\nolimits_{j=1}^{r} h_i(\theta(t))h_j(\theta(t_k))\left[A_i x(t) + B_i K_j x(t_k) + B_{wi}(t)\omega(t)\right] \\ z(t) = \sum\nolimits_{i=1}^{r}\sum\nolimits_{j=1}^{r} h_i(\theta(t))h_j(\theta(t_k))\left[C_i x(t) + D_i K_j x(t_k) + D_{wi}(t)\omega(t)\right] \end{cases} \tag{3.1.6}$$

Before ending this section, the following assumption, definitions and lemmas, which will be used to develop the main results in sequel, are introduced.

Lemma 3.1 *[109] For any matrix $M \in \mathbb{R}^{n\times n}$ and $R_3 \in \mathbb{R}^{n\times n}$ satisfying $\begin{bmatrix} R_3 & M \\ \star & R_3 \end{bmatrix} \geq 0$, and given scalars $0 < \kappa < 1$ and $0 \leq h(t) < h$, then*

$$-h\int_{t-h}^{t} \dot{x}^T(s)R_3\dot{x}(s)ds \leq \upsilon^T(t)\Delta\upsilon(t)$$

where $\upsilon^T(t) = \left[x^T(t)\ x^T(t-h(t))\ x^T(t-h)\ \frac{1}{h}\int_{t-h}^{t} x^T(s)ds\right]$ and Δ is defined as

$$\Delta = \begin{bmatrix} \Delta_{11} & \kappa(R_3 - M) & \Delta_{13} & 0.5(1-\kappa)\pi^2 R_3 \\ \star & \kappa(-2R_3 + M + M^T) & \kappa(R_3 - M) & 0 \\ \star & \star & -R_3 - 0.25(1-\kappa)R_3\pi^2 & 0.5(1-\kappa)\pi^2 R_3 \\ \star & \star & \star & (\kappa-1)\pi^2 R_3 \end{bmatrix} \tag{3.1.7}$$

$\Delta_{11} = -R_3 - 0.25(1-\kappa)R_3\pi^2,\ \Delta_{13} = (1-\kappa)(1-0.25\pi^2)R_3 + \kappa M.$

Lemma 3.2 *[138] For any constant matrix $R_2 = R_2^T$, $R_4 = R_4^T$ and a scalar $h > 0$, then the following inequalities hold:*

$$-\int_{t-h}^{t} x^T(s)R_2x(s)ds \leq -\frac{1}{h}\left(\int_{t-h}^{t} x^T(s)ds\right) R_2 \left(\int_{t-h}^{t} x(s)ds\right) \tag{3.1.8}$$

$$-\int_{-h}^{0}\int_{t+\theta}^{t} \dot{x}^T(s)R_4\dot{x}(s)dsd\theta \leq -\frac{2}{h^2}\left(\int_{-h}^{0}\int_{t+\theta}^{t} \dot{x}^T(s)dsd\theta\right) R_4 \left(\int_{-h}^{0}\int_{t+\theta}^{t} \dot{x}(s)dsd\theta\right)$$
$$= -\frac{2}{h^2}\left(hx(t) - \int_{t-h}^{t} x(s)ds\right)^T R_4 \left(hx(t) - \int_{t-h}^{t} x(s)ds\right) \tag{3.1.9}$$

Assumption 3.1 *[84] For given real matrices $\Phi = \Phi^T \geq 0$, $\Psi_1 = \Psi_1^T \leq 0$, Ψ_2 and $\Psi_3 = \Psi_3^T$, assume that the following conditions are satisfied, $\forall i,\ j \in \{1,\ 2\ ,\cdots,r\}$:*

1) $\|D_{wi}\| \cdot \|\Phi\| = 0$;

2) $(\|\Psi_1\| + \|\Psi_2\|)\|\Phi\| = 0$;

3) $D_{wi}^T\Psi_1D_{wi} + D_{wi}^T\Psi_2 + \Psi_2^TD_{wi} + \Psi_3 > 0$.

Definition 3.1 *[84] System (3.1.5) is said to be extended dissipative if (3.1.10) holds for all $w(t) \in \mathcal{L}_2[0,\ \infty)$*

$$\int_{0}^{t_f} J(t)dt \geq z^T(t)\Phi z(t) + \rho, t \in [0, t_f] \tag{3.1.10}$$

where $J(t) = z^T(t)\Psi_1z(t) + 2z^T(t)\Psi_2w(t) + w^T(t)\Psi_3w(t)$, Φ, Ψ_1, Ψ_2 and Ψ_3 are known matrices satisfying Assumption 3.1, ρ is a scalar.

Remark 3.1 *The extended dissipative control performance for fuzzy sampled-data system in this chapter is more general than other control performance indices, such as H_∞, $L_2 - L_\infty$, passive and dissipative. For instance, when $(\Phi, \Psi_1, \Psi_2, \Psi_3, \rho) = (0, -I, 0, \gamma^2 I, 0)$, the control performance index (3.1.10) becomes the H_∞ control performance considered in [43, 74, 77]; when $(\Phi, \Psi_1, \Psi_2, \Psi_3, \rho) = (I, 0, 0, \gamma^2 I, 0)$, the control performance index (3.1.10) reduces to $L_2 - L_\infty$ (energy-to-peak) control* *performance in [81]; when* $(\Phi, \Psi_1, \Psi_2, \Psi_3, \rho) = (0, 0, I, \gamma I, 0)$*, and* $z(t)$*,* $w(t)$ *have the same dimension, the control performance index (3.1.10) becomes the passivity performance [82]; when* $(\Phi, \Psi_1, \Psi_2, \Psi_3, \rho) = (0, Q, S, R - \alpha I, 0)$*, the control performance index (3.1.10) reduces to the strict (Q, S, R)-dissipativity [83]; when* $(\Phi, \Psi_1, \Psi_2, \Psi_3) = (0, -\epsilon I, I, -\sigma I)$*,* $(\epsilon > 0, \sigma > 0)$ *the control performance index (3.1.10) reduces to the very-strict passivity performance index.* ρ *is not necessary to be zero in sense of the very-strict passivity. [139] shows that* ρ *should be non-positive in this case, which can also be checked in Assumption 3.1 and Definition 3.1. In fact, when* $w(t) = 0$*, (3.1.10) becomes*

$$\rho \leq \int_0^{t_f} z(t)^T \Psi_1 z(t) dt - z^T(t) \Phi z(t), t \in [0, t_f]$$

Then it is easy to get that $\rho \leq 0$ *since* $\Phi \geq 0$ *and* $\Psi_1 \leq 0$ *according to Assumption 3.1.*

Definition 3.2 *[83] Given two constant scalars* $\lambda^* > 0$ *and* $c > 0$*, if*

$$\|x(t)\| \leq ce^{-\lambda^* t} \sup_{-h \leq s \leq 0} \{\|x(s)\|, \|\dot{x}(s)\|\} \tag{3.1.11}$$

holds. Then the closed-loop fuzzy sampled-data system (3.1.6) is exponentially stable with a decay rate λ^* *when* $w(t) = 0$*.*

The problems to be addressed in this chapter are formulated as follows:

1) The closed-loop fuzzy sampled-data system (3.1.6) with $w(t) = 0$ is exponentially stable;

2) The closed-loop fuzzy sampled-data system (3.1.6) guarantees the new performance index proposed in (3.1.10) for all nonzero $w(t) \in \mathcal{L}_2[0, \infty)$.

3.2 Main results on fuzzy sampled-data control

In this section, a new exponential stability condition which can guarantee the prescribed extended dissipative performance for sampled-data fuzzy system is presented. Based on the input delay approach proposed in [71], the sampling instant t_k can be represented in the form of a special time-varying delay as follows:

$$t_k = t - (t - t_k) = t - h(t) \tag{3.2.1}$$

where $h(t) = t - t_k$, which satisfies

$$0 \leq h(t) < h_k = t_{k+1} - t_k \leq h, t_k \leq t < t_{k+1} \tag{3.2.2}$$

Substitute (3.2.1) into (3.1.6), we can rewrite the closed-loop fuzzy sampled-data system as:

$$\begin{cases} \dot{x}(t) = \sum_{i=1}^{r}\sum_{j=1}^{r} h_i(\theta(t))h_j(\theta(t_k))[A_i x(t) + B_i K_j x(t-h(t)) + B_{wi}\omega(t)] \\ z(t) = \sum_{i=1}^{r}\sum_{j=1}^{r} h_i(\theta(t))h_j(\theta(t_k))[C_i x(t) + D_i K_j x(t-h(t)) + D_{wi}\omega(t)] \end{cases} \tag{3.2.3}$$

The initial condition of $x(t)$ is given as $x(t) = \varphi(t)$ for $t \in [-h, 0]$, where $\varphi(t)$ is a differentiable function.

By now, we have transformed the asynchronous sampling fuzzy system (3.1.6) into a continuous time delay T-S fuzzy system. Thus the exponential stability of system (3.2.3) can guarantee that system (3.1.6) is exponentially stable.

First we consider the exponential stability criterions for system (3.2.4).

$$\dot{x}(t) = \sum\nolimits_{i=1}^{r}\sum\nolimits_{j=1}^{r} h_i(\theta(t))h_j(\theta(t_k))[A_i x(t) + B_i K_j x(t-h(t))] \tag{3.2.4}$$

Theorem 3.1 *Given scalars $0 < \epsilon < 1$, $0 < \kappa < 1$, $0 < \lambda$, system (3.2.4) is exponentially stable with a decay rate $\lambda^* = \lambda/2$ for any admissible sampling* *period $h > 0$ if there exist matrices $P > 0$, $Q_2 > 0$, $R_1 > 0$, $R_2 > 0$, $R_3 > 0$, $R_4 > 0$, arbitrary matrices Q_1, M such that linear matrix inequalities (LMIs) (3.2.5)–(3.2.7) hold:*

$$\begin{bmatrix} P & Q_1 \\ \star & Q_2 \end{bmatrix} > 0 \tag{3.2.5}$$

$$\begin{bmatrix} R_3 & M \\ \star & R_3 \end{bmatrix} > 0 \tag{3.2.6}$$

$$\begin{bmatrix} \Xi_{11}^{i} & \Xi_{12}^{ij} & \Xi_{13} & \Xi_{14}^{i} & A_i^T\tilde{R} \\ \star & \Xi_{22} & \Xi_{23} & \Xi_{24}^{ij} & K_j^TB_i^T\tilde{R} \\ \star & \star & \Xi_{33} & \Xi_{34} & 0 \\ \star & \star & \star & \Xi_{44} & 0 \\ \star & \star & \star & \star & -\tilde{R} \end{bmatrix} < 0 \tag{3.2.7}$$

where

$$\begin{aligned}
\Xi_{11}^{i} &= \lambda P+P^TA_i+A_i^TP+Q_1+Q_1^T+e^{\lambda h}R_1+he^{\lambda h}R_2-2R_4-R_3-0.25(1-\kappa)R_3\pi^2 \\
\Xi_{12}^{ij} &= PB_iK_j+\kappa(R_3-M), \Xi_{13} = -Q_1+(1-\kappa)(1-0.25\pi^2)R_3+\kappa M \\
\Xi_{14}^{i} &= hA_i^TQ_1+\lambda hQ_1+hQ_2+2R_4+0.5(1-\kappa)\pi^2R_3 \\
\Xi_{22} &= \kappa(M+M^T-2R_3), \Xi_{23} = \kappa(R_3-M), \tilde{R} = \frac{he^{\lambda h}-h}{\lambda}R_3+\frac{e^{\lambda h}-h\lambda-1}{\lambda^2}R_4 \\
\Xi_{24}^{ij} &= hK_j^TB_i^TQ_1\Xi_{33} = -R_1-R_3-0.25(1-\kappa)\pi^2R_3 \\
\Xi_{34} &= -hQ_2+0.5(1-\kappa)\pi^2R_3, \Xi_{44} = \lambda h^2Q_2-hR_2-2R_4-(1-\kappa)\pi^2R_3
\end{aligned}$$

Proof: Consider the following Lyapunov-Krasovskii function:

$$V(t) = V_1(t)+V_2(t)+V_3(t)+V_4(t) \tag{3.2.8}$$

where

$$\begin{aligned}
V_1(t) =& e^{\lambda t} \begin{bmatrix} x(t) \\ \int_{t-h}^{t} x(s)ds \end{bmatrix}^T \begin{bmatrix} P & Q_1 \\ Q_1^T & Q_2 \end{bmatrix} \begin{bmatrix} x(t) \\ \int_{t-h}^{t} x(s)ds \end{bmatrix} \\
V_2(t) =& \int_{t-h}^{t} e^{\lambda(s+h)} x^T(s) R_1 x(s) ds + \int_{-h}^{0} \int_{t+\theta}^{t} e^{\lambda(s+h)} x^T(s) R_2 x(s) ds d\theta \\
V_3(t) =& h \int_{-h}^{0} \int_{t+\theta}^{t} e^{\lambda(s-\theta)} \dot{x}^T(s) R_3 \dot{x}(s) ds d\theta \\
V_4(t) =& \int_{-h}^{0} \int_{v}^{0} \int_{t+\theta}^{t} e^{\lambda(s-\theta)} \dot{x}^T(s) R_4 \dot{x}(s) ds d\theta dv
\end{aligned}$$

P, Q_2, R_1, R_2, R_3 and R_4 are symmetric positive-definite matrices. It is easy to see that there exists sufficiently small scalar $\delta > 0$ such that

$$V(t) \geq \delta e^{\lambda t} \|x(t)\|^2 \tag{3.2.9}$$

The time derivative of $V(t)$ along the trajectories of system (3.2.4) can be expressed as:

$$\dot{V}(t) = \dot{V}_1(t) + \dot{V}_2(t) + \dot{V}_3(t) + \dot{V}_4(t) \tag{3.2.10}$$

where

$$\begin{aligned}
\dot{V}_1(t) =& \lambda e^{\lambda t} \begin{bmatrix} x(t) \\ \int_{t-h}^{t} x(s)ds \end{bmatrix}^T \begin{bmatrix} P & Q_1 \\ Q_1^T & Q_2 \end{bmatrix} \begin{bmatrix} x(t) \\ \int_{t-h}^{t} x(s)ds \end{bmatrix} \\
&+ 2e^{\lambda t} \begin{bmatrix} x(t) \\ \int_{t-h}^{t} x(s)ds \end{bmatrix}^T \begin{bmatrix} P & Q_1 \\ Q_1^T & Q_2 \end{bmatrix} \begin{bmatrix} \dot{x}(t) \\ x(t) - x(t-h) \end{bmatrix} \\
\dot{V}_2(t) =& e^{\lambda(t+h)} x^T(t) R_1 x(t) - e^{\lambda t} x^T(t-h) R_1 x(t-h) \\
&+ h e^{\lambda(t+h)} x^T(t) R_2 x(t) - e^{\lambda h} \int_{t-h}^{t} e^{\lambda s} x^T(s) R_2 x(s) ds \\
\dot{V}_3(t) =& \frac{h e^{\lambda h} - h}{\lambda} e^{\lambda t} \dot{x}^T(t) R_3 \dot{x}(t) - h e^{\lambda t} \int_{t-h}^{t} \dot{x}^T(s) R_3 \dot{x}(s) ds \\
\dot{V}_4(t) =& \frac{e^{\lambda h} - \lambda h - 1}{\lambda^2} e^{\lambda t} \dot{x}^T(t) R_4 \dot{x}(t) - e^{\lambda t} \int_{-h}^{0} \int_{t+\theta}^{t} \dot{x}^T(s) R_4 \dot{x}(s) ds d\theta
\end{aligned}$$

Recalling and applying Lemma 3.1 under condition (3.2.6), we have

$$-he^{\lambda t}\int_{t-h}^{t}\dot{x}^T(s)R_3\dot{x}(s)ds \leq e^{\lambda t}\upsilon^T(t)\Delta\upsilon(t) \tag{3.2.11}$$

where Δ is defined in (3.1.7).

By Lemma 3.2,we can obtain

$$-e^{\lambda h}\int_{t-h}^{t}e^{\lambda s}x^T(s)R_2x(s)ds \leq -\frac{e^{\lambda t}}{h}\left(\int_{t-h}^{t}x^T(s)ds\right)R_2\left(\int_{t-h}^{t}x(s)ds\right) \tag{3.2.12}$$

$$\begin{aligned}
&-e^{\lambda t}\int_{-h}^{0}\int_{t+\theta}^{t}\dot{x}^T(s)R_4\dot{x}(s)ds\\
&\leq -\frac{2e^{\lambda t}}{h^2}\left(\int_{-h}^{0}\int_{t+\theta}^{t}\dot{x}^T(s)ds\right)R_4\left(\int_{-h}^{0}\int_{t+\theta}^{t}\dot{x}(s)ds\right)\\
&= -\frac{2e^{\lambda t}}{h^2}\left(hx(t)-\int_{t-h}^{t}x(s)ds\right)^T R_4\left(hx(t)-\int_{t-h}^{t}x(s)ds\right)
\end{aligned} \tag{3.2.13}$$

Considering (3.2.10)-(3.2.13), we can get (3.2.14)

$$\dot{V}(t) \leq \sum_{i=1}^{r}\sum_{j=1}^{r}h_i(\theta(t))h_j(\theta(t_k))e^{\lambda t}\eta^T(t)\Xi_{ij}\eta(t) \tag{3.2.14}$$

where

$$\begin{aligned}
\eta^T(t) &= \left[x^T(t)\ x^T(t-h(t))\ x^T(t-h)\ \frac{1}{h}\int_{t-h}^{t}x^T(s)ds\right]\\
\Xi_{ij} &= \begin{bmatrix}\Xi_{11}^i & \Xi_{12}^{ij} & \Xi_{13} & \Xi_{14}^i\\ \star & \Xi_{22}^{ij} & \Xi_{23} & \Xi_{24}^{ij}\\ \star & \star & \Xi_{33} & \Xi_{34}\\ \star & \star & \star & \Xi_{44}\end{bmatrix} + \begin{bmatrix}A_i^T\\ K_j^TB_i^T\\ 0\\ 0\end{bmatrix}\tilde{R}\begin{bmatrix}A_i^T\\ K_j^TB_i^T\\ 0\\ 0\end{bmatrix}^T
\end{aligned}$$

Applying Schur Complement to (3.2.7), one can get $\Xi_{ij} < 0$, which implies that

$$\dot{V}(t) < 0 \tag{3.2.15}$$

Then there always exists a sufficiently small scalar $c > 0$, such that

$$\dot{V}(t) \leq -ce^{\lambda t}\|x(t)\|^2 < 0 \tag{3.2.16}$$

Thus

$$V(t) < V(0) \tag{3.2.17}$$

On the other hand, denote $\mathcal{Q} = \begin{bmatrix} P & Q_1 \\ \star & Q_2 \end{bmatrix} > 0$, then

$$V_1(0) \leq \lambda_{max}(\mathcal{Q}) \begin{bmatrix} x(0) \\ \int_{-h}^{0} \varphi(s)ds \end{bmatrix}^T \begin{bmatrix} x(0) \\ \int_{-h}^{0} \varphi(s)ds \end{bmatrix}$$

$\varphi(s)$ is continuous in $[-h, 0]$, then there exists a positive scalar $\delta_1 > 0$ such that $\int_{-h}^{0} \varphi(s)ds \leq \delta_1\|x(0)\|$. Then we have $V_1(0) \leq (1 + \delta_1^2)\lambda_{max}(\mathcal{Q})\|x(0)\|^2$.

$$\begin{aligned}
V(0) =& \sum\nolimits_{i=1}^{4} V_i(0) \\
\leq& (1 + \delta_1^2)\lambda_{max}\{\mathcal{Q}\}\|x(0)\|^2 + he^{\lambda h}\lambda_{max}\{R_1\} \sup_{-h\leq s\leq 0} \|x(s)\|^2 \\
&+ \frac{\lambda he^{\lambda h}+1}{\lambda^2}\lambda_{max}\{R_2\} \sup_{-h\leq s\leq 0} \|x(s)\|^2 + \frac{he^{\lambda h}}{\lambda^2}\lambda_{max}\{R_3\} \sup_{-h\leq s\leq 0} \|\dot{x}(s)\|^2 \\
&+ \frac{2e^{\lambda h}}{\lambda^3}\lambda_{max}\{R_4\} \sup_{-h\leq s\leq 0} \|\dot{x}(s)\|^2 \qquad (3.2.18) \\
\leq& a_1 \sup_{-h\leq s\leq 0} \|x(s)\|^2 + a_2 \sup_{-h\leq s\leq 0} \|\dot{x}(s)\|^2 \\
\leq& (a_1 + a_2) \left(\sup_{-h\leq s\leq 0} \{\|x(s)\|^2, \|\dot{x}(s)\|^2\} \right)
\end{aligned}$$

where

$$\begin{aligned}
a_1 &= (1 + \delta_1^2)\lambda_{max}\{\mathcal{Q}\} + he^{\lambda h}\lambda_{max}\{R_1\} + \frac{\lambda he^{\lambda h} + 1}{\lambda^2}\lambda_{max}\{R_2\} \\
a_2 &= \frac{he^{\lambda h}}{\lambda^2}\lambda_{max}\{R_3\} + \frac{2e^{\lambda h}}{\lambda^3}\lambda_{max}\{R_4\}
\end{aligned}$$

Then based on (3.2.9), (3.2.17) and (3.2.18), the following inequality holds

$$\delta e^{\lambda t}\|x(t)\|^2 \le (a_1+a_2)\left(\sup_{-h\le s\le 0}\{\|x(s)\|^2, \|\dot{x}(s)\|^2\}\right)$$

which indicates that

$$\|x(t)\| \le \sqrt{\frac{a_1+a_2}{\delta}}e^{-\frac{\lambda t}{2}}\left(\sup_{-h\le s\le 0}\{\|x(s)\|, \|\dot{x}(s)\|\}\right) \tag{3.2.19}$$

According to Definition 3.2 and (3.2.19), it is easy to tell that system (3.2.4) is exponentially stable with decay rate $\lambda^* = \lambda/2$. This completes the proof. ■

Based on Theorem 3.1, we give the following exponential extended dissipative conditions for system (3.1.6).

Theorem 3.2 *Given scalars $0<\epsilon<1$, $0<\kappa<1$, $0<\lambda$ and matrices $\Phi = \overline{\Phi}^T\overline{\Phi}$, $\Psi_1 = -\overline{\Psi}_1^T\overline{\Psi}_1$, Ψ_2, Ψ_3 satisfying Assumption 1, system (3.2.3) is extended dissipative and exponentially stable with a decay rate $\lambda^* = \lambda/2$ for any admissible sampling period $h>0$ if there exist matrices $P>0$, $Q_2>0$, $R_1>0$, $R_2>0$, $R_3>0$, $R_4>0$, arbitrary matrices Q_1, M such that LMIs (3.2.20)–(3.2.22) hold.*

$$\begin{bmatrix} P & Q_1 \\ \star & Q_2 \end{bmatrix} > 0 \tag{3.2.20}$$

$$\begin{bmatrix} R_3 & M \\ \star & R_3 \end{bmatrix} > 0 \tag{3.2.21}$$

$$\begin{bmatrix} \Xi_{11}^i & \Xi_{12}^{ij} & \Xi_{13} & \Xi_{14}^i & \Xi_{15}^i & A_i^T\tilde{R} & C_i^T\overline{\Psi}_1^T \\ \star & \Xi_{22} & \Xi_{23} & \Xi_{24} & \Xi_{25}^{ij} & K_j^TB_i^T\tilde{R} & K_j^TD_i^T\overline{\Psi}_1^T \\ \star & \star & \Xi_{33} & \Xi_{34} & 0 & 0 & 0 \\ \star & \star & \star & \Xi_{44} & \Xi_{45}^i & 0 & 0 \\ \star & \star & \star & \star & \Xi_{55}^i & B_{wi}^T\tilde{R} & D_{wi}^T\overline{\Psi}_1^T \\ \star & \star & \star & \star & \star & -\tilde{R} & 0 \\ \star & \star & \star & \star & \star & \star & -I \end{bmatrix} < 0 \tag{3.2.22}$$

$$\mathcal{G}_{ij} = \begin{bmatrix} \varepsilon P - C_i^T \Phi C_i & -C_i^T \Phi D_i K_j \\ \star & \mathcal{G}_{22}^{ij} \end{bmatrix} > 0 \tag{3.2.23}$$

where

$$\begin{aligned} \mathcal{G}_{22}^{ij} =& (1-\varepsilon)e^{-\lambda h} P - K_j^T D_i^T \Phi D_i K_j, \Xi_{15}^i = PB_{wi} - C_i^T \Psi_2 \\ \Xi_{25}^{ij} =& -K_j^T D_i^T \Psi_2, \Xi_{45}^i = hQ_1^T B_{wi}, \Xi_{55}^i = -\Psi_3 - D_{wi}^T \Psi_2 - \Psi_2 D_{wi} \end{aligned}$$

and scalar ρ in Definition 3.1 is defined as

$$\rho = -V(0) - e^{\lambda h} \|P\| \sup_{-h \le \sigma \le 0} \|\varphi(\sigma)\|^2 \tag{3.2.24}$$

Other notations are the same as defined in Theorem 3.1.

Proof: It is easy to obtain (3.2.7) by pre- and post-multiplying (3.2.22) with

$$\begin{bmatrix} I_{4n} & 0 & 0 & 0 \\ 0 & 0 & I_{2n} & 0 \end{bmatrix}$$

and its transpose. Then according to Theorem 3.1, system (3.1.6) with $w(t) = 0$ is exponentially stable.

Take the time derivative of $V(t)$ along system (3.1.6), then it follows from (3.2.10)-(3.2.13) that

$$\dot{V}(t) - e^{\lambda t} J(t) \le \sum_{i=1}^{r} \sum_{j=1}^{r} h_i(\theta(t)) h_j(\theta(t_k)) e^{\lambda t} \eta_1^T(t) \check{\Xi}_{ij} \eta_1(t) \tag{3.2.25}$$

where

$$\begin{aligned} J(t) &= z^T(t)\Psi_1 z(t) + 2z^T(t)\Psi_2 w(t) + w^T(t)\Psi_3 w(t) \\ \eta_1^T(t) &= \left[x^T(t)\; x^T(t-h(t))\; x^T(t-h)\; \frac{1}{h}\int_{t-h}^{t} x^T(s)ds\; w^T(t) \right] \end{aligned}$$

$$\breve{\Xi}_{ij} = \begin{bmatrix} \Xi_{11}^i & \Xi_{12}^{ij} & \Xi_{13} & \Xi_{14}^i & \Xi_{15}^i \\ \star & \Xi_{22} & \Xi_{23} & \Xi_{24}^{ij} & \Xi_{25}^{ij} \\ \star & \star & \Xi_{33} & \Xi_{34} & 0 \\ \star & \star & \star & \Xi_{44} & hQ_1 B_{wi} \\ \star & \star & \star & \star & \Xi_{55}^i \end{bmatrix} + \begin{bmatrix} A_i^T \\ K_j^T B_i^T \\ 0 \\ 0 \\ B_{wi}^T \end{bmatrix} \tilde{R} \begin{bmatrix} A_i^T \\ K_j^T B_i^T \\ 0 \\ 0 \\ B_{wi}^T \end{bmatrix}^T \tag{3.2.26}$$

$$+ \begin{bmatrix} C_i^T \overline{\Psi}_1^T \\ K_j^T D_i^T \overline{\Psi}_1^T \\ 0 \\ 0 \\ D_{wi}^T \overline{\Psi}_1^T \end{bmatrix} \begin{bmatrix} C_i^T \overline{\Psi}_1^T \\ K_j^T D_i^T \overline{\Psi}_1^T \\ 0 \\ 0 \\ D_{wi}^T \overline{\Psi}_1^T \end{bmatrix}^T$$

Applying Schur Complement to (3.2.22), one can obtain that $\breve{\Xi}_{ij} < 0$, which means that

$$\dot{V}(t) - e^{\lambda t} J(t) < 0 \tag{3.2.27}$$

According to Definition 1, we need to prove inequality (3.2.28) holds

$$\int_0^{t_f} J(t)dt - z^T(t)\Phi z(t) \geq \rho \tag{3.2.28}$$

When $\|\Phi\| = 0$, we need to prove

$$\int_0^{t_f} J(t)dt \geq \rho \tag{3.2.29}$$

Integrating both sides of (3.2.27) yields

$$\int_0^t e^{\lambda t} J(t)dt \geq V(t) - V(0) \tag{3.2.30}$$

From (3.2.8), we can obtain

$$V(0) + \int_0^t e^{\lambda t} J(t)dt \geq V(t) \geq e^{\lambda t} x^T(t) P x(t) \geq 0 \tag{3.2.31}$$

If $J(t) \geq 0$, then $\int_0^{t_f} J(t)dt \geq -V(0) \geq \rho$. And if $J(t) < 0$, for any $t \in [0, t_f]$, $e^{\lambda t} \geq 1$, it is easy to see that $\int_0^{t_f} J(t)dt \geq \int_0^{t_f} e^{\lambda t} J(t)dt \geq -V(0) \geq \rho$. Then we can conclude that (3.2.29) holds.

On the other hand, when $\|\Phi\| > 0$, according to Assumption 1, it is required that $\|\Psi_1\| + \|\Psi_2\| = 0$ and $\|D_{wi}\| = 0$, which implies that $\Psi_1 = 0$, $\Psi_2 = 0$ and $\Psi_3 > 0$. Thus $J(t) = w^T(t)\Psi_3 w(t) \geq 0$. Then according to (3.2.31), inequality (3.2.32) holds for any $t \in [0,\ t_f]$.

$$e^{\lambda t} x^T(t)Px(t) \leq V(0) + e^{\lambda t}\int_0^t J(t)dt \leq -e^{\lambda t}\rho + e^{\lambda t}\int_0^{t_f} J(t)dt \tag{3.2.32}$$

When $t > h(t)$, it is clear that $0 < t - h(t) < t_f$. Then we have

$$e^{\lambda(t-h)} x^T(t-h(t))Px(t-h(t)) \leq -e^{\lambda t}\rho + e^{\lambda t}\int_0^t J(t)dt \tag{3.2.33}$$

When $t < h(t)$, it is obvious that $t - h(t) < 0 < t_f$. In this circumstance, it can be verified that

$$\begin{aligned} e^{\lambda(t-h)} x^T(t-h(t))Px(t-h(t)) &\leq e^{\lambda(t-h)}\|P\| \sup_{-h\leq\sigma\leq 0}\|\varphi(\sigma)\|^2 \\ &\leq -e^{\lambda t}\rho + e^{\lambda t}\int_0^{t_f} J(t)dt \end{aligned} \tag{3.2.34}$$

This, together with (3.2.32), (3.2.33) implies that for any $t \in [0,\ t_f]$ and scalar $\varepsilon \in (0,\ 1)$, the following condition holds:

$$e^{\lambda t}\int_0^{t_f} J(t)dt - e^{\lambda t}\rho \geq e^{\lambda t}\left[(1-\epsilon)e^{-h} x^T(t-h(t))Px(t-h(t)) + \epsilon x^T(t)Px(t)\right] \tag{3.2.35}$$

Recalling (3.1.6) with $D_{wi} = 0$, we have

$$\begin{aligned} z^T(t)\Phi z(t) = &-\sum_{i=1}^{r}\sum_{j=1}^{r} h_i h_j \begin{bmatrix} x(t) \\ x(t-h(t)) \end{bmatrix}^T \mathcal{G}_{ij} \begin{bmatrix} x(t) \\ x(t-h(t)) \end{bmatrix} \\ &+ e^{-\lambda h}(1-\epsilon)x^T(t-h(t))Px(t-h(t)) + \epsilon x^T(t)Px(t) \end{aligned} \tag{3.2.36}$$

We can see that $\mathcal{G}_{ij} > 0$ from (3.2.23). Then

$$z^T(t)\Phi z(t) \leq (1-\epsilon)e^{-\lambda h}x^T(t-h(t))Px(t-h(t)) + \epsilon x^T(t)Px(t) \tag{3.2.37}$$

Then according to (3.2.35), (3.2.37), inequality (3.2.28) holds for any $t_f \geq 0$. Taking the aforementioned discussion into consideration, we can draw the conclusion that system (3.1.6) is extended dissipative.

In conclusion, system (3.1.6) is exponentially stable and can satisfy the prescribed performance index-extended dissipative. This completes the proof. ■

Remark 3.2 *Similar to [68] and [83], Theorem 3.2 is applicable to aperiodic sampled-data systems as long as the length between adjacent sampling instants does not exceed the admissible sampling period h. Theorem 3.2 provides some sufficient conditions that guarantee system (3.1.6) exponential stability and extended dissipativity. The conditions in Theorem 3.2 are expressed in the form of LMIs, which can be solved via standard software easily. By tuning the weighting matrices* Φ, Ψ_1, Ψ_2, Ψ_3 *as discussed in Remark 3.1, Theorem 3.2 can be used to check the* H_∞ *performance,* $L_2 - L_\infty$ *performance, passivity and dissipativity, respectively. Additionally, a newly developed integral inequality in Lemma 3.1, which involves less decision variables is adopted in this chapter to reduce conservatism.*

It is easy to tell that when the sub-controller gains $K_j, j = 1, \cdots, r$ are not given in advance, conditions in Theorem 3.2 are nonconvex, which makes the performance criteria cannot be directly extended to the controller design. In what follows, we aim to give a controller design method for system (3.1.2), which can guarantee system (3.1.6) is exponential extended dissipative. In the following theorem, sufficient conditions for the existence of an exponential stabilization fuzzy controller under aperiodic sampling measurements are developed based on Theorem 3.2.

Theorem 3.3 *Given scalars* $0 < \epsilon < 1$, $0 < \kappa < 1$, $\lambda > 0$ *and matrices* $\Phi = \overline{\Phi}^T\overline{\Phi}$, $\Psi_1 = -\overline{\Psi}_1^T\overline{\Psi}_1$, Ψ_2, Ψ_3 *satisfying Assumption 1, system (3.1.6) is exponentially stable with a decay rate* $\lambda^* = \lambda/2$ *and guarantees the new performance defined in Definition 3.1 for any admissible sampled-data period* $0 < h$, *if there exist symmetric positive matrices* $\overline{P}$, $\overline{Q}_2$, $\overline{R}_1$, $\overline{R}_2$, $\overline{R}_3$, $\overline{R}_4$, X, *arbitrary matrices* $\overline{Q}_1$, $\overline{M}$, Y_j, *such that LMIs (3.2.38)-(3.2.41) hold:*

$$\begin{bmatrix} \overline{P} & \overline{Q}_1 \\ \star & \overline{Q}_2 \end{bmatrix} > 0 \tag{3.2.38}$$

$$\begin{bmatrix} \overline{R}_3 & \overline{M} \\ \star & \overline{R}_3 \end{bmatrix} > 0 \tag{3.2.39}$$

$$\overline{\mathcal{G}}_{ij} = \begin{bmatrix} \varepsilon\overline{P} & 0 & X^T C_i^T \overline{\Phi}^T \\ \star & (1-\varepsilon)e^{-\lambda h}\overline{P} & Y_j D_i^T \overline{\Phi}^T \\ \star & \star & I \end{bmatrix} > 0 \tag{3.2.40}$$

$$\begin{bmatrix} \overline{\Xi}_{11}^i & \overline{\Xi}_{12}^{ij} & \overline{\Xi}_{13} & \overline{\Xi}_{14} & \overline{\Xi}_{15}^i & \overline{\Xi}_{16}^i & \overline{\Xi}_{17}^i \\ \star & \overline{\Xi}_{22} & \overline{\Xi}_{23} & 0 & \overline{\Xi}_{25}^{ij} & \overline{\Xi}_{26}^{ij} & \overline{\Xi}_{27}^{ij} \\ \star & \star & \overline{\Xi}_{33} & \overline{\Xi}_{34} & 0 & 0 & 0 \\ \star & \star & \star & \overline{\Xi}_{44} & 0 & h\overline{Q}_1^T & 0 \\ \star & \star & \star & \star & \overline{\Xi}_{55}^i & \beta_2 B_{wi}^T & D_{wi}^T \overline{\Psi}_1^T \\ \star & \star & \star & \star & \star & \overline{\Xi}_{66} & 0 \\ \star & \star & \star & \star & \star & \star & -I \end{bmatrix} < 0 \tag{3.2.41}$$

where

$\overline{\Xi}_{11}^i = \lambda\overline{P} + \beta_1(A_iL + L^TA_i^T) + \overline{Q}_1 + \overline{Q}_1^T + e^{\lambda h}(\overline{R}_1 + h\overline{R}_2) - 2\overline{R}_4 - \overline{R}_3 - 0.25(1-\kappa)\overline{R}_3\pi^2$

$\overline{\Xi}_{12}^{ij} = \beta_1 B_i Y_j + \kappa(\overline{R}_3 - \overline{M})l$, $\overline{\Xi}_{13} = (1-\kappa)(1-0.25\pi^2)\overline{R}_3 + \kappa\overline{M} - \overline{Q}_1$

$\overline{\Xi}_{14} = \lambda h\overline{Q}_1 + h\overline{Q}_2 + 2\overline{R}_4 + 0.5(1-\kappa)\pi^2\overline{R}_3$, $\overline{\Xi}_{15}^i = -\beta_1 B_{wi} - L^T C_i^T \Psi_2$,

$\overline{\Xi}_{16}^i = \overline{P} - \beta_1 L + \beta_2 L^T A_i^T$, $\overline{\Xi}_{17}^i = L^T C_i^T \overline{\Psi}_1^T$, $\overline{\Xi}_{22} = -2\kappa\overline{R}_3 + \kappa\overline{M} + \kappa\overline{M}^T$

$\overline{\Xi}_{23} = \kappa(\overline{R}_3 - \overline{M})$, $\overline{\Xi}_{25}^{ij} = -Y_j^T D_i^T \Psi_2$, $\overline{\Xi}_{26}^{ij} = \beta_2 Y_j^T B_i^T$, $\overline{\Xi}_{27}^{ij} = Y_j^T D_i^T \overline{\Psi}_1^T$

$$\overline{\Xi}_{33} = -\overline{R}_1 - \overline{R}_3 - 0.25(1-\kappa)\pi^2\overline{R}_3,\ \overline{\Xi}_{34} = -h\overline{Q}_2^T + 0.5(1-\kappa)\pi^2\overline{R}_3$$
$$\overline{\Xi}_{44} = \lambda h^2\overline{Q}_2 - h\overline{R}_2 - 2\overline{R}_4 - (1-\kappa)\pi^2\overline{R}_3,\ \overline{\Xi}_{55}^i = -\Psi_3 - D_{wi}^T\Psi_2 - \Psi_2^T D_{wi}$$
$$\overline{\Xi}_{66} = -\beta_2(L+L^T) + \overline{R},\ \overline{R} = \frac{he^{\lambda h} - h}{\lambda}\overline{R}_3 + \frac{e^{\lambda h} - h\lambda - 1}{\lambda^2}\overline{R}_4$$

Moreover, if the above LMIs have feasible solutions, the desired fuzzy sampled-data controller can be obtained with parameters given by

$$K_j = Y_j L^{-1} \tag{3.2.42}$$

Proof: Define the following new matrix variables $L = X^{-1}, P_1 = \beta_1 L, P_2 = \beta_2 L, P = L^T\overline{P}L, Q_1 = L^T\overline{Q}_1 L, Q_2 = L^T\overline{Q}_2 L, R_1 = L^T\overline{R}_1 L, R_2 = L^T\overline{R}_2 L, R_3 = L^T\overline{R}_3 L, R_4 = L^T\overline{R}_4 L, M = L^T\overline{M}L, Y_j = K_j L.$

Then $\begin{bmatrix} \overline{P} & \overline{Q}_1 \\ \star & \overline{Q}_2 \end{bmatrix} = diag\{L^T\ \ L^T\}\begin{bmatrix} P & Q_1 \\ \star & Q_2 \end{bmatrix} diag\{L\ \ L\} > 0$, $\begin{bmatrix} \overline{R}_3 & \overline{M} \\ \star & \overline{R}_3 \end{bmatrix} = diag\{L^T\ \ L^T\}\begin{bmatrix} R_3 & M \\ \star & R_3 \end{bmatrix} diag\{L\ \ L\} > 0$ which indicate that (3.2.38), (3.2.39) hold. Noting that for any appropriate dimension matrices P_1 and P_2, the following equation holds

$$\sum_{i=1}^{r}\sum_{j=1}^{r} h_i(\theta(t))h_j(\theta(t_k))2e^{\lambda t}\left[x^T(t)P_1^T + \dot{x}^T(t)P_2^T\right]$$
$$[A_i x(t) + B_i K_j x(t-h(t)) + B_{wi}w(t) - \dot{x}(t)] = 0 \tag{3.2.43}$$

Add (3.2.43) to $\dot{V}(t)$. Then we have

$$\dot{V}(t) \le \sum_{i=1}^{r}\sum_{j=1}^{r} h_i(\theta(t))h_j(\theta(t_k))\bar{\eta}_1^T(t)\hat{\Xi}_{ij}\bar{\eta}_1(t) \le c_1\|\bar{\eta}_1(t)\|^2$$

for some $c_1 > 0$ if (3.2.44) holds.

$$\hat{\Xi}_{ij} < 0 \tag{3.2.44}$$

where $\bar{\eta}_1^T(t) = \left[\eta_1^T(t)\ \dot{x}^T(t)\right]$,

$$\hat{\Xi}_{ij} = \begin{bmatrix} \hat{\Xi}_{11}^{i} & \hat{\Xi}_{12}^{ij} & \hat{\Xi}_{13} & \hat{\Xi}_{14} & \hat{\Xi}_{15}^{i} & \hat{\Xi}_{16}^{i} \\ \star & \hat{\Xi}_{22} & \hat{\Xi}_{23} & 0 & \hat{\Xi}_{25}^{ij} & \hat{\Xi}_{26}^{ij} \\ \star & \star & \hat{\Xi}_{33} & \hat{\Xi}_{34} & 0 & 0 \\ \star & \star & \star & \hat{\Xi}_{44} & 0 & hQ_1^T \\ \star & \star & \star & \star & \hat{\Xi}_{55}^{i} & B_{wi}^T P_2 \\ \star & \star & \star & \star & \star & \hat{\Xi}_{66} \end{bmatrix},$$

$\hat{\Xi}_{11}^{i} = \lambda P + [Q_1]_s + e^{\lambda h}(R_1 + hR_2) - 2R_4 - R_3 - 0.25(1-\kappa)R_3\pi^2 + P_1^T A_i + A_i^T P_1 - C_i^T \Psi_1 C_i$

$\hat{\Xi}_{12}^{ij} = P_1^T B_i K_j + \kappa(R_3 - M) - C_i^T \Psi_1 D_i K_j,\ \hat{\Xi}_{13} = -Q_1 + (1-\kappa)(1-0.25\pi^2)R_3 + \kappa M$

$\hat{\Xi}_{14} = \lambda h Q_1 + hQ_2^T + 2R_4 + 0.5(1-\kappa)\pi^2 R_3,\ \hat{\Xi}_{22} = \kappa(M + M^T - 2R_3) - K_j^T D_i^T \Psi_1 D_i K_j$

$\hat{\Xi}_{23} = \kappa(R_3 - M),\ \hat{\Xi}_{33} = -R_1 - R_3 - 0.25(1-\kappa)\pi^2 R_3$

$\hat{\Xi}_{34} = -hQ_2^T + 0.5(1-\kappa)\pi^2 R_3,\ \hat{\Xi}_{44} = \lambda h^2 Q_2 - hR_2 - 2R_4 - (1-\kappa)\pi^2 R_3$

$\hat{\Xi}_{16}^{i} = P - P_1^T + A_i^T P_2,\ \hat{\Xi}_{15}^{i} = P_1^T B_{wi} - C_i^T \Psi_2 - C_i^T \Psi_1 D_{wi}$

$\hat{\Xi}_{26}^{ij} = K_j^T B_i^T P_2,\ \hat{\Xi}_{25}^{ij} = -K_j^T D_i^T \Psi_2 - -K_j^T D_i^T \Psi_1 D_{wi}$

$\hat{\Xi}_{55}^{i} = -\Psi_3 - D_{wi}^T \Psi_2 - \Psi_2^T D_{wi} - D_{wi}^T \Psi_1 D_{wi},\ \hat{\Xi}_{66} = \tilde{R} - P_2^T - P_2$

By applying Schur Complement to (3.2.44) under condition $\Psi_1 = -\overline{\Psi}_1^T \overline{\Psi}_1$ and pre- and post- multiplying the transformed inequation by $diag\{L^T\ L^T\ L^T\ L^T\ I\ L^T\ I\}$ and its transpose respectively, (3.2.41) can be obtained. Perform congruence transformation to (3.2.23) with $diag\{L^T,\ L^T\}$ and its transpose gives the condition in (3.2.45).

$$\begin{bmatrix} \varepsilon\overline{P} - C_i^T \Phi C_i & -C_i^T \Phi D_i K_j \\ \star & (1-\varepsilon)e^{-\lambda h} P - K_j^T D_i^T \Phi D_i K_j \end{bmatrix} > 0 \tag{3.2.45}$$

Apply Schur Complement to (3.2.45) with the condition $\Phi = \overline{\Phi}^T \overline{\Phi}$ one can easily obtain (3.2.40).

Therefore, according to Theorem 3.2, the designed sampled-data fuzzy controller can exponentially stabilize system (3.1.6) and guarantee the prescribed extended dissipative performance. This completes the proof. ■

Remark 3.3 *Theorem 3.3 provides an approach to design a sampled-data fuzzy controller so as to guarantee that system (3.1.6) is exponential extended dissipative. Besides, we can design the controllers by setting appropriate λ in advance to achieve better performance. Moreover, the performance scalar γ is included as a optimization parameter in the MI conditions in Theorem 3.3, which means that we can optimize the attenuation level γ if the following convex optimization problem has feasible solution:*

$$\textit{Minimize } \gamma \textit{ subject to (3.2.38)-(3.2.41)}$$

3.3 Application to uncertain suspension system

Here, an example of quarter-vehicle active suspension system with considering uncertain payload and aperiodic sampling is considered. This example is provided to evaluate the validity and superiority of the extended dissipative and exponential controller design approach proposed in this chapter over some ones of the existing literatures. Comparison results are mainly conducted from the aspects of disturbance attenuation level and closed-loop system dynamic performance.

Example 1: Consider the two-degree-of-freedom quarter vehicle model which is shown in Fig.3.1 borrowed from [77]. The dynamic equation of the active suspension model is built as follows

$$\begin{aligned} m_u(t)\ddot{z}_u(t)+c_s\left[\dot{z}_u(t)-\dot{z}_s(t)\right]+k_s\left[z_u(t)-z_s(t)\right] \\ +k_t\left[z_u(t)-z_r(t)\right]+c_t\left[\dot{z}_u(t)-\dot{z}_r(t)\right]=-u(t) \\ m_s(t)\ddot{z}_s(t)+c_s\left[\dot{z}_s(t)-\dot{z}_u(t)\right]+k_s\left[z_s(t)-z_u(t)\right]=u(t) \end{aligned} \tag{3.3.1}$$

where

z_s : sprung massed displacement;

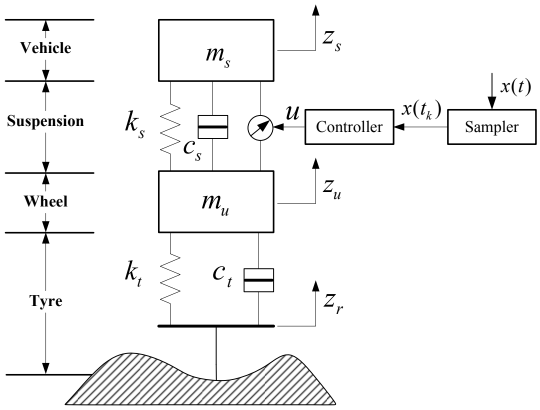

Fig. 3.1: Quarter vehicle model

z_u : unsprung massed displacement;

z_r : road displacement input;

c_s : damping coefficient of the suspension system;

k_s : stiffness coefficient of the suspension system;

k_t : compressibility coefficient of the pneumatic tire;

c_t : damping coefficient of the pneumatic tire;

m_s : sprung mass which represents the car chassis;

m_u : unsprung mass of the wheel assembly;

$u(t)$: active input of the suspension system;

As a result of the payload change, vehicle mass cannot remain constant. Thus, the quarter vehicle model is an uncertain system that contains uncertain parameters $m_s(t)$ and $m_u(t)$. The uncertain parameter is supposed to vary in a given range, which indicates that $m_s(t) \in [m_{s\min},\ m_{s\max}]$ and $m_u(t) \in [m_{u\min},\ m_{u\max}]$.

Consider the following performance constraints:

1. The suspension deflection is no larger than a maximum value constrained

by mechanical structure.

$$\|z_s(t) - z_u(t)\| \leq z_{\max} \tag{3.3.2}$$

2. The dynamic tire load should not exceed the static tire load to guarantee that the wheels contact the road uninterruptedly.

$$k_t(z_u(t) - z_r(t)) < (m_s(t) + m_u(t))g \tag{3.3.3}$$

The following controlled outputs are defined to achieve the aforementioned performance constraints

$$\begin{aligned} z_1(t) &= \ddot{z}_s(t), \\ z_2(t) &= \begin{bmatrix} \dfrac{z_s(t) - z_u(t)}{z_{\max}} & \dfrac{k_t(z_u(t) - z_r(t))}{(m_s(t) + m_u(t))g} \end{bmatrix}^T \end{aligned}$$

Define $x_1(t) = z_s(t) - z_u(t)$, which represents the suspension deflection, $x_2(t) = z_u(t) - z_r(t)$, which denotes the tire deflection, $x_3(t) = \dot{z}_s(t)$, which is the sprung mass speed, $x_4(t) = \dot{z}_u(t)$, which is the unsprung mass speed, and $\omega(t) = \dot{z}_r(t)$, which is the disturbance input. Then system dynamical equation (3.3.1) is rewritten in the state space form:

$$\begin{cases} \dot{x}(t) = A(t)x(t) + B(t)u(t) + B_w(t)\omega(t) \\ z_1(t) = C_1(t)x(t) + D_1(t)u(t) \\ z_2(t) = C_2(t)x(t) \end{cases} \tag{3.3.4}$$

where

$$A(t) = \begin{bmatrix} 0 & 0 & 1 & -1 \\ 0 & 0 & 0 & 1 \\ -\frac{k_s}{m_s(t)} & 0 & -\frac{c_s}{m_s(t)} & \frac{c_s}{m_s(t)} \\ \frac{k_s}{m_u(t)} & -\frac{k_t}{m_u(t)} & \frac{c_s}{m_u(t)} & -\frac{c_s+c_t}{m_u(t)} \end{bmatrix}$$

$$B(t) = \begin{bmatrix} 0 \\ 0 \\ \frac{1}{m_s(t)} \\ -\frac{1}{m_u(t)} \end{bmatrix}, B_w(t) = \begin{bmatrix} 0 \\ -1 \\ 0 \\ \frac{c_t}{m_u(t)} \end{bmatrix}$$

$$C_1(t) = \begin{bmatrix} -\frac{k_s}{m_s(t)} & 0 & -\frac{c_s}{m_s(t)} & \frac{c_s}{m_s(t)} \end{bmatrix}, D_1(t) = \frac{1}{m_s(t)}$$

$$C_2(t) = \begin{bmatrix} \frac{1}{z_{\max}} & 0 & 0 & 0 \\ 0 & \frac{k_t}{(m_s(t)+m_u(t))g} & 0 & 0 \end{bmatrix}$$

Similar to [140] and [77], the T-S fuzzy model of the quarter vehicle system can be derived as follows: define $\xi_1(t) = \frac{1}{m_s(t)}, \xi_2(t) = \frac{1}{m_u(t)}$. Since $m_s(t)$ and $m_u(t)$ are bounded, then we have

$$\hat{m}_s \triangleq \max \xi_1(t) = \frac{1}{m_{s\min}}, \ \check{m}_s \triangleq \min \xi_1(t) = \frac{1}{m_{s\max}}$$
$$\hat{m}_u \triangleq \max \xi_2(t) = \frac{1}{m_{u\min}}, \ \check{m}_u \triangleq \min \xi_2(t) = \frac{1}{m_{u\max}}$$

By employing the sector nonlinear method, premise variables $\xi_1(t)$ and $\xi_2(t)$ can be represented by $\xi_1(t) = M_1(\xi_1(t))\hat{m}_s + M_2(\xi_1(t))\check{m}_s, \xi_2(t) = N_1(\xi_2(t))\hat{m}_u + N_2(\xi_2(t))\check{m}_u$ where

$$M_1(\xi_1(t)) + M_2(\xi_1(t)) = 1, N_1(\xi_2(t)) + N_2(\xi_2(t)) = 1$$

The membership functions $M_1(\xi_1(t))$, $M_2(\xi_1(t))$, $N_1(\xi_2(t))$, $N_2(\xi_2(t))$ can be calculated as follows

$$M_1(\xi_1(t)) = \frac{\frac{1}{m_s(t)} - \check{m}_s}{\hat{m}_s - \check{m}_s}, \quad M_2(\xi_1(t)) = \frac{\hat{m}_s - \frac{1}{m_s(t)}}{\hat{m}_s - \check{m}_s}$$
$$N_1(\xi_2(t)) = \frac{\frac{1}{m_u(t)} - \check{m}_u}{\hat{m}_u - \check{m}_u}, \quad N_2(\xi_2(t)) = \frac{\hat{m}_u - \frac{1}{m_u(t)}}{\hat{m}_u - \check{m}_u}$$

These membership functions are named as "**Heavy**" ($M_1(\xi_1(t))$), "**Light**" ($M_2(\xi_1(t))$), "**Heavy**" ($N_1(\xi_2(t))$) and "**Light**" ($N_1(\xi_2(t))$), respectively. Following the similar line in [77], we can obtain the T-S fuzzy model of the active suspension system:

Model Rule 1: IF $\xi_1(t)$ is Light and $\xi_2(t)$ is Light, Then

$$\begin{aligned}\dot{x}(t) &= A_1x(t) + B_1u(t) + B_{w1}\omega(t)\\ z_1(t) &= C_{11}x(t) + D_{11}u(t)\\ z_2(t) &= C_{21}x(t)\end{aligned}$$

Replace $\frac{1}{m_s(t)}$ and $\frac{1}{m_u(t)}$ with $\hat{m}_s$ and $\hat{m}_u$ in matrices $A(t)$, $B(t)$, $B_w(t)$, $C_1(t)$, $D_1(t)$, $C_2(t)$, we can obtain matrices A_1, B_1, B_{w1}, C_{11}, D_{11}, C_{21}.

Model Rule 2: IF $\xi_1(t)$ is Heavy and $\xi_2(t)$ is Heavy, Then

$$\begin{aligned}\dot{x}(t) &= A_2x(t) + B_2u(t) + B_{w2}\omega(t)\\ z_1(t) &= C_{12}x(t) + D_{12}u(t)\\ z_2(t) &= C_{22}x(t)\end{aligned}$$

Replace $\frac{1}{m_s(t)}$ and $\frac{1}{m_u(t)}$ with $\check{m}_s$ and $\check{m}_u$ in matrices $A(t)$, $B(t)$, $B_w(t)$, $C_1(t)$, $D_1(t)$, $C_2(t)$, we can obtain matrices A_2, B_2, B_{w2}, C_{12}, D_{12}, C_{22}.

Model Rule 3: IF $\xi_1(t)$ is Light and $\xi_2(t)$ is Heavy, Then

$$\begin{aligned}\dot{x}(t) &= A_3x(t) + B_3u(t) + B_{w3}\omega(t)\\ z_1(t) &= C_{13}x(t) + D_{13}u(t)\\ z_2(t) &= C_{23}x(t)\end{aligned}$$

Replace $\frac{1}{m_s(t)}$ and $\frac{1}{m_u(t)}$ with $\hat{m}_s$ and $\check{m}_u$ in matrices $A(t)$, $B(t)$, $B_w(t)$, $C_1(t)$, $D_1(t)$, $C_2(t)$, we can obtain matrices A_3, B_3, B_{w3}, C_{13}, D_{13}, C_{23}.

Model Rule 4: IF $\xi_1(t)$ is Heavy and $\xi_2(t)$ is Light, Then

$$\begin{aligned}\dot{x}(t) &= A_4x(t) + B_4u(t) + B_{w4}\omega(t)\\ z_1(t) &= C_{14}x(t) + D_{14}u(t)\end{aligned}$$

$$z_2(t) = C_{24}x(t)$$

Replace $\frac{1}{m_s(t)}$ and $\frac{1}{m_u(t)}$ with $\check{m}_s$ and $\hat{m}_u$ in matrices $A(t)$, $B(t)$, $B_w(t)$, $C_1(t)$, $D_1(t)$, $C_2(t)$, we can obtain matrices A_4, B_4, B_{w4}, C_{14}, D_{14}, C_{24}.

By fuzzy blending, we can obtain the following overall fuzzy model

$$\begin{cases} \dot{x}(t) = \sum_{i=1}^{r} h_i(\xi(t)) \left[A_i x(t) + B_i u(t) + B_{wi}\omega(t)\right] \\ z_1(t) = \sum_{i=1}^{r} h_i(\xi(t)) \left[C_{1i}x(t) + D_{1i}u(t)\right] \\ z_2(t) = \sum_{i=1}^{r} h_i(\xi(t)) C_{2i}x(t) \end{cases} \tag{3.3.5}$$

where $\xi(t) = \{\xi_1(t), \xi_2(t)\}$,

$$h_1(\xi(t)) = M_1(\xi_1(t)) \times N_1(\xi_2(t)), h_2(\xi(t)) = M_2(\xi_1(t)) \times N_2(\xi_2(t)),$$
$$h_3(\xi(t)) = M_1(\xi_1(t)) \times N_2(\xi_2(t)), h_4(\xi(t)) = M_2(\xi_1(t)) \times N_1(\xi_2(t)),$$

The membership functions $h_i(\xi(t))$, $i = 1, 2, \cdots, r$, represent the degree of uncertain parameter $m_s(t)$ and $m_u(t)$ in the fuzzy set $\{Heavy,\ Light\}$, i.e., how heavy or how light the unsprung and sprung mass are at current moment.

Remark 3.4 *In general there are two approaches for constructing fuzzy models: 1). Identification (fuzzy modeling) using input-output data; 2). Derivation from given nonlinear system equations.*
The identification approach to fuzzy modeling is suitable for plants that are unable or too difficult to be represented by analytical and/or physical models. On the other hand, nonlinear dynamic models for mechanical systems can be readily obtained by, for example, the Lagrange method and the Newton-Euler method. In such cases, the second approach, which derives a fuzzy model from given nonlinear dynamical models, is more appropriate. There are two ways to convert a given nonlinear dynamical system into a fuzzy model: sector nonlinearity and local approximation

in fuzzy partition spaces. The fuzzy model builded by sector nonlinearity method exactly represents the original nonlinear system in given conditions. However, the latter is just an approximation fuzzy model, which can reduce the number of fuzzy model rules. In this chapter, the sector nonlinear method is adopted to construct the uncertain active suspension system by T-S fuzzy model. More detailed information on fuzzy modeling can be referenced to [88].

Based on the above T-S fuzzy model of uncertain active suspension system, we aim at designing a sampled-data PDC fuzzy controller in the form of (3.1.5). By employing the input delay approach, closed-loop T-S fuzzy sampled-data system can be easily rewritten as the form of (3.2.3).

To satisfy the performance constraints (3.3.2) and (3.3.3), the following condition should be taken into consideration [77]:

$$\begin{bmatrix} -\overline{P} & \sqrt{\rho}\overline{P}\{C_{2i}\}_q^T \\ \star & -I \end{bmatrix} < 0, q = 1, 2 \tag{3.3.6}$$

where $\{C_{2i}\}_q^T$ denotes the q_{th} row vector of C_{2i}^T.

The corresponding quarter-vehicle model parameters are given in Table 3.1.

Table 3.1: Parameters for Quarter-vehicle Model

k_s	k_t	c_s	c_t
$42720N/m$	$101115N/m$	$1095Ns/m$	$14.6Ns/m$

The sprung mass $m_s(t) \in [950kg,\ 996kg]$, and the unsprung mass $m_u(t) \in [110kg,\ 118kg]$. The maximum allowable suspension stroke is set as $z_{\max} = 0.1\,\mathrm{m}$ with $\rho = 1$. To compare with the recently developed fuzzy H_∞ sampled-data control method, only the H_∞ sampled-data controller design is considered in this chapter. We consider different h to find the minimum index γ. In Theorem 3.3, let $\lambda^\star = 0.1(i.e.\lambda = 0.2)$, $\rho_1 = 0.9$, $\rho_2 = 0.4$, $\varepsilon = 0.5$, $\kappa = 0.99$, $\Phi = 0$, $\Psi_1 = -1$,

Table 3.2: Comparison of Minimum Disturbance Attenuation Index γ Obtained by [77] and Theorem 3.3

h	1ms	5ms	10ms	20ms	30ms
[77]	21.65	21.98	22.43	23.40	24.51
Theorem 3.3	10.58	11	11.66	14.25	21.84

$\Psi_2 = 0$, $\Psi_3 = \gamma^2$, for several values of h, the obtained minimum H_∞ disturbance attenuation performance indices γ_{min} are listed in Table 3.2.

It is worth noting that the guaranteed performance index $\gamma_{\min}$ obtained by the convex optimization problem formulated in Theorem 3.3 has much to do with the sampling period. The guaranteed performance index $\gamma_{\min}$ under different sampling periods derived from Theorem 3.3 are listed in Table 3.2, from which we can see that $\gamma_{\min}$ is larger as the sampling periods increases. Moreover, it can be clearly seen from Table 3.2 that the minimum H_∞ disturbance attenuation levels γ_{min} obtained by our approach are smaller than those obtained in [77]. Fig.3.2 shows control inputs with different sampling period h.

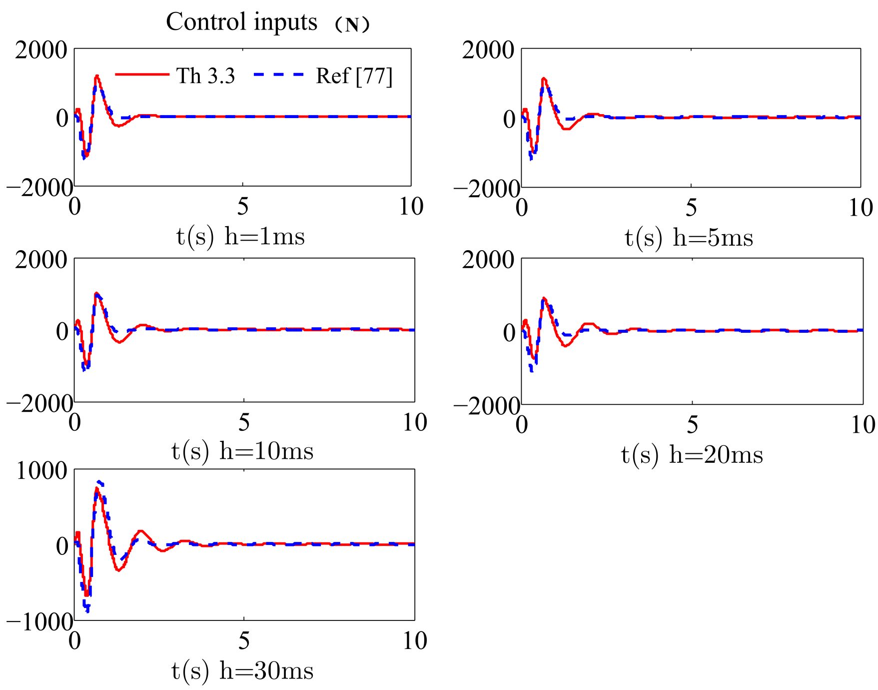

Fig. 3.2: Control inputs under different sampling period h

Remark 3.5 *In [77],* $2+r$ *matrices variables are involved, and the number of LMIs is* $(r^2+r+4)/2$ *(where* r *is the number of fuzzy if-then rules), the largest dimension of LMIs is* $3n+m+v$*, where* m *is the dimension of control input and* v *is the dimension of measurement output. While Theorem 3 contains* $9+r$ *matrices variables,* r^2+r+7 *LMIs and the largest dimension of LMIs is* $5n+m+v$*. And the computational time of our method is 2.6404s(when* $h = 30ms, \lambda^* = 0.1$*. All simulations were performed using SeDuMi [141] and YALMIP [142] with MATLAB 2013b on an Athlon (3.20 GHz), 4 GB RAM , running Windows 7.), which is tolerable and acceptable. On the other hand, in [77]only the* H_∞ *control problem is investigated for the uncertain suspension system. However, in this chapter, the* H_∞*,* L_2-L_∞*, passive and dissipative control problems for T-S fuzzy sampled-data systems can be solved successfully under the unified framework of extended dissipative control, instead of addressing these control problems in a separate way, which is a most important distinction between the work being undertaken and the existing literatures [74, 75, 77–80, 82, 83]. This can allow us to choose a suitable control strategy by adjusting the weighting matrices in the new performance index according to the practical applications or noise levels. What is more, the desired dynamic performance of closed-loop sampled-data system is guaranteed through setting an exponential decay rate in advance for arbitrary admissible sampling period. In addition,a new integral inequality in* ***3.1*** *is adopted instead of Jensen's inequality in this chapter to derive LMI based conditions, which is conductive to less conservative results.*

To further verify the effectiveness of the controller design method proposed in this chapter, consider the case of an isolated bump on a smooth road surface [43, 77]. Road displacement $z_r(t)$ is defined as follows

$$z_r(t) = \begin{cases} \frac{A}{2}(1-\cos(\frac{2\pi V}{L}t)), & 0 \le t \le \frac{L}{V} \\ 0, & t > \frac{L}{V} \end{cases} \tag{3.3.7}$$

where the height and length of the bump are $A = 50$mm and $L = 6$m and

$V = 35(\mathrm{km/h})$. The designed state-feedback fuzzy sampled-data controller in the form of (3.1.5) is expected to meet the following requirements: 1) minimize the sprung mass acceleration $z_1(t)$; 2) the suspension deflection is no larger than the upper bound of suspension stroke $z_{\max} = 0.1\mathrm{m}$, which is equivalent to $z_2(t)_1 < 1$; 3) the dynamic tire load , i.e., $z_2(t)_2$ is less than 1.

State-feedback fuzzy sampled-data controller gains under different decay rates λ^* are given in Table 3.3.

Table 3.3: Controller feedback gains for $h = 10ms$ and different values of decay rate λ^*

λ^*	The Controller Gains
$\lambda^* = 0.05$	$K_1 = 10^4 \times [1.9594\ 0.8610\ \ -0.2692\ 0.3360]$
	$K_2 = 10^4 \times [1.9399\ 1.1792\ \ -0.2972\ 0.3577]$
	$K_3 = 10^4 \times [1.9402\ 1.1758\ \ -0.2961\ 0.3566]$
	$K_4 = 10^4 \times [1.9384\ 0.8140\ \ -0.2755\ 0.3317]$
$\lambda^* = 0.25$	$K_1 = 10^4 \times [2.0069\ 1.0657\ \ -0.2780\ 0.3228]$
	$K_2 = 10^4 \times [2.0130\ 1.4524\ \ -0.3011\ 0.3494]$
	$K_3 = 10^4 \times [2.0134\ 1.4481\ \ -0.3000\ 0.3484]$
	$K_4 = 10^4 \times [2.0070\ 1.0694\ \ -0.2790\ 0.3238]$
$\lambda^* = 0.50$	$K_1 = 10^4 \times [2.0789\ 1.2658\ \ -0.2764\ 0.2935]$
	$K_2 = 10^4 \times [2.0915\ 1.6658\ \ -0.2991\ 0.3180]$
	$K_3 = 10^4 \times [2.0914\ 1.6629\ \ -0.2982\ 0.3173]$
	$K_4 = 10^4 \times [2.0793\ 1.2694\ \ -0.2772\ 0.2943]$
$\lambda^* = 0.75$	$K_1 = 10^4 \times [2.1256\ 1.0969\ \ -0.2434\ 0.2480]$
	$K_2 = 10^4 \times [2.1429\ 1.4748\ \ -0.2636\ 0.2690]$
	$K_3 = 10^4 \times [2.1419\ 1.4724\ \ -0.2630\ 0.2683]$
	$K_4 = 10^4 \times [2.1266\ 1.0995\ \ -0.2441\ 0.2487]$

Fig.3.3-Fig.3.5 depict the responses of the open-loop system ($u(t) = 0$, passive mode) and the sampled-data closed-loop system, which is composed by the controller we designed in previous section. These figures show the bump responses of body accelerations, suspension deflection, and tire deflection of the active suspension system under different decay rates λ^*, when the maximum sampling interval is chosen as $h = 10$ ms. From Fig.3.3, one can observe that the body acceleration of the closed loop system is much less than that of the open loop system, thus the designed fuzzy sampled-data controller improves the ride comfort. Moreover,

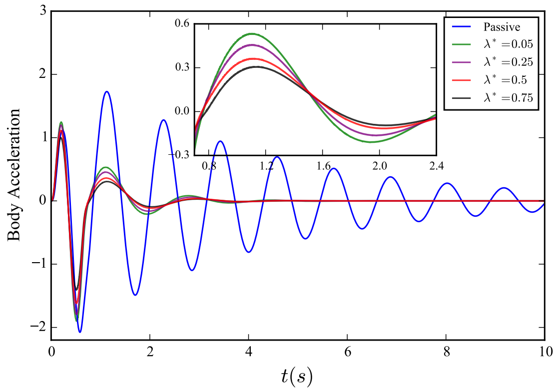

Fig. 3.3: Body acceleration of the open and closed-loop active suspension systems with different decay rate λ^* (h=10 ms)

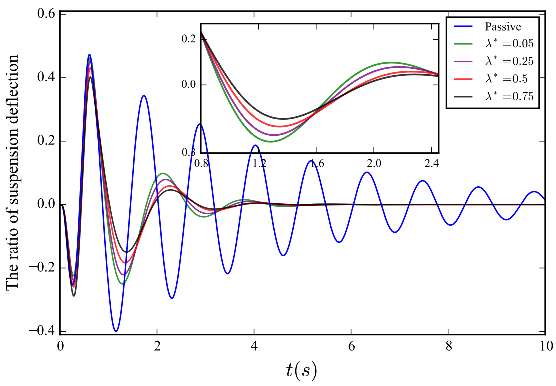

Fig. 3.4: Suspension deflection of the open and closed-loop active suspension systems with different decay rate λ^* (h=10 ms)

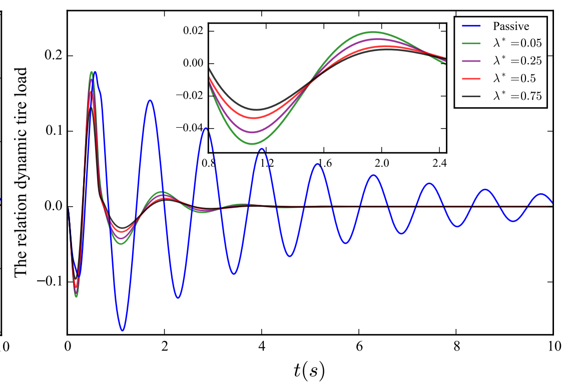

Fig. 3.5: Tire deflection of the open and closed-loop active suspension systems with different decay rate λ^* (h=10 ms)

it can be seen from Fig.3.4 and Fig.3.5 that the suspension deflection constraint, which is equivalent to $x_1(t)/z_{\max} < 1$ and the dynamic tire load constraint i.e. $k_t x_2(t)/(m_s(t) + m_u(t))g < 1$ are satisfied, which implies that the designed controller guarantees the road holding capability. In a word, Fig.3.3-Fig.3.5 validate that better ride comfort, road holding capability can be achieved and constraint suspension deflection can be guaranteed for the active suspension system with the designed sampled-data controller. In addition, one can easily see that better performance can be achieved when the decay rate λ^* is sufficiently bigger.

Fig.3.6-Fig.3.8 depict the responses of body accelerations, constrained suspension

deflection, and constrained tire deflection of the active suspension system under different sampling periods h when decay rate $\lambda^* = 0.5$. We can see that the smaller sampling period h is, the better body acceleration, suspension deflection and tire deflection performance can be achieved, which in turn verifies the results in Table 3.2.

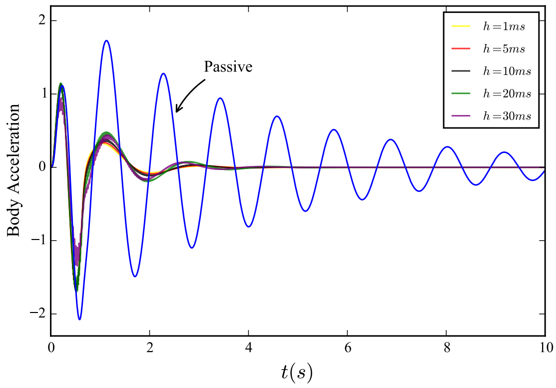

Fig. 3.6: Body acceleration under different sampling period h

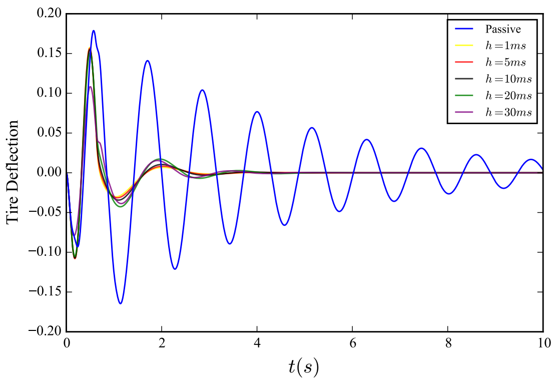

Fig. 3.7: Tire Deflection under different sampling period h

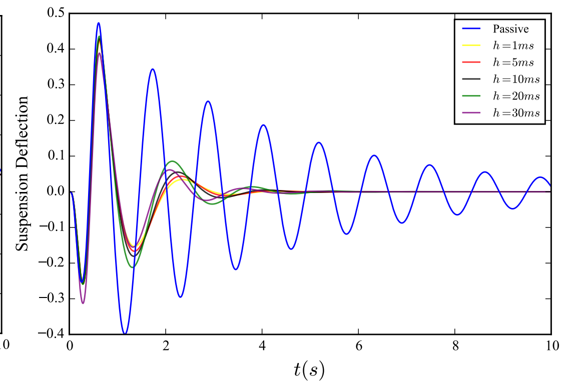

Fig. 3.8: Suspension Deflection under different sampling period h

3.4 Conclusion

This chapter has addressed the exponential stability analysis and stabilization problems for T-S fuzzy systems under aperiodic sampling. Some classical problems (such as H_∞, $L_2 - L_\infty$, passive and dissipative stability and stabilization problems) have been solved successfully under a unified framework by resorting to a novel performance index−extended dissipative performance index. Through adopting a sampling period dependent Lyapunov-Krasovskii function together with a novel efficient integral inequality, which has the advantages of reducing conservativeness, new stability conditions consisting of both exponential stability and extended dissipativity criterion have been established. Furthermore, a sampled-data controller that cannot only exponentially stabilize the system but also guarantee the prescribed extended-dissipativity performance has been designed. A quarter-vehicle active suspension system with taking into account the uncertain payload and aperiodic sampling has been provided for evaluating the validity and superiority (from the aspects of disturbance attenuation level and closed-loop system dynamic performance) of the extended dissipative control approach proposed in this thesis over some ones of the existing literatures.

Chapter 4

Imperfect premise matching fuzzy filtering of nonlinear system with time-varying delays

Fuzzy sampled-data controller designed in the previous chapter shares the same fuzzy membership functions with fuzzy model. Compared with fuzzy controller or filter with matched premise variables, controller and filter designed under imperfect premise matching can enhance design flexibility and robustness. So imperfect premise matching fuzzy filtering problem for nonlinear systems with time-varying delay is considered in this chapter. Firstly, T-S fuzzy time-varying delay model and fuzzy filter with imperfect premise variables are established. Then the unified performance index, which covers H_∞, $L_2 - L_\infty$, passive and dissipative performance as special cases, is introduced. Furthermore, new extended dissipative filter design approach based on the above unified performance for the considered fuzzy time delay system is developed through employing the Lyapunov stability theory together with an efficient integral inequality. As a result, the extended dissipative filter can be designed in terms of solutions to a set of convex optimization problems. Finally, two examples are provided to verify the effectiveness and advantages of the extended dissipative filter design approach based on the unified performance index proposed in this chapter.

The rest of this chapter is organized as follows: the problem to be analyzed and the unified performance index are presented in Section 4.1. Main results, including filter performance criterion and filter design approach are given in Section 4.2. Numerical examples are shown in Section 4.3 to demonstrate the effectiveness and advantages of the proposed method. Conclusion is drawn in Section 4.4.

4.1 Problem formulation and preliminaries

Consider the following time-delay T-S fuzzy model with r plant rules:

◆ Plant Rule i: IF $\theta_1(t)$ is M_{i1} and $\theta_2(t)$ is M_{i2} and $\cdots$ and $\theta_p(t)$ is M_{ip}, THEN

$$\begin{cases} \dot{x}(t) = A_{1i}x(t) + A_{2i}x(t-\tau(t)) + D_{1i}\omega(t) \\ z(t) = C_{1i}x(t) + C_{2i}x(t-\tau(t)) + D_{2i}\omega(t) \\ y(t) = E_{1i}x(t) + E_{2i}x(t-\tau(t)) + D_{3i}\omega(t) \\ x(t) = \phi(t), t \in [-\bar{\tau}, 0], \end{cases} \tag{4.1.1}$$

where $\theta_j(t)$ and M_{ij} ($i = 1, \cdots, r, j = 1, \cdots, p$) are the premise variables (which are measurable) and the fuzzy sets respectively, r is the number of fuzzy IF-THEN rules, p is a positive integer. $x(t) \in \mathbb{R}^n$ is the state vector and $\omega(t) \in \mathbb{R}^q$ is the disturbance input; $z(t) \in \mathbb{R}^v$ is the signal to be estimated; $y(t) \in \mathbb{R}^m$ is the measured output; A_{1i}, A_{2i}, D_{1i}, C_{1i}, C_{2i}, D_{2i}, E_{1i}, E_{2i} and D_{3i} are known constant matrices of compatible dimensions; $\tau(t)$ is time-varying delay, which satisfies $0 < \tau(t) \leq \bar{\tau}$, where $\bar{\tau} > 0$ is a known constant scalar; $\phi(t)$ is a continuous vector-valued initial function on $[-\bar{\tau}, 0]$.

By fuzzy blending, the overall fuzzy system can be inferred as follows:

$$\begin{cases} \dot{x}(t) = \sum_{i=1}^{r} h_i(\theta(t)) \left[A_{1i}x(t) + A_{2i}x(t-\tau(t)) + D_{1i}\omega(t)\right] \\ z(t) = \sum_{i=1}^{r} h_i(\theta(t)) \left[C_{1i}x(t) + C_{2i}x(t-\tau(t)) + D_{2i}\omega(t)\right] \\ y(t) = \sum_{i=1}^{r} h_i(\theta(t)) \left[E_{1i}x(t) + E_{2i}x(t-\tau(t)) + D_{3i}\omega(t)\right] \\ x(t) = \phi(t), t \in [-\bar{\tau}, 0] \end{cases} \tag{4.1.2}$$

where $h_i(\theta(t)) = \omega_i(\theta(t))/\sum_{i=1}^{r}\omega_i(\theta(t))$, $\omega_i(\theta(t)) = \prod_{j=1}^{p}M_{ij}(\theta_j(t))$. $\omega_i(\theta(t)) \geq 0$, $i = 1, 2, \cdots, r$ hold for all t. Therefore, we have $h_i(\theta(t)) \geq 0$, $i = 1, 2, \cdots, r$, $\sum_{i=1}^{r}h_i(\theta(t)) = 1$.

For system (4.1.2), consider a full order fuzzy filter with r rules taking the following form:

♦ Filter Rule j: IF $\eta_1(t)$ is N_{j1} and $\eta_2(t)$ is N_{j2} and $\cdots$ and $\eta_p(t)$ is N_{jp}, THEN

$$\begin{cases} \dot{x}_f(t) = A_{fj}x_f(t) + B_{fj}y(t) \\ z_f(t) = C_{fj}x_f(t) \end{cases} \tag{4.1.3}$$

where $N_{j\beta}$, j=1, 2, $\cdots$, r, $\beta = 1, 2, \cdots, p$, denote the fuzzy sets. A_{fj}, B_{fj} and C_{fj}, j=1, 2, $\cdots$, r, are filter parameters to be designed. Thus the overall fuzzy filter system is represented by the following form:

$$\begin{cases} \dot{x}_f(t) = \sum\limits_{j=1}^{r}m_j(\eta(t))\left[A_{fj}x_f(t) + B_{fj}y(t)\right] \\ z_f(t) = \sum\limits_{j=1}^{r}m_j(\eta(t))C_{fj}x_f(t) \\ x_f(t) = x_f(0), t \in [-\bar{\tau},\ 0] \end{cases} \tag{4.1.4}$$

where $m_j(\eta(t)) \geq 0$, $j = 1, \cdots, r$, $\sum_{j=1}^{r}m_j(\eta(t)) = 1$. For simple description, we denote $h_i(\theta(t)) = h_i$ and $m_j(\eta(t)) = m_j$ in the rest of this chapter.

Define an augmented state vector $\xi(t) = [x^T(t)\ x_f^T(t)]^T$ and a filtering error vector $e(t) = z(t) - z_f(t)$, one can easily obtain the following filtering error system:

$$\begin{cases} \dot{\xi}(t) = \sum\limits_{i=1}^{r}\sum\limits_{j=1}^{r}h_i m_j[\overline{A}_{1ij}\xi(t) + \overline{A}_{2ij}\xi(t-\tau(t)) + \overline{D}_{1ij}\omega(t)] \\ e(t) = \sum\limits_{i=1}^{r}\sum\limits_{j=1}^{r}h_i m_j[\overline{C}_{1ij}\xi(t) + \overline{C}_{2ij}\xi(t-\tau(t)) + \overline{D}_{2ij}\omega(t)] \\ \varphi(t) = [\phi^T(t)\ \ x_f^T(0)]^T, t \in [-\bar{\tau},\ 0] \end{cases} \tag{4.1.5}$$

where

$$\overline{A}_{1ij} = \begin{bmatrix} A_{1i} & 0 \\ B_{fj}E_{1i} & A_{fj} \end{bmatrix},\ \overline{A}_{2ij} = \begin{bmatrix} A_{2i} & 0 \\ B_{fj}E_{2i} & 0 \end{bmatrix},\ \overline{D}_{1ij} = \begin{bmatrix} D_{1i} \\ B_{fj}D_{3i} \end{bmatrix},$$

$$\overline{C}_{1ij} = \begin{bmatrix} C_{1i} & -C_{fj} \end{bmatrix}, \ \overline{C}_{2ij} = \begin{bmatrix} C_{2i} & 0 \end{bmatrix}, \ \overline{D}_{2ij} = D_{2i}.$$

Before ending this section, the following assumption, definition and lemma, which will be useful to develop the main results in sequel, are introduced.

Lemma 4.1 *[109] For any matrices $Z \in \mathbb{R}^{n\times n}$ and $R_1 \in \mathbb{R}^{n\times n}$ satisfying $\begin{bmatrix} R_1 & Z \\ \star & R_1 \end{bmatrix} \geq 0$, and given scalars $0 < \kappa < 1$ and $c \leq b < a$, if there exists a vector function $x : [c, a] \to \mathbb{R}^n$ such that the integrations in the following inequality are well defined, then*

$$-(a-c)\int_c^a \dot{x}^T(\alpha)R_1\dot{x}(\alpha)d\alpha \leq \upsilon^T(t)\Delta\upsilon(t)$$

where $\upsilon^T(t) = \left[x^T(a)\ x^T(b)\ x^T(c)\ \frac{1}{a-c}\int_c^a x^T(\alpha)d\alpha\right]$,

$$\Delta = \begin{bmatrix} \Delta_{11} & \kappa(R_1 - Z) & \Delta_{13} & 0.5(1-\kappa)\pi^2 R_1 \\ \star & \Delta_{22} & \kappa(R_1 - Z) & 0 \\ \star & \star & -R_1 - 0.25(1-\kappa)R_1\pi^2 & 0.5(1-\kappa)\pi^2 R_1 \\ \star & \star & \star & -(1-\kappa)\pi^2 R_1 \end{bmatrix} \tag{4.1.6}$$

where

$$\begin{aligned} \Delta_{11} &= -R_1 - 0.25(1-\kappa)R_1\pi^2, \\ \Delta_{13} &= (1-\kappa)(1-0.25\pi^2)R_1 + \kappa Z, \\ \Delta_{22} &= \kappa(-2R_1 + Z + Z^T). \end{aligned}$$

Remark 4.1 *In fact, Lemma 4.1 is a convex combination of the following two integral inequalities for any $k \in [0, 1]$,*

$$\begin{aligned} &-(a-c)\int_c^a \dot{x}^T(\alpha)R_1\dot{x}(\alpha)d\alpha \\ &= -k(a-c)\int_c^a \dot{x}^T(\alpha)R_1\dot{x}(\alpha)d\alpha - (1-k)(a-c)\int_c^a \dot{x}^T(\alpha)R_1\dot{x}(\alpha)d\alpha \end{aligned} \tag{4.1.7}$$

Then according to [143, 144], we have:

$$
\begin{aligned}
&-k(a-c)\int_c^a \dot{x}^T(\alpha)R_1\dot{x}(\alpha)d\alpha \\
&\leq \begin{bmatrix} x(a) \\ x(b) \\ x(c) \end{bmatrix}^T \begin{bmatrix} -kR_1 & k(R_1-Z) & kG \\ \star & -2kR_1+kZ+kZ^T & k(R_1-Z) \\ \star & \star & -kR_1 \end{bmatrix} \begin{bmatrix} x(a) \\ x(b) \\ x(c) \end{bmatrix} \qquad (4.1.8) \\
&-(1-k)(a-c)\int_c^a \dot{x}^T(\alpha)R_1\dot{x}(\alpha)d\alpha \\
&\leq -(1-k)\eta^T(t)\begin{bmatrix} (0.25\pi^2+1)R_1 & 0 & (0.25\pi^2-1)R_1 & -0.5\pi^2R_1 \\ \star & 0 & 0 & 0 \\ \star & \star & (0.25\pi^2+1)R_1 & -0.5\pi^2R_1 \\ \star & \star & \star & \pi^2R_1 \end{bmatrix}\eta(t) \qquad (4.1.9)
\end{aligned}
$$

where $c \leq b \leq a$ *and* $\eta^T(t) = [x^T(a)\ x^T(b)\ x^T(c)\ \frac{1}{a-c}\int_c^a x^T(s)ds]^T$. *Then according to (4.1.7)-(4.1.9), we can get Lemma 2.1. Details of the proof can be referenced in [109]. Parameter k represents the weights of inequality (4.1.8) and (4.1.9). A general way to select k is to find an optimal k along the decreasing direction of disturbance attenuation performance level* γ *for a given initial value (e.g.* $k = 0.5$*, inequality (4.1.8) plays the same role as inequality (4.1.9)). Certainly, the obtained k may be a locally optimal parameter. In order to obtain a globally optimal parameter, conducting global search is necessary.*

Lemma 4.2 *[138] For any constant matrix* $\Sigma = \Sigma^T$ *and a scalar* $\bar{\tau} > 0$*, then the following inequalities hold:*

$$
-\int_{t-\bar{\tau}}^t x^T(s)\Sigma x(s)ds \leq -\frac{1}{\bar{\tau}}\left(\int_{t-\bar{\tau}}^t x^T(s)ds\right)\Sigma\left(\int_{t-\bar{\tau}}^t x(s)ds\right) \qquad (4.1.10)
$$

$$
\begin{aligned}
&-\int_{-\bar{\tau}}^0\int_{t+\theta}^t \dot{x}^T(s)\Sigma\dot{x}(s)ds \leq -\frac{2}{\bar{\tau}^2}\left(\int_{-\bar{\tau}}^0\int_{t+\theta}^t \dot{x}^T(s)ds\right)\Sigma\left(\int_{-\bar{\tau}}^0\int_{t+\theta}^t \dot{x}(s)ds\right) \\
&= -\frac{2}{\bar{\tau}^2}\left[\bar{\tau}x(t) - \int_{t-\bar{\tau}}^t x(s)ds\right]^T \Sigma \left[\bar{\tau}x(t) - \int_{t-\bar{\tau}}^t x(s)ds\right] \qquad (4.1.11)
\end{aligned}
$$

Assumption 4.1 *[84] For given real matrices* $\Phi = \Phi^T \geq 0$, $\Psi_1 = \Psi_1^T \leq 0$, Ψ_2 *and* $\Psi_3 = \Psi_3^T$ *satisfy the following conditions,* $\forall i,\ j \in \{1,\ 2\ , \cdots, r\}$*:*

1) $\|\overline{D}_{2ij}\| \cdot \|\Phi\| = 0$*;*

2) $(\|\Psi_1\| + \|\Psi_2\|)\|\Phi\| = 0$*;*

3) $\overline{D}_{2ij}^T \Psi_1 \overline{D}_{2ij} + \overline{D}_{2ij}^T \Psi_2 + \Psi_2^T \overline{D}_{2ij} + \Psi_3 > 0.$

Definition 4.1 *[84] For given matrices* Φ, Ψ_1, Ψ_2 *and* Ψ_3 *satisfying Assumption 1, system (4.1.5) can guarantee the prescribed* H_∞, $L_2 - L_\infty$, *passive and dissipative performance if there exits a scalar* ρ *such that the following inequality holds for any* $t_f \geq 0$ *and all* $w(t) \in \mathcal{L}_2[0,\ \infty)$

$$\int_0^{t_f} J(t)dt \geq e^T(t)\Phi e(t) + \rho, \quad t \in [0,\ t_f] \tag{4.1.12}$$

where $J(t) = e^T(t)\Psi_1 e(t) + 2e^T(t)\Psi_2 w(t) + w^T(t)\Psi_3 w(t)$.

Remark 4.2 *In Assumption 1,* $\Phi = \Phi^T, \Psi_1 = \Psi_1^T, \Psi_3 = \Psi_3^T$ *guarantee that the inequality in Definition 1 is well defined.* $\Phi \geq 0, \Psi_1 \leq 0$ *are conducive to deriving MI-based conditions for the filter design problem in Theorem 4.2 and Corollary 4.1. Item 3) is a standard condition for the investigation of dissipativity problem. Assumptions similar to these items have been used in [145, 146]. It is well known that, when considering the* $L_2 - L_\infty$ *performance, there should not be disturbance input in output equation [147], which can be guaranteed by item 1) in Assumption 1. The second term is technically necessary for the development of our analysis and design method. The only limitation is that when considering the* H_∞, $L_2 - L_\infty$, *passivity and dissipativity performance, zero initial condition is required, which is a common assumption in performance analysis problem, see [82, 148, 149].*

Remark 4.3 *The left-hand side of inequality (4.1.12) is often regarded as the energy supply function. The extended dissipative filter for fuzzy delay system is more general than other filter performance indices, such as* H_∞, $L_2 - L_\infty$, *passive and dissipative performances. For instance,*

1) *Let $\Phi = 0$, $\Psi_1 = -I$, $\Psi_2 = 0$, $\Psi_3 = \gamma^2 I$ and $\rho = 0$, inequality (4.1.12) reduces to H_∞ performance [93];*

2) *Let $\Phi = I$, $\Psi_1 = 0$, $\Psi_2 = 0$, $\Psi_3 = \gamma^2 I$ and $\rho = 0$, inequality (4.1.12) becomes $L_2 - L_\infty$ (energy-to-peak) performance considered in [98]*

3) *If the dimension of output $z(t)$ is the same as that of disturbance $w(t)$, then inequality (4.1.12) with $\Phi = 0$, $\Psi_1 = 0$, $\Psi_2 = I$, $\Psi_3 = \gamma I$ and $\rho = 0$ become the passivity performance index [150];*

4) *Let $\Phi = 0$, $\Psi_1 = Q$, $\Psi_2 = S$, $\Psi_3 = R - \alpha I$ and $\rho = 0$, inequality (4.1.12) reduces to the strict (Q,S,R)-dissipativity [151];*

5) *Let $\Phi = 0$, $\Psi_1 = -\epsilon I$, $\Psi_2 = I$, $\Psi_3 = -\sigma I$ with $\varepsilon > 0$ and $\sigma > 0$, the inequality (4.1.12) becomes the very-strict passivity performance index.*

In the definition of very-strict passivity, scalar ρ is not required to be zero. It was shown in [139] that ρ should be a non-positive scalar. This fact can also be verified from Assumption 1 and Definition 1. Indeed, when $w(t) = 0$, it follows from (4.1.12) that

$$\rho \leq \int_0^{t_f} e^T(t)\Psi_1 e(t)dt - e^T(t)\Phi e(t), \quad t \in [0,\ t_f]$$

Note from Assumption 1 that $\Phi \geq 0$ and $\Psi_1 \leq 0$. Thus, the above inequality indicates that $\rho \leq 0$.

The problems to be addressed in this chapter are formulated as follows:

1) The filtering error system (4.1.5) with $w(t) = 0$ is asymptotically stable;

2) The filtering error system (4.1.5) guarantees the unified performance index proposed in (4.1.12) for all nonzero $w(t) \in \mathcal{L}_2[0,\ \infty)$.

4.2 Main Results on fuzzy filter design

In this section, the extended dissipative filter design issue for time-varying delay fuzzy systems will be considered. We first present a performance criterion for the filtering error system (4.1.5) where the filter matrices in (4.1.4) are assumed to be given.

Theorem 4.1 *Given scalars $0 < \epsilon < 1$, $0 < \kappa < 1$, $\bar{\tau} > 0$ and matrices Φ, Ψ_1, Ψ_2, Ψ_3 satisfying Assumption 1, the filtering error system (4.1.5) is asymptotically stable and satisfies the performance index in Definition 4.1 for any admissible time-varying delay $0 < \tau(t) \leq \bar{\tau}$ under condition $m_j - \lambda_j h_j \geq 0, (0 < \lambda_j < 1)$, if there exist matrices $P > 0$, $Q_1 > 0$, $R_1 > 0$, $R_2 > 0$, $R_3 > 0$, $G > 0$, arbitrary matrices Λ_i, Z and , $L_i, i = 1, \cdots, 5$ such that the following conditions hold, $\forall i,\ j \in \{1,\ 2\ , \cdots, r\}$:*

$$G - P < 0 \tag{4.2.1}$$

$$\begin{bmatrix} R_1 & Z \\ \star & R_1 \end{bmatrix} > 0 \tag{4.2.2}$$

$$\mathcal{G}_{ij} = \begin{bmatrix} \varepsilon G - \overline{C}_{1ij}^T \Phi \overline{C}_{1ij} & -\overline{C}_{1ij}^T \Phi \overline{C}_{2ij} \\ \star & (1-\varepsilon) G - \overline{C}_{2ij}^T \Phi \overline{C}_{2ij} \end{bmatrix} > 0 \tag{4.2.3}$$

$$\Xi_{ij} - \Lambda_i < 0 \tag{4.2.4}$$

$$\lambda_i \Xi_{ii} - \lambda_i \Lambda_i + \Lambda_i < 0 \tag{4.2.5}$$

$$\lambda_j \Xi_{ij} - \lambda_i \Xi_{ji} - \lambda_j \Lambda_i - \lambda_i \Lambda_j + \Lambda_i + \Lambda_j < 0,\ i < j \tag{4.2.6}$$

where

$$\Xi_{ij} = \begin{bmatrix} \Xi_{11}^{ij} & \Xi_{12}^{ij} & \Xi_{13}^{ij} & \Xi_{14}^{ij} & \Xi_{15}^{ij} & \Xi_{16}^{ij} \\ \star & \Xi_{22}^{ij} & \Xi_{23}^{ij} & \overline{A}_{2ij}^T L_4^T & -L_2 + \overline{A}_{2ij}^T L_5^T & \Xi_{26}^{ij} \\ \star & \star & \Xi_{33} & \Xi_{34} & -L_3 & L_3 \overline{D}_{1ij} \\ \star & \star & \star & \Xi_{44} & -L_4 & L_4 \overline{D}_{1ij} \\ \star & \star & \star & \star & \Xi_{55} & L_5 \overline{D}_{1ij} \\ \star & \star & \star & \star & \star & \Xi_{66}^{ij} \end{bmatrix} \tag{4.2.7}$$

$$\Xi_{11}^{ij} = Q_1 + \bar{\tau}R_2 - R_1 - 0.25(1-\kappa)R_1\pi^2 - 2R_3 + L_1\overline{A}_{1ij} + \overline{A}_{1ij}^T L_1^T - \overline{C}_{1ij}^T\Psi_1\overline{C}_{1ij}$$
$$\Xi_{12}^{ij} = \kappa(R_1 - Z) + L_1\overline{A}_{2ij} + \overline{A}_{1ij}^T L_2^T - \overline{C}_{1ij}^T\Psi_1\overline{C}_{2ij}$$
$$\Xi_{13}^{ij} = (1-\kappa)(1-0.25\pi^2)R_1 + \kappa Z + \overline{A}_{1ij}^T L_3^T$$
$$\Xi_{14}^{ij} = 0.5(1-\kappa)R_1\pi^2 + 2R_3 + \overline{A}_{1ij}^T L_4^T,\ \Xi_{15}^{ij} = P - L_1 + \overline{A}_{1ij}^T L_5^T$$
$$\Xi_{22}^{ij} = \kappa(-2R_1 + Z + Z^T) + L_2\overline{A}_{2ij} + \overline{A}_{2ij}^T L_2^T - \overline{C}_{2ij}^T\Psi_1\overline{C}_{2ij}$$
$$\Xi_{23}^{ij} = \kappa(R_1 - Z) + \overline{A}_{2ij}^T L_3^T,\ \Xi_{33} = -Q_1 - R_1 - 0.25(1-\kappa)R_1\pi^2$$
$$\Xi_{34} = 0.5(1-\kappa)R_1\pi^2,\ \Xi_{44} = -(1-\kappa)R_1\pi^2 - \bar{\tau}R_2 - 2R_3$$
$$\Xi_{55} = \bar{\tau}^2 R_1 + \frac{\bar{\tau}^2}{2}R_3 - L_5 - L_5^T,\ \Xi_{16}^{ij} = L_1\overline{D}_{1ij} - \overline{C}_{1ij}^T\Psi_1\overline{D}_{2ij} - \overline{C}_{1ij}^T\Psi_2$$
$$\Xi_{26}^{ij} = L_2\overline{D}_{1ij} - \overline{C}_{2ij}^T\Psi_1\overline{D}_{2ij} - \overline{C}_{2ij}^T\Psi_2$$
$$\Xi_{66}^{ij} = -\overline{D}_{2ij}^T\Psi_1\overline{D}_{2ij} - \overline{D}_{2ij}^T\Psi_2 - \Psi_2^T\overline{D}_{2ij} - \Psi_3$$

In this case, scalar ρ involved in Definition 1 can be chosen as

$$\rho = -V(0) - \|G\| \sup_{-\bar{\tau}\le\sigma\le 0} |\varphi(\sigma)|^2 \tag{4.2.8}$$

Proof: Consider the following Lyapunov-Krasovskii functional:

$$V(t,\xi(t)) = V_1(t,\xi(t)) + V_2(t,\xi(t)) \tag{4.2.9}$$

where

$$\begin{aligned}
V_1(t,\xi(t)) =& \xi^T(t)P\xi(t) + \int_{t-\bar{\tau}}^{t} \xi^T(s)Q_1\xi(s)ds \\
V_2(t,\xi(t)) =& \bar{\tau}\int_{-\bar{\tau}}^{0}\int_{t+\theta}^{t} \dot{\xi}^T(s)R_1\dot{\xi}(s)dsd\theta + \int_{-\bar{\tau}}^{0}\int_{t+\theta}^{t} \xi^T(s)R_2\xi(s)dsd\theta \\
&+ \int_{-\bar{\tau}}^{0}\int_{\theta}^{0}\int_{t+\beta}^{t} \dot{\xi}^T(\alpha)R_3\dot{\xi}(\alpha)d\alpha d\beta d\theta
\end{aligned}$$

P, Q_1, R_1, R_2 and R_3 are symmetric positive definite matrices. Then the time derivative of $V(t,\xi(t))$ along the trajectories of system (4.1.5) can be expressed as:

$$
\begin{aligned}
\dot{V}(t,\xi(t)) =& \dot{V}_1(t,\xi(t)) + \dot{V}_2(t,\xi(t)) \\
\dot{V}_1(t,\xi(t)) =& 2\xi^T(t)P\sum\nolimits_{i=1}^{r}\sum\nolimits_{j=1}^{r} h_i m_j[\overline{A}_{1ij}\xi(t) + \overline{A}_{2ij}\xi(t-\tau(t)) + \overline{D}_{1ij}\omega(t)] \\
&+ \xi^T(t)Q_1\xi(t) - \xi^T(t-\bar{\tau})Q_1\xi(t-\bar{\tau}) \\
\dot{V}_2(t,\xi(t)) =& \bar{\tau}^2\dot{\xi}^T(t)R_1\dot{\xi}(t) - \bar{\tau}\int_{t-\bar{\tau}}^{t}\dot{\xi}^T(s)R_1\dot{\xi}(s)ds + \bar{\tau}\xi^T(t)R_2\xi(t) + \frac{\bar{\tau}^2}{2}\dot{\xi}^T(t)R_3\dot{\xi}(t) \\
&- \int_{t-\bar{\tau}}^{t}\xi^T(s)R_2\xi(s)ds - \int_{-\bar{\tau}}^{0}\int_{t+\theta}^{t}\dot{\xi}^T(s)R_3\dot{\xi}(s)dsd\theta
\end{aligned}
$$

Recalling and applying Lemma 4.1 under condition (4.2.2), we have

$$
-\bar{\tau}\int_{t-\bar{\tau}}^{t}\dot{\xi}^T(\alpha)R_1\dot{\xi}(\alpha)d\alpha \le \zeta^T(t)\Gamma\zeta(t)
$$

where $\zeta^T(t) = \begin{bmatrix}\xi^T(t) & \xi^T(t-\tau(t)) & \xi^T(t-\bar{\tau}) & \frac{1}{\bar{\tau}}\int_{t-\bar{\tau}}^{t}\xi^T(s)ds & \dot{\xi}^T(t) & \omega^T(t)\end{bmatrix}$.

$$
\Gamma = \begin{bmatrix}
\Gamma_{11} & \Gamma_{12} & \Gamma_{13} & 0.5(1-\kappa)\pi^2R_1 & 0 & 0 \\
\star & \Gamma_{22} & \kappa(R_1 - Z) & 0 & 0 & 0 \\
\star & \star & -R_1 - 0.25(1-\kappa)\pi^2R_1 & 0.5(1-\kappa)\pi^2R_1 & 0 & 0 \\
\star & \star & \star & -(1-\kappa)\pi^2R_1 & 0 & 0 \\
\star & \star & \star & \star & 0 & 0 \\
\star & \star & \star & \star & \star & 0
\end{bmatrix} \tag{4.2.10}
$$

$$
\begin{aligned}
\Gamma_{11} =& -R_1 - 0.25(1-\kappa)R_1\pi^2, \Gamma_{12} = \kappa(R_1 - Z), \\
\Gamma_{13} =& (1-\kappa)(1-0.25\pi^2)R_1 + \kappa Z, \Gamma_{22} = \kappa(-2R_1 + Z + Z^T).
\end{aligned}
$$

By Lemma 4.2,

$$
-\int_{t-\bar{\tau}}^{t}\xi^T(s)R_2\xi(s)ds \le -\frac{1}{\bar{\tau}}\left(\int_{t-\bar{\tau}}^{t}\xi^T(s)ds\right)R_2\left(\int_{t-\bar{\tau}}^{t}\xi(s)ds\right)
$$

$$
-\int_{-\bar{\tau}}^{0}\int_{t+\theta}^{t}\dot{\xi}^T(s)R_3\dot{\xi}(s)dsd\theta \le -\frac{2}{\bar{\tau}^2}\left(\int_{-\bar{\tau}}^{0}\int_{t+\theta}^{t}\dot{\xi}^T(s)dsd\theta\right)R_3\left(\int_{-\bar{\tau}}^{0}\int_{t+\theta}^{t}\dot{\xi}(s)dsd\theta\right)
$$

$$= -\frac{2}{\bar{\tau}^2}\left[\bar{\tau}\xi(t) - \int_{t-\bar{\tau}}^{t}\xi(s)ds\right]^T R_3\left[\bar{\tau}\xi(t) - \int_{t-\bar{\tau}}^{t}\xi(s)ds\right]$$

By considering the dynamic constraint of system (4.1.5), we have the following equation

$$2\beta^T(t)L\left[\sum_{i=1}^{r}\sum_{j=1}^{r}h_i m_j\left(\overline{A}_{1ij}\xi(t)+\overline{A}_{2ij}\xi(t-\tau(t))+\overline{D}_{1ij}\omega(t)\right) - \dot{\xi}(t)\right] = 0 \quad (4.2.11)$$

where $\beta^T(t) = \begin{bmatrix}\xi^T(t) & \xi^T(t-\tau(t)) & \xi^T(t-\bar{\tau}) & \frac{1}{\bar{\tau}}\int_{t-\bar{\tau}}^{t}\xi^T(s)ds & \dot{\xi}^T(t)\end{bmatrix}$ and $L^T = \begin{bmatrix}L_1^T & L_2^T & L_3^T & L_4^T & L_5^T\end{bmatrix}$. Add (4.2.11) to the right side of $\dot{V}(t,\xi(t))$, we can have

$$\dot{V}(t,\xi(t)) - J(t) \leq \zeta^T(t)\left(\sum_{i=1}^{r}\sum_{j=1}^{r}h_i m_j\Xi_{ij}\right)\zeta(t) \quad (4.2.12)$$

where

$$J(t) = e^T(t)\Psi_1 e(t) + 2e^T(t)\Psi_2 w(t) + w^T(t)\Psi_3 w(t) \quad (4.2.13)$$

It can be seen from (4.2.12) that if $\sum_{i=1}^{r}\sum_{j=1}^{r}h_i m_j\Xi_{ij} < 0$, then $\dot{V}(t,\xi(t)) - J(t) < 0$. Consider $\sum_{i=1}^{r}\sum_{j=1}^{r}h_i(h_j - m_j\Lambda_i) = 0$, where $\Lambda_i = \Lambda_i^T, i = 1,\cdots,r$ are arbitrary matrices with appropriate dimensions. Then we have

$$\begin{aligned}\sum_{i=1}^{r}\sum_{j=1}^{r}h_i m_j\Xi_{ij} =& \sum_{i=1}^{r}\sum_{j=1}^{r}h_i(h_j - m_j + \lambda_j h_j - \lambda_j h_j)\Lambda_i + \sum_{i=1}^{r}\sum_{j=1}^{r}h_i m_j\Xi_{ij}\\ =& \sum_{i=1}^{r}\sum_{i=1}^{r}h_i^2(\lambda_i\Xi_{ii} - \lambda_i\Lambda_i + \Lambda_i) + \sum_{i=1}^{r-1}\sum_{j=i+1}^{r}h_i h_j(\lambda_j\Xi_{ij} - \lambda_j\Lambda_i\\ &+\Lambda_i + \lambda_i\Xi_{ji} - \lambda_i\Lambda_j + \Lambda_j) + \sum_{i=1}^{r}\sum_{j=1}^{r}h_i(m_j - \lambda_j h_j)(\Xi_{ij} - \Lambda_i)\end{aligned}$$

Under the condition of $m_j - \lambda_j h_j \geq 0$ for all j, it is easy to obtain (4.2.14) from inequalities (4.2.4)-(4.2.6).

$$\dot{V}(t,\xi(t)) - J(t) \leq \zeta^T(t)\left(\sum_{i=1}^{r}\sum_{j=1}^{r}h_i m_j\Xi_{ij}\right)\zeta(t) < 0 \quad (4.2.14)$$

Then, there always exists a sufficiently small scalar $c > 0$, such that (4.2.15) holds.

$$\dot{V}(t,\xi(t)) - J(t) \leq -c \mid \zeta(t) \mid^2 \leq -c \mid \xi(t) \mid^2 \tag{4.2.15}$$

According to Definition 1, we need to prove that the following inequality holds for any matrices Φ, Ψ_1, Ψ_2, Ψ_3 satisfying Assumption 1:

$$\int_0^{t_f} J(t)dt - e^T(t)\Phi e(t) \geq \rho \tag{4.2.16}$$

where t_f is any nonnegative scalar. We consider the following two cases of $\|\Phi\| = 0$ and $\|\Phi\| \neq 0$, respectively.

First, consider the case of $\|\Phi\| = 0$. When $\|\Phi\| = 0$, we need to prove

$$\int_0^{t_f} J(t)dt \geq \rho \tag{4.2.17}$$

It follows from (4.2.15) that $J(t) - \dot{V}(t,\xi(t)) \geq 0$ holds for any $t > 0$. Integrating both sides of it yields

$$\int_0^{t} J(t_v)dt_v \geq V(t,\xi(t)) - V(0) \tag{4.2.18}$$

From (4.2.9) and (4.2.1), we can obtain

$$V(t,\xi(t)) \geq \xi^T(t)P\xi(t) \geq \xi^T(t)G\xi(t) \geq 0 \tag{4.2.19}$$

Notice from (4.2.8) that $\rho \leq -V(0)$. Thus it follows from (4.2.18) and (4.2.19) that

$$\int_0^{t_f} J(t_v)dt_v \geq \xi^T(t_f)G\xi(t_f) + \rho \tag{4.2.20}$$

Thus, it is obvious that (4.2.17) holds.

For another case of $\|\Phi\| \neq 0$, under Assumption 1, it is required that $\|\Psi_1\| + \|\Psi_2\| = 0$ and $\|\overline{D}_{2ij}\| = 0$, which imply $\Psi_1 = 0$, $\Psi_2 = 0$ and $\Psi_3 > 0$. Thus, $J(t) = w^T(t)\Psi_3 w(t) \geq 0$. Then according to (4.2.20), the following inequality holds for any $t \in [0,\ t_f]$.

$$\int_0^{t_f} J(t_v)dt_v \geq \int_0^{t} J(t_v)dt_v \geq \xi^T(t)G\xi(t) + \rho \tag{4.2.21}$$

When $t > \tau(t)$, it is obvious that $0 < t - \tau(t) < t_f$. Thus it follows from (4.2.21) that

$$\int_0^{t_f} J(t_v)dt_v \geq \int_0^{t-\tau(t)} J(t_v)dt_v \geq \xi^T(t-\tau(t))G\xi(t-\tau(t)) + \rho \tag{4.2.22}$$

When $t < \tau(t)$, it gives that $-\bar{\tau} \leq -\tau(t) \leq t - \tau(t) < 0$. In this circumstance, it can be verified that

$$\begin{aligned} \rho + \xi^T(t-\tau(t))G\xi(t-\tau(t)) &\leq \rho + \|G\|\,|\xi(t-\tau(t))|^2 \\ &\leq \rho + \|G\| \sup_{-\bar{\tau}\leq\sigma\leq 0} |\phi(\sigma)|^2 \\ &= -V(0) \leq \int_0^{t_f} J(t_v)dt_v \end{aligned} \tag{4.2.23}$$

This, together with (4.2.22), indicates that for any $t \in [0,\ t_f]$ and scalar $\varepsilon \in (0, 1)$, (4.2.24) holds:

$$\int_0^{t_f} J(t_v)dt_v \geq (1-\epsilon)\xi^T(t-\tau(t))G\xi(t-\tau(t)) + \epsilon\xi^T(t)G\xi(t) + \rho \tag{4.2.24}$$

Recalling (4.1.5) with $\overline{D}_{2ij} = 0$, we have

$$\begin{aligned} e^T(t)\Phi e(t) = \sum_{i=1}^{r}\sum_{j=1}^{r} h_i m_j \Bigg\{ &- \begin{bmatrix} \xi(t) \\ \xi(t-\tau(t)) \end{bmatrix}^T \mathcal{G}_{ij} \begin{bmatrix} \xi(t) \\ \xi(t-\tau(t)) \end{bmatrix} \\ &+ (1-\epsilon)\xi^T(t-\tau(t))G\xi(t-\tau(t)) + \epsilon\xi^T(t)G\xi(t) \Bigg\} \end{aligned} \tag{4.2.25}$$

where $\mathcal{G}_{ij}$ is defined in (4.2.3) and $\mathcal{G}_{ij} > 0$. Then for any $t > 0$,

$$e^T(t)\Phi e(t) \leq (1-\epsilon)\xi^T(t-\tau(t))G\xi(t-\tau(t)) + \epsilon\xi^T(t)G\xi(t) \tag{4.2.26}$$

(4.2.24) and (4.2.26) imply that for any $t \in [0,\ t_f]$ the following inequality holds:

$$\int_0^{t_f} J(t_v)dt_v \geq e^T(t)\Phi e(t) + \rho \tag{4.2.27}$$

Since (4.2.27) holds for any $t \in [0,\ t_f]$. Then (4.2.16) holds for any $t_f \geq 0$. In view of the two cases of $\|\Phi\| = 0$ and $\|\Phi\| \neq 0$ discussed above, one can easily obtain the conclusion that system (4.1.5) is extended dissipative according to Definition 1. When $w(t) \equiv 0$, it follows from (4.2.15) that

$$\dot{V}(t, \xi(t)) \leq e^T(t)\Psi_1 e(t) - c|\xi(t)|^2 \tag{4.2.28}$$

Moreover, $\Psi_1 \leq 0$ under Assumption 1, then we have $\dot{V}(t) \leq -c|\xi(t)|^2$, which indicates that filtering error system (4.1.5) is asymptotically stable with $w(t) \equiv 0$. This completes the proof. ■

Remark 4.4 *Theorem 4.1 provides a performance criterion for the filtering error system (4.1.5) with given filter matrices. The performance criteria in Theorem 4.1 are expressed in the form of linear matrix inequalities (LMIs), which can be easily solved via standard software. It is easy to get that $\rho = 0$ under zero initial condition from (4.2.8). By tuning the weighting matrices Φ, Ψ_1, Ψ_2, Ψ_3 as discussed in Remark 4.3, Theorem 4.1 can be used to check the H_∞ performance, $L_2 - L_\infty$ performance, passivity and dissipativity, respectively. Additionally, the terms $-\int_{t-\bar{\tau}}^{t} \xi^T(s)R_2\xi(s)ds$ and $-\int_{-\bar{\tau}}^{0}\int_{t+\theta}^{t} \dot{\xi}^T(s)R_3\dot{\xi}(s)dsd\theta$ in the derivative of the Lyapunov-Krasovskii functional were ignored in [84], but are made full use of in condition (4.2.4), (4.2.5) and (4.2.6) of Theorem 4.1. This improvement can contribute to less conservativeness.*

Moreover, it should be pointed out that some existing results [84, 93–95] require information of the derivative of $\tau(t)$ to design filters. In this study, such requirement is removed since the derivative of delay is usually unknown in practical complex nonlinear systems.

Remark 4.5 *Compared with the perfectly matched premise fuzzy filter design method in [91, 152, 153], the method proposed in Theorem 4.1 can enhance design flexibility and lower the implementation cost of the fuzzy filter to some extent when simple membership functions are used instead of complicated ones. Free matrices* $\Lambda_i, i = 1, 2, \cdots, r$. *are introduced in the design of filter for fuzzy delay system to alleviate the conservativeness, which we will discuss later in Example 1. The condition* $m_j - \lambda_j h_j \geq 0$, $(0 < \lambda_j < 1)$ *presents a simple description of relationship between system membership function* h_j *and filter membership function* m_j. *For convenient of developing the filter analysis and design method, the parameter* λ_j *is technically limited in* $0 < \lambda_j < 1$. *In practice, we can always find simple membership functions satisfying this condition. When parameter* λ_j *approaches near* 1, *filter membership function* m_j *is more closely approximated to the system membership function* h_j.

It is worth pointing out that if the filter matrices are not given in advance, conditions in Theorem 4.1 are nonconvex, which makes the performance criteria can not be directly extended to the filter design. By employing the convex linearization technique, we are in a position to develop extended dissipative filter design approach for fuzzy time-delay system (4.1.2) based on the performance criteria of Theorem 4.1. Recalling Assumption 1 and noticing that $\Phi \geq 0$ and $\Psi_1 \leq 0$, there always exist matrices $\overline{\Phi}$ and $\overline{\Psi}_1$ such that

$$\Phi = \overline{\Phi}^T \overline{\Phi}, \quad \Psi_1 = -\overline{\Psi}_1^T \overline{\Psi}_1. \tag{4.2.29}$$

Under imperfect premise matching, the extended dissipative filter design approach for fuzzy time-delay system (4.1.2) is stated as follows.

Theorem 4.2 *Given scalars* $0 < \epsilon < 1$, $0 < \kappa < 1$, $\bar{\tau} > 0$, $l_i, i = 1, \cdots, 5$, *fuzzy filter error system is asymptotically stable and satisfies the extended dissipative performance for any time-varying delay* $0 < \tau(t) \leq \bar{\tau}$ *under condition* $m_j - \lambda_j h_j \geq 0, (0 < \lambda_j < 1)$, *if there exist matrices* $X > 0$, $Y > 0$, $\overline{Q}_1 > 0$, $\overline{R}_1 > 0$, $\overline{R}_2 > 0$,

$\overline{R}_3 > 0$, $\overline{G} > 0$, $\overline{L}$, $\overline{\Lambda}_i$, $\overline{Z}$, $\overline{A}_{fj}$, $\overline{B}_{fj}$ *and* $\overline{C}_{fj}$ *such that the following conditions hold,* $\forall i,\ j \in \{1,\ 2\ , \cdots, r\}$*:*

$$\overline{G} - \overline{P} < 0 \tag{4.2.30}$$

$$\begin{bmatrix} \overline{R}_1 & \overline{Z} \\ \star & \overline{R}_1 \end{bmatrix} > 0 \tag{4.2.31}$$

$$\overline{\mathcal{G}}_{ij} = \begin{bmatrix} \varepsilon\overline{G} & 0 & \Upsilon_{4ij}\overline{\Phi}^T \\ \star & (1-\varepsilon)\overline{G} & \Upsilon_{5ij}\overline{\Phi}^T \\ \star & \star & I \end{bmatrix} > 0 \tag{4.2.32}$$

$$\overline{\Xi}_{ij} - \overline{\Lambda}_i < 0 \tag{4.2.33}$$

$$\lambda_i\overline{\Xi}_{ii} - \lambda_i\overline{\Lambda}_i + \overline{\Lambda}_i < 0 \tag{4.2.34}$$

$$\lambda_j\overline{\Xi}_{ij} - \lambda_i\overline{\Xi}_{ji} - \lambda_j\overline{\Lambda}_i - \lambda_i\overline{\Lambda}_j + \overline{\Lambda}_i + \overline{\Lambda}_j < 0,\ i < j \tag{4.2.35}$$

$$\overline{\Xi}_{ij} = \begin{bmatrix} \overline{\Xi}_{11}^{ij} & \overline{\Xi}_{12}^{ij} & \overline{\Xi}_{13}^{ij} & \overline{\Xi}_{14}^{ij} & \overline{\Xi}_{15}^{ij} & l_1\Upsilon_{3ij} - \Upsilon_{4ij}\Psi_2 & \Upsilon_{4ij}\Psi_1^T \\ \star & \overline{\Xi}_{22}^{ij} & \overline{\Xi}_{23}^{ij} & l_4\Upsilon_{2ij}^T & -l_2\overline{L} + l_5\Upsilon_{2ij}^T & l_2\Upsilon_{3ij} - \Upsilon_{5i}\Psi_2 & \Upsilon_{5i}\Psi_1^T \\ \star & \star & \overline{\Xi}_{33} & \overline{\Xi}_{34} & -l_3\overline{L} & l_3\Upsilon_{3ij} & 0 \\ \star & \star & \star & \overline{\Xi}_{44} & -l_4\overline{L} & l_4\Upsilon_{3ij} & 0 \\ \star & \star & \star & \star & \overline{\Xi}_{55} & l_5\Upsilon_{3ij} & 0 \\ \star & \star & \star & \star & \star & \overline{\Xi}_{66}^{ij} & \overline{D}_{2ij}\overline{\Psi}_1^T \\ \star & \star & \star & \star & \star & \star & -I \end{bmatrix} \tag{4.2.36}$$

$$\overline{\Xi}_{11}^{ij} = \overline{Q}_1 + \bar{\tau}\overline{R}_2 - \overline{R}_1 - 0.25(1-\kappa)\overline{R}_1\pi^2 - 2\overline{R}_3 + l_1\Upsilon_{1ij} + l_1\Upsilon_{1ij}^T$$

$$\overline{\Xi}_{12}^{ij} = \kappa(\overline{R}_1 - \overline{Z}) + l_1\Upsilon_{2ij} + l_2\Upsilon_{1ij}^T, \overline{\Xi}_{13}^{ij} = (1-\kappa)(1-0.25\pi^2)\overline{R}_1 + \kappa\overline{Z} + l_3\Upsilon_{1ij}^T$$

$$\overline{\Xi}_{14}^{ij} = 0.5(1-\kappa)\overline{R}_1\pi^2 + 2\overline{R}_3 + l_4\Upsilon_{1ij}^T, \overline{\Xi}_{15}^{ij} = \overline{P} - l_1\overline{L} + l_5\Upsilon_{1ij}^T$$

$$\overline{\Xi}_{22}^{ij} = \kappa(-2\overline{R}_1 + \overline{Z} + \overline{Z}^T) + l_2\Upsilon_{2ij} + l_2\Upsilon_{2ij}^T, \overline{\Xi}_{23}^{ij} = \kappa(\overline{R}_1 - \overline{Z}) + l_3\Upsilon_{2ij}^T$$

$$\overline{\Xi}_{33} = -\overline{Q}_1 - \overline{R}_1 - 0.25(1-\kappa)\overline{R}_1\pi^2\overline{\Xi}_{34} = 0.5(1-\kappa)\overline{R}_1\pi^2$$

$$\overline{\Xi}_{44} = -(1-\kappa)\overline{R}_1\pi^2 - \bar{\tau}\overline{R}_2 - 2\overline{R}_3, \overline{\Xi}_{55} = \bar{\tau}^2\overline{R}_1 + \frac{\bar{\tau}^2}{2}\overline{R}_3 - l_5\overline{L} - l_5\overline{L}^T$$

$$\overline{\Xi}_{66}^{ij} = -\overline{D}_{2ij}^T\Psi_2 - \Psi_2^T\overline{D}_{2ij} - \Psi_3$$

$$\Upsilon_{1ij} = \begin{bmatrix} XA_{1i} + \overline{B}_{fj}E_{1i} & \overline{A}_{fj} \\ YA_{1i} + \overline{B}_{fj}E_{1i} & \overline{A}_{fj} \end{bmatrix}, \Upsilon_{2ij} = \begin{bmatrix} XA_{2i} + \overline{B}_{fj}E_{2i} & 0 \\ YA_{2i} + \overline{B}_{fj}E_{2i} & 0 \end{bmatrix},$$

$$\overline{L} = \begin{bmatrix} X & Y \\ \star & Y \end{bmatrix}, \Upsilon_{3ij} = \begin{bmatrix} XD_{1i} + \overline{B}_{fj}D_{3i} \\ YD_{1i} + \overline{B}_{fj}D_{3i} \end{bmatrix}, \Upsilon_{4ij} = \begin{bmatrix} C_{1i}^T \\ \overline{C}_{fj}^T \end{bmatrix}, \Upsilon_{5i} = \begin{bmatrix} C_{2i}^T \\ 0 \end{bmatrix}$$

Moreover, if above LMIs have feasible solutions, the desired delay dependent filter is obtained with parameters given by

$$\begin{cases} A_{fj} = Y^{-1}\overline{A}_{fj} \\ B_{fj} = Y^{-1}\overline{B}_{fj} \\ C_{fj} = \overline{C}_{fj}. \end{cases} \tag{4.2.37}$$

Proof: From inequality (4.2.14), we can obtain that

$$\Xi_{ij} < 0 \tag{4.2.38}$$

Under the condition of $\Psi_1 = -\overline{\Psi}_1^T\overline{\Psi}_1$, applying Schur Complement to (4.2.38) yields $\tilde{\Xi}_{ij} < 0$, which is defined in (4.2.39):

$$\tilde{\Xi}_{ij} = \begin{bmatrix} \tilde{\Xi}_{11}^{ij} & \tilde{\Xi}_{12}^{ij} & \tilde{\Xi}_{13}^{ij} & \tilde{\Xi}_{14}^{ij} & \tilde{\Xi}_{15}^{ij} & L_1\overline{D}_{1ij} - \overline{C}_{1ij}^T\Psi_2 & \overline{C}_{1ij}^T\overline{\Psi}_1^T \\ \star & \tilde{\Xi}_{22}^{ij} & \tilde{\Xi}_{23}^{ij} & \overline{A}_{2ij}^T L_4^T & -L_2+\overline{A}_{2ij}^T L_5^T & L_2\overline{D}_{1ij} - \overline{C}_{2ij}^T\Psi_2 & \overline{C}_{2ij}^T\overline{\Psi}_1^T \\ \star & \star & \tilde{\Xi}_{33} & \tilde{\Xi}_{34} & -L_3 & L_3\overline{D}_{1ij} & 0 \\ \star & \star & \star & \tilde{\Xi}_{44} & -L_4 & L_4\overline{D}_{1ij} & 0 \\ \star & \star & \star & \star & \tilde{\Xi}_{55} & L_5\overline{D}_{1ij} & 0 \\ \star & \star & \star & \star & \star & \Xi_{66}^{ij} & \overline{D}_{2ij}\overline{\Psi}_1^T \\ \star & \star & \star & \star & \star & \star & -I \end{bmatrix} \tag{4.2.39}$$

where

$$\tilde{\Xi}_{11}^{ij} = Q_1 + \bar{\tau}R_2 - R_1 - 0.25(1-\kappa)R_1\pi^2 - 2R_3 + L_1\overline{A}_{1ij} + \overline{A}_{1ij}^T L_1^T$$

$$\tilde{\Xi}_{12}^{ij} = \kappa(R_1 - Z) + L_1\overline{A}_{2ij} + \overline{A}_{1ij}^T L_2^T, \tilde{\Xi}_{13}^{ij} = (1-\kappa)(1 - 0.25\pi^2)R_1 + \kappa Z + \overline{A}_{1ij}^T L_3^T$$

$$\tilde{\Xi}_{14}^{ij} = 0.5(1-\kappa)R_1\pi^2 + 2R_3 + \overline{A}_{1ij}^T L_4^T, \tilde{\Xi}_{15}^{ij} = P - L_1 + \overline{A}_{1ij}^T L_5^T$$

$$\tilde{\Xi}_{22}^{ij} = \kappa(-2R_1 + Z + Z^T) + L_2\overline{A}_{2ij} + \overline{A}_{2ij}^T L_2^T, \tilde{\Xi}_{23}^{ij} = \kappa(R_1 - Z) + \overline{A}_{2ij}^T L_3^T$$

$$\tilde{\Xi}_{33} = -Q_1 - R_1 - 0.25(1-\kappa)R_1\pi^2, \tilde{\Xi}_{34} = 0.5(1-\kappa)R_1\pi^2$$

$$\tilde{\Xi}_{44} = -(1-\kappa)R_1\pi^2 - \bar{\tau}R_2 - 2R_3, \tilde{\Xi}_{55} = \bar{\tau}^2 R_1 + \frac{\bar{\tau}^2}{2}R_3 - L_5 - L_5^T$$

Let $L_i = l_i L$, partition L as $L = \begin{bmatrix} X & S \\ S^T & W \end{bmatrix}$. Then define $H = \begin{bmatrix} I & 0 \\ 0 & SW^{-1} \end{bmatrix}$, $Y = SW^{-1}S^T, \overline{A}_{fj} = SA_{fj}W^{-1}S^T$, $\overline{B}_{fj} = SB_{fj}$, $\overline{C}_{fj} = C_{fj}W^{-1}S^T$. Replacing Ξ_{ij} and Λ_i with $\tilde{\Xi}_{ij}$ and $\tilde{\Lambda}_i$ in inequalities (4.2.4)-(4.2.6), where $\tilde{\Lambda}_i$ is an arbitrary matrix with appropriate dimensions, these inequalities still hold. After replacing Ξ_{ij} and Λ_i with $\tilde{\Xi}_{ij}$ and $\tilde{\Lambda}_i$, then pre- and post- multiplying these inequalities by $diag\{H,\ H,\ H,\ H,\ H,\ I,\ I\}$ and its transpose with change of matrix variables defined by: $\overline{\Lambda}_i = diag\{H, H, H, H, H, I, I\}\Lambda_i diag\{H, H, H, H, H, I, I\}^T, \overline{G} = HGH^T, \overline{Q}_1 = HQ_1H^T, \overline{R}_1 = HR_1H^T, \overline{R}_2 = HR_2H^T, \overline{R}_3 = HR_3H^T, \overline{Z} = HZH^T, \overline{P} = HPH^T$. One can easily get (4.2.33)-(4.2.35). By Schur Complement with the condition $\Phi = \overline{\Phi}^T\overline{\Phi}$ it can be seen from (4.2.3) that

$$\tilde{\mathcal{G}}_{ij} = \begin{bmatrix} \varepsilon G & 0 & \overline{C}_{1ij}^T\overline{\Phi}^T \\ \star & (1-\varepsilon)G & \overline{C}_{2ij}^T\overline{\Phi}^T \\ \star & \star & I \end{bmatrix} > 0 \tag{4.2.40}$$

Then, perform congruence transformation to (4.2.40) with $diag\{H,\ H,\ I\}$ and its transpose gives the condition in (4.2.32). Therefore, if inequalities (4.2.30)-(4.2.35) in Theorem 4.2 hold, the filtering error system (4.1.5) is asymptotically stable and extended dissipative with the filter parameters given as follows:

$$A_{fj} = S^{-1}\overline{A}_{fj}S^{-T}W,\ B_{fj} = S^{-1}\overline{B}_{fj},\ C_{fj} = \overline{C}_{fj}S^{-T}W.$$

Or equivalently under transformation $S^{-T}Wx(t)$, the filter parameters can be yielded as:

$$\begin{aligned} A_{fj} &= S^{-T}W(S^{-1}\overline{A}_{fj}S^{-T}W)W^{-1}S^T = Y^{-1}\overline{A}_{fj}, \\ B_{fj} &= S^{-T}W(S^{-1}\overline{B}_{fj}) = Y^{-1}\overline{B}_{fj}, \\ C_{fj} &= (\overline{C}_{fj}S^{-T}W)W^{-1}S^T = \overline{C}_{fj}. \end{aligned}$$

This completes the proof. ■

Remark 4.6 *In terms of LMIs, Theorem 4.2 provides sufficient conditions for the design of a delay-dependent filter so as to guarantee that the filtering error system is extended dissipative. It is worth noting that the conditions in Theorem 4.2 are LMIs not only over the matrix variables, but also over the matrix* Ψ_3*. In Definition 4.1,* $\Psi_3 = \gamma^2 I$ *for* H_∞ *and* $L_2 - L_\infty$ *filtering problem,* $\Psi_3 = \gamma I$*, for passivity filtering problem, respectively, which imply that the scalar* γ*,* γ^2 *can be included as optimization variable to obtain optimal attenuation level* γ *for* $H_\infty, L_2 - L_\infty$*, passivity filtering problems, and can be readily obtained by solving the following convex optimization problem:*

Minimize γ *or* γ^2 *subject to (4.2.30)-(4.2.35)*

In Theorem 4.2, let $\Lambda_i = 0, \lambda_i = 0, i = 1, 2, \cdots, r$, we can easily obtain the following corollary related to filter design for fuzzy delay systems with matched membership functions.

Corollary 4.1 *Given scalars* $0 < \epsilon < 1$*,* $0 < \kappa < 1$*,* $\bar{\tau} > 0$*,* $l_i, i = 1, \cdots, 5$*, and matrices* $\overline{\Phi}$*,* $\overline{\Psi}_1$*,* Ψ_2*,* Ψ_3 *satisfying (4.2.29) and Assumption 1, system (4.1.5) is asymptotically stable and satisfies the unified performance index in Definition 1 for any time-varying delay* $0 < \tau(t) \leq \bar{\tau}$*, if there exist matrices* $X > 0$*,* $Y > 0$*,* $\overline{Q}_1 > 0$*,* $\overline{R}_1 > 0$*,* $\overline{R}_2 > 0$*,* $\overline{R}_3 > 0$*,* $\overline{G} > 0$*,* $\overline{L}$*,* $\overline{Z}$*,* $\overline{A}_{fj}$*,* $\overline{B}_{fj}$ *and* $\overline{C}_{fj}$ *such that the following conditions hold,* $\forall i,\ j \in \{1,\ 2, \cdots, r\}$*:*

$$\overline{G} - \overline{P} < 0 \tag{4.2.41}$$

$$\begin{bmatrix} \overline{R}_1 & \overline{Z} \\ \star & \overline{R}_1 \end{bmatrix} > 0 \tag{4.2.42}$$

$$\overline{\mathcal{G}}_{ij} = \begin{bmatrix} \varepsilon\overline{G} & 0 & \Upsilon_{4ij}\overline{\Phi}^T \\ \star & (1-\varepsilon)\overline{G} & \Upsilon_{5ij}\overline{\Phi}^T \\ \star & \star & I \end{bmatrix} > 0 \tag{4.2.43}$$

$$\bar{\Xi}_{ij} < 0 \tag{4.2.44}$$

Moreover, if above LMIs have feasible solutions, the desired delay dependent filter is obtained with parameters given by

$$\begin{cases} A_{fj} = Y^{-1}\overline{A}_{fj} \\ B_{fj} = Y^{-1}\overline{B}_{fj} \\ C_{fj} = \overline{C}_{fj}. \end{cases} \tag{4.2.45}$$

Other notations are the same as defined in Theorem 4.2.

Remark 4.7 *In general, if the premise variable of the original fuzzy model $\theta(t)$ is available, we can use the information of $\theta(t)$ to construct simple filter membership functions instead of complicated ones. Then, fuzzy filter with imperfect premise variables can be implemented based the obtained simple filter membership functions. For the case of T-S fuzzy system with unmeasurable parameters or uncertain parameters, a simple and effective solution is to construct a model-independent filter. Due to the fact that the fuzzy-rule-independent filter ignores the fuzzy rule, it has more conservativeness than the fuzzy-rule-dependent one. Until present, some approaches have been developed well to deal with the fuzzy-rule-dependent filter design problems of T-S fuzzy system with unmeasurable parameters (unmeasurable premise variables) or uncertain parameters, such as uncertain system approach [154] and switching filtering approach [155]. On the other side, implementation of the fuzzy-rule-dependent filter is more complex than that of fuzzy-rule-independent filter. Thus, how to reduce the implementation cost of the fuzzy-rule-dependent filtering, and simultaneously obtain low conservativeness for T-S fuzzy system with unmeasurable parameters or uncertain parameters by resorting to the imperfect premise matching method are interesting and challenging issues. Whereas it is not investigated in the present chapter due to the space limitation.*

4.3 Simulation results

In this section, two examples are given to verify the effectiveness and less conservativeness of the method proposed in this chapter.

Example 1: Consider T-S fuzzy system (4.1.2) with two plant rules($r = 2$) borrowed from [93], the parameters are as followings:

$$\begin{bmatrix} A_{11} & A_{21} & D_{11} \\ A_{12} & A_{22} & D_{12} \end{bmatrix} = \left[\begin{array}{cc|cc|c} -2.1 & 0.1 & -1.1 & 0.1 & 1 \\ 1 & -2 & -0.2 & -1.1 & -0.2 \\ \hline -1.9 & 0 & -0.9 & 0 & -0.3 \\ -0.2 & -1.1 & -1.1 & -1.2 & 0.1 \end{array}\right],$$

$$\begin{bmatrix} C_{11} & C_{21} & D_{21} \\ C_{12} & C_{22} & D_{22} \end{bmatrix} = \left[\begin{array}{cc|cc|c} 1 & -0.5 & 0.1 & 0 & 0 \\ \hline 0.5 & -0.6 & -0.2 & 1 & 0.1 \end{array}\right],$$

$$\begin{bmatrix} E_{11} & E_{21} & D_{31} \\ E_{12} & E_{22} & D_{32} \end{bmatrix} = \left[\begin{array}{cc|cc|c} 1 & 0 & -0.8 & 0.6 & 0.3 \\ \hline -0.2 & 0.3 & 0 & 0.2 & -0.6 \end{array}\right].$$

Membership functions for Rule 1 and Rule 2 are given as follows:

$$h_1(x_1(t)) = 1 - \frac{1}{1+e^{-3(x_1(t)+\frac{\pi}{2})}}\left(1 - \frac{1}{1+e^{-3(x_1(t)-\frac{\pi}{2})}}\right),\ h_2(x_1(t)) = 1 - h_1(x_1(t)),$$
$$m_1(x_1(t)) = 1 - 0.96e^{\frac{-x_1(t)^2}{2\times 1.6^2}},\ m_2(x_1(t)) = 1 - m_1(x_1(t)).$$

Remark 4.8 *An easy way to choose the membership function for the fuzzy filter is to find some simple membership functions whose profiles are similar to the system membership function. It only requires some simple trial processes to determine the filter membership functions that satisfy the unmatched condition $m_j - \lambda_j h_j \geq 0$, ($0 < \lambda_j < 1$) while preserving performance of the filter.*

The fuzzy filter, designed according to Theorem 4.2, can satisfy the prescribed

H_∞, $L_2 - L_\infty$, passive and dissipative performances. Due to limited space, only H_∞ performance is considered in this example.

To compare with the recently developed fuzzy H_∞ filter, set $\lambda_1 = 0.6$, $\lambda_2 = 0.9$, $\varepsilon = 0.5$, $\kappa = 0.9$, $\Phi = 0$, $\Psi_1 = -1$, $\Psi_2 = 0$, $\Psi_3 = \gamma^2$, $\bar{\tau} = 0.8$ in Theorem 4.2, the comparison results of minimum γ_{min} are listed in Table 4.1.

Table 4.1: Comparison of Minimum index γ in Example 1

Ref.	[94]	[93]	[106]	Th. 4.2	Cor 4.1
γ	0.35	0.22	0.32	0.22	0.23
Number of Variables	$11r+5$	$42r^2+8r+11$	$5r+9$	$4r+9$	$3r+9$

It can be clearly seen that the minimum disturbance attenuation level γ_{min} obtained by our approach is smaller than those obtained in Ref. [94]($\delta = 20$) and Ref. [106]. Although Theorem 4.2 in this chapter and Ref. [93] obtain the same minimum γ, Theorem 4.2 in this chapter involves $4r + 9$ decision variables, which are significantly fewer than $42r^2+8r+11$ decision variables contained in Ref. [93]. The simulation results in Table.4.1 demonstrate that the filter design approach proposed in this chapter is less conservativeness or more computational efficiency or both than those in Ref. [94], Ref. [106], Ref. [93] and Corollary 4.1. It is worth pointing out that the minimum attenuation level γ obtained by Theorem 4.2 is smaller than that obtained by Corollary 4.1, which verifies that imperfect premise filter can reduce conservativeness.

When $\bar{\tau} = 0.8$, we obtain a desired delay-dependent H_∞ fuzzy filter in the form of (4.1.4) with the following filter parameters

$$\begin{aligned}
\begin{bmatrix} A_{f1} & B_{f1} \\ A_{f2} & B_{f2} \end{bmatrix} &= \left[\begin{array}{cc|c} -4.3031 & -5.3024 & -2.4623 \\ -0.2069 & -4.3285 & 0.1056 \\ \hline -5.3295 & -1.9101 & -1.5309 \\ -1.8154 & -3.4272 & 0.0347 \end{array}\right], \\
\begin{bmatrix} C_{f1} & C_{f2} \end{bmatrix} &= \left[\begin{array}{cc|cc} -0.259 & 0.1335 & -0.0026 & -0.8033 \end{array}\right].
\end{aligned}$$

Fig. 4.1 depicts the responses of $z(t)$ and $z_f(t)$, and Fig. 4.2 shows the error response of $z(t)$-$z_f(t)$.

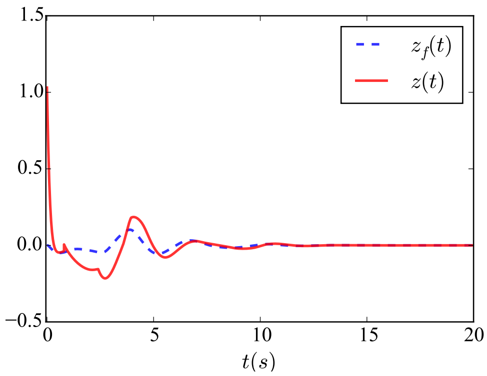

Fig. 4.1: Responses of $z(t)$ and $z_f(t)$

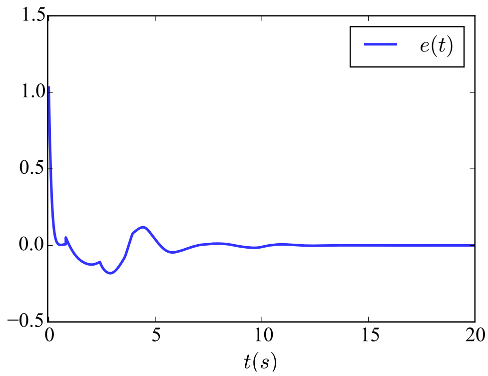

Fig. 4.2: Response of filtering error signal $e(t) = z(t) - z_f(t)$

Example 2: To further illustrate the effectiveness of the filter design method proposed in this chapter, we apply Theorem 4.2 to the continuous stirred tank reactor (CSTR) system borrowed from Ref. [156]. The system parameters and membership functions are given as follows:

$$A_{11} = \begin{bmatrix} -1.427 & 0.076 \\ 1.375 & -1.635 \end{bmatrix}, A_{12} = \begin{bmatrix} -2.051 & 0.396 \\ -5.343 & 0.724 \end{bmatrix}, A_{13} = \begin{bmatrix} -4.528 & 0.317 \\ -20.759 & -0.105 \end{bmatrix},$$
$$A_{21} = A_{22} = A_{23} = \begin{bmatrix} 0.25 & 0 \\ 0 & 0.25 \end{bmatrix}, D_{11} = D_{12} = D_{13} = \begin{bmatrix} -0.5 \\ 1 \end{bmatrix}$$
$$C_{11} = C_{12} = C_{13} = \begin{bmatrix} 5 & 2 \end{bmatrix}, C_{21} = C_{22} = C_{23} = \begin{bmatrix} 0 & 0 \end{bmatrix}, D_{21} = D_{22} = D_{23} = 0$$
$$E_{11} = E_{12} = E_{13} = \begin{bmatrix} 0 & 1 \end{bmatrix}, E_{21} = E_{22} = E_{23} = \begin{bmatrix} 0 & 0 \end{bmatrix}, D_{31} = D_{32} = D_{33} = 1$$

$$h_1(x_1(t)) = \begin{cases} 1 - \frac{1}{1+e^{-4x_1(t)+6}}, & x_1(t) \leq 2.7520 \\ 0, & x_1(t) > 2.7520 \end{cases}$$
$$h_2(x_1(t)) = \begin{cases} 1 - h_1(x_1(t)), & x_1(t) \leq 2.7520 \\ 1 - h_3(x_1(t)), & x_1(t) > 2.7520 \end{cases}$$

$$h_3(x_1(t)) = \begin{cases} 0, & x_1(t) \leq 2.7520 \\ \frac{1}{1+e^{-4x_1(t)+8}}, & x_1(t) > 2.7520 \end{cases}$$

$$m_1(x_1(t)) = \begin{cases} 1, & x_1(t) \leq 0.8882 \\ 1 - \frac{x_1(t)-0.8882}{2.7520-0.8882}, & 0.8882 < x_1(t) \leq 2.7520 \\ 0, & x_1(t) > 2.7520 \end{cases}$$

$$m_2(x_1(t)) = \begin{cases} 1 - m_1(x_1(t)), & x_1(t) \leq 2.7520 \\ 1 - m_3(x_1(t)), & x_1(t) > 2.7520 \end{cases}$$

$$m_3(x_1(t)) = \begin{cases} 0, & x_1(t) \leq 2.7520 \\ \frac{x_1(t)-2.7520}{4.7052-2.7520}, & 2.7520 < x_1(t) \leq 4.7052 \\ 1, & x_1(t) > 4.7052 \end{cases}$$

Now similar to Example 1, we use the filter design approach proposed in this chapter to design a $L_2 - L_\infty$ filter for the above fuzzy CSTR system. By using standard Matlab software, let $\lambda_1 = 0.75$, $\lambda_2 = 0.5$, $\varepsilon = 0.6$, $\kappa = 0.9$, $\bar{\tau} = 0.3$, $\Phi = 1$, $\Psi_1 = 0$, $\Psi_2 = 0$, $\Psi_3 = \gamma^2$, we can see that LMIs (4.2.30)-(4.2.35) in Theorem 4.2 are feasible. Then we can obtain that $\gamma_{min} = 2.24$, and the desired $L_2 - L_\infty$ filter parameters are given as follows:

$$\left[\begin{array}{c|c} A_{f1} & B_{f1} \\ \hline C_{f1} & \end{array}\right] = \left[\begin{array}{cc|c} -1.2237 & -0.0197 & -0.1147 \\ 1.6904 & -3.0930 & -1.6765 \\ \hline -4.8763 & -1.9885 & \end{array}\right]$$

$$\left[\begin{array}{c|c} A_{f2} & B_{f2} \\ \hline C_{f2} & \end{array}\right] = \left[\begin{array}{cc|c} -1.6641 & 0.2504 & -0.1155 \\ -2.7217 & -1.2159 & -1.6759 \\ \hline -4.8763 & -1.9885 & \end{array}\right]$$

$$\left[\begin{array}{c|c} A_{f3} & B_{f3} \\ \hline C_{f3} & \end{array}\right] = \left[\begin{array}{cc|c} -4.2883 & 0.3143 & -0.1180 \\ -20.8035 & -0.8783 & -1.6734 \\ \hline -4.8763 & -1.9885 & \end{array}\right]$$

In simulation, the disturbance input is defined as $w(t) = \frac{1}{2+t}, t \geq 0$. The initial condition of the system (4.1.2) is $x(0) = [-1 \ 0.2]^T$ and the initial condition of the corresponding filter system is $x_f(0) = [0\ 0]^T$. Fig.4.3 depicts the system state $x(t)$ and filter state $x_f(t)$. Fig.4.4 shows the response of filtering error signal $e(t)$, which shows that the filtering error finally reduces to zero. From these simulation

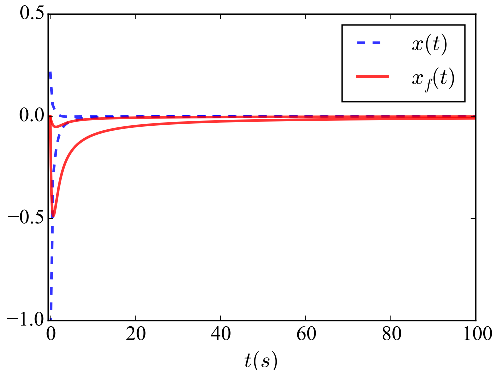

Fig. 4.3: Responses of system state $x(t)$ and filter state $x_f(t)$

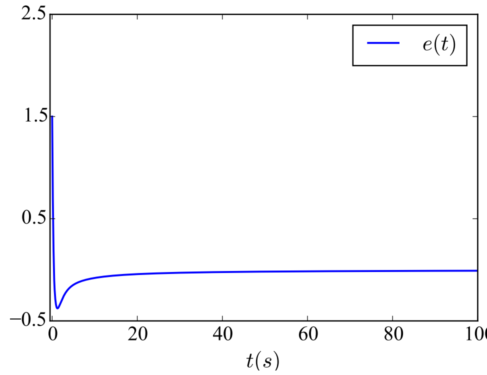

Fig. 4.4: Response of filtering error signal ~ $e(t) = z(t) - z_f(t)$

results, it can be seen that the filter design approach proposed in Theorem 4.2 can provide an accurate estimation of the desired signal in presence of external noise $w(t)$ and the designed $L_2 - L_\infty$ filter satisfies the specified requirements. The above results indicate again that the delay-dependent filter design method proposed in this chapter is effective.

4.4 Conclusion

This chapter focuses on extended dissipative filter design problem for fuzzy systems with time-varying delay under imperfect premise matching. Based on extended dissipative performance index, the H_∞, $L_2 - L_\infty$, passive and dissipative filter problems have been investigated. New delay-dependent conditions for performance analysis and filter design have been established in terms of LMIs by employing an efficient integral inequality. Finally, some numerical simulation results specific to H_∞ and $L_2 - L_\infty$ filtering problems have been provided to demonstrate the advantages of the method proposed in this chapter over some recent ones in the literature.

Chapter 5

Analysis and optimization of fuzzy membership functions with a frequency domain method

Although fuzzy control with imperfect premise matching can enhance design flexibility and reduce conservativeness, it also brings difficulty to parameters selection of membership functions. NCOS function based mismatched fuzzy membership function parameter optimization problems are studied in this chapter. In this chapter, finite frequency H_∞ controller design method for T-S fuzzy-model-based control system under imperfect premise matching is first given. Then to further improve the disturbance attenuation performance of the concerned frequency band, parameter optimization method of mismatched controller membership function based on the nCOS function is presented. GA is also given to verify the validity of the nCOS function based optimization method.

The novelty and contribution of this study lie in several aspects. (a) It is the first time that a frequency domain method is used for the analysis and optimization of Gaussian membership functions under imperfect premise matching control and to this aim a novel systematic frequency domain method for calculating the nCOS function of such a fuzzy system with nonlinear Gaussian membership function is developed; (b) The new nCOS function can greatly facilitate optimization of the mismatched membership parameters and gives an in-depth understanding of nonlinear influence on system performance due to membership function; (c)

Comparison results indicate that the disturbance suppression capability of the fuzzy controller is further enhanced by combining the finite frequency H_∞ control with the nCOS function based frequency domain optimization method.

The rest of the chapter is organized as follows: system description and problem formulation are given in section 5.1. Fuzzy controller design with mismatched membership function is given in section 5.2. nCOS function based optimization algorithm and GA optimization method are also presented in section 5.2. Applications of the method proposed in this chapter to nonlinear systems are given in Section 5.3. Conclusions are drawn in Section 5.4.

5.1 System description and problem formulation

In this section, T-S fuzzy model of nonlinear system and fuzzy controller with mismatched membership functions will be established.

Consider the following nonlinear system

$$\begin{cases} \dot{x}(t) = F_1(x(t), u(t), \omega(t)) \\ z(t) = F_2(x(t), u(t), \omega(t)) \end{cases} \tag{5.1.1}$$

where $F_1(x(t), u(t), \omega(t))$ and $F_2(x(t), u(t), \omega(t))$ are nonlinear functions, $x(t) \in \mathbb{R}^n$ is the system state vector, $\omega(t) \in \mathbb{R}^\omega$ is the disturbance input, $u(t) \in \mathbb{R}^m$ is the control input, and $z(t) \in \mathbb{R}^z$ is the controlled output. It is well known that any smooth nonlinear systems can be approximated by a T-S fuzzy model [88], then nonlinear system (5.1.1) can be expressed in the following form

Plant Rule i: IF $\theta_1(t)$ is μ_{i1} and $\theta_2(t)$ is μ_{i2} and $\cdots$ and $\theta_p(t)$ is μ_{ip}, THEN

$$\begin{cases} \dot{x}(t) = A_i x(t) + B_i u(t) + B_{\omega i}\omega(t) \\ z(t) = C_i x(t) + D_i u(t) \end{cases} \tag{5.1.2}$$

where $\mu_{i1}, \mu_{i2}, \cdots, \mu_{ip}$ are fuzzy sets, A_i, B_i, $B_{\omega i}$, C_i and D_i are constant matrices with compatible dimensions, $\theta(t) = [\theta_1(t), \theta_2(t), \cdots, \theta_p(t)]$ is the premise variable vector, and r is the number of fuzzy IF-THEN rules, $i = 1, 2, \cdots, r$. Throughout this thesis, it is assumed that the premise variables only depend on the system state $x(t)$. So the overall fuzzy system is inferred as follows

$$\begin{cases} \dot{x}(t) = \sum_{i=1}^{r} h_i(\theta(t)) \left[A_i x(t) + B_i u(t) + B_{\omega i}\omega(t)\right] \\ z(t) = \sum_{i=1}^{r} h_i(\theta(t)) \left[C_i x(t) + D_i u(t)\right] \end{cases} \tag{5.1.3}$$

where $h_i(\theta(t)) \geq 0, \sum_{i=1}^{r} h_i(\theta(t)) = 1$.

In this section, we consider a fuzzy controller that shares different premise variables with the fuzzy system, which is in the following structure:

Controller Rule j: IF $\eta_1(t)$ is N_{j1} and $\eta_2(t)$ is N_{j2} and $\cdots$ and $\eta_p(t)$ is N_{jp}, THEN

$$u(t) = K_j x(t), \tag{5.1.4}$$

where $j = 1, 2, \cdots, r$. The output of the mismatched fuzzy controller can be represented by the following form:

$$u(t) = \sum_{j=1}^{r} m_j(\eta(t)) K_j x(t) \tag{5.1.5}$$

$\eta(t) = [\eta_1(t), \eta_2(t), \cdots, \eta_p(t)]$ is the imperfect premise variable vector. Then the closed-loop fuzzy system can be represented as

$$\begin{cases} \dot{x}(t) = \overline{\boldsymbol{A}}(h, m)x(t) + \overline{\boldsymbol{B}}(h, m)\omega(t) \\ z(t) = \overline{\boldsymbol{C}}(h, m)x(t) \end{cases} \tag{5.1.6}$$

where

$$\overline{\boldsymbol{A}}(h, m) = \sum_{i=1}^{r}\sum_{j=1}^{r} h_i(\theta(t)) m_j(\eta(t)) \left[A_i + B_i K_j\right], \ \overline{\boldsymbol{B}}(h) = \sum_{i=1}^{r} h_i(\theta(t)) B_{\omega i},$$

$$\overline{\boldsymbol{C}}(h, m) = \sum_{i=1}^{r}\sum_{j=1}^{r} h_i(\theta(t)) m_j(\eta(t)) \left[C_i + D_i K_j\right].$$

$m_j(\eta(t)) \geq 0$, $\sum_{j=1}^{r} m_j(\eta(t)) = 1$. For simple description, we denote $h_i(\theta(t)) = h_i$, $m_j(\eta(t)) = m_j$, $\overline{\boldsymbol{A}}(h,m) = \overline{\boldsymbol{A}}$, $\overline{\boldsymbol{B}}(h) = \overline{\boldsymbol{B}}$, $\overline{\boldsymbol{C}}(h,m) = \overline{\boldsymbol{C}}$. For T-S fuzzy control with mismatched premise variables, various membership functions can be employed to enhance the design flexibility and/or lower the structural complexity of the fuzzy controller as long as the following conditions [110] are satisfied:

$$m_i - \lambda_i h_i \geq 0, 1 > \lambda_i > 0, i = 1, \cdots, r. \tag{5.1.7}$$

Remark 5.1 *Condition (5.1.7) only presents boundary constraint on the mismatched membership function. It is worth noting that except for this design condition, there are still some subjectively decided parameters in the mismatched controller membership function, which will also influence system performance. For example, Gaussian membership function, which is smooth and nonzero at all points has been extensively adopted as imperfect membership functions in some existing research work [23, 110, 116–118, 157]. But none of these works have systematically investigated the parameter selection of Gaussian membership function. Thus it is of great importance to explore how the parameters of mismatched controller membership function affect the closed-loop system performance.*

5.2 H_∞ controller design and membership function parameters optimization

5.2.1 Finite frequency H_∞ controller design

The finite frequency H_∞ control problem is to design a fuzzy controller such that the following inequality holds for all nonzero $\omega(t) \in \mathcal{L}_2[0,\ \infty)$ over a specified frequency band $[w_1\ w_2]$, where w_1 and w_2 correspondingly represent the lower and upper boundaries of the concerned frequency band.

$$\int_{w_1<w<w_2} Z^T(w)Z(w)dw - \gamma^2 \int_{w_1<w<w_2} W^T(w)W(w)dw \leq 0, w \in [w_1, w_2] \tag{5.2.1}$$

In addition, the following actuator saturation constraint is also considered

$$|u(t)| \leq u_{\max} \tag{5.2.2}$$

where $u_{\max}$ is the upper bound of the actuator force amplitude. The following lemma, which will be used to develop the main results in sequel, are introduced here.

Lemma 5.1 *(Projection Lemma) [158]: Given* Γ, Λ, Θ, *there exists a matrix* F *satisfying* $\Gamma F \Lambda + (\Gamma F \Lambda)^T + \Theta < 0$ *if and only if the following inequalities hold*

$$\Gamma^{\perp} \Theta \Gamma^{\perp T} < 0, \;\; \Lambda^{T^{\perp}} \Theta \Lambda^{T^{\perp T}} < 0$$

Finite frequency H_∞ controller design for the T-S fuzzy system under imperfect premise mismatching is presented in the following theorem.

Theorem 5.1 *For given scalars* η, δ, *the T-S fuzzy system (5.1.3) with controller (5.1.4) under condition* $m_j - \lambda_j h_j \geq 0, (0 < \lambda_j < 1)$ *is asymptotically stable with disturbance input* $\omega(t) = 0$ *and satisfies* H_∞ *disturbance attenuation performance* γ *over a given frequency band* $[w_1 \; w_2]$ *under energy-bounded disturbance* $\omega_{max} = (\eta - V(0))/\delta$, *if there exist symmetric matrices* P, Λ_i, $P_1 > 0$, $Q > 0$, $\forall i, j \in \{1,\ 2\ , \cdots, r\}$, *such that the following matrix inequalities hold*

$$\begin{bmatrix} [P_1 \overline{\boldsymbol{A}}]_s & P_1 \overline{\boldsymbol{B}} \\ \star & -\eta I \end{bmatrix} < 0 \tag{5.2.3}$$

$$\begin{bmatrix} \overline{\boldsymbol{A}} \, \overline{\boldsymbol{B}} \\ I \;\; 0 \end{bmatrix}^T \begin{bmatrix} -Q & P + jw_c Q \\ P - jw_c Q & -w_1 w_2 Q \end{bmatrix} \begin{bmatrix} \overline{\boldsymbol{A}} \, \overline{\boldsymbol{B}} \\ I \;\; 0 \end{bmatrix} + \begin{bmatrix} \overline{\boldsymbol{C}}^T \overline{\boldsymbol{C}} & 0 \\ 0 & -\gamma^2 I \end{bmatrix} < 0 \tag{5.2.4}$$

$$\begin{bmatrix} -I & \sqrt{\delta} K_j \\ \star & -u_{max}^2 P_1 \end{bmatrix} < 0 \tag{5.2.5}$$

where $w_c = (w_1 + w_2)/2$.

Proof: First, we prove that the closed-loop system is asymptotically stable when $\omega(t) = 0$. Consider the following quadratic Lyapunov function

$$V(t) = x^T(t)P_1x(t) \tag{5.2.6}$$

P_1 is a positive definite matrix. Time derivative of $V(t)$ can be expressed as

$$\begin{aligned}\dot{V}(t) =& \dot{x}^T(t)P_1x(t) + x^T(t)P_1\dot{x}(t) \\ =& \sum_{i=1}^{r}\sum_{j=1}^{r} h_i m_j x^T(t)\left[\bar{A}_{ij}^T P_1 + P_1\bar{A}_{ij}\right]x(t) \\ \leq& \sum_{i=1}^{r}\sum_{j=1}^{r} h_i m_j x^T(t)\left[\bar{A}_{ij}^T P_1 + P_1\bar{A}_{ij} + \frac{1}{\eta}P_1\bar{B}_{ij}\bar{B}_{ij}^T P_1\right]x(t)\end{aligned} \tag{5.2.7}$$

By using Schur complement, inequality (5.2.3) can be rewritten as

$$[P_1\overline{\boldsymbol{A}}]_s + \frac{1}{\eta}P_1\overline{\boldsymbol{B}}\overline{\boldsymbol{B}}^T P_1 < 0$$

Then we can obtain

$$\dot{V}(t) \leq 0 \tag{5.2.8}$$

Thus we come to the conclusion that the closed-loop system is asymptotically stable with disturbance $\omega(t) = 0$.

For any constant $\eta > 0$, the following inequality holds

$$2x^T(t)P_1\overline{\boldsymbol{B}}\omega(t) \leq \frac{1}{\eta}x^T(t)P_1\overline{\boldsymbol{B}}\overline{\boldsymbol{B}}^T P_1x(t) + \eta\omega^T(t)\omega(t) \tag{5.2.9}$$

According to (5.2.7), (5.2.8) and (5.2.9), for $\forall\ \omega(t) \neq 0$, we can obtain

$$\begin{aligned}\dot{V}(t) \leq& x^T(t)\left[\overline{\boldsymbol{A}}P_1 + P_1\overline{\boldsymbol{A}} + \frac{1}{\eta}P_1\overline{\boldsymbol{B}}\overline{\boldsymbol{B}}^T P_1\right]x(t) + \eta\omega^T(t)\omega(t) \\ \leq& \eta\omega^T(t)\omega(t)\end{aligned} \tag{5.2.10}$$

Integrate both sides of inequality (5.2.10) from 0 to t, the following inequality can be obtained

$$V(t) - V(0) \leq \eta\int_0^t \omega^T(t)\omega(t)dt \leq \eta\|\omega(t)\| = \eta\omega_{\max}$$

which indicates that

$$x^T(t)P_1x(t) \leq V(0) + \eta\omega_{\max} \triangleq \delta \tag{5.2.11}$$

Consider control input, we have

$$\begin{aligned}\max_{t\geq 0}|u(t)|^2 &\leq \max_{t\geq 0}\left\|\sum_{j=1}^{r} m_j[x^T(t)K_j^TK_jx(t)]\right\|_2 \qquad (5.2.12)\\ &= \max_{t\geq 0}\left\|\sum_{j=1}^{r} m_j[x^T(t)P_1^{\frac{1}{2}}P_1^{-\frac{1}{2}}K_j^TK_jP_1^{-\frac{1}{2}}P_1^{\frac{1}{2}}x(t)]\right\|_2\\ &\leq \delta\lambda_{\max}\left\{\sum_{j=1}^{r} m_j[P_1^{-\frac{1}{2}}K_j^TK_jP_1^{-\frac{1}{2}}]\right\}\end{aligned}$$

Then one can obtain that constraints on control input are satisfied if the following inequality holds

$$\delta P_1^{-\frac{1}{2}}K_j^TK_jP_1^{-\frac{1}{2}} < u_{\max}^2 I \tag{5.2.13}$$

Apply Schur complement to inequality (5.2.5), (5.2.13) can be obtained.

Next we prove that the frequency performance constraints hold. For inequality (5.2.4), multiply $[x^T(t)\ \omega^T(t)]$ and its conjugate transpose on the left and right side of inequality (5.2.4), we can obtain

$$2\dot{x}^T(t)Px(t)-\dot{x}^T(t)P\dot{x}(t)+jw_cx^T(t)Q\dot{x}(t)+z^T(t)z(t)-\gamma^2\omega^T(t)\omega(t) \leq 0 \tag{5.2.14}$$

Note that for any vectors ζ and φ, equation $\zeta^TQ\varphi = \mathrm{tr}\left(\varphi\zeta^TQ\right)$ always holds. Thus inequality (5.2.14) can be rewritten as

$$\begin{aligned}&\frac{dx^T(t)Px(t)}{dt}+z^T(t)z(t)-\gamma^2\omega^T(t)\omega(t)\\ &\leq \mathrm{tr}\left[\mathbf{He}\left((w_1x(t)+j\dot{x}(t))(w_2x(t)+j\dot{x}(t))^T\right)Q\right] \qquad (5.2.15)\end{aligned}$$

where $\mathbf{He}(A) = \frac{A+A^T}{2}$. Integrating both sides of (5.2.15) from 0 to t yields

$$\int_0^t x^T(t)Px(t)dt + \int_0^t z^T(t)z(t)dt - \int_0^\infty \gamma^2\omega^T(t)\omega(t)dt \leq \mathrm{tr}\left[\mathbf{He}(S)Q\right] \tag{5.2.16}$$

where $S = \int_0^\infty (w_1 x(t) + j\dot{x}(t))(w_2 x(t) + j\dot{x}(t))^T dt$. $\int_0^t x^T(t)Px(t)dt \geq 0$ holds when $P > 0$, then the following inequality can be obtained

$$\int_0^t z^T(t)z(t)dt - \int_0^\infty \gamma^2 \omega^T(t)\omega(t)dt \leq \mathrm{tr}\left[\mathbf{He}(S)Q\right] \tag{5.2.17}$$

Then according to the Parseval's theorem [159], we have

$$S = \frac{1}{2\pi}\int_{-\infty}^{\infty}(w_1 - w)(w_2 - w)X^T(w)X(w)dw$$
$$\int_0^\infty x^T(t)x(t)dt = \frac{1}{2\pi}\int_{-\infty}^{\infty} X^T(w)X(w)dw$$
$$\int_0^\infty \omega^T(t)\omega(t) = \frac{1}{2\pi}\int_{-\infty}^{\infty} W^T(w)W(w)dw$$

where $X(w)$, $W(w)$ are continuous Fourier transform of $x(t)$ and $\omega(t)$.

$\mathrm{tr}\left[\mathbf{He}(S)Q\right] < 0$, $w \in [w_1,\ w_2]$ holds when $(w_1 - w)(w_2 - w) < 0$, then inequality (5.2.1) holds, which indicates that the closed-loop system satisfies the finite frequency H_∞ performance. This completes the proof. ■

Since conditions (5.2.3)-(5.2.5) are not strictly linear matric inequalities, hence, it cannot be handled directly by MATLAB LMI optimization tools. In order to solve the nonlinear problem, the following theorem is obtained through linearization.

Theorem 5.2 *For given scalars η, δ, the closed-loop fuzzy system under condition $m_j - \lambda_j h_j \geq 0, (0 < \lambda_j < 1)$, is asymptotically stable with disturbance input $\omega(t) = 0$ and satisfies H_∞ disturbance attenuation performance γ over given frequency band $[w_1\ w_2]$, if there exist symmetric matrices $\bar{P}$, $\bar{\Lambda}_i$, and positive definite symmetric matrices $F > 0$, $\bar{Q} > 0$, $\forall i, j \in \{1,\ 2\ , \cdots\ , r\}$, such that the following matrix inequalities hold*

$$\bar{\Theta}_{ii} - \bar{\Lambda}_i < 0 \tag{5.2.18}$$

$$\bar{\Theta}_{ii} - \lambda_i\bar{\Lambda}_i + \bar{\Lambda}_i < 0 \tag{5.2.19}$$

$$\bar{\Theta}_{ij} - \lambda_j\bar{\Lambda}_i - \lambda_i\bar{\Lambda}_j + \bar{\Lambda}_i + \bar{\Lambda}_j < 0,\ i < j \tag{5.2.20}$$

$$\begin{bmatrix} -\bar{Q} & \bar{P}+jw_c\bar{Q}-F & 0 & 0 \\ \star & \bar{\Omega}_{ij} & B_{\omega i} & F^T C_i^T+\bar{K}_j^T D_i^T \\ \star & \star & -\gamma^2 I & 0 \\ \star & \star & \star & -I \end{bmatrix} < 0 \tag{5.2.21}$$

$$\begin{bmatrix} -I & \sqrt{\delta}\bar{K}_j \\ \star & -u_{max}^2 F \end{bmatrix} < 0 \tag{5.2.22}$$

where

$$w_c = (w_1 + w_2)/2, \bar{\Omega}_{ij} = -w_1 w_2 \bar{Q}+[A_i F+B_i\bar{K}_j]_s$$

$$\bar{\Theta}_{ij} = \begin{bmatrix} [A_i F+B_i\overline{K}_j]_s & B_{\omega i} \\ \star & -\eta I \end{bmatrix}$$

Then the fuzzy controller gain can be obtained as

$$K_j = \bar{K}_j F^{-1} \tag{5.2.23}$$

Proof: It's easy to verify that (5.2.4) and the following inequality are equivalent

$$\begin{bmatrix} \overline{\boldsymbol{A}} & \overline{\boldsymbol{B}} \\ I & 0 \\ 0 & I \end{bmatrix}^T \Phi \begin{bmatrix} \overline{\boldsymbol{A}} & \overline{\boldsymbol{B}} \\ I & 0 \\ 0 & I \end{bmatrix} < 0 \tag{5.2.24}$$

where

$$\Phi = \begin{bmatrix} -Q & P + jw_c Q & 0 \\ P - jw_c Q & w_1 w_2 Q + \overline{\boldsymbol{C}}^T\overline{\boldsymbol{C}} & 0 \\ 0 & 0 & -\gamma^2 I \end{bmatrix} \tag{5.2.25}$$

We also know that the following equation always holds

$$\begin{bmatrix} I & 0 \\ 0 & 0 \\ I & I \end{bmatrix}^T \Phi \begin{bmatrix} I & 0 \\ 0 & 0 \\ I & I \end{bmatrix} = \begin{bmatrix} -Q & 0 \\ 0 & -\gamma^2 I \end{bmatrix} < 0 \tag{5.2.26}$$

According to Lemma 5.1 with

$$\Gamma^{\perp} = \begin{bmatrix} \overline{\boldsymbol{A}}\, I\, 0 \\ \overline{\boldsymbol{B}}\, 0\, I \end{bmatrix},\ \Pi^{\perp} = \begin{bmatrix} I\, 0\, 0 \\ 0\, 0\, I \end{bmatrix}$$

the following inequality is sufficient condition for (5.2.4)

$$\Phi + \begin{bmatrix} -I \\ \overline{\boldsymbol{A}}^T \\ \bar{\boldsymbol{b}}^T \end{bmatrix} P_1 \begin{bmatrix} 0\, I\, 0 \end{bmatrix} + \begin{bmatrix} 0\, I\, 0 \end{bmatrix}^T P_1 \begin{bmatrix} -I \\ \overline{\boldsymbol{A}}^T \\ \overline{\boldsymbol{B}}^T \end{bmatrix}^T < 0 \qquad (5.2.27)$$

Then substitute $\overline{\boldsymbol{A}} = \sum_{i=1}^{r}\sum_{j=1}^{r} h_i m_j \left[A_i + B_i K_j\right]$, $\overline{\boldsymbol{C}} = \sum_{i=1}^{r}\sum_{j=1}^{r} h_i m_j \left[C_i + D_i K_j\right]$, $\overline{\boldsymbol{B}} = \sum_{i=1}^{r} h_i B_{\omega i}$ into inequality (5.2.27), the following inequality can be obtained

$$\sum_{i=1}^{r}\sum_{j=1}^{r} h_i m_j \Xi_{ij} < 0 \qquad (5.2.28)$$

where

$$\Xi_{ij} = \begin{bmatrix} -Q & -P_1 + P + jw_c Q & 0 \\ \star & \Omega_{ij} & P_1 B_{\omega i} \\ \star & \star & -\gamma^2 I \end{bmatrix}$$

$$\Omega_{ij} = \left[A_i P_1 + B_i K_j P_1\right]_s + w_1 w_2 Q + \left[C_i + D_i K_j\right]^T \left[C_i + D_i K_j\right]$$

Since $h_i, m_j > 0$, thus we have $\Xi_{ij} < 0$. According to Schur Complement $\Xi_{ij} < 0$ can be equivalently transformed into

$$\begin{bmatrix} -Q & -P_1 + P + jw_c Q & 0 & 0 \\ \star & \left[A_i P_1 + B_i K_j P_1\right]_s + w_1 w_2 Q & P_1 B_{\omega i} & C_i + D_i K_j \\ \star & \star & -\gamma^2 I & 0 \\ \star & \star & \star & -I \end{bmatrix} < 0 \qquad (5.2.29)$$

Define following new matrix variables $\bar{Q} = F^{-T} Q F^{-1}, \bar{P} = F^{-T} P F^{-1}, \bar{P}_1 =$

$F^{-1}, \bar{K}_j = K_j F^{-1}$, $\Upsilon_1 = \mathrm{diag}\{F^{-1}, F^{-1}, I, I\}$, then perform congruence transformation to (5.2.29) by pre- and post-multiplying Υ_1^T and its conjugate transpose, (5.2.21) can be obtained.

Substitute $\overline{\boldsymbol{A}} = \sum_{i=1}^r \sum_{j=1}^r h_i m_j [A_i + B_i K_j]$, $\overline{\boldsymbol{C}} = \sum_{i=1}^r \sum_{j=1}^r h_i m_j [C_i + D_i K_j]$, $\overline{\boldsymbol{B}} = \sum_{i=1}^r h_i B_{\omega i}$ into inequality (5.2.3), the following inequality can be obtained

$$\sum_{i=1}^r \sum_{j=1}^r h_i m_j \Theta_{ij} < 0 \tag{5.2.30}$$

where

$$\Theta_{ij} = \begin{bmatrix} [P_1 A_i + B_i K_j]_s & P_1 B_{\omega i} \\ \star & -\eta I \end{bmatrix}$$

Taking property of fuzzy membership function into consideration, we have

$$\sum_{i=1}^r \sum_{j=1}^r h_i (h_j - m_j) \Lambda_i = 0 \tag{5.2.31}$$

where $\Lambda_i = \Lambda_i^T$ is arbitrary matrix with appropriate dimension, add 5.2.31)to inequality (5.2.30), the following results can be obtained

$$\begin{aligned}
\sum_{i=1}^r \sum_{j=1}^r h_i m_j \Theta_{ij} =& \sum_{i=1}^r \sum_{j=1}^r h_i (h_j - m_j + \lambda_j h_j - \lambda_j h_j) \Lambda_i + \sum_{i=1}^r \sum_{j=1}^r h_i m_j \Theta_{ij} \\
=& \sum_{i=1}^r \sum_{i=1}^r h_i^2 (\lambda_i \Theta_{ii} - \lambda_i \Lambda_i + \Lambda_i) + \sum_{i=1}^{r-1} \sum_{j=i+1}^r h_i h_j (\lambda_j \Theta_{ij} - \lambda_j \Lambda_i \\
&+ \Lambda_i + \lambda_i \Theta_{ji} - \lambda_i \Lambda_j + \Lambda_j) + \sum_{i=1}^r \sum_{j=1}^r h_i (m_j - \lambda_j h_j)(\Theta_{ij} - \Lambda_i)
\end{aligned}$$

Then if (5.2.32)-(5.2.34) hold

$$\Theta_{ij} - \Lambda_i < 0 \tag{5.2.32}$$

$$\lambda_i \Theta_{ii} - \lambda_i \Lambda_i + \Lambda_i < 0 \tag{5.2.33}$$

$$\lambda_j \Theta_{ij} + \lambda_i \Theta_{ji} - \lambda_j \Lambda_i - \lambda_i \Lambda_j + \Lambda_i + \Lambda_j < 0,\ i < j \tag{5.2.34}$$

then (5.2.30) also holds. Define $\Upsilon_2 = \mathrm{diag}\{F^{-1}, I\}$, pre- and post-multiply

(5.2.32)-(5.2.34) by Υ_2^T and its transpose, inequality (5.2.18)-(5.2.20) can be obtained. This completes the proof. ■

5.2.2 Optimization of mismatched membership functions' parameters based on nCOS function

In this part, nCOS function based optimization method is applied to obtain the optimal parameters of the mismatched controller membership functions. Some basic definitions are first introduced.

Nonlinear output spectrum for single-input multiple-output system

Nonlinear systems can usually be identified or modeled into parametric model such as nonlinear differential equation (NDE), nonlinear autoregressive with exogenous input (NARX) and nonlinear block oriented (NBO) in practice. Nonlinear output spectrum of those nonlinear systems is not only a function of frequency variables but also functions of model parameters and input magnitude. Volterra model of a single-input multiple-output (SIMO) nonlinear differential equation system is given as follows [26]:

$$\begin{cases} y_i(t) = \sum_{n=1}^{N} y_i^n(t) \\ y_i^n(t) = y_i^0(t) + \int_{-\infty}^{\infty} \cdots \int_{-\infty}^{\infty} h_i^n(\tau_1, \cdots, \tau_n) \prod_{k=1}^{n} u(t-\tau_k) d\tau_k \end{cases} \tag{5.2.35}$$

where $y_i(t)$ and $u(t)$ are the ith subsystem output and input of the system, respectively, N is the maximum order of the system nonlinearity, $h_i^n(\tau_1, \cdots, \tau_n)$ is the nth order Volterra kernel, y_i^0 is zero or the DC constant. Then the nth order GFRF can be defined by the multi-dimensional Fourier transform as [126]

$$H_i^n(jw_1, \cdots, jw_n) = \int_{-\infty}^{\infty} \cdots \int_{-\infty}^{\infty} h_i^n(\tau_1, \cdots, \tau_n) e^{-j(w_1\tau_1 + \cdots + w_n\tau_n)} d\tau_1 \cdots d\tau_n \tag{5.2.36}$$

Then (5.2.35) can also be rewritten as [160]

$$y_i(t) = \sum_{n=1}^{N} y_i^n(t) \tag{5.2.37}$$

$$= H_i^0 + \frac{1}{2\pi}\int_{-\infty}^{\infty}\left[\frac{1}{(2\pi)^{n-1}}\underbrace{\int_{-\infty}^{\infty}\cdots\int_{-\infty}^{\infty}}_{n-1}\Xi_i^n dw_1\cdots dw_{n-1}\right]e^{jwt}dw$$

where

$$\Xi_i^n = H_i^n(jw_1,\cdots,jw_{n-1},j(w-w_1-\cdots-w_{n-1}))\times U_n(jw_1,\cdots,jw_{n-1})$$

$U_n(jw_1,\cdots,jw_{n-1}) = U(jw_1)\cdots U(jw_{n-1})U(j(w-w_1-\cdots-w_{n-1}))$, $w_n = w - w_1 - \cdots - w_{n-1}$, $U(jw)$ is the input spectrum, H_i^0 is associated with the 0th order output y_i^0, which is independent of input. The output y_i^n in the frequency domain is written as

$$Y_i^n(jw) = \frac{1}{(2\pi)^{n-1}}\underbrace{\int_{-\infty}^{\infty}\cdots\int_{-\infty}^{\infty}}_{n-1}\Xi_i^n dw_1\cdots dw_{n-1} \tag{5.2.38}$$

$$Y_i(jw) = \sum\nolimits_{n=1}^{N} Y_i^n(jw). \tag{5.2.39}$$

5.2.3 Computation of the nonlinear output spectrum

The nonlinear output spectrum of a SIMO system from the first order to the nth order can be analytically computed based on numerical or experimental data using least square method [49,124,125]. Considering the truncation error $\sigma_{[N]}(jw)$ and input $\rho U(jw)$ with magnitude ρ, the nonlinear output spectrum in (5.2.39) is presented as

$$\begin{aligned} Y_i(jw)_\rho &= \sum\nolimits_{n=1}^{\infty} \rho^n Y_i^n(jw) \\ &= \rho Y_i^1(jw) + \rho^2 Y_i^2(jw) + \rho^3 Y_i^3(jw) + \cdots \\ &= \sum\nolimits_{i=1}^{N} \rho^n Y_i^n(jw) + \sigma_{[N]}(jw) \end{aligned} \tag{5.2.40}$$

where $\sigma_{[N]}(jw)$ is the truncation error, which includes all the remaining higher order output spectrum components in Volterra series expansion, ρ represents different magnitudes of input. To determine $Y_i(jw)_\rho$, the system can be excited by the same input $U(jw)$ with different magnitudes $\rho_1, \rho_2, \cdots, \rho_N$ and there will be a series of output denoted by $Y_i(jw)_{\rho_1}, Y_i(jw)_{\rho_2}, \cdots, Y_i(jw)_{\rho_N}$. Then the nth order output spectrum $Y_i^n(jw)$, $n \in \{1, 2, \cdots, N\}$ is calculated as

$$\begin{bmatrix} Y_i^1(jw) \\ Y_i^2(jw) \\ \vdots \\ Y_i^N(jw) \end{bmatrix} = \begin{bmatrix} \rho_1 & \rho_1^2 & \cdots & \rho_1^N \\ \rho_2 & \rho_2^2 & \cdots & \rho_2^N \\ \vdots & \vdots & \ddots & \vdots \\ \rho_N & \rho_N^2 & \cdots & \rho_N^N \end{bmatrix}^{-1} \begin{bmatrix} Y_i(jw)_{\rho_1} \\ Y_i(jw)_{\rho_2} \\ \vdots \\ Y_i(jw)_{\rho_N} \end{bmatrix} \tag{5.2.41}$$

The square matrix is nonsingular if $\rho_1 \neq \rho_2 \neq \cdots \neq \rho_N$. An important issue of applying the above method for estimation of the output spectrum is how to select appropriate excitation magnitude ρ with consistent accuracy. To find the best excitation parameter ρ, a ρ-selection method in [49] can be adopted. Generally, ρ can start with a small number and increases regularly by δ until a larger number. For each ρ, run the method above to estimate first-, second- and third-order output spectrum, and eventually generate the $|Y_i^n(jw)| \backsim \rho$ curve; the best value of ρ corresponds to the bottom of the resulting U-shaped curve which results in a smaller estimation error for $|Y_i^n(jw)|$.

5.2.4 Optimization of fuzzy membership function parameters by nCOS function

The controller gains K_j are obtained according to the finite frequency H_∞ controller design method in Theorem 5.2. For the mismatched fuzzy controller adopting the Gaussian shape membership function, the closed-loop T-S fuzzy system can be reformulated as the following general exponential-type nonlinear system [161] by substituting the fuzzy controller (5.1.5) into the original nonlinear plant

$$f_1(\hat{x}, \hat{\omega}) + f_2(\hat{x}, \hat{\omega})\, e^{g(\hat{x},\hat{\omega})} = \sum_{l=0}^{L} \frac{d^l \omega}{dt^l} \tag{5.2.42}$$

where $\quad \hat{x} = \left\{ x, \frac{d^1 x}{dt}, \frac{d^2 x}{dt^2}, \cdots, \frac{d^L x}{dt^L} \right\}, \hat{\omega} = \left\{ \omega, \frac{d^1 \omega}{dt}, \frac{d^2 \omega}{dt^2}, \cdots, \frac{d^L \omega}{dt^L} \right\}$

and $f_1(\hat{x}, \hat{\omega})$, $f_2(\hat{x}, \hat{\omega})$ and $g(\hat{x}, \hat{\omega})$ are polynomial functions of system state x and input ω, l is the differential order with maximum order L.

According to equation (5.2.41), the nonlinear characteristic output spectrum can be analytically computed based on experimental data and least square method, which will be very useful for the analysis and optimization of membership function parameters. The optimization process for mismatched fuzzy controller with Gaussian shape membership function is summarized in **Algorithm 1**.

Algorithm 1: Optimization of fuzzy membership function parameters

---

(1) Define new state variables $y_1 = x$ and $y_2 = e^{g(\hat{x}, \hat{\omega})}$, then by taking derivative of y_2 with respect to time, the following equation can be obtained:

$$\frac{dy_2}{dt} = e^{g(\hat{x}, \hat{\omega})} \frac{d\, g(\hat{x}, \hat{\omega})}{dt} = y_2 \frac{d\, g(\hat{y}_1, \hat{\omega})}{dt} \tag{5.2.43}$$

Then the closed-loop system (5.2.42) can be equivalently transformed into the following single input multiple output polynomial nonlinear system with the same initial conditions of (5.2.42) and $y_2(0) = e^{g(\hat{x}(0), \hat{\omega}(0))}$:

$$\begin{cases} f_1(\hat{y}_1, \hat{\omega}) + f_2(\hat{y}_1, \hat{\omega}) y_2 = \sum_{l=0}^{L} \frac{d^l \omega}{dt^l} \\ \frac{dy_2}{dt} = y_2 \frac{d\, g(\hat{y}_1, \hat{\omega})}{dt} \end{cases} \tag{5.2.44}$$

(2) Based on the probing method [26], assume the input is $\omega(t) = e^{j(w_1 + \cdots + w_n)t}$, system state of (5.2.44) is expressed as

$$y_i = H_i^0 + \sum_{\substack{\text{all combinations} \\ \text{of } w_{i1} \text{ in } w}} H_i^1(w_{i1}) e^{j w_{i1} t} + \cdots \tag{5.2.45}$$

$$+ \sum_{\substack{\text{all permutations} \\ \text{of } (w_{i1},\cdots,w_{in})}} \sum_{\text{all combinationsof } w_{i1} \text{ in } w} H_i^n(w_{i1},\cdots,w_{in})e^{j(w_{i1}+\cdots+w_{in})t}$$

where $w=(w_1,\cdots,w_n)$. Substitute (5.2.45) into (5.2.44) and equate the coefficients of $e^{j(w_1+\cdots+w_n)t}$ to zero, the explicit formula of the nth order GFRFs can be obtained. Substitute GFRFs into (5.2.38) with some manipulation, the output spectrum can be obtained.

(3) With the estimated $Y_i(jw)_\rho$ from (5.2.40), the unknown frequency coefficients regarding to w in nCOS function are determined by using the least square method. Then the relationship between the nonlinear parameters that we are interested in and the output spectrum of (5.2.42) can thus be obtained, which can clearly demonstrate how the parameters of interest affect system frequency response. The optimal parameters of membership function for the mismatched controller can be obtained where the output spectrum is minimized.

Remark 5.2 *The nCOS function based optimization method in Algorithm 1 can be applied to analysis and design of the control systems with exponential type nonlinearities. Parameters optimization for the mismatched fuzzy controller adopting Gaussian shape membership function is one of the applications of nCOS function based frequency domain method. If the mismatched membership function is polynomial type, the methods in [27, 48, 49, 160] can easily obtain the nCOS function for polynomial type nonlinear system and thus determine the optimal parameters.*

5.2.5 GA-based optimization of mismatched membership functions' parameters

Another solution to the aforementioned parameters optimization problem of the T-S fuzzy system adopting Gaussian shape mismatched membership function is using search-based optimization method. In this chapter, GA is adopted to verify the validity and effectiveness of the nCOS function based frequency domain method. The objective is to seek optimal parameters in fuzzy membership functions to minimize the output frequency response $|Y(jw)|$. GA has great potential in global optimization, is appropriate to deal with the optimization problem in this chapter. In the following, standard GA is applied to search the parameter space to seek for the optimal fuzzy membership function. The process of GA optimization is summarized in **Algorithm 2**.

Algorithm 2: Optimization of fuzzy membership function parameters using GA

(1) Specify bounds of the parameters in Gaussian membership function.

(2) Encode the parameters to a binary string and generate an initial population of N chromosomes randomly.

(3) Decode the initial population into practical values of system's parameters.

(4) For each set of parameters, calculate the output frequency response $|Y(jw)|$ of the closed-loop fuzzy system.

(5) Cross over with a probability p_c and mutate with a probability p_m.

(6) Retain the best chromosomes in the population.

(7) Check if the maximum number of iterations is reached or the convergent conditions are satisfied. If so, stop and output the result. If not, repeat Step 4-7.

5.3 Applications to nonlinear mechanical systems

In this section, two nonlinear systems are considered: one is a simple numerical nonlinear system and another is a nonlinear quarter suspension systems. These examples are provided to evaluate the validity and superiority of the frequency domain based optimization approach proposed in this chapter.

5.3.1 Numerical example

First we consider a simple nonlinear system in [162]

$$\ddot{\xi}(t) = -0.02\xi(t) - 0.67\xi(t)^3 + u(t) + \omega(t) \tag{5.3.1}$$

Assume $\xi(t) \in [-d, d]$, $d \geq 0$. Denote $x_1(t) = \xi(t)$ and $x_2(t) = \dot{\xi}(t)$, according to sector nonlinearity method, the nonlinear system can be exactly represented on $[-d,\ d]$ by the following overall fuzzy system

$$\begin{cases} \dot{x}(t) = \sum_{i=1}^{2} h_i(x(t))\left[A_i x(t) + B_i u(t) + B_{\omega i}\omega(t)\right] \\ z(t) = \sum_{i=1}^{2} h_i(x(t)) C_i x(t) \end{cases} \tag{5.3.2}$$

where $x(t) = [x_1^T(t)\ \ x_2^T(t)]^T$.

$$h_1(x(t)) = 1 - x_1(t)^2/d^2,\ h_2(x(t)) = x_1(t)^2/d^2 \tag{5.3.3}$$

$$A_1 = \begin{bmatrix} 0 & 1 \\ -0.02 & 0 \end{bmatrix}, A_2 = \begin{bmatrix} 0 & 1 \\ -0.02 - 0.67d^2 & 0 \end{bmatrix}, B_1 = B_2 = \begin{bmatrix} 0 \\ 1 \end{bmatrix}, B_{w1} = B_{w2} = \begin{bmatrix} 0 \\ 1 \end{bmatrix},$$

$C_1 = [0\ 0.5],\ C_2 = [0\ 0.5]$

Controller membership functions are chosen as

$$m_1(x(t)) = 1 - a\,e^{-\frac{(x_1-b)^2}{2\times c^2}},\ m_2(x(t)) = a\,e^{-\frac{(x_1-b)^2}{2\times c^2}} \tag{5.3.4}$$

where $d = 2$, $a = 0.95$, $b \in [-6,\ 6]$, $c \in [0.84,\ 6]$, $w_1 = 0.01$, $w_2 = 1$ with permissible parameters $\lambda_1 = 0.05$ and $\lambda_2 = 0.0011$. Controller gains obtained from Theorem 5.2 can be written as $K_1 = [k_{11}\ k_{12}]$, $K_2 = [k_{21}\ k_{22}]$, so the overall controller is

$$\begin{aligned} u(t) =& \sum_{i=1}^{2} m_i(\xi(t))K_i x(t) \\ =& k_{11}\xi(t)+k_{12}\dot{\xi}(t)+\Big[(k_{21}-k_{11})\xi(t)+(k_{22}-k_{12})\dot{\xi}(t)\Big]\,ae^{-\frac{(\xi-b)^2}{2c^2}} \end{aligned} \tag{5.3.5}$$

According to Theorem 5.2, assume initial condition $x(0) = 0$, $\dot{x}(0) = 0$, $\mu = 500$, the fuzzy controller is calculated as

$$K_1 = [-223.4033\ \ -46.2517], K_2 = [-255.4280\ \ -56.0321]$$

By substituting (6.3.9) into (5.3.1), the closed-loop system can be written as

$$\ddot{\xi}(t) = n_1\xi(t)+n_2\dot{\xi}(t)+n_3\xi(t)e^{-\frac{(\xi(t)-b)^2}{2c^2}}+n_4\dot{\xi}(t)e^{-\frac{(\xi(t)-b)^2}{2c^2}}+n_5\xi(t)^3+\omega(t) \tag{5.3.6}$$

where $n_1 = k_{11}-0.02$, $n_2 = k_{12}, n_3 = a(k_{21}-k_{11}), n_4 = a(k_{22}-k_{12})$, $n_5 = -0.67$.

It is obvious that the closed-loop system is a nonlinear system with exponential type nonlinearity: $e^{(\xi-b)^2/2c^2}$. Then following the steps in **Algorithm 1**, the relationship between system nCOS function and parameters b and c can be analytically calculated as follows:

First define new variables $y_1(t) = \xi(t)$ and $y_2(t) = e^{-\frac{(\xi(t)-b)^2}{2c^2}}$, the closed-loop system can be equivalently transformed into the polynomial nonlinear system

$$\begin{cases} \ddot{y}_1(t) = n_1(t)y_1(t)+n_2\dot{y}_1(t)+n_3y_1(t)y_2(t)+n_4\dot{y}_1(t)y_2(t)+n_5y_1(t)^3+\omega(t) \\ \dot{y}_2(t) = -\dfrac{1}{c^2}y_1(t)\dot{y}_1(t)y_2(t) + \dfrac{b}{c^2}\dot{y}_1(t)y_2(t) \end{cases} \tag{5.3.7}$$

Following Step 2 of **Algorithm 1**, each order GFRF $H_i^n(jw)$ can be easily obtained:

$$
\begin{aligned}
&H_1^0 = 0, \quad H_2^0 = e^{-\frac{b^2}{2c^2}} \\
&H_1^1(jw_1) = \frac{1}{H_2^0(-m_4 jw_1 - m_3) - (m_2 jw_1 + w_1^2 + m_1)}, \quad H_2^1(jw_1) = H_2^0 H_1^1(jw_1) \\
&H_1^2(jw_1, jw_2) = \frac{(m_4 jw_1 + m_3) H_1^1(jw_1) H_2^1(jw_2)/H_2^0}{[-m_4 j(w_1+w_2) - m_3] - [m_2 j(w_1+w_2) + (w_1+w_2)^2 + m_1]} \\
&H_2^2(jw_1, jw_2) = -\frac{H_2^0}{c^2}\frac{jw_1 H_1^1(jw_1) H_1^1(jw_2)}{j(w_1+w_2)} + \frac{b}{c^2}\frac{jw_1}{j(w_1+w_2)} H_1^1(jw_1) H_2^1(jw_2) \\
&\qquad + \frac{bH_2^0}{c^2} H_1^2(jw_1, jw_2) \\
&H_1^3(jw_1, jw_2, jw_3) = \left\{ H_2^0 \left[(m_4 jw_1 + m_3) H_1^1(jw_1) H_2^2(jw_2, jw_3) \right.\right. \\
&\left.\left. + m_4 j(w_1+w_2) H_1^2(jw_1, jw_2) H_2^1(jw_3) \right] - m_5 H_1^1(jw_1) H_1^1(jw_2) H_1^1(jw_3)/H_2^0 \right\} \\
&/ \left[-m_4 j(w_1+w_2+w_3) - m_3\right] - \left[m_2 j(w_1+w_2+w_3) + (w_1+w_2+w_3)^2 + m_1 \right]
\end{aligned}
$$

Choose $y(t) = \ddot{\xi}(t)$ as the output. Input is $\omega(t) = \rho sin(wt)$ and denote $f = -\frac{1}{c^2}$, $g = \frac{b}{c^2}$. Substitute $H_i^n(jw)$ into (5.2.38) with some manipulation, the output spectrum can be calculated as:

$$
Y_1(jw) = \rho Y_1^1(jw_1) + \rho^2 Y_1^2(jw_1, jw_2) + \rho^3 Y_1^3(jw_1, jw_2, jw_3) + \cdots
$$

where

$$
Y_1^1(jw_1) = \frac{1}{\varphi_1^1(jw_1) H_2^0 + \varphi_1^0(jw_1)} \tag{5.3.8}
$$

$$
Y_1^2(jw_1, jw_2) = \frac{H_2^0}{\sum_{i=0}^3 \varphi_2^i(jw_1, jw_2)(H_2^0)^i} \tag{5.3.9}
$$

$$
\begin{aligned}
Y_1^3(jw_1, jw_2, jw_3) = &\frac{1}{\sum_{i=0}^6 \varphi_3^i(w_1, w_2, w_3)(H_2^0)^i} + \\
&\frac{\sum_{i=1}^3 \left[\varphi_{3f}^i(w_1, w_2, w_3) f + \varphi_{3g}^i(w_1, w_2, w_3) g + \varphi_{3c}^i(w_1, w_2, w_3) \right] (H_2^0)^i}{\sum_{i=0}^6 \varphi_3^i(w_1, w_2, w_3)(H_2^0)^i}
\end{aligned} \tag{5.3.10}
$$

The coefficients $\varphi(\cdot)$ which are given in the following tables, are independent of those parameters of interest, i.e., f and g and can be determined by using least square method.

According to the ρ−selection method aforementioned, curves of $|Y_1^2(jw)| \backsim \rho$ and $|Y_1^3(jw)| \backsim \rho$ are given in Fig.5.1, from which it can be seen that the best excitation magnitude should be 0.6.

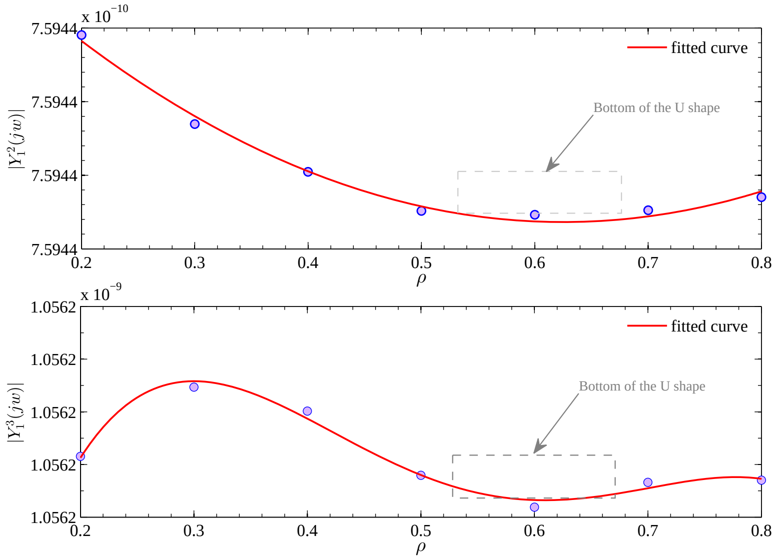

Fig. 5.1: Estimation of $Y_1^2(jw)$ and $Y_1^3(jw)$ under different excitation

Then choose input as $\omega(t) = 0.6\sin(\pi \cdot t)$, the coefficients of the output spectrum can be obtained via least square method, which are shown in Table 5.3.1 as follows:

Coefficient	Value	Coefficient	Value
$\varphi_1^1(jw_1)$	0.7394+0.1926i	$\varphi_1^0(jw_1)$	3.6805 + 0.4148i
$\varphi_2^0(jw_1, jw_2)$	-7.2e09 - 4.2e09i	$\varphi_2^1(jw_1, jw_2)$	1.1e10 + 6.4e09i
$\varphi_2^2(jw_1, jw_2)$	-4.3e09-2.5e09i	$\varphi_2^3(jw_1, jw_2)$	5.3e08+3.2e08i
$\varphi_3^0(jw_1, jw_2, jw_3)$	-2.5e07 + 2.1e07i	$\varphi_3^1(jw_1, jw_2, jw_3)$	2.8e08 - 2.2e08i
$\varphi_3^2(jw_1, jw_2, jw_3)$	-1.2e09 + 9.4e+08i	$\varphi_3^3(jw_1, jw_2, jw_3)$	2.6e09 - 2.0e09i
$\varphi_3^4(jw_1, jw_2, jw_3)$	-3.1e09 + 2.3e09i	$\varphi_3^5(jw_1, jw_2, jw_3)$	1.8e08 - 1.4e09i
$\varphi_3^6(jw_1, jw_2, jw_3)$	-4.6e08 + 3.5e08i	$\varphi_{3f}^1(jw_1, jw_2, jw_3)$	-56.279 - 2.1556i
$\varphi_{3f}^2(jw_1, jw_2, jw_3)$	-166.06 - 10.417i	$\varphi_{3f}^3(jw_1, jw_2, jw_3)$	-41.369 - 1.7803i
$\varphi_{3g}^1(jw_1, jw_2, jw_3)$	40.147 + 1.6309i	$\varphi_{3g}^2(jw_1, jw_2, jw_3)$	119.33 + 7.2823i
$\varphi_{3g}^3(jw_1, jw_2, jw_3)$	29.447 + 1.3701i	$\varphi_{3c}^1(jw_1, jw_2, jw_3)$	29.658 + 1.7477i
$\varphi_{3c}^2(jw_1, jw_2, jw_3)$	-19.469 - 1.1247i	$\varphi_{3c}^3(jw_1, jw_2, jw_3)$	-34.687 - 1.9019i

To verify the output prediction, output spectrum in terms of different parameters b and c are calculated via simulation, which are shown in Fig.5.2.

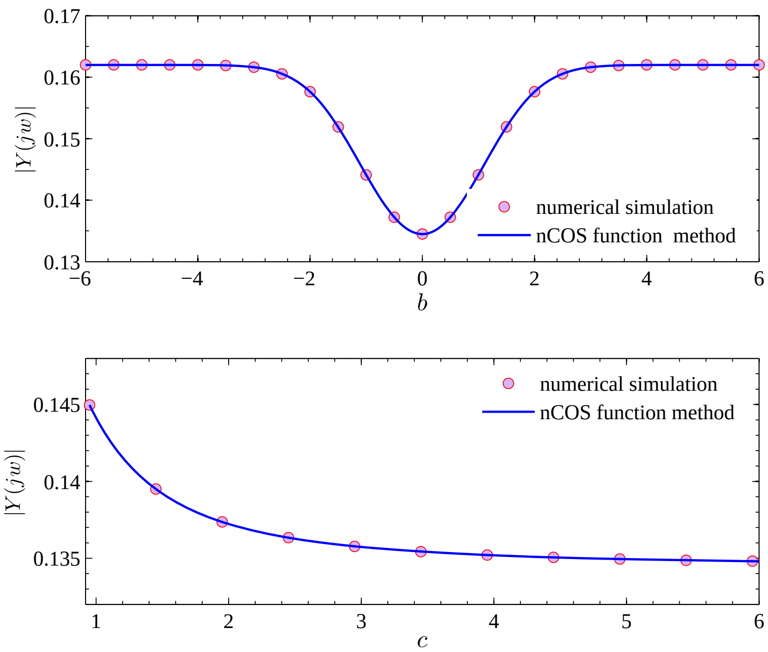

Fig. 5.2: Amplitude of $Y(jw)$ with different b $(c = 1)$ and c $(b = 1)$

From these two results, it can be seen that the output spectrum calculated by the nCOS function based method has a good agreement with the numerical simulation results.

Output spectrum in terms of different parameters of b and c, can then be easily calculated, which is shown in Fig.5.3. It can be seen from Fig.5.3 that parame-

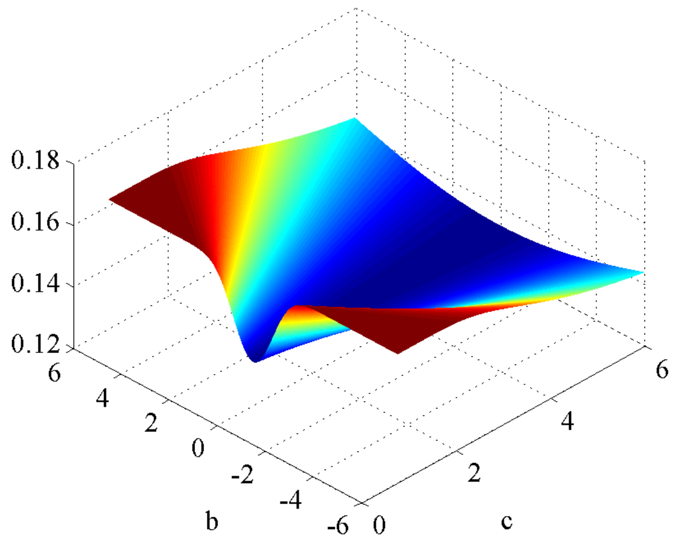

Fig. 5.3: Amplitude of $|Y(jw)|$ with different b and c

ters b and c in the controller membership functions have a significant impact on system output, which has not been studied in existing research works yet. The output spectrum can provide insight guidance in choosing parameters of controller membership functions in imperfect premise variables fuzzy control. For example, when $b = 2, c = 0.955, |Y(jw)| = 0.1561$. $b = -0.285, c = 5.595, |Y(jw)| = 0.1346$. The amplitude of output is reduced about 13.77%.

Then GA optimization method is applied to verify the results obtained by the nCOS function based optimization method, choose the initial population as $N = 120$, the crossover rate as $p_c = 0.6$, the mutation rate as $p_m = 0.05$ and the parameters space of b and c are $[-6, 6]$ and $[0.84, 6]$ respectively. The GA-based

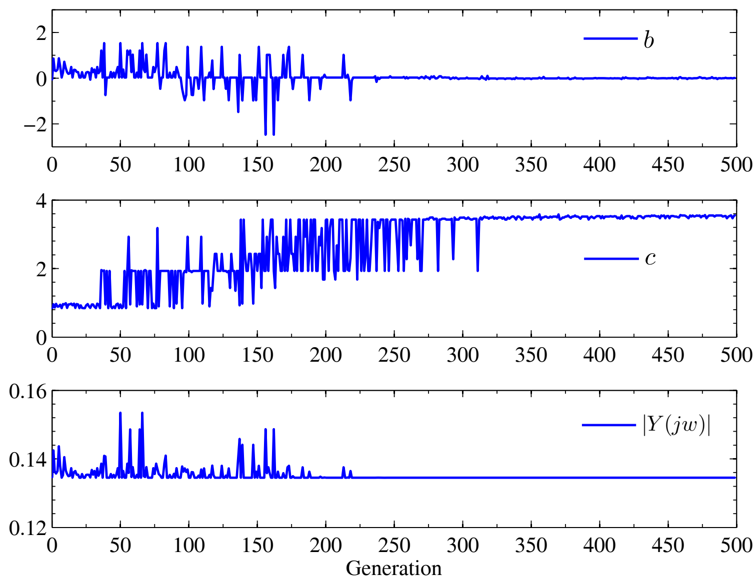

Fig. 5.4: GA-based optimization process

optimization process is shown in Fig.5.4. It is obtained that the final optimal output is $|Y(jw)| = 0.13448$, and the corresponding optimal parameters are approximately $b = 0$ and $c = 3.5$, which is almost identical to the result $|Y(jw)| = 0.1345$ calculated by the frequency response based method. This again verifies the effectiveness of frequency response based optimization method. It is also worth pointing out that the GA approach can only obtain optimal value of $|Y(jw)|$ and the corresponding parameters b and c. Moreover, the time consumption increases tremendously with larger parameter space. On the other hand, the nCOS function based method, can provide analytical relationship between the parameters b, c and the desired performance. As shown in Fig.5.3, the output response of the closed-loop system in the concerned parameter space can be calculated analytically. And the computing burden does not increase with parameters' range.

5.3.2 Nonlinear vehicle suspension system

A more complicated 2-DOF nonlinear vehicle suspension system is given in this part. According to Newton's second law, nonlinear dynamic equation of the system is built as follows:

$$\begin{aligned} m_s\ddot{z}_s &= -F_s - F_d + u \\ m_u\ddot{z}_u &= F_s + F_d - F_t - F_b - u \end{aligned} \tag{5.3.11}$$

where m_s and m_u are sprung and unsprung mass, z_s, z_u and z_r are the vertical displacements of sprung mass, unsprung mass and road input, u is the control force applied on the suspension system. F_s, F_d, F_t are the forces produced by the nonlinear spring, nonlinear damper and the tire, which are represented as:$F_s = k_{s1}(z_s - z_u) + k_{s3}(z_s - z_u)^3,\ F_b = c_t(\dot{z}_u - \dot{z}_r), F_d = c_{s1}(\dot{z}_s - \dot{z}_u) + c_{s2}(\dot{z}_s - \dot{z}_u)^2,\ F_t = k_t(z_u - z_r)$, where k_{s1} and k_{s3} are nonlinear stiffness coefficients, c_{s1} and c_{s2} are damping coefficients, k_t and c_t are stiffness and damping coefficients of the tire.

Define $x_1(t) = z_s(t) - z_u(t)$, which represents the suspension deflection, $x_2(t) = \dot{z}_s(t)$, which is the sprung mass speed, $x_3(t) = z_u(t) - z_r(t)$, which denotes the tire deflection, $x_4(t) = \dot{z}_u(t)$, which is the unsprung mass speed, and $\omega(t) = \dot{z}_r(t)$ is the disturbance input. Then system dynamical equation (5.3.11) is rewritten in the following form:

$$\begin{cases} \dot{x}_1 = x_2 - x_4, \\ \dot{x}_2 = -\dfrac{k_{s1}}{m_s}x_1 - \dfrac{k_{s3}}{m_s}x_1^3 - \dfrac{c_{s1}}{m_s}(x_2 - x_4) - \dfrac{c_{s2}}{m_s}\dot{x}_1^2 + \dfrac{u}{m_s}, \\ \dot{x}_3 = x_4 - \omega, \\ \dot{x}_4 = \dfrac{k_{s1}x_1}{m_u} + \dfrac{k_{s3}x_1^3}{m_u} + \dfrac{c_{s1}(x_2 - x_4)}{m_u} + \dfrac{c_{s2}\dot{x}_1^2}{m_u} - \dfrac{k_t x_3}{m_u} - \dfrac{c_t x_4}{m_u} + \dfrac{c_t\omega}{m_u} \end{cases}$$

In suspension control, the following performance constraints should also be taken into consideration:

1. The suspension deflection is no larger than a maximum value constrained by mechanical structure, i.e., $\|z_s(t) - z_u(t)\| \leq z_{\max}$
2. The dynamic tire load should not exceed the static tire load to guarantee that the wheels contact the road uninterruptedly, i.e., $k_t(z_u(t) - z_r(t)) < (m_s + m_u)g$

The following controlled outputs are defined to achieve the aforementioned performance constraints

$$\begin{aligned} z_1(t) &= \ddot{z}_s(t), \\ z_2(t) &= \begin{bmatrix} \frac{z_s(t) - z_u(t)}{z_{\max}} & \frac{k_t(z_u(t) - z_r(t))}{(m_s + m_u)g} \end{bmatrix}^T \end{aligned}$$

Assume $x_1(t) \in [-d_1, d_1]$, $\dot{x}_1(t) \in [-d_2, d_2]$, d_1, $d_2 \geq 0$. Then according to the fuzzy modeling method in [88], the following fuzzy model can exactly represent the nonlinear suspension system in region $[-d_1, d_1] \times [-d_2, d_2]$

$$\begin{cases} \dot{x}(t) = \sum_{i=1}^{4} h_i(\xi(t))[A_i x(t) + B_i u(t) + B_{wi}\omega(t)] \\ z_1(t) = \sum_{i=1}^{4} h_i(\xi(t))[C_{1i}x(t) + D_i u(t)] \\ z_2(t) = \sum_{i=1}^{4} h_i(\xi(t))C_{2i}x(t) \end{cases}$$

where $\xi(t) = \{x_1(t), \dot{x}_1(t)\}$, $M_1(x_1(t)) = 1 - \frac{x_1(t)^2}{d_1^2}$, $M_2(x_1(t)) = \frac{x_1(t)^2}{d_1^2}$, $N_1(\dot{x}_1(t)) = \frac{1}{2}(1 - \frac{\dot{x}_1(t)}{d_2})$, $N_2(\dot{x}_1(t)) = \frac{1}{2}(1 + \frac{\dot{x}_1(t)}{d_2})$,

$h_1(\xi(t)) = M_1(x_1(t)) \cdot N_1(\dot{x}_1(t)), h_2(\xi(t)) = M_1(x_1(t)) \cdot N_2(\dot{x}_1(t))$,

$h_3(\xi(t)) = M_2(x_1(t)) \cdot N_1(\dot{x}_1(t)), h_4(\xi(t)) = M_2(x_1(t)) \cdot N_2(\dot{x}_1(t))$,

$$A_i = \begin{bmatrix} 0 & 1 & 0 & -1 \\ a_{21}^i & a_{22}^i & 0 & a_{24}^i \\ 0 & 0 & 0 & 1 \\ a_{41}^i & a_{42}^i & -\frac{k_t}{m_u} & a_{44}^i \end{bmatrix}, B_i = \begin{bmatrix} 0 \\ \frac{1}{m_s} \\ 0 \\ -\frac{1}{m_u} \end{bmatrix}, B_{\omega i} = \begin{bmatrix} 0 \\ 0 \\ -1 \\ \frac{c_t}{m_u} \end{bmatrix},$$

$$a_{21}^1 = a_{21}^2 = -\frac{k_{s1}}{m_s}, a_{21}^3 = a_{21}^4 = -\frac{k_{s1} + k_{s3}d_1^2}{m_s}, a_{41}^1 = a_{41}^2 = \frac{k_{s1}}{m_u},$$
$$a_{41}^3 = a_{41}^4 = \frac{k_{s1} + k_{s3}d_1^2}{m_u}, a_{22}^1 = a_{22}^3 = \frac{c_{s2}d_2 - c_{s1}}{m_s},\ a_{24}^1 = a_{24}^3 = \frac{c_{s1} - c_{s2}d_2}{m_s},$$
$$a_{42}^1 = a_{42}^3 = \frac{c_{s1} - d_2c_{s2}}{m_u},\ a_{44}^1 = a_{44}^3 = \frac{d_2c_{s2} - c_{s1} - c_t}{m_u}, a_{22}^2 = a_{22}^4 = \frac{-c_{s2}d_2 - c_{s1}}{m_s},$$
$$a_{24}^2 = a_{24}^4 = \frac{c_{s1} + c_{s2}d_2}{m_s}, a_{42}^2 = a_{42}^4 = \frac{c_{s1} + d_2c_{s2}}{m_u},\ a_{44}^2 = a_{44}^4 = \frac{-d_2c_{s2} - c_{s1} - c_t}{m_u},$$
$$C_{11} = \begin{bmatrix} -\frac{k_{s1}}{m_s} & \frac{c_{s2}d_2 - c_{s1}}{m_s} & 0 & \frac{c_{s1} - c_{s2}d_2}{m_s} \end{bmatrix}, C_{12} = \begin{bmatrix} -\frac{k_{s1}}{m_s} & \frac{-c_{s2}d_2 - c_{s1}}{m_s} & 0 & \frac{c_{s1} + c_{s2}d_2}{m_s} \end{bmatrix},$$
$$C_{13} = \begin{bmatrix} -\frac{k_{s1} + k_{s3}d^2}{m_s} & \frac{c_{s2}d_2 - c_{s1}}{m_s} & 0 & \frac{c_{s1} - c_{s2}d_2}{m_s} \end{bmatrix}, C_{14} = \begin{bmatrix} -\frac{k_{s1} + k_{s3}d^2}{m_s} & \frac{-c_{s2}d_2 - c_{s1}}{m_s} & 0 & \frac{c_{s1} + c_{s2}d_2}{m_s} \end{bmatrix},$$
$$C_{2i} = \begin{bmatrix} \frac{1}{z_{\max}} & 0 & 0 & 0 \\ 0 & 0 & \frac{k_t}{(m_s + m_u)g} & 0 \end{bmatrix},\ D_i = \frac{1}{m_s}.$$

To satisfy the performance constraints, the following condition should be taken into consideration:

$$\begin{bmatrix} -\bar{P}_1 & \sqrt{\delta}\bar{P}_1\{C_{2i}\}_q^T \\ \star & -I \end{bmatrix} < 0, q = 1, 2 \tag{5.3.12}$$

where $\{C_{2i}\}_q^T$ denotes the q_{th} row vector of C_{2i}^T.

Parameters of this nonlinear quarter vehicle suspension system are listed in Table 5.1.

Table 5.1: Parameters of Quarter vehicle Suspension Model

Parameter	Value	Parameter	Value
m_s	900 kg	m_u	50 kg
k_{s1}	20000 N/m	k_{s3}	3170400N/m^3
c_{s1}	1500 Ns/m	c_{s2}	54.28 Ns^2/m^2
k_t	200000 N/m	c_t	170 Ns/m

The mismatched controller membership functions are chosen as

$$m_1(\xi(t)) = (1 - 0.5e^{-\frac{(x_1(t)-b)^2}{2c^2}})(\frac{1}{2} - \frac{\dot{x}_1(t)}{2d_2}), m_2(\xi(t)) = (1 - 0.5e^{-\frac{(x_1(t)-b)^2}{2c^2}})(\frac{1}{2} + \frac{\dot{x}_1(t)}{2d_2})$$
$$m_3(\xi(t)) = 0.5e^{-\frac{(x_1(t)-b)^2}{2c^2}}(\frac{1}{2} - \frac{\dot{x}_1(t)}{2d_2}), m_4(\xi(t)) = 0.5e^{-\frac{(x_1(t)-b)^2}{2c^2}}(\frac{1}{2} + \frac{\dot{x}_1(t)}{2d_2})$$

where $d_1 = 0.1$, $d_2 = 1$, $b \in [-6,\ 6]$, $c \in [1.5,\ 6]$ with permitted $\lambda_1 = 0.00014$, $\lambda_2 = 0.00014$, $\lambda_3 = 0.00014$, $\lambda_4 = 0.00016$, $w_1 = 4$, $w_2 = 8$. Then according to Theorem 5.2, assume initial conditions are 0 , $\mu = 3000$, γ and fuzzy controller gains are calculated as $\gamma = 4$,

$$K_1 = 10^4 \times [-1.8874 \quad -1.2846 \quad -0.7848 \quad -0.0107],$$

$$K_2 = 10^4 \times [-1.8750 \quad -1.2824 \quad -0.7726 \quad -0.0114],$$

$$K_3 = 10^4 \times [1.0075 \quad -0.7257 \quad 2.7113 \quad -0.0103],$$

$$K_4 = 10^4 \times [1.0048 \quad -0.7199 \quad 2.8760 \quad -0.0143]$$

Choose $\ddot{z}_s$ as the output, then following the same procedure as in Example.1, given input $\omega(t) = 0.02\sin(12\pi t)$, the output spectrum can be easily calculated with different parameters of b and c. Fig.5.5 show the effectiveness of the output spectrum calculation method. Then the curve $|Y(jw)| \backsim b\&c$ can be easily obtained, which is shown in Fig.5.6.

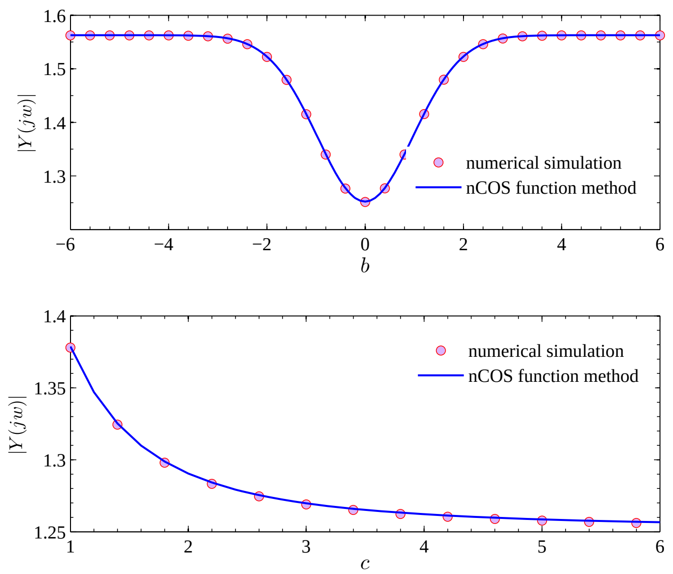

Fig. 5.5: Amplitude of $Y(jw)$ with different b ($c = 1$) and c ($b = 1$)

According to the GA optimization method, the optimal value of $|Y(jw)|$ and optimal b and c are $|Y(jw)|_{\min} = 1.2525$, $b = 0.7005$, $c = 6$, which are easy to

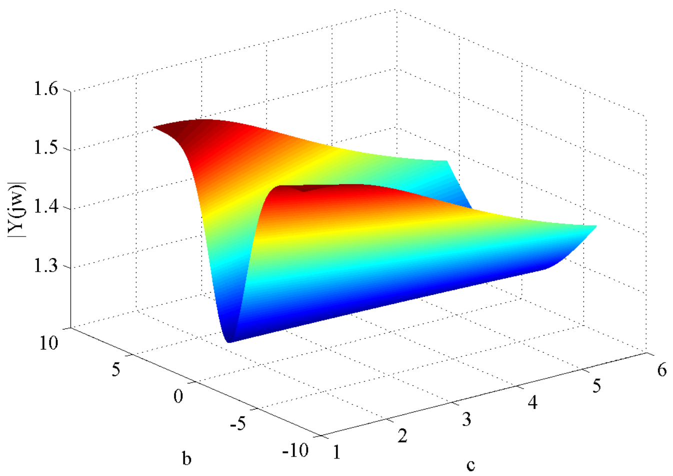

Fig. 5.6: Amplitude of $Y(jw)$ with different b and c

obtain via the nCOS function based optimization method. In addition to optimal value, from the curve we can easily come to the conclusion that parameters in the dark blue area are all eligible candidate for the mismatched controller, whereas parameters that fall in red area should be avoided. Also, from Fig.5.6, we can tell that parameter b in the controller membership functions has more influence on system performance than parameter c. None of these can be observed via GA or other existing optimization methods.

For comparison, we choose parameters $b = 0.01$, $c = 1.5$ from the dark blue area as optimized parameters and $b = 5, c = 1.6$, from the red area as randomly chosen parameters in the curve $|Y(jw)| \backsim b\&c$. To test performance of the suspension system, filtered white noise borrowed from [163] with road roughness class E is adopted in the simulation. The equation of road excitation can be expressed as $\dot{q}(t) = -2\pi n_q u q(t) + 2\pi n_0 \sqrt{G_q(n_0)u} G(t)$, where $n_q = 0.0001 m^{-1}$ is the lowest frequency, $G(t)$ is standard Gaussian white noise with 0 mean and unit variance, $G_q(n_0) = 4096 \times 10^{-6} m^2/m^{-1}$(class E), u is the vehicle forward velocity. Vehicle forward velocities $V = 30$ m/s is used to test performance of the proposed control approach. Fig.5.7 presents the body acceleration response and FFT of the acceleration signal, from which we can see active suspension outperforms passive one, and the controller with optimized b, c can achieve better performance than the one with randomly chosen parameters between 4Hz-8Hz.

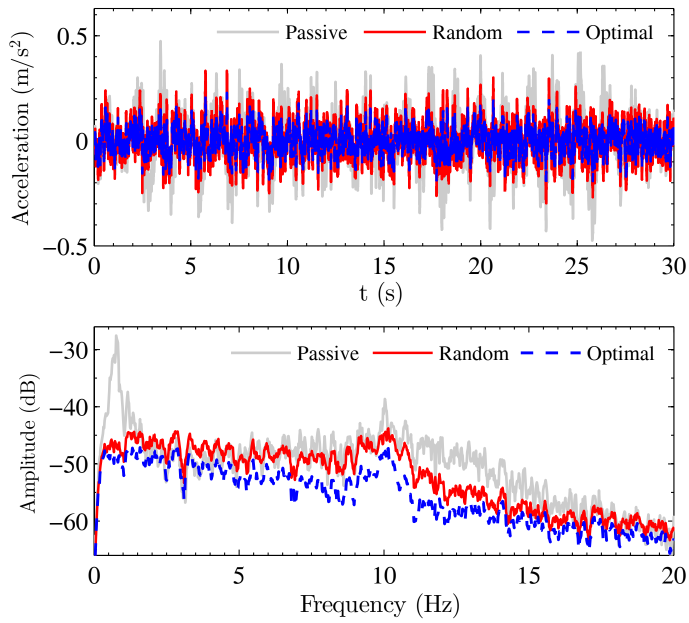

Fig. 5.7: Acceleration response and FFT of acceleration

Suspension deflection $z_s - z_u$ is given in Fig.5.8, from which one can observe that the controlled suspension spaces all fall into acceptable ranges. Thus, these physical constraints are guaranteed. The dynamic tire load is illustrated in Fig.5.8, which demonstrates that the dynamic tire load constraint $\frac{F_t+F_b}{(m_s+m_u)g} < 1$ is satisfied. In a word, Fig.5.8 validates that road holding capability and constraint suspension deflection can be guaranteed with improved ride comfort.

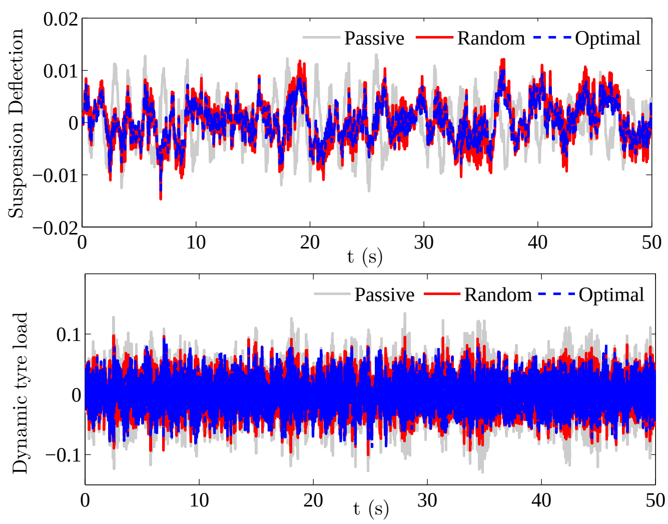

Fig. 5.8: Suspension deflection and dynamic tyre load

Then to evaluate robustness of the designed fuzzy controller, a general disturbance $F_d = 0.2\sin1.5\pi t + \sin12\pi t$ is added to the sprung mass. The disturbance contains disturbance components at 6Hz, which falls in 4Hz-8Hz. Following the same analysis procedure, Fig.5.9 shows acceleration of the suspension system both in time and frequency domain, from which we can see that the controller designed based on optimal parameters outperforms the one designed based on randomly chosen parameters over the frequency range 4Hz-8Hz.

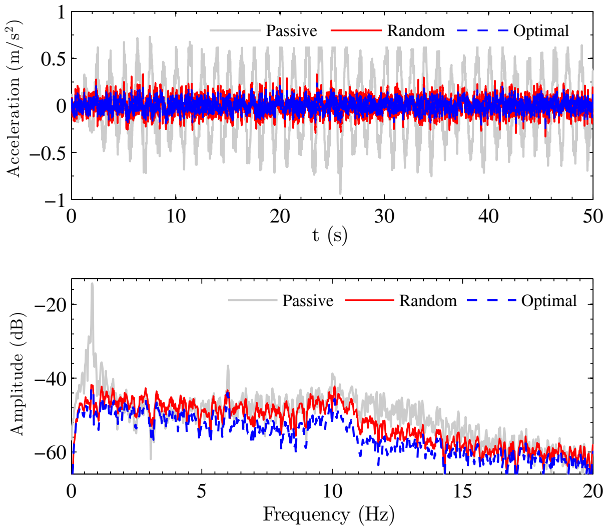

Fig. 5.9: Acceleration response and FFT subject to disturbance

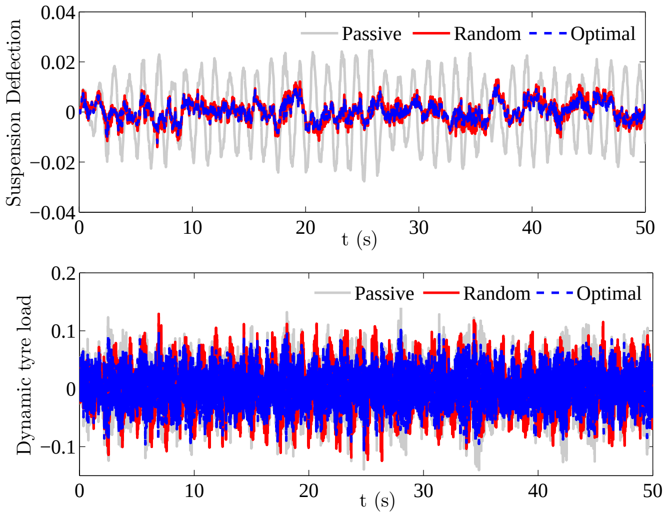

Fig. 5.10: Suspension deflection and dynamic tyre load

Fig.5.10 are the suspension deflection and dynamic tyre load, which demonstrates that the physical constraints of the suspension system are all satisfied when subject to general disturbance.

It can be seen from the results above that the proposed nCOS function based method provides a unique frequency domain insight into the nonlinear influence incurred by exponential-type nonlinearity (i.e., the Gaussian membership functions of the controller) on system output response, and therefore offers an alternative solution to parameters optimization problem in fuzzy control with mismatched controllers. This has never been explored in existing research work but can be done readily with the proposed frequency based method.

5.4 Conclusion

A novel finite frequency H_∞ controller with mismatched premise variables has been designed. A novel nCOS function based optimization method, which aims to optimize the Gaussian membership functions' parameters has been proposed in this chapter. Compared to GA optimization method, the nCOS function based frequency domain optimization approach can provide analytical relationship between system output spectrum and fuzzy membership function parameters and is time efficient. Simulation results of nonlinear suspension system demonstrate that suspension performance over a concerned frequency band has been further enhanced by combining the finite frequency H_∞ control with the nCOS function based frequency domain optimization method.

Chapter 6

A novel parametric characteristic output spectrum function for nonlinear systems

In general, nonlinear system output spectrum is jointly determined by linear parameters, nonlinear parameters, excitation amplitude and frequency variables [49]. Frequency domain method used in Chapter 5 and most of the existing results about nCOS function based method mainly focus on nonlinear model parameters' influence on system output spectrum [27, 49, 124, 160, 164]. Linear model parameters' influence on systems output nonlinear spectrum has been systemically investigated in [134]. It is worth pointing out that analysis of linear and nonlinear parameters' influence on system output spectrum in a separated manner is not comprehensive enough for in-depth understanding of the system characteristics. To solve this problem, a novel parametric characteristic output spectrum (pCOS) function simultaneously including linear and nonlinear model parameters will be developed in this chapter. Based on the proposed novel pCOS function, nonlinear output spectrum can be determined as a polynomial of system parameters (both linear and nonlinear). This result will be a strong complement to existing nCOS function based methods, which can provide a more comprehensive solution to in-depth analysis and design of nonlinear systems. Moreover, coefficients of the novel parametric characteristic output spectrum are independent of linear and nonlinear model parameters of interest. Only measured output data are required to calculate these coefficients, which is very convenient for nondestructive evaluations of practical systems. Detailed procedures to determine these coefficients are presented in this chapter. To verify effectiveness of the proposed method, an example of designing linear and nonlinear parameters for a mechanical system is first given. Then together with a nonlinear output spectrum calculation method [49], the approach proposed in this chapter is applied to fault detection of closed-loop control systems with plant and controller faults. The fault characteristics can be decoupled by using the nth-order output spectrum. Therefore, identification and location of multi-faults can be determined according to the nth-order output spectrum.

6.1 Volterra series in the frequency domain and nonlinear output spectrum

A considerably large class of nonlinear systems, for example, mechanical systems [29,30,165–167], circuit systems [134,168], can be modeled or identified as general Nonlinear Differential Equation (NDE) model as follows:

$$\sum_{m=1}^{M}\sum_{p=0}^{m}\sum_{k_1,\cdots,k_{p+q}=0}^{K} c_{p,q}(k_1,\cdots,k_{p+q})\prod_{i=1}^{p}\frac{d^{k_i}y(t)}{dt^{k_i}}\prod_{i=p+1}^{p+q}\frac{d^{k_i}u(t)}{dt^{k_i}}=0 \tag{6.1.1}$$

where $\frac{d^k u(t)}{dt^k}|_{k=0} = u(t)$, $p+q=m$, $\sum_{k_1,\cdots,k_{p+q}=0}^{K} = \sum_{k_1=0}^{K}(\cdot)\cdots\sum_{k_{p+q}=0}^{K}(\cdot)$, M is the maximum degree of nonlinearity in terms of $y(t)$ and $u(t)$, and K is the maximum order of the derivative. In this model, the parameters such as $c_{0,1}(\cdot)$ and $c_{1,0}(\cdot)$ are linear parameters corresponding to the linear terms in the model, i.e., $\frac{d^k y(t)}{dt^k}$ and $\frac{d^k u(t)}{dt^k}$ for $k = 0, 1, \cdots, L$, and $c_{p,q}(\cdot)$ for $p+q > 1$ are referred to as nonlinear parameters corresponding to nonlinear terms in the model of the form $\prod_{i=1}^{p}\frac{d^{k_i}y(t)}{dt^{k_i}}\prod_{i=p+1}^{p+q}\frac{d^{k_i}u(t)}{dt^{k_i}}$, i.e., $y^p(t)u^q(t)$. $p+q$ is referred to as the nonlinear degree of parameter $c_{p,q}(\cdot)$.

The input-output relationship for a considerably large class of nonlinear systems described by the NDE model (6.1.1) can be approximately represented by a Volterra series of order N as [48, 160, 169]

$$y(t) = \sum_{n=1}^{N} y_n(t) \tag{6.1.2}$$

$$y_n(t) = \int_{-\infty}^{\infty} \cdots \int_{-\infty}^{\infty} h_n(\tau_1, \cdots, \tau_n) \prod_{i=1}^{n} u(t - \tau_i) d\tau_i \tag{6.1.3}$$

where $u(t)$ is input of system, $y(t)$ is output of system, N is maximum nonlinearity order of system, $h_n(\tau_1, \cdots, \tau_n)$ is the nth-order Volterra kernel. The nth-order GFRF is defined as [24]

$$H_n(j\omega_1, \cdots, j\omega_n) = \int_{-\infty}^{\infty} \cdots \int_{-\infty}^{\infty} h_n(\tau_1, \cdots, \tau_n) \mathrm{e}^{-j(\omega_1\tau_1 + \cdots + \omega_n\tau_n)} d\tau_1 \cdots d\tau_n \tag{6.1.4}$$

Then in the frequency domain, (6.1.2) and (6.1.3) can be written as

$$Y(j\omega) = \sum_{n=1}^{N} Y_n(j\omega) \tag{6.1.5}$$

$$Y_n(j\omega) = \frac{1}{\sqrt{n}(2\pi)^{n-1}} \int_{\omega_1 + \cdots + \omega_n = \omega} H_n(j\omega_1, \cdots, j\omega_n) \prod_{i=1}^{n} U(j\omega_i) d\sigma_\omega \tag{6.1.6}$$

where $\int_{\omega_1 + \cdots + \omega_n = \omega} (\cdot) d\sigma_\omega$ is integration on the super plane $\omega_1 + \cdots + \omega_n = \omega$. $Y(j\omega)$ is output spectrum, $Y_n(j\omega)$ is referred to as the nth-order output spectrum.

According to [124, 164], GFRFs for the NDE model (6.1.1) in terms of model parameters can be recursively calculated as:

$$\begin{aligned} & L_n(j\omega_1, \cdots, \omega_n) \cdot H_n(j\omega_1, \cdots, j\omega_n) \\ = & \sum_{k_1, \cdots, k_n = 1}^{K} c_{0,n}(k_1, \cdots, k_n)(j\omega_1)^{k_1} \cdots (j\omega_n)^{k_n} \\ & + \sum_{q=1}^{n-1} \sum_{p=1}^{n-q} \sum_{k_1, \cdots, k_{p+q} = 0}^{K} c_{p,q}(k_1, \cdots, k_{p+q}) \left(\prod_{i=1}^{q} (j\omega_{n-q+i})^{k_{p+i}} \right) \\ & \times H_{n-q,p}(j\omega_1, \cdots, j\omega_{n-q}) \end{aligned} \tag{6.1.7}$$

$$+\sum_{p=2}^{n}\sum_{k_1,\cdots,k_p=0}^{K} c_{p,0}(k_1,\cdots,k_p)H_{n,p}(j\omega_1,\cdots,j\omega_n)$$

where

$$H_{n,p}(\cdot)=\sum_{i=1}^{n-p+1} H_i(j\omega_1,\cdots,j\omega_n)H_{n-i,p-1}(j\omega_{i+1},\cdots,j\omega_n)(j\omega_1+\cdots+j\omega_i)^{k_p}$$

$$H_{n,1}(j\omega_1,\cdots,j\omega_n)=H_n(j\omega_1,\cdots,j\omega_n)(j\omega_1+\cdots+j\omega_n)^{k_1}$$

$$L_n(j\omega_1,\cdots,j\omega_n)=-\sum_{k_1=0}^{K} c_{1,0}(k_1)(j\omega_1+\cdots+j\omega_n)^{k_1}$$

Moreover, $H_{n,p}(j\omega_1,\cdots,j\omega_n)$ can also be written as

$$H_{n,p}(j\omega_1,\cdots,j\omega_n)=\sum_{\substack{r_1\cdots r_p=1\\ \sum r_i=n}}^{n-p+1}\prod_{i=1}^{p} H_{r_i}(j\omega_{X+1},\cdots,j\omega_{X+r_i})(j\omega_{X+1},\cdots,j\omega_{X+r_i})^{k_i}$$

where $X=\sum_{x=1}^{i-1} r_x$. Then (6.1.7) can be written in a more concise form as

$$H_n(j\omega_1,\cdots,j\omega_n)=\frac{1}{L_n\left(j\sum\limits_{i=1}^{n}\omega_i\right)}\sum_{q=0}^{n}\sum_{p=0}^{n-q}\sum_{k_1,k_p=0}^{K} c_{p,q}(k_1,\cdots,k_p)$$
$$\times\left(\prod_{i=1}^{q}(j\omega_{n-q+1})^{k_{p+i}}\right)H_{n-q,p}(j\omega_1,\cdots,j\omega_{n-q}) \tag{6.1.8}$$

Higher order GFRFs can be recursively calculated from lower-order GFRFs. The first order GFRF is given as

$$H_1(j\omega_1)=-\frac{\sum_{k_1=0}^{K} c_{0,1}(k_1)(j\omega_1)^k}{L_1(j\omega_1)} \tag{6.1.9}$$

6.2 A novel parametric characteristic output spectrum function for nonlinear systems

Nonlinear output spectrum is not only function of frequency variables but also function of input magnitude and model parameters of interest. Based on the parametric characteristic analysis results in [124], the nth-order GFRF can be expressed as

$$H_n(j\omega_1, \cdots, j\omega_n) = CE(H_n(j\omega_1, \cdots, j\omega_n)) \cdot f_n(j\omega_1, \cdots, j\omega_n) \qquad (6.2.1)$$

where $f_n(j\omega_1, \cdots, j\omega_n)$ is a complex valued function vector with appropriate dimension, which is referred to as the correlative function of the parametric characteristic $CE(H_n(j\omega_1, \cdots, j\omega_n))$.

Equation (6.2.1) explicitly demonstrates the analytical relationship between system GFRFs and system time domain nonlinear model parameters. Based on the parametric characteristic analysis, system nonlinear characteristics can be studied in the frequency domain from a novel perspective such as frequency characteristics of system output frequency response, parametric sensitivity analysis and so on.

Substitute (6.2.1) into (6.1.6)

$$\begin{aligned} Y(j\omega) &= \sum_{n=1}^{N} CE(H_n(j\omega_1, \cdots, j\omega_n)) \frac{1}{\sqrt{n}(2\pi)^{n-1}} \int_{\omega_1+\cdots+\omega_n=\omega} f_n(j\omega_1, \cdots, j\omega_n) \prod_{n=1}^{n} U(j\omega_i) d\sigma_\omega \\ &= \sum_{n=1}^{N} CE(H_n(j\omega_1, \cdots, j\omega_n)) \cdot F_n(j\omega_1, \cdots, j\omega_n) \qquad (6.2.2) \end{aligned}$$

Obviously, nonlinear parametric characteristic can be obtained as

$$CE(Y(j\omega)) = \underset{i=1}{\overset{N}{\oplus}} CE(H_n(j\omega_1, \cdots, j\omega_n)) \qquad (6.2.3)$$

Operation $\oplus$ is reduced vectorized sum which has the same definition as in [124].

(6.2.1) and (6.2.2) are nonlinear parameter characteristics of GFRF and system output frequency response function, which clearly demonstrate analytical relationship between nonlinear system model parameters and system GFRF, frequency response functions. Nonlinear parameter characteristic analysis, such as influence of certain nonlinear parameters on output frequency response, sensitivity analysis of nonlinear parameters, detailed results can be referenced to [27, 164, 170]. In [125], correlative function $f_n(j\omega_1, \cdots, j\omega_n)$ are determined as functions of first order GFRF and system nonlinear parameters, which has greatly enriched the nonlinear parametric characteristics analysis theory. In this chapter, we take this result one step further, correlative function $f_n(j\omega_1, \cdots, j\omega_n)$ are explicitly determined as polynomials of system linear and nonlinear parameters.

In the following section, based on parametric characteristic vector $CE(H_n(\cdot))$, algorithms are provided to explicitly and rigorously determine the correlative function $f_n(j\omega_1, \cdots, j\omega_n)$ and $F_n(j\omega_1, \cdots, j\omega_n)$ directly in terms of system linear parameters, in a more analytical form. Then system's GFRF and output frequency spectrum can be easily expressed as a clear structure in terms of linear and nonlinear parameters. The proposed algorithms enable simultaneous analysis of linear and nonlinear parameters' effect on system GFRF and output frequency response functions.

6.2.1 GFRFs with respect to system parameters

For convenience, linear parameters in $L_n(\cdot)$ are separated into the following two parts:

$$c_{p,q} = \hat{c}_{p,q}(k_1) + \tilde{c}_{p,q}(k_1), p + q = 1, k_1 = 0, 1, \cdots, K$$

where $\hat{c}_{p,q}(k_1)$ denotes linear components of no interest and $\tilde{c}_{p,q}(k_1)$ are linear parameters to be analyzed and designed. Moreover, define $\boldsymbol{\varepsilon} = [\varepsilon_0, \varepsilon_1, \cdots, \varepsilon_K]$, $\varepsilon_{k_1} \in \mathbb{N}^+, k_1 = 0, \cdots, K$. $\tilde{c}^{\boldsymbol{\varepsilon}} = \prod_{k_1=0}^{K} \tilde{c}_{1,0}^{\varepsilon_{k_1}}$, which only involves linear parameters of interest.

Proposition 6.1 *[134]: If $|\hat{L}_n^{-1}(\omega_n)\tilde{L}_n(\omega_n)| < 1$, then the following equation holds:*

$$L_n^{-1}(\omega_n) = \phi_n^{\mathbf{0}}(\omega_n) + \sum_{\varepsilon_0+\varepsilon_1+\cdots+\varepsilon_K=1}^{\infty} \phi_n^{\varepsilon}(\omega_n)\tilde{c}^{\varepsilon} \tag{6.2.4}$$

where

$$\begin{aligned}
\phi_n^{\varepsilon}(\omega_n) &= (-1)^{\sum_{k_1=0}^{K}\varepsilon_{k_1}}[\hat{L}_n^{-1}(\omega_n)]^{\sum_{k_1=0}^{K}\varepsilon_{k_1}+1}(j\omega_1+\cdots+j\omega_n)^{\sum_{k_1=0}^{K}k_1\times\varepsilon_{k_1}} \qquad (6.2.5)\\
\tilde{L}_n(\omega_n) &= \sum_{k_1=0}^{K}\tilde{c}_{1,0}(k_1)(j\omega_1+\cdots+j\omega_n)^{k_1}\\
\phi_n^{\mathbf{0}}(\omega_n) &= \hat{L}_n(\omega_n) = \frac{1}{\sum_{k_1=0}^{K}\hat{c}_{1,0}(k_1)(j\omega_1+\cdots+j\omega_n)^{k_1}}
\end{aligned}$$

(6.2.4) can also be written in the following concise form:

$$L_n^{-1}(\omega_n) = \chi^{Ly}\cdot\varphi_n^{y}(\omega_n) \tag{6.2.6}$$

where $\chi^{Ly} = [1, \tilde{c}^{\varepsilon}]$, which only involves the output linear parameters of interest. $\varphi_n^{y}(\omega_n) = [\phi_n^{\mathbf{0}}(\omega_n), \sum_{\varepsilon_0+\varepsilon_1+\cdots+\varepsilon_K=1}^{\infty}\phi_n^{\varepsilon}(\omega_n)]^T$, which only involves output linear parameters of no interest and frequency variables ω_n.

Proposition 6.2 *The first order GFRF of the nonlinear system can be given as product of two polynomials consisted of system linear parameters*

$$H_1(j\omega_1) = \chi^{Ly}\otimes\chi^{Lu}\cdot\Phi_1(\hat{c}_{p,q}(k_1); j\omega_1) \tag{6.2.7}$$

where $p+q = 1$, $\chi^{Lu} = [1, \tilde{c}_{0,1}(k_1)], k_1 = 0, \cdots, K$, $\chi^{Ly} = [1, \tilde{c}^{\varepsilon}]$. $\Phi_1(\hat{c}_{p,q}(k_1); j\omega_1), k_1 = 0, \cdots, K$ is a complex valued function vector with appropriate dimension, which involves only linear parameters of no interest and frequency variables. Operation $\otimes$ is reduced Kronecker product, which has same definition as in [124].

Proof: The first order GFRF (6.1.9) can be rewritten as:

$$
\begin{aligned}
H_1(j\omega_1) =& -\frac{\sum_{k_1=0}^{K}\hat{c}_{0,1}(k_1)(j\omega_1)^{k_1}+\sum_{k_1=0}^{K}\tilde{c}_{0,1}(k_1)(j\omega_1)^{k_1}}{L_1(j\omega_1)} \\
=&\frac{[1,\ \tilde{c}_{0,1}(k_1)][\hat{c}_{0,1}(k_1)(j\omega_1)^{k_1}\ \ (j\omega_1)^{k_1}]^T}{L_1(j\omega_1)}
\end{aligned}
\tag{6.2.8}
$$

Then substitute (6.2.6) into (6.2.8), the following equation can be obtained

$$
H_1(j\omega_1) = \chi^{Lu}\cdot\varphi_1^u(\omega_1)\cdot\chi^{Ly}\cdot\varphi_1^y(\omega_1) \tag{6.2.9}
$$

where $\varphi_1^u(\omega_1) = [\hat{c}_{0,1}(k_1)(j\omega_{k_1})^{k_1},\ (j\omega_1)^{k_1}]^T$. In (6.2.9), $\varphi_1^u(\omega_1)$, $\varphi_1^y(\omega_1)$ are functions of linear parameters of no interest, which are independent of system linear parameter to be analyzed in χ^{Lu} and χ^{Ly}. So the first order GFRF can be written as a polynomial of linear parameters in $\chi^{Lu}\otimes\chi^{Ly}$. Thus (6.2.9) can be written in a more concise form as

$$
H_1(j\omega_1) = \chi^{Ly}\otimes\chi^{Lu}\cdot\Phi_1(\hat{c}_{p,q}(k_1);j\omega_1), p+q=1.
$$

This completes the proof.

Based on the results in Proposition 6.2, the nth order GFRF of system (6.1.1) can be rewritten as a polynomial function with respect to system linear and nonlinear parameters as follows:

Proposition 6.3 *Let $s_n^{x_\iota} = c_{p_0,q_0}(\cdot)c_{p_1,q_1}(\cdot)\cdots c_{p_k,q_k}(\cdot)$ $(\iota = 1,\cdots,\mathfrak{L})$, which is the ι-th nonlinear parametric monomial in $CE(H_n(\cdot))$. $n(s_n^{x_\iota})$ is the order of the GFRF, in which the monomial $s_n^{x_\iota}$ is generated, $n(s_n^{x_\iota}) = \sum_{i=1}^{x_\iota}(p_i+q_i)-x_\iota+1$, x_ι is the number of parameters in $s_n^{x_\iota}$, $\sum_{i=1}^{x_\iota}(p_i+q_i)$ is summation of the subscript of all the parameters in $s_n^{x_\iota}$, if $x_\iota<1$, $\sum_{i=1}^{x_\iota}(\cdot)=0$, $n(1)=1$. The n-th order GFRF for system (6.1.1) can be formulated as*

$$
H_n(\cdot) = \sum_{\iota=1}^{\mathfrak{L}} s_n^{x_\iota}\mathcal{F}_{n(s_n^{x_\iota})}(s_n^{x_\iota};\omega_{l_1}\cdots\omega_{l_{n(s_n^{x_\iota})}}) \tag{6.2.10}
$$

$$
\mathcal{F}_{n(s_n^{x_\iota})}(s_n^{x_\iota};\omega_{l_1}\cdots\omega_{l_{n(s_n^{x_\iota})}}) = \varphi_{n(s_n^{x_\iota})}(s_n^{x_\iota};\omega_{l_1}\cdots\omega_{l_{n(s_x)}})[\chi^{Ly}]^{\rho+x}[\chi^{Lu}]^{\rho} \tag{6.2.11}
$$

where $\varphi_{n(s_n^{x_\iota})}(s_n^{x_\iota};\omega_{l_1}\cdots\omega_{l_{n(s_x)}})$ *represents function of frequencies* $\omega_{l_1}\cdots\omega_{l_n}$ *and output linear parameters of no interest, and* $\rho = n-\sum_{i=0}^{k} q_i$, l_i *for* $i = 1,\cdots,n(s_n^{x_\iota})$ *is a positive integer representing the index of the frequency variables.* $[\chi^{Ly}]^{\rho+x} = \underbrace{\left[\chi^{Ly}\otimes\cdots\otimes\chi^{Ly}\right]}_{\rho+x}$, $[\chi^{Lu}]^{\rho} = \underbrace{\left[\chi^{Lu}\otimes\cdots\otimes\chi^{Lu}\right]}_{\rho}$.

Proof: Let $\Gamma_{CE}(n)$ be a set composed of all the elements in $CE(H_n(\cdot)$, and $\Gamma_f(n)$ be a set of complex valued functions $f_n(\cdot)$. Based on results in [125], the nth-order GFRF can be expressed as

$$H_n(\cdot) = CE(H_n(\cdot))\cdot\Psi_n(CE(H_n(\cdot)))$$

where Ψ_n is a mapping

$$\Psi_n : \Gamma_{CE}(n) \to \Gamma_f(n)$$

Then for any nonlinear parameter monomial $s_n^{x_\iota}$ in $CE(H_n(\cdot))$, there exists a complex valued correlative function $\mathcal{F}_{n(s_n^{x_\iota})}(s_n^{x_\iota};\omega_{l_1}\cdots\omega_{l_{n(s_n^{x_\iota})}})$, which indicates that the nth order GFRF $H_n(\cdot)$ can be written as (6.2.10).

Based on results in [125], the correlative function can be written as a function of first order GFRF and $L_i(\cdot)$

$$\mathcal{F}_{n(s_n^{x_\iota})}(s_n^{x_\iota};\omega_{l_1}\cdots\omega_{l_{n(s_n^{x_\iota})}}) = \frac{\varphi_n(s_n^{x_\iota};\omega_{l_1}\cdots\omega_{l_{n(s_n^{x_\iota})}})}{\left[L(\omega_{l_1}\cdots\omega_{l_{n(s_n^{x_\iota})}})\right]^x}\prod_{i=1}^{\rho} H_1(j\omega_{\bar{l}_i}) \qquad (6.2.12)$$

where $r_1,\cdots,r_\rho$ are ρ integers taken from $[1,2,\cdots,n(s_n^{x_\iota})]$ without repetitions, $\bar{l} = [r_1,\cdots,r_\rho]$ is a set of integer representing the index of the frequency variables.

Substitute (6.2.6) and (6.2.7) into (6.2.12), (6.2.11) can be obtained. This complete the proof.

Remark 6.1 *In Proposition 6.3, the GFRFs are given in an explicit and straightforward structure in terms of system nonlinear parameters, the first order GFRF*

$H_1(\cdot)$ and $L_i^{-1}(.)$, thus influence of system linear and nonlinear parameters on system GFRFs can be simultaneously investigated based on results in Proposition 6.3.

6.2.2 Novel pCOS function with respect to both linear and nonlinear parameters

The analytic relationship between GFRFs and system linear and nonlinear parameters has been shown in Proposition 6.3. Nonlinear output spectrum is determined by GFRFs and input spectrum, thus how system linear and nonlinear parameters affect nonlinear output spectrum can be directly obtained based on results in Proposition 6.3.

Proposition 6.4 *A novel parametric characteristic output spectrum of system (6.1.2) in terms of system linear and nonlinear parameters can be given as*

$$Y(j\omega) = \sum_{n=1}^{N} Y_n(j\omega) \tag{6.2.13}$$

$$Y_n(j\omega) = \sum_{\iota=1}^{\mathfrak{L}} s_n^{x_\iota} [\chi^{Ly}]^{\rho+x} [\chi^{Lu}]^{\rho} \psi_{n(s_n^{x_\iota})}(s_n^{x_\iota}; \omega_{l_1} \cdots \omega_{l_{n(s_n^{x_\iota})}}) \tag{6.2.14}$$

where $\psi_{n(s_n^{x_\iota})}(s_n^{x_\iota}; \omega_{l_1} \cdots \omega_{l_{n(s_n^{x_\iota})}})$ is function of frequency variables, input magnitude and irrelevant linear parameters.

Proof: According to (6.1.5) and (6.1.6), nonlinear output spectrum can be written as:

$$Y(j\omega) = \sum_{n=1}^{N} \frac{1}{(2\pi)^{n-1}} \int \cdots \int_{\omega_1+\cdots+\omega_n=\omega} H_n(j\omega_1, \cdots, j\omega_n) \prod_{i=1}^{n} U(\omega_i) d\omega_i$$

Since $s_n^{x_\iota}$, $[\chi_n^{Ly}]^{\rho+x}$ and $[\chi_n^{Lu}]^{\rho}$ are all system parameters, substitute (6.2.10) into the above equation, (6.2.14) can be obtained. This completes the proof.

Procedure for calculation of the novel pCOS is given as follows:

Procedure 1: Calculation of the novel pCOS function

---

(1) Determine the polynomial representation of $L_i(\cdot)$ and $H_1(\cdot)$ based on methods in Proposition 6.1 and Proposition 6.2

(2) Determine structure of the novel pCOS function based on method proposed in Proposition 6.4.

(3) Calculate coefficients $\psi_{n(s_n^{x_\iota})}(s_n^{x_\iota}; \omega_{l_1} \cdots \omega_{l_{n(s_n^{x_\iota})}})$.

Remark 6.2 $\psi_{n(s_n^{x_\iota})}(s_n^{x_\iota}; \omega_{l_1} \cdots \omega_{l_{n(s_n^{x_\iota})}})$ *can be determined based on simulation or experimental data by Least Square method in terms of concerned linear and nonlinear characteristic parameter over given parameter's range.*

Remark 6.3 *It is noticed that the novel parametric characteristic output spectrum is a polynomial function with respect to system linear and nonlinear parameters. This relationship between the nonlinear output spectrum and system linear and nonlinear parameters in (6.2.14) is referred to as the novel parametric characteristic output spectrum function, which is not only function of frequency variables, but also functions of system's linear and nonlinear parameters (to be designed and analyzed). The novel pCOS function proposed in this chapter is a strong complement to the nCOS function-based method proposed in [49, 124, 125], which developed a systematic method to express the nonlinear output spectrum function as an explicit polynomial function of nonlinear characteristic parameters and the new nCOS function proposed in [134], which only investigated the relationship between nonlinear output spectrum and system linear parameters.*

6.3 A case study

The NDE model (6.1.1) has been widely used in mechanical system modelling. For example, NDE model of a single degree-of-freedom suspension system with cubic nonlinear damping is given by

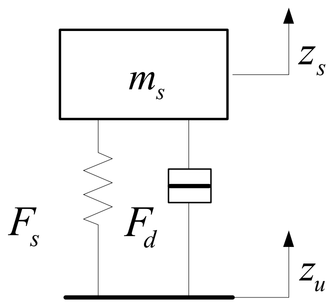

Fig. 6.1: 1-DOF suspension system

$$m_s\, \ddot{z}_s(t) + k\,(z_s(t) - z_u(t)) + c_1\,(\dot{z}_s(t) - \dot{z}_u(t)) + c_3\,(\dot{z}_s(t) - \dot{z}_u(t))^3 = 0 \quad (6.3.1)$$

Denote $z(t) = z_s(t) - z_u(t)$, equation (6.3.1) can be rewritten as

$$m_s\, \ddot{z}(t) + k\, z(t) + c_1\, \dot{z}(t) + c_3\, \dot{z}(t)^3 = F_\omega(t) \qquad (6.3.2)$$

where $F_\omega(t) = -m_s\, \ddot{z}_u(t)$. Equation (6.3.2) is a specific case of (6.1.1) with

$$c_{0,1}(2) = m_s,\;\; c_{1,0}(2) = m_s,\;\; c_{1,0}(0) = k,$$
$$c_{1,0}(1) = c_1,\;\; c_{3,0}(1,1,1) = c_3, \text{else } c_{p,q}(\cdot) = 0.$$

6.3.1 Analysis and design of nonlinear system

The main objective of this section is to study the effect of system damping parameters c_1 and c_3 on system output responses over the concern ranges. The output frequency response of the 1-DOF suspension system up to 5th order can be calculated as follows:

(1) Determine the polynomial representation of $L_n(\cdot)$ and $H_1(\cdot)$ in terms of system damping coefficients c_1 and c_3 based on methods in **Proposition** 6.1 and 6.2. In this case, only parameter $c_{1,0}(1)$ is the linear parameter of interest, so $\boldsymbol{\varepsilon} = [\varepsilon_1]$, where ε_1 represents the nonlinear order of linear parameters $c_{1,0}(1)$ in χ^{Ly}.

$$\begin{aligned}
L_n^{-1}\left(j\sum\nolimits_{i=1}^{n}\omega_i\right) &= \chi^{Ly}\cdot\varphi_n^y(\omega_n) = [1\ c_1\ \ \cdots\ \ c_1^{\varepsilon_1}\ ]\varphi_n^y(\omega_n) \\
H_1(j\omega) &= \chi^{Ly}\otimes\chi^{Lu}\cdot\Phi_1(\hat{c}_{p,q}(k_1);j\omega_1) \\
&= [1\ c_1\ \ \cdots\ \ c_1^{\varepsilon_1}]\Phi_1(\hat{c}_{p,q}(k_1);j\omega_1), p+q=1.
\end{aligned}$$

(2) Determine structure of system output spectrum. Nonlinear characteristic parameters of the system are obtained as

$$\mathrm{CE}(H_1(\cdot)) = [1],\ \mathrm{CE}(H_3(\cdot)) = [c_3],\ \mathrm{CE}(H_5(\cdot)) = [c_3^2].$$

According to **Proposition** 6.3, GFRFs up to fifth order can be obtained as following:

For first order GFRF: $x=0$, $s_0=1$, $\rho=1$.

$$H_1(j\omega) = 1\cdot\mathcal{F}_1(1;\omega) = \chi^{Ly}\cdot\varphi_1(1;\omega)$$

For third order GFRF: $x=1$, $s_1=c_{3,0}(1,1,1)$, $\rho=3$.

$$H_3(j\omega) = c_{3,0}(1,1,1)\cdot\mathcal{F}_3(c_{3,0}(1,1,1);\omega) = c_{3,0}(1,1,1)\cdot[\chi^{Ly}]^{3+1}\cdot\varphi_3(c_{3,0}(1,1,1);\omega)$$

For fifth order GFRF: $x=2$, $s_2=c_{3,0}^2(1,1,1)$, $\rho=5$

$$H_5(j\omega) = c_{3,0}^2(1,1,1)\cdot\mathcal{F}_5(c_{3,0}^2(1,1,1);\omega) = c_{3,0}^2(1,1,1)\cdot[\chi^{Ly}]^{5+2}\cdot\varphi_5(c_{3,0}^2(1,1,1);\omega)$$

(3) Determine output spectrum.

$$Y_1(j\omega) = \chi^{Ly}\cdot\psi_1(1;\omega)$$

$$Y_3(j\omega) = c_{3,0}(1,1,1) \cdot [\chi^{Ly}]^{3+1} \cdot \psi_3(c_{3,0}(1,1,1);\omega)$$
$$Y_5(j\omega) = c_{3,0}^2(1,1,1) \cdot [\chi^{Ly}]^{5+2} \cdot \psi_5(c_{3,0}^2(1,1,1);\omega)$$

where $\psi_i(\cdot), i = 1,3,5$ are coefficients to be calculated. Then system output spectrum up to fifth order can be obtained as:

$$Y(j\omega) = \sum\nolimits_{n=1}^{5} Y_n(j\omega)$$

Parameters for the single-DOF suspension system are given as: $m_s = 240$, and $k = 15394$. System output frequency response at resonant frequency is always of great importance. So resonant frequency ω_r is first chosen as input frequency. Although high linear damping can effectively suppress the resonant peak, it will also degrade system isolation performance at higher frequency domain. Thus, system response out of resonant frequency domain should also be taken into consideration. The excitation input are chosen as $\ddot{z}_u(t) = 4.2\sin(\omega_r t)$ and $\ddot{z}_u(t) = 4.2\sin(6\omega_r t)$, where $\omega_r = \sqrt{k/m_s}$ is the resonant frequency of the suspension system. Then coefficients can be calculated from system characteristic output spectrum responses subject to given input when damping parameters c_1 and c_3 are over the following concern ranges $c_1 \in [500,\ 1300],\ c_3 \in [800,\ 2800]$.

To verify validity of the proposed approach, comparisons of output frequency response that obtained via simulation and the method proposed are given in Fig.6.2, from which it can be seen that larger truncation order ε_1 for linear parameters c_1 results in better match between simulation results and estimated output spectrum. This verifies the effectiveness the approach proposed in this chapter.

Then output frequency response in terms of linear damping c_1 and nonlinear damping c_3 at resonant frequency ω_r and high frequency $6\omega_r$ are given in Fig.6.3 and Fig.6.4, respectively.

From Fig.6.3, it can be seen that both high linear damping and high nonlinear damping are helpful to suppress the resonant peak. But the performance improved

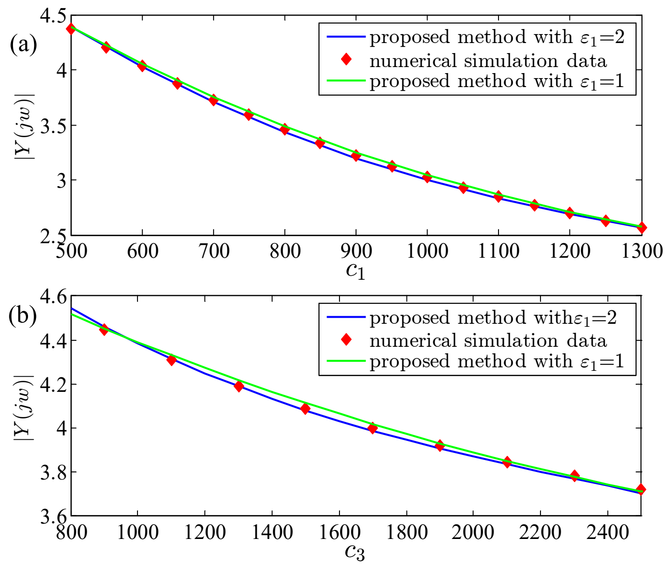

Fig. 6.2: Amplitude of $Y(j\omega)$ under $\ddot{z}_u(t) = 4.2\sin(\omega_r t)$ (a) $c_3 = 1000$ and (b) $c_1 = 500$.

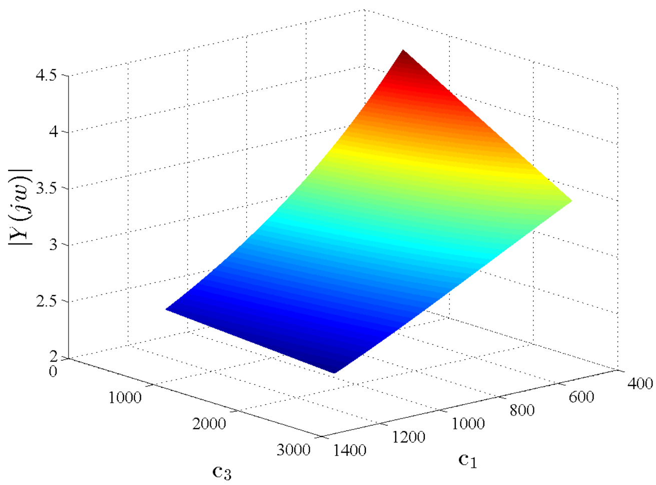

Fig. 6.3: Amplitude of $Y(j\omega)$ with c_1 and c_3 under input $\ddot{z}_u(t) = 4.2\sin(\omega_r t)$

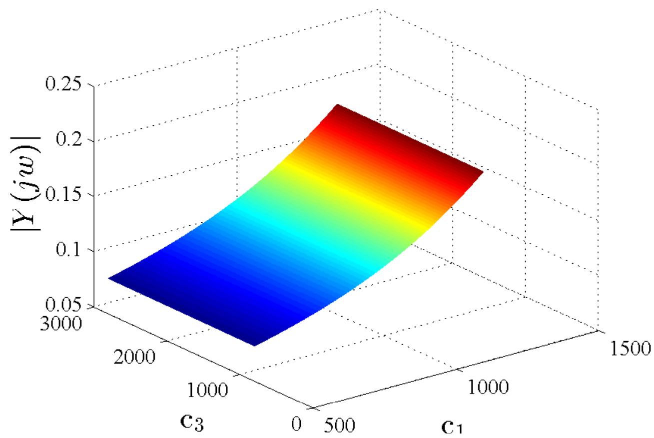

Fig. 6.4: Amplitude of $Y(j\omega)$ with c_1 and c_3 under input $\ddot{z}_u(t) = 4.2\sin(6\omega_r t)$

by increasing the linear damping is more obvious. From Fig.6.4, it is observed that high frequency performance is sharply degraded by linear damping, but almost not affected by the nonlinear damping. Then we can come to the conclusion that suspension system with proper small linear damping and large nonlinear damping can achieve better performance at both resonant and high frequency domains.

To further test vibration isolation performance of the suspension system with the above damping design strategy, random input including low and high frequency disturbances are respectively applied to the system. The disturbances are correspondingly chosen as $\ddot{z}_u(t) = 0.2\sin(\omega_r t)$ and $\ddot{z}_u(t) = 2.0\sin(6\omega_r t)$, ω_r is the resonant frequency. Suspension acceleration response in time domain with different damping are given in Fig.6.5.

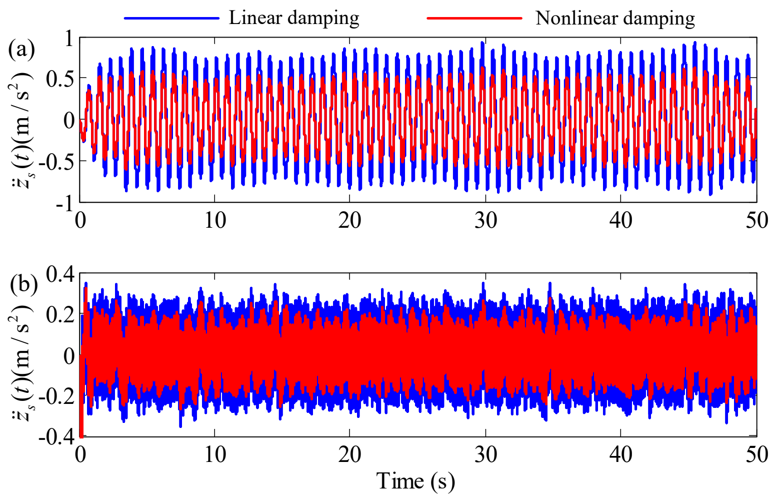

Fig. 6.5: Acceleration response under different damping. (a) linear damping ($c_1 = 500$, $c_3 = 0$) and nonlinear damping ($c_1 = 800$, $c_3 = 2800$), (b) linear damping ($c_1 = 1300$, $c_3 = 0$) and nonlinear damping ($c_1 = 800$, $c_3 = 2800$).

Fig.6.5(a) shows acceleration under linear damping and nonlinear damping, from which it is observed that nonlinear damping outperforms linear damping. Fig.6.5(b) are comparison results of acceleration response with high linear damping and high nonlinear damping, from which we can see that large linear damping degrades high frequency performance. The linear and nonlinear parameters analysis method proposed in this chapter can be seen as a powerful tool in passive suspension, or passive vibration isolation system design. With this method, both linear and nonlinear parameters can be designed to guarantee better performance. This method can also be applied to parameter analysis and design of multi-degree-of-freedom system. In that case, more frequencies should be included.

6.3.2 Application to fault identification of closed-loop nonlinear control system

In this part, the parameter analysis approach is applied to identify controller and plant faults of the closed-loop system. Generally, in practical systems, only measured output data can be obtained for nondestructive evaluation. Hence, the hybrid parameters analysis method proposed in this chapter, together with an n-th order nonlinear output spectrum calculation method via measured output [49] can provide an in-depth insight of fault characteristics analysis and identification.

Computation of the nth-order output spectrum

The output spectrum of a single input single output system up to nth-order can be analytically computed based on simulation or experimental data and least square method [49, 124, 125]. Considering excitation input $\beta_p U(j\omega)$ with magnitude β_p, the nonlinear output spectrum in (6.1.5) is presented as

$$Y(j\omega)_{\beta_p} = \sum_{n=1}^{\infty} \beta_p^n \hat{Y}_n(j\omega) = \sum_{n=1}^{N} \beta_p^n \hat{Y}_n(j\omega) + \sigma_{[N]}(j\omega) \tag{6.3.3}$$

where $\sigma_{[N]}(j\omega)$ represents the truncation error. To calculate nth-order output spectrum $\hat{Y}_n(j\omega)$, the system is excited by input $\beta_p U(j\omega)$ with the same frequency but different amplitude, where $p = \{1, 2, \cdots, N\}$. Correspondingly, system output $Y(j\omega)_{\beta_1}$, $Y(j\omega)_{\beta_2}$, $\cdots$, $Y(j\omega)_{\beta_N}$ can be obtained. Then the nth-order output spectrum $Y_n(j\omega)$, $n \in \{1, 2, \cdots, N\}$ is calculated by least square method

$$\begin{bmatrix} \hat{Y}_1(j\omega) \\ \hat{Y}_2(j\omega) \\ \vdots \\ \hat{Y}_N(j\omega) \end{bmatrix} = \begin{bmatrix} \beta_1 & \beta_1^2 & \cdots & \beta_1^N \\ \beta_2 & \beta_2^2 & \cdots & \beta_2^N \\ \vdots & \vdots & \ddots & \vdots \\ \beta_N & \beta_N^2 & \cdots & \beta_N^N \end{bmatrix}^{-1} \begin{bmatrix} Y(j\omega)_{\beta_1} \\ Y(j\omega)_{\beta_2} \\ \vdots \\ Y(j\omega)_{\beta_N} \end{bmatrix} \tag{6.3.4}$$

The square matrix is nonsingular if $\beta_1 \neq \beta_2 \neq \cdots \neq \beta_N$. An excitation magnitude β selection method in [49] can be adopted. U-shaped $|\hat{Y}_n(j\omega)| \backsim \beta_p$ curve can be obtained with a series of β_p, which starts from a small value. The optimal β_p should locate around the bottom of the curve which corresponds to the minimum estimation error for $|\hat{Y}_n(j\omega)|$.

Then according to (6.2.14), we can obtain:

$$\begin{aligned} Y_n(j\omega) &= \beta^n \hat{Y}_n(j\omega) \\ &= \beta^n \left[\sum_{\iota}^{\mathfrak{L}} s_n^{x_\iota} [\chi^{Ly}]^{\rho+x} [\chi^{Lu}]^{\rho} \hat{\psi}_{n(s_n^{x_\iota})}(s_n^{x_\iota}; \omega_{l_1} \cdots \omega_{l_{n(s_n^{x_\iota})}}) \right] \end{aligned} \tag{6.3.5}$$

where $\hat{\psi}_{n(s_n^{x_\iota})}(s_n^{x_\iota}; \omega_{l_1} \cdots \omega_{l_{n(s_n^{x_\iota})}})$ is a function of frequency variables and linear parameters of no interest.

Fault identification of closed-loop system

For practical systems modeled as the NDE model (6.1.1), consider a state feedback controller $u(t) = K(x(t))\, x(t)$, then the closed-loop system is still a NDE model. Then output spectrum of the closed-loop system can be explicitly formulated as (6.2.13) and (6.2.14). The output spectrum value can also be directly estimated via the aforementioned decomposition method in (6.3.4). Thus parameters including actuator parameters and plant parameters in the output spectrum can be determined. Finally, compare the estimated parameters with known systems' information, the fault can be easily detected and located. The fault detection method can be summarized as follows:

Procedure 2: Fault detection of closed-loop control system

---

(1) Determine the optimal β with the excitation magnitude selection method.

(2) Determine structure of $Y_n(j\omega)$ according to method proposed in **Proposition** 6.4. Then output spectrum $\hat{Y}_n(j\omega)$ can be calculated as

$$\hat{Y}_n(j\omega)=\sum_{\iota}^{\mathfrak{L}} s_n^{x_\iota}[\chi^{Ly}]^{\rho+x}[\chi^{Lu}]^{\rho}\hat{\psi}_{n(s_n^{x_\iota})}(s_n^{x_\iota};\omega_{l_1}\cdots\omega_{l_{n(s_n^{x_\iota})}}) \tag{6.3.6}$$

(3) Calculate the nth order output frequency response $\hat{Y}_n(j\omega)$ using the decomposition method with excitation input $\beta U(j\omega)$. Coefficients $\hat{\psi}_{n(s_n^{x_\iota})}(s_n^{x_\iota};\omega_{l_1}\cdots\omega_{l_{n(s_n^{x_\iota})}})$ can be calculated over given parameters' ranges (c_{p_0,q_0}, $\cdots$, c_{p_k,q_k}).

(4) Then $c_{p_0,q_0}(\cdot),\cdots,c_{p_k,q_k}(\cdot)$ can accordingly be calculated. Compare them to known system parameters, fault can be identified and located.

Case study

In this part, we still consider the example in Section 6.3. To achieve better vibration isolation performance, active control method based on T-S fuzzy nonlinear controller will be used in this system. Define $x_1(t) = z(t)$ and $x_2(t) = \dot{z}(t)$, denote $x(t) = [x_1(t)\ x_2(t)]^T$, then the nonlinear system can be represented on $x_2(t) \in [-d,\ d]$ by the following T-S fuzzy system

$$\dot{x}(t) = \sum\nolimits_{i=1}^{2} h_i(x(t))\,[A_i\,x(t) + B_i\,u(t) + B_{\omega i}\,F_\omega(t)] \tag{6.3.7}$$

where membership functions are $h_1(x(t)) = 1 - x_2(t)^2/d^2$, and $h_2(x(t)) = x_2(t)^2/d^2$. System matrices are given as follows:

$$
\begin{aligned}
A_1 &= \begin{bmatrix} 0 & 1 \\ -\frac{k}{m_s} & -\frac{c_1}{m_s} \end{bmatrix}, \; A_2 = \begin{bmatrix} 0 & 1 \\ -\frac{k}{m_s} & -\frac{c_1}{m_s} - \frac{c_3 d^2}{m_s} \end{bmatrix} \\
B_1 &= B_2 = \begin{bmatrix} 0 & 1 \end{bmatrix}^T, \; B_{\omega_1} = B_{\omega_2} = \begin{bmatrix} 0 & \frac{1}{m_s} \end{bmatrix}^T
\end{aligned}
$$

For the aforementioned fuzzy system, a fuzzy controller will be designed to achieve better vibration isolation performance. Controller gains are expressed as:

$$K_1 = [k_{11} \; k_{12}], \; K_2 = [k_{21} \; k_{22}] \tag{6.3.8}$$

The overall controller can be represented as:

$$
\begin{aligned}
u(t) &= \sum\nolimits_{i=1}^{2} h_i(x(t))K_i x(t) \\
&= k_{11}x_1(t) + k_{12}x_2(t) + \frac{k_{21} - k_{11}}{d^2} x_1(t)x_2^2(t) + \frac{k_{22} - k_{12}}{d^2} x_2^3(t)
\end{aligned} \tag{6.3.9}
$$

By substituting (6.3.9) into (6.3.2), the closed-loop system is obtained as:

$$m_s \, \ddot{z}(t) + a_1 \, z(t) + a_2 \, \dot{z}(t) + a_3 \, \dot{z}^3(t) + a_4 \, z(t)\dot{z}^2(t) = F_\omega(t) \tag{6.3.10}$$

where $a_1 = (k - k_{11}), a_2 = (c_1 - k_{12}), a_3 = (c_3 - \frac{k_{22} - k_{12}}{d^2})$, and $a_4 = -\frac{k_{21} - k_{11}}{d^2}$. Obviously, the stiffness and damping coefficients of the closed-loop system (6.3.10) are reconfigured by the controller to achieve better performance. The system output $y(t)$ is chosen as $y(t) = \ddot{z}_s(t)$. For given system parameters $m_s = 240$, $k = 15394$, $c_1 = 385.4$, $c_3 = 100$, and $d = 5$, a fuzzy controller is designed based on the method in [171] and the controller gains are given as follows

$$K_1 = [7661.5089, \; -4785.8861], \; K_2 = [7664.1038 \; -4685.0831].$$

As shown in Fig.6.6, we mainly consider multiplicative faults caused by the non-

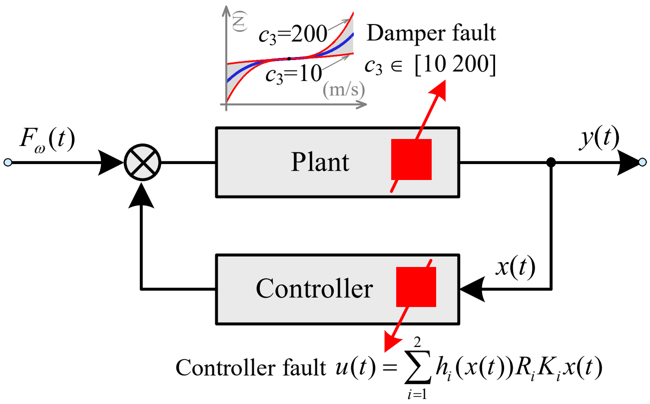

Fig. 6.6: Damper and controller faults in the closed-loop control system

linear damper and controller. A typical fault of nonlinear damper is the damper force drift caused by oil leakage, physical deformation and other factors. Nonlinear damping coefficient c_3 varying in the range of $c_3 \in [10\ 200]$ is used to mimic the damper fault. The normal value of c_3 is 100. For convenient analysis, the controller fault distribution matrix R_i is defined as

$$R_1 = \begin{bmatrix} 1 & 0 \\ 0 & r_c \end{bmatrix}, \; R_2 = \begin{bmatrix} 1 & 0 \\ 0 & r_c \end{bmatrix}. \tag{6.3.11}$$

where controller fault rate $r_c \in [0\ 1]$ is used to describe the fault extent. $r_c = 1$ means no fault occurs in the controller. The controller fault is mimicked by adopting controller rate varying in the range of $r_c \in [0.40\ 0.95]$. The faults are assumed to be slow time-varying, then the parameters at the moment of estimation will remain constant.

The closed-loop system (6.3.10) can be viewed as a specific case of (6.1.1) with the following parameters

$$c_{1,0}(2) = m_s, \; c_{1,0}(0) = a_1, \; c_{1,0}(1) = a_2,$$
$$c_{3,0}(1,1,1) = a_3, \; c_{3,0}(0,1,1) = a_4, \text{else } c_{p,q}(\cdot) = 0.$$

Since parameters c_3, k_{12}, and k_{22} are closely related to system faults, a_2 and a_3

are the concerned parameters in the closed-loop control system (6.3.10). Thus, parameter $c_{1,0}(1)$ is the linear parameters of interest, $\boldsymbol{\varepsilon} = [\varepsilon_1]$, where ε_1 represents the nonlinear order of linear parameters $c_{1,0}(1)$ in χ^{Ly}. Consequently, the polynomial representation of $L_n^{-1}(\cdot)$ and $H_1(\cdot)$ in terms of system linear parameters $c_{1,0}(1)$ can be determined as:

$$\begin{aligned}
L_n^{-1}\left(j\sum\nolimits_{i=1}^{n}\omega_i\right) =&\chi^{Ly}\cdot\varphi_n^y(\boldsymbol{\omega_n}) = [1\ a_2\ \cdots\ a_2^{\varepsilon_1}\ ]\varphi_n^y(\omega)\\
H_1(j\omega) =&\chi^{Ly}\otimes\chi^{Lu}\cdot\Phi_1(\hat{c}_{0,1}(l);j\omega)\\
=&[1\ a_2\ \cdots\ a_2^{\varepsilon_1}]\Phi_1(\hat{c}_{0,1}(l);j\omega)
\end{aligned}$$

Further, nonlinear characteristic parameter of the system can be obtained as $\mathrm{CE}(H_1(\cdot)) = [1], \mathrm{CE}(H_3(\cdot)) = [a_3,\ a_4]$. Then output spectrum up to third order can be written as:

$$Y(j\omega) = Y_1(j\omega) + \underbrace{a_3F_3(a_3;\omega) + a_4F_3(a_4;\omega)}_{Y_3(j\omega)} \tag{6.3.12}$$

Based on output spectrum estimation (6.3.3), (6.3.12) can be reformed as:

$$Y(j\omega) =\beta\hat{Y}_1(j\omega) + \beta^3\underbrace{[a_3\hat{F}_3(a_3;\omega) + a_4\hat{F}_3(a_4;\omega)]}_{\hat{Y}_3(j\omega)} \tag{6.3.13}$$

According to Proposition 6.4, $\hat{F}_3(a_3;\omega)$ and $\hat{F}_3(a_4;\omega)$ can be calculated as:

$$\hat{F}_3(a_3;\omega) = [\chi^{Ly}]^{3+1}\cdot\hat{\boldsymbol{\psi}}_3(a_3;\omega), \hat{F}_3(a_4;\omega) = [\chi^{Ly}]^{3+1}\cdot\hat{\boldsymbol{\psi}}_3(a_4;\omega)$$

Then it is easy to obtain

$$\hat{Y}_1(j\omega) =[1\ a_2\ \cdots\ a_2^{\varepsilon_1}\ ]\hat{\boldsymbol{\psi}}_1(1;\omega) \tag{6.3.14}$$

$$\hat{Y}_3(j\omega) =a_3[1\ a_2\ \cdots\ a_2^{\varepsilon_1}\ ]^4\,\hat{\boldsymbol{\psi}}_3(a_3;\omega)a_4[1\ a_2\ \cdots\ a_2^{\varepsilon_1}\ ]^4\,\hat{\boldsymbol{\psi}}_3(a_4;\omega) \tag{6.3.15}$$

where $\hat{\boldsymbol{\psi}}_i(\cdot), i = 1, 2, 3$ are column vectors, which are independent of a_2, a_3, a_4 and can be determined based on simulation or experimental data.

The linear parameters truncation order $\varepsilon_1 = 2$, excitation magnitude is selected as $\beta = 0.02$ based on the excitation magnitude selection method, then coefficients $\hat{\boldsymbol{\psi}}_1(1;\omega)$, $\hat{\boldsymbol{\psi}}_3(a_3;\omega)$, and $\hat{\boldsymbol{\psi}}_3(a_4;\omega)$ are obtained as shown in Table 6.1 and 6.2.

Table 6.1: Coefficients of first-order output spectrum

Coefficient	Value
$\hat{\boldsymbol{\psi}}_1(1;\omega)(1,1)$	0.9103 - 0.0811i
$\hat{\boldsymbol{\psi}}_1(1;\omega)(2,1)$	-1.4505e-04 - 1.2784e-04i
$\hat{\boldsymbol{\psi}}_1(1;\omega)(3,1)$	1.2201e-08 + 1.1116e-08i

Table 6.2: Coefficients of third-order output spectrum

Coefficient	Value	Coefficient	Value
$\hat{\boldsymbol{\psi}}_3(a_3;\omega)(1,1)$	-7.64e-05 - 9.34e-05i	$\hat{\boldsymbol{\psi}}_3(a_4;\omega)(1,1)$	3.88e-05 + 6.40e-05i
$\hat{\boldsymbol{\psi}}_3(a_3;\omega)(2,1)$	1.24e-07 + 1.56e-07i	$\hat{\boldsymbol{\psi}}_3(a_4;\omega)(2,1)$	-8.56e-08 - 1.34e-07i
$\hat{\boldsymbol{\psi}}_3(a_3;\omega)(3,1)$	-8.82e-11 - 1.13e-10i	$\hat{\boldsymbol{\psi}}_3(a_4;\omega)(3,1)$	7.72e-11 + 1.17e-10i
$\hat{\boldsymbol{\psi}}_3(a_3;\omega)(4,1)$	3.54e-14 + 4.57e-14i	$\hat{\boldsymbol{\psi}}_3(a_4;\omega)(4,1)$	-3.75e-14 - 5.58e-14i
$\hat{\boldsymbol{\psi}}_3(a_3;\omega)(5,1)$	-8.71e-18 - 1.14e-17i	$\hat{\boldsymbol{\psi}}_3(a_4;\omega)(5,1)$	1.08e-17 + 1.58e-17i
$\hat{\boldsymbol{\psi}}_3(a_3;\omega)(6,1)$	1.34e-21 + 1.77e-21i	$\hat{\boldsymbol{\psi}}_3(a_4;\omega)(6,1)$	-1.90e-21 - 2.75e-21i
$\hat{\boldsymbol{\psi}}_3(a_3;\omega)(7,1)$	-1.27e-25 - 1.68e-25i	$\hat{\boldsymbol{\psi}}_3(a_4;\omega)(7,1)$	2.00e-25 + 2.88e-25i
$\hat{\boldsymbol{\psi}}_3(a_3;\omega)(8,1)$	6.69e-30 + 8.89e-30i	$\hat{\boldsymbol{\psi}}_3(a_4;\omega)(8,1)$	-1.16e-29 - 1.66e-29i
$\hat{\boldsymbol{\psi}}_3(a_3;\omega)(9,1)$	-1.51e-34 - 2.02e-34i	$\hat{\boldsymbol{\psi}}_3(a_4;\omega)(9,1)$	2.85e-34 + 4.04e-34i

To identify the fault, excitation input with different amplitude is imposed to the system and the values of output spectrum $Y_1(j\omega)$ and $Y_3(j\omega)$ are obtained by measuring the input and the corresponding output based on the equation (6.3.4). According to the explicit relationships in (6.3.14) and (6.3.15), the concerned parameters a_2 and a_3 can be obtained. For the real values of c_3 and r_c selected from $c_3 \in [20\ 200]$ and $r_c \in [0.40\ 95]$, the estimation results of controller and damper faults are demonstrated in Table 6.3.

Since the first-order output spectrum $Y_1(\omega)$ is only dependent on the parameter a_2, the estimation results of control fault rate r_c remain constant for different damping coefficient c_3. The detailed estimation errors of controller and nonlinear

Table 6.3: Estimation results of controller and nonlinear damper faults

	r_c = **0.40**	r_c = **0.45**	r_c = **0.50**	r_c = **0.55**	r_c = **0.60**	r_c = **0.65**
c_3 = **10**	0.3974	0.4586	0.5144	0.5659	0.6141	0.6597
	9.9858	10.7255	10.7577	10.4922	10.2348	10.1106
c_3 = **50**	0.3974	0.4586	0.5144	0.5659	0.6141	0.6597
	49.9714	54.1588	54.3237	52.7272	51.1501	50.3968
c_3 = **100**	0.3974	0.4586	0.5144	0.5659	0.6141	0.6597
	99.9535	108.4473	108.7815	105.5199	102.2946	100.7545
c_3 = **150**	0.3974	0.4586	0.5144	0.5659	0.6141	0.6597
	149.9356	162.7364	163.2392	158.3139	158.4384	151.1112
c_3 = **200**	0.3974	0.4586	0.5144	0.5659	0.6141	0.6597
	199.9177	217.0255	217.6971	211.1071	204.5823	201.4683
	r_c = **0.70**	r_c = **0.75**	r_c = **0.80**	r_c = **0.85**	r_c = **0.90**	r_c = **0.95**
c_3 = **10**	0.7034	0.7460	0.7878	0.8299	0.8729	0.9184
	10.1344	10.2569	10.3796	10.3625	10.0775	9.5177
c_3 = **50**	0.7034	0.7460	0.7878	0.8299	0.8729	0.9184
	50.6233	51.5919	52.6894	52.9502	51.3555	47.6075
c_3 = **100**	0.7034	0.7460	0.7878	0.8299	0.8729	0.9184
	101.2351	103.2590	105.5777	106.1875	102.9577	95.2199
c_3 = **150**	0.7034	0.7460	0.7878	0.8299	0.8729	0.9184
	151.8470	154.9245	158.4658	159.4253	154.5580	142.8336
c_3 = **200**	0.7034	0.7460	0.7878	0.8299	0.8729	0.9184
	202.4587	206.5917	211.3527	212.6602	206.1589	190.4450

damper faults are summarized in the Fig.6.7. The estimation error of controller fault rate r_c is less than 4%. The estimation error of nonlinear damper fault is less than 8%. The estimation error is mainly introduced by the least-squares method. Since the damper fault estimation is based on the estimation result of controller fault rate r_c, thus the estimation error on damper fault estimation is further enlarged. Overall, the estimation errors are in an acceptable level.

Remark 6.4 *For closed-loop control systems including multiple faults from plant and controller, the proposed fault detection method uses only one single output as a reference of evaluation. By resorting to a nonlinear decomposition method, multiple fault characteristics can be independently extracted from the single output data with relatively high accuracy. Compared with other methods using multiple output data, the proposed fault detection method significantly improves the efficiency and*

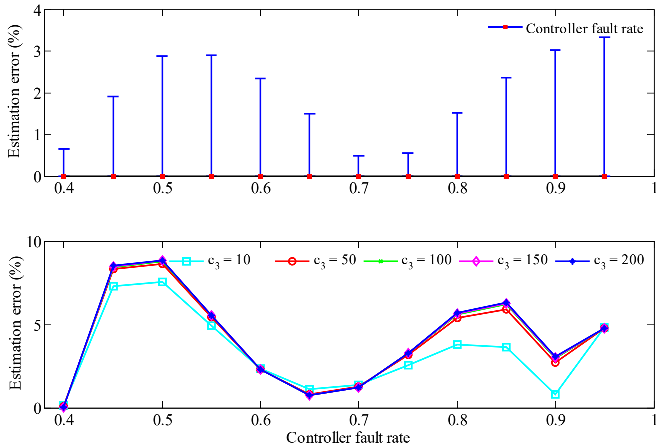

Fig. 6.7: Estimation errors of controller and nonlinear damper faults

convenience of detection procedures especially in nondestructive evaluation cases with high dimension. Moreover, higher order unmodeled dynamics or disturbances do not affect the identification results. Taking the case in this chapter for example, only first- and third-order output spectrum are used to identify faults, thus unmodeled dynamics or disturbances higher than third order in the system have no influence on the identification results, which further confirms the robustness of the proposed method.

6.4 Conclusion

A novel parametric characteristic function is proposed for analysis and design of nonlinear systems in this chapter. The relationship between system parameters and output spectrum is explicitly revealed and effects of both linear and nonlinear parameters of interest on system output spectrum are simultaneously considered and analyzed. This proposed approach serves as a strong complement to existing nCOS function based method, which can only analyze and design system parameters in a separated manner, either linear or nonlinear and can provide a more comprehensive and powerful solution for nonlinear system analysis and design. Then together with a nonlinear decomposition method, the approach proposed in this paper are applied to fault detection of closed-loop control systems with plant and controller faults.

Chapter 7

Conclusions

This thesis has presented some novel control and analysis methods that can improve nonlinear dynamic systems performance with disturbance, uncertainty, time-delay, etc. The results obtained in this thesis foster the flexibility of fuzzy model based control, enrich research on frequency domain method based on nCOS function and offer solutions to some existing technical problems. More specifically, the conclusions have been summarized as follows:

Chapter 2 studies the fuzzy adaptive control for nonlinear suspension systems based on a bio-inspired reference model. A general bio-inspired nonlinear structure, which can present ideal nonlinear quasi-zero stiffness for vibration isolation, is adopted as tracking reference model. Fuzzy logic systems are used to approximate unknown nonlinear terms in nonlinear suspension systems. Particularly, a nonlinear damping is designed to improve damping characteristics of the bio-inspired reference model. With beneficial nonlinear stiffness and improved nonlinear damping of the bio-inspired reference model, the proposed fuzzy adaptive controller can effectively suppress vibration of suspension systems with less actuator force and much improved ride comfort, thus energy saving performance can be achieved. Finally, a quarter-vehicle active suspension system with considering payload uncertainties, general disturbance and actuator saturation is provided for evaluating the validity and superiority of the bio-inspired nonlinear dynamics based fuzzy adaptive control approach proposed in this chapter.

Chapter 3 deals with the fuzzy sampled-data control for nonlinear systems. First, exponential stability analysis and stabilization problems for T-S fuzzy systems under aperiodic sampling have been investigated. Some classical problems (such as H_∞, $L_2 - L_\infty$, passive and dissipative stability and stabilization problems) have been solved successfully under a unified framework by resorting to a novel performance index−extended dissipative performance index. Through adopting a sampling period dependent Lyapunov-Krasovskii function together with a novel efficient integral inequality, which has the advantages of reducing conservativeness, new stability conditions consisting of both exponential stability and extended dissipativity criterion have been established. Furthermore, a sampled-data controller that can not only exponentially stabilize the system but also guarantee the prescribed extended-dissipativity performance has been designed. A quarter-vehicle active suspension system with taking into account the uncertain payload and aperiodic sampling has been provided for evaluating the validity and superiority (from the aspects of disturbance attenuation level and closed-loop system dynamic performance) of the extended dissipative control approach proposed in this thesis over some ones of the existing literatures.

Chapter 4 focuses on imperfect premise matching fuzzy filter design problem for nonlinear systems with time-varying delay. Based on extended dissipative performance index, the H_∞, $L_2 - L_\infty$, passive and dissipative filter problems have been investigated. New delay-dependent conditions for performance analysis of filtering error system have been established in terms of LMIs by employing an efficient integral inequality. Finally, some numerical simulation results specific to H_∞ and $L_2 - L_\infty$ filter problems have been provided to demonstrate the advantages of the method proposed in this chapter over some recent ones in the literature.

In Chapter 5, optimization problems of mismatched fuzzy membership function parameters based on frequency domain method is investigated. Finite frequency fuzzy H_∞ control for nonlinear mechanical system with mismatched premise variables is first studied. Then the H_∞ index from disturbance to controlled output has been minimized by designing a finite frequency fuzzy controller over the concerned frequency band. A novel nCOS function based optimization method, which aims to optimize the Gaussian membership functions' parameters, has been proposed in this thesis. Compared to GA optimization method, the nCOS function based frequency domain optimization approach can provide a more analytical relationship between system output spectrum and fuzzy membership function parameters and is time efficient. Then the controller design and optimization methods are applied to a nonlinear quarter suspension system. Simulation results demonstrate that suspension performance over a concerned frequency band has been further enhanced by combining the finite frequency H_∞ control with the nCOS function based frequency domain optimization method.

On the basis of nCOS function, a novel pCOS function for the analysis and design of nonlinear systems is proposed in Chapter 6. The relationship between system parameters and output spectrum is explicitly revealed through the novel pCOS function, and effects of both linear and nonlinear parameters of interest on system output spectrum are considered and analyzed. This parameter analysis approach is used to analyze and design linear damping and nonlinear damping of passive suspension system. Then together with a nonlinear decomposition method, the approach proposed in this paper are applied to fault detection of closed-loop control systems with plant and controller faults.

7.1 Future work

Following are the future research that will further verify and enhance the concepts presented in this thesis:

1. The novel pCOS function proposed in Chapter 6 of this thesis aims at analysis and design of SISO systems. The problem of pCOS function of MIMO systems is worth further study.

2. Experimental validation: The control methods presented in this thesis are all theoretical research. Thus, experimental test platform such as quarter suspension setup can be designed to experimentally validate control approaches.

Bibliography

[1] R. M. Murray, *Control in an information rich world: Report of the panel on future directions in control, dynamics, and systems.* SIAM, 2003.

[2] T. Takagi and M. Sugeno, "Fuzzy identification of systems and its applications to modeling and control," *IEEE Trans. Systems, Man and Cybernetics*, vol. SMC-15, no. 1, pp. 116–132, Jan. 1985.

[3] K. Tanaka, T. Ikeda, and H. Wang, "Fuzzy regulators and fuzzy observers: relaxed stability conditions and LMI-based designs," *IEEE Trans. Fuzzy Syst.*, vol. 6, no. 2, pp. 250–265, May 1998.

[4] J. Qiu, G. Feng, and H. Gao, "Fuzzy-model-based piecewise H_∞ static-output-feedback controller design for networked nonlinear systems," *IEEE Trans. Fuzzy Syst.*, vol. 18, no. 5, pp. 919–934, Oct. 2010.

[5] ——, "Static-output-feedback H_∞ control of continuous-time T-S fuzzy affine systems via piecewise Lyapunov functions," *IEEE Trans. Fuzzy Syst.*, vol. 21, no. 2, pp. 245–261, Apr. 2013.

[6] H. K. Lam, M. Narimani, H. Li, and H. Liu, "Stability analysis of polynomial-fuzzy-model-based control systems using switching polynomial Lyapunov function," *IEEE Trans. Fuzzy Syst.*, vol. 21, no. 5, pp. 800–813, Oct. 2013.

[7] J. Qiu, G. Feng, and J. Yang, "A new design of delay-dependent robust H_∞ filtering for discrete-time T–S fuzzy systems with time-varying delay," *IEEE Trans. Fuzzy. Syst.*, vol. 17, no. 5, pp. 1044–1058, Oct. 2009.

[8] X. Zhao, L. Zhang, P. Shi, and H. Karimi, "Novel stability criteria for T-S fuzzy systems," *IEEE Trans. Fuzzy Syst.*, vol. 22, no. 2, pp. 313–323, Mar. 2014.

[9] J. Qiu, S. Ding, H. Gao, and S. Yin, "Fuzzy-model-based reliable static output feedback H_∞ control of nonlinear hyperbolic PDE systems," *IEEE Trans. Fuzzy Syst.*, vol. 24, no. 2, pp. 388–400, Mar. 2016.

[10] X. Zhao, Y. Yin, L. Zhang, and H. Yang, "Control of switched nonlinear systems via T-S fuzzy modeling," *IEEE Trans. Fuzzy Syst.*, vol. 24, no. 1, pp. 235–241, Feb. 2016.

[11] H. Li, J. Yu, C. Hilton, and H. Liu, "Adaptive sliding-mode control for nonlinear active suspension vehicle systems using T-S fuzzy approach," *IEEE Trans. Ind. Electron.*, vol. 60, no. 8, pp. 3328–3338, Aug. 2013.

[12] J. Qiu, H. Gao, and S. Ding, "Recent advances on fuzzy-model-based nonlinear networked control systems: A survey," *IEEE Trans. Ind. Electron.*, vol. 63, no. 2, pp. 1207–1217, Feb. 2016.

[13] D. Zhang, S. Nguang, D. Srinivasan, and L. Yu, "Distributed filtering for discrete-time T-S fuzzy systems with incomplete measurements," *IEEE Trans. Fuzzy. Syst.*, vol. 26, no. 3, pp. 1459–1471, Jun. 2018.

[14] F. Yang, S. Guan, and D. Wang, "Quadratically convex combination approach to stability of T-S fuzzy systems with time-varying delay," *Journal of the Franklin Institute*, vol. 351, no. 7, pp. 3752 – 3765, Jul. 2014.

[15] H. Shao, Q.-L. Han, Z. Zhang, and X. Zhu, "Sampling-interval-dependent stability for sampled-data systems with state quantization," *Int. J. Robust & Nonlinear Control*, vol. 24, no. 17, pp. 2995–3008, 2014.

[16] D. Zhang, Q.-L. Han, and X. Jia, "Network-based output tracking control for T-S fuzzy systems using an event-triggered communication scheme," *Fuzzy Sets Syst.*, vol. 273, pp. 26 – 48, Aug. 2015.

[17] H. Li, X. Sun, P. Shi, and H.-K. Lam, "Control design of interval type-2 fuzzy systems with actuator fault: Sampled-data control approach," *Inform. Sci.*, vol. 302, no. 0, pp. 1 – 13, May 2015.

[18] H. K. Lam and S. H. Tsai, "Stability analysis of polynomial-fuzzy-model-based control systems with mismatched premise membership functions," *IEEE Trans. Fuzzy Syst.*, vol. 22, no. 1, pp. 223–229, Feb. 2014.

[19] X. Su, P. Shi, L. Wu, and Y. D. Song, "Fault detection filtering for nonlinear switched stochastic systems," *IEEE Trans. Automat. Contr.*, vol. 61, no. 5, pp. 1310–1315, May 2016.

[20] X. Su, P. Shi, L. Wu, and M. V. Basin, "Reliable filtering with strict dissipativity for t-s fuzzy time-delay systems," *IEEE Trans. Cybern.*, vol. 44, no. 12, pp. 2470–2483, Dec. 2014.

[21] C. Liu and H. K. Lam, "Design of a polynomial fuzzy observer controller with sampled-output measurements for nonlinear systems considering unmeasurable premise variables," *IEEE Trans. Fuzzy Syst.*, vol. 23, no. 6, pp. 2067–2079, Dec. 2015.

[22] X. Su, P. Shi, L. Wu, and S. K. Nguang, "Induced l_2 filtering of fuzzy stochastic systems with time-varying delays," *IEEE Trans. Cybern.*, vol. 43, no. 4, pp. 1251–1264, Aug. 2013.

[23] J. Li, X. Huang, and Z. Li, "Extended dissipative filtering of fuzzy systems with time-varying delay under imperfect premise matching," *Int. J. Syst. Sci.*, vol. 48, no. 8, pp. 1731–1743, 2017.

[24] J. C. P. JONES and S. A. BILLINGS, "Recursive algorithm for computing the frequency response of a class of non-linear difference equation models," *Int. J. Control*, vol. 50, no. 5, pp. 1925–1940, 1989.

[25] S. A. BILLINGS and J. C. P. JONES, "Mapping non-linear integro-differential equations into the frequency domain," *International Journal of Control*, vol. 52, no. 4, pp. 863–879, 1990.

[26] A. K. Swain and S. A. Billings, "Generalized frequency response function

matrix for MIMO non-linear systems," *Int. J. Control*, vol. 74, no. 8, pp. 829–844, 2001.

[27] X. Jing, "Frequency domain analysis and identification of block-oriented nonlinear systems," *J. of Sound and Vibration*, vol. 330, no. 22, pp. 5427 – 5442, 2011.

[28] Z. Xiao and X. Jing, "Frequency-domain analysis and design of linear feedback of nonlinear systems and applications in vehicle suspensions," *IEEE/ASME Trans. Mechatronics*, vol. 21, no. 1, pp. 506–517, Feb 2016.

[29] Q. Li and X. Jing, "A second-order output spectrum approach for fault detection of bolt loosening in a satellite-like structure with a sensor chain," *Nonlinear Dyn.*, vol. 89, no. 1, pp. 587–606, Jul 2017.

[30] ——, "Fault diagnosis of bolt loosening in structures with a novel second-order output spectrum–based method," *Structural Health Monitoring*, 2019.

[31] J. Song, Y. Niu, and Y. Zou, "A parameter-dependent sliding mode approach for finite-time bounded control of uncertain stochastic systems with randomly varying actuator faults and its application to a parallel active suspension system," *IEEE Trans. Ind. Electron.*, vol. 65, no. 10, pp. 8124–8132, Oct. 2018.

[32] H. Li, X. Jing, and H. Karimi, "Output-feedback-based H_∞ control for vehicle suspension systems with control delay," *IEEE Trans. Ind. Electron.*, vol. 61, no. 1, pp. 436–446, Jan. 2014.

[33] W. Sun, Z. Zhao, and H. Gao, "Saturated adaptive robust control for active suspension systems," *IEEE Trans. Ind. Electron.*, vol. 60, no. 9, pp. 3889–3896, Sept. 2013.

[34] T. Yoshimura, A. Kume, M. Kurimoto, and J. Hino, "Construction of an active suspension system of a quarter car model using the concept of sliding

mode control," *J. of Sound and Vibration*, vol. 239, no. 2, pp. 187 – 199, 2001.

[35] M. Gaid, A. Cela, and Y. Hamam, "Optimal integrated control and scheduling of networked control systems with communication constraints: application to a car suspension system," *IEEE Trans. Control Syst. Technol.*, vol. 14, no. 4, pp. 776–787, Jul. 2006.

[36] S. Yin and Z. Huang, "Performance monitoring for vehicle suspension system via fuzzy positivistic c-means clustering based on accelerometer measurements," *IEEE/ASME Trans. Mechatronics*, vol. 20, no. 5, pp. 2613–2620, Oct. 2015.

[37] H. Pan, W. Sun, X. Jing, H. Gao, and J. Yao, "Adaptive tracking control for active suspension systems with non-ideal actuators," *J. of Sound and Vibration*, vol. 399, pp. 2 – 20, 2017.

[38] G. Yao, F. Yap, G. Chen, W. Li, and S. Yeo, "MR damper and its application for semi-active control of vehicle suspension system," *Mechatronics*, vol. 12, no. 7, pp. 963 – 973, 2002.

[39] R. Sharp and D. Crolla, "Road vehicle suspension system design - a review," *Vehicle System Dynamics*, vol. 16, no. 3, pp. 167–192, 1987.

[40] J. Li, X. Huang, and Z. Li, "Exponential stabilization for fuzzy sampled-data system based on a unified framework and its application," *Journal of the Franklin Institute*, vol. 354, no. 13, pp. 5302 – 5327, 2017.

[41] S. Liu, H. Zhou, X. Luo, and J. Xiao, "Adaptive sliding fault tolerant control for nonlinear uncertain active suspension systems," *Journal of the Franklin Institute*, vol. 353, no. 1, pp. 180 – 199, 2016.

[42] W. Sun, Y. Zhao, J. Li, L. Zhang, and H. Gao, "Active suspension control with frequency band constraints and actuator input delay," *IEEE Trans. Ind. Electron.*, vol. 59, no. 1, pp. 530–537, Jan. 2012.

[43] H. Gao, W. Sun, and P. Shi, "Robust sampled-data H_∞ control for vehicle active suspension systems," *IEEE Trans. Control Syst. Technol.*, vol. 18, no. 1, pp. 238–245, Jan. 2010.

[44] Z. Lang, X. Jing, S. Billings, G. Tomlinson, and Z. Peng, "Theoretical study of the effects of nonlinear viscous damping on vibration isolation of sdof systems," *J. of Sound and Vibration*, vol. 323, no. 1, pp. 352 – 365, 2009.

[45] X. Jing, Z. Lang, S. Billings, and G. Tomlinson, "Frequency domain analysis for suppression of output vibration from periodic disturbance using nonlinearities," *J. of Sound and Vibration*, vol. 314, no. 3, pp. 536 – 557, 2008.

[46] X. Jing and Z. Lang, "Frequency domain analysis of a dimensionless cubic nonlinear damping system subject to harmonic input," *Nonlinear Dyn.*, vol. 58, no. 3, p. 469, Apr 2009.

[47] Z. Xiao, X. Jing, and L. Cheng, "The transmissibility of vibration isolators with cubic nonlinear damping under both force and base excitations," *J. of Sound and Vibration*, vol. 332, no. 5, pp. 1335 – 1354, 2013.

[48] X. Jing and Z. Lang, "Frequency domain analysis and design of nonlinear systems based on volterra series expansion — a parametric characteristic approach," *Springer International Publishing Switzerland*, 2015.

[49] X. Jing, "Nonlinear characteristic output spectrum for nonlinear analysis and design," *IEEE/ASME Trans. Mechatronics*, vol. 19, no. 1, pp. 171–183, Feb. 2014.

[50] X. Jing, Z. Lang, and S. Billings, "Frequency domain analysis for non-linear volterra systems with a general non-linear output function," *Int. J. Control*, vol. 81, no. 2, pp. 235–251, 2008.

[51] ——, "Nonlinear influence in the frequency domain: Alternating series," *Systems & Control Letters*, vol. 60, no. 5, pp. 295 – 309, 2011.

[52] N. Yagiz and L. Sakman, "Robust sliding mode control of a full vehicle without suspension gap loss," *Modal Analysis*, vol. 11, no. 11, pp. 1357–1374, 2005.

[53] J. Yu, R. Ding, Q. Yang, M. Tan, W. Wang, and J. Zhang, "On a bio-inspired amphibious robot capable of multimodal motion," *IEEE/ASME Trans. Mechatronics*, vol. 17, no. 5, pp. 847–856, Oct. 2012.

[54] O. Castillo, R. Marroquin, P. Melin, F. Valdez, and J. Soria, "Comparative study of bio-inspired algorithms applied to the optimization of type-1 and type-2 fuzzy controllers for an autonomous mobile robot," *Inform. Sci.*, vol. 192, pp. 19 – 38, 2012.

[55] I. Kovacic, M. Brennan, and T. Waters, "A study of a nonlinear vibration isolator with a quasi-zero stiffness characteristic," *J. of Sound and Vibration*, vol. 315, no. 3, pp. 700 – 711, 2008.

[56] Y. Wang, F. Li, and Y. Wang, "Homoclinic behaviors and chaotic motions of double layered viscoelastic nanoplates based on nonlocal theory and extended melnikov method," *Chaos*, vol. 25, no. 6, pp. 063–108, 2015.

[57] Z. Wu, X. Jing, J. Bian, F. Li, and R. Allen, "Vibration isolation by exploring bio-inspired structural nonlinearity," *Bioinspiration & biomimetics*, vol. 10, no. 5, pp. 056–015, 2015.

[58] X. Sun and X. Jing, "A nonlinear vibration isolator achieving high-static-low-dynamic stiffness and tunable anti-resonance frequency band," *Mechanical Systems and Signal Processing*, vol. 80, pp. 166 – 188, 2016.

[59] Y. Wang and X. Jing, "Nonlinear stiffness and dynamical response characteristics of an asymmetric X-shaped structure," *Mechanical Systems and Signal Processing*, vol. 125, pp. 142 – 169, 2019.

[60] H. Pan, X. Jing, W. Sun, and H. Gao, "A bioinspired dynamics-based adaptive tracking control for nonlinear suspension systems," *IEEE Trans. Control Syst. Technol.*, vol. 26, no. 3, pp. 903–914, May 2018.

[61] W. Liu, C. Lim, P. Shi, and S. Xu, "Backstepping fuzzy adaptive control for a class of quantized nonlinear systems," *IEEE Trans. Fuzzy. Syst.*, vol. 25, no. 5, pp. 1090–1101, Oct. 2017.

[62] H. Li, L. Wang, H. Du, and A. Boulkroune, "Adaptive fuzzy backstepping tracking control for strict-feedback systems with input delay," *IEEE Trans. Fuzzy. Syst.*, vol. 25, no. 3, pp. 642–652, 2016.

[63] H. Ma, H. Liang, Q. Zhou, and C. K. Ahn, "Adaptive dynamic surface control design for uncertain nonlinear strict-feedback systems with unknown control direction and disturbances," *IEEE Trans. Syst., Man, Cybern. B, Cybern.*, vol. 49, no. 3, pp. 506–515, Mar. 2019.

[64] Y. Zhang, H. Liang, H. Ma, Q. Zhou, and Z. Yu, "Distributed adaptive consensus tracking control for nonlinear multi-agent systems with state constraints," *Applied Mathematics and Computation*, vol. 326, pp. 16 – 32, 2018.

[65] D. Zhang, P. Shi, and L. Yu, "Containment control of linear multiagent systems with aperiodic sampling and measurement size reduction," *IEEE Trans. Neural Netw. Learn. Syst.*, vol. 29, no. 10, pp. 5020–5029, Oct. 2018.

[66] D. Zhang, Z. Xu, H. Karimi, Q. Wang, and L. Yu, "Distributed H_∞ output-feedback control for consensus of heterogeneous linear multiagent systems with aperiodic sampled-data communications," *IEEE Trans. Ind. Electron.*, vol. 65, no. 5, pp. 4145–4155, May 2018.

[67] D. Zhang, L. Liu, and G. Feng, "Consensus of heterogeneous linear multiagent systems subject to aperiodic sampled-data and dos attack," *IEEE Trans. Cybern.*, vol. 49, no. 4, pp. 1501–1511, 2018.

[68] H. Gao and T. Chen, "Stabilization of nonlinear systems under variable sampling: A fuzzy control approach," *IEEE Trans. Fuzzy Syst.*, vol. 15, no. 5, pp. 972–983, Oct. 2007.

[69] Y. S. Suh, "Stability and stabilization of nonuniform sampling systems," *Automatica*, vol. 44, no. 12, pp. 3222–3226, Dec. 2008.

[70] A. Seuret and C. Briat, "Stability analysis of uncertain sampled-data systems with incremental delay using looped-functionals," *Automatica*, vol. 55, pp. 274 – 278, May 2015.

[71] E. Fridman, "A refined input delay approach to sampled-data control," *Automatica*, vol. 46, no. 2, pp. 421 – 427, Feb. 2010.

[72] X. Ge, Q.-L. Han, and X. Jiang, "Sampled-data $\mathcal{H}\infty$ filtering of Takagi-Sugeno fuzzy systems with interval time-varying delays," *Journal of the Franklin Institute*, vol. 351, no. 5, pp. 2515 – 2542, May 2014.

[73] F. Yang, H. Zhang, and Y. Wang, "An enhanced input-delay approach to sampled-data stabilization of T-S fuzzy systems via mixed convex combination," *Nonlinear Dyn.*, vol. 75, no. 3, pp. 501–512, Feb. 2014.

[74] J. Yoneyama, "Robust H_∞ control of uncertain fuzzy systems under time-varying sampling," *Fuzzy Sets Syst.*, vol. 161, no. 6, pp. 859 – 871, Mar. 2010.

[75] X.-L. Zhu, B. Chen, Y. Wang, and D. Yue, "H_∞ stabilization criterion with less complexity for nonuniform sampling fuzzy systems," *Fuzzy Sets Syst.*, vol. 225, pp. 58 – 73, Aug. 2013.

[76] C. Peng, Q.-L. Han, D. Yue, and E. Tian, "Sampled-data robust H_∞ control for T-S fuzzy systems with time delay and uncertainties," *Fuzzy Sets Syst.*, vol. 179, no. 1, pp. 20 – 33, Sep. 2011.

[77] H. Li, X. Jing, H.-K. Lam, and P. Shi, “Fuzzy sampled-data control for uncertain vehicle suspension systems,” *IEEE Trans. Cybern.*, vol. 44, no. 7, pp. 1111–1126, Jul. 2014.

[78] H.-Q. Xiao, Y. He, M. Wu, S.-P. Xiao, and J. She, “New results on H_∞ tracking control based on the T-S fuzzy model for sampled-data networked control system,” *IEEE Trans. Fuzzy Syst.*, vol. 23, no. 6, pp. 2439–2448, Dec. 2015.

[79] S. Wen and Z. Zeng, “Robust sampled-data H_∞ output tracking control for a class of nonlinear networked systems with stochastic sampling,” *Int. J. Syst. Sci.*, vol. 44, no. 9, pp. 1626–1638, Sep. 2013.

[80] J. Huang, Y. Shi, H. Huang, and Z. Li, “$L_2 - L_\infty$ filtering for multirate nonlinear sampled-data systems using T-S fuzzy models,” *Digital Signal Processing*, vol. 23, no. 1, pp. 418 – 426, Jan. 2013.

[81] M. Kchaou, M. Souissi, and A. Toumi, “Delay-dependent stability and robust $L_2 - L_\infty$ control for a class of fuzzy descriptor systems with time-varying delay,” *Int. J. Robust & Nonlinear Control*, vol. 23, no. 3, pp. 284–304, 2013.

[82] Z.-G. Wu, P. Shi, H. Su, and J. Chu, “Network-based robust passive control for fuzzy systems with randomly occurring uncertainties,” *IEEE Trans. Fuzzy Syst.*, vol. 21, no. 5, pp. 966–971, Oct. 2013.

[83] Z. Wu, P. Shi, H. Su, and R. Lu, “Dissipativity-based sampled-data fuzzy control design and its application to truck-trailer system,” *IEEE Trans. Fuzzy Syst.*, vol. 23, no. 5, pp. 1669–1679, Oct. 2015.

[84] B. Zhang, W. X. Zheng, and S. Xu, “Filtering of Markovian jump delay systems based on a new performance index,” *IEEE Trans. Circuits Syst. I, Reg. Papers*, vol. 60, no. 5, pp. 1250–1263, May 2013.

[85] Z. Li, J. Li, J. Yu, and X. Zhao, “Robust filter design for a class of uncertain systems with stability constraints under a unified framework,” *Journal of the Franklin Institute*, vol. 353, no. 16, pp. 4233 – 4252, 2016.

[86] G. Welch, G. Bishop *et al.*, “An introduction to the kalman filter,” 1995.

[87] R. Van Der Merwe and E. A. Wan, “The square-root unscented kalman filter for state and parameter-estimation,” in *2001 IEEE international conference on acoustics, speech, and signal processing. Proceedings*, vol. 6. IEEE, 2001, pp. 3461–3464.

[88] K. Tanaka and H. O. Wang, *Fuzzy control systems design and analysis: a linear matrix inequality approach.* John Wiley & Sons, 2004.

[89] F. Li and X. Zhang, “A delay-dependent bounded real lemma for singular LPV systems with time-variant delay,” *Int. J. Robust & Nonlinear Control*, vol. 22, no. 5, pp. 559–574, 2012.

[90] H. Gao, Y. Zhao, J. Lam, and K. Chen, “H_∞ fuzzy filtering of nonlinear systems with intermittent measurements,” *IEEE Trans. Fuzzy Syst.*, vol. 17, no. 2, pp. 291–300, Apr. 2009.

[91] Y. Zhao, H. Gao, and J. Lam, “New results on H_∞ filtering for fuzzy systems with interval time-varying delays,” *Inform. Sci.*, vol. 181, no. 11, pp. 2356–2369, Jun. 2011.

[92] J. Zhang and Y. Xia, “New LMI approach to fuzzy H_∞ filter designs,” *IEEE Trans. Circuits Syst. II, Exp. Briefs*, vol. 56, no. 9, pp. 739–743, Sep. 2009.

[93] J. Liu, Z. Gu, E. Tian, and R. Yan, “New results on H_∞ filter design for nonlinear systems with time-delay through a T-S fuzzy model approach,” *Int. J. Syst. Sci.*, vol. 43, no. 3, pp. 426–442, Mar. 2012.

[94] S.-J. Huang, X.-Q. He, and N.-N. Zhang, “New results on H_∞ filter design for nonlinear systems with time delay via T-S fuzzy models,” *IEEE Trans. Fuzzy Syst.*, vol. 19, no. 1, pp. 193–199, Feb. 2011.

[95] J. An, G. Wen, C. Lin, and R. Li, "New results on a delay-derivative-dependent fuzzy H_∞ filter design for T-S fuzzy systems," *IEEE Trans. Fuzzy Syst.*, vol. 19, no. 4, pp. 770–779, Aug. 2011.

[96] H. D. Choi, C. K. Ahn, P. Shi, M. T. Lim, and M. K. Song, "$L_2 - L_\infty$ filtering for Takagi-Sugeno fuzzy neural networks based on Wirtinger-type inequalities," *Neurocomputing*, vol. 153, no. 0, pp. 117–125, Apr. 2015.

[97] R. Yang, H. Gao, and P. Shi, "Delay-dependent $L_2 - L_\infty$ filter design for stochastic time-delay systems," *IET Control Theory Appl.*, vol. 5, no. 1, pp. 1–8, Jan. 2011.

[98] Z. Li and S. Xu, "Fuzzy weighting-dependent approach to robust filter design for delayed fuzzy systems," *Signal Processing*, vol. 89, no. 4, pp. 463–471, Apr. 2009.

[99] J. Qiu, G. Feng, and J. Yang, "New results on robust energy-to-peak filtering for discrete-time switched polytopic linear systems with time-varying delay," *IET Control Theory Appl.*, vol. 2, no. 9, pp. 795–806, Sep. 2008.

[100] H. Gao, J. Lam, and C. Wang, "Robust energy-to-peak filter design for stochastic time-delay systems," *Systems Control Lett.*, vol. 55, no. 2, pp. 101–111, Feb. 2006.

[101] H. Zhang, Y. Shi, and A. S. Mehr, "Robust energy-to-peak filtering for networked systems with time-varying delays and randomly missing data," *IET Control Theory Appl.*, vol. 4, no. 12, pp. 2921–2936, Dec. 2010.

[102] P. Shi, Y. Zhang, M. Chadli, and R. K. Agarwal, "Mixed H_∞ and passive filtering for discrete fuzzy neural networks with stochastic jumps and time delays," *IEEE Trans. Neural Netw. Learn. Syst.*, vol. 27, no. 4, pp. 903–909, Apr. 2016.

[103] C. K. Ahn, "Passive and exponential filter design for fuzzy neural networks," *Inform. Sci.*, vol. 238, no. 0, pp. 126–137, Jul. 2013.

[104] P. Shi, F. Li, L. Wu, and C. Lim, "Neural network-based passive filtering for delayed neutral-type semi-Markovian jump systems," *IEEE Trans. Neural Netw. Learn. Syst.*, vol. 28, no. 9, pp. 2101–2114, Sep. 2017.

[105] J. Wang, X. Zhang, and Q. Han, "Event-triggered generalized dissipativity filtering for neural networks with time-varying delays," *IEEE Trans. Neural Netw. Learn. Syst.*, vol. 27, no. 1, pp. 77–88, Jan. 2016.

[106] Y. Ma and M. Chen, "Delay-dependent robust dissipative filter for T-S fuzzy descriptor time-varying delay systems," *Journal of Control, Automation and Electrical Systems*, vol. 26, no. 5, pp. 476–483, 2015.

[107] Z. Feng and J. Lam, "Robust reliable dissipative filtering for discrete delay singular systems," *Signal Processing*, vol. 92, no. 12, pp. 3010–3025, Dec. 2012.

[108] Y. Li and G.-p. Liu, "Delay-dependent robust dissipative filtering of stochastic genetic regulatory networks with time-varying delays," *IET Control Theory Appl.*, vol. 7, no. 11, pp. 1520–1528, 2013.

[109] H. Shen, J. H. Park, L. Zhang, and Z.-G. Wu, "Robust extended dissipative control for sampled-data markov jump systems," *Int. J. Control*, vol. 87, no. 8, pp. 1549–1564, 2014.

[110] H. Lam and M. Narimani, "Stability analysis and performance design for fuzzy-model-based control system under imperfect premise matching," *IEEE Trans. Fuzzy Syst.*, vol. 17, no. 4, pp. 949–961, Aug. 2009.

[111] H. Lam and L. Seneviratne, "Stability analysis of polynomial fuzzy-model-based control systems under perfect/imperfect premise matching," *IET Control Theory Appl.*, vol. 5, no. 15, pp. 1689–1697, Oct. 2011.

[112] S. H. Kim, "Robust Takagi-Sugeno fuzzy control design for nonlinear networked control systems with asynchronous premise variables," *IET Control Theory Appl.*, vol. 7, no. 6, pp. 910–919, Apr. 2013.

[113] H. Li, Y. Pan, and Q. Zhou, "Filter design for interval type-2 fuzzy systems with d stability constraints under a unified frame," *IEEE Trans. Fuzzy. Syst.*, vol. 23, no. 3, pp. 719–725, Jun. 2015.

[114] H. J. Kim, J. B. Park, and Y. H. Joo, "Decentralised H_∞ fuzzy filter for non-linear large-scale systems under imperfect premise matching," *IET Control Theory Appl.*, vol. 9, no. 18, pp. 2704–2714, 2015.

[115] C. Zhang, H. Lam, J. Qiu, C. Liu, and Q. Chen, "A new design of membership-function-dependent controller for T-S fuzzy systems under imperfect premise matching," *IEEE Trans. Fuzzy. Syst.*, vol. 27, no. 7, pp. 1428–1440, Jul. 2019.

[116] H. J. Kim, J. B. Park, and Y. H. Joo, "H_∞ fuzzy filter for non-linear sampled-data systems under imperfect premise matching," *IET Control Theory Appl.*, vol. 11, no. 5, pp. 747–755, 2017.

[117] ——, "Decentralised H_∞ fuzzy filter for non-linear large-scale systems under imperfect premise matching," *IET Control Theory Appl.*, vol. 9, no. 18, pp. 2704–2714, 2015.

[118] T. Zhao and S. Dian, "Fuzzy dynamic output feedback H_∞ control for continuous-time T-S fuzzy systems under imperfect premise matching," *ISA Transactions*, vol. 70, pp. 248 – 259, 2017.

[119] E. Nakamura and N. Kehtarnavaz, "Optimization of fuzzy membership function parameters," in *1995 IEEE International Conference on Systems, Man and Cybernetics. Intelligent Systems for the 21st Century*, vol. 1, Oct. 1995, pp. 1–6 vol.1.

[120] A. Homaifar and E. McCormick, "Simultaneous design of membership functions and rule sets for fuzzy controllers using genetic algorithms," *IEEE Trans. Fuzzy. Syst.*, vol. 3, no. 2, pp. 129–139, May 1995.

[121] C. Larbes, S. A. Cheikh, T. Obeidi, and A. Zerguerras, "Genetic algorithms optimized fuzzy logic control for the maximum power point tracking in photovoltaic system," *Renewable Energy*, vol. 34, no. 10, pp. 2093 – 2100, 2009.

[122] E. E. Omizegba and G. E. Adebayo, "Optimizing fuzzy membership functions using particle swarm algorithm," in *2009 IEEE International Conference on Systems, Man and Cybernetics*, Oct. 2009, pp. 3866–3870.

[123] G. Fang, N. M. Kwok, and Q. Ha, "Automatic fuzzy membership function tuning using the particle swarm optimization," in *2008 IEEE Pacific-Asia Workshop on Computational Intelligence and Industrial Application*, vol. 2, Dec. 2008, pp. 324–328.

[124] X. Jing, Z.Lang, S. Billings, and G. Tomlinson, "The parametric characteristic of frequency response functions for nonlinear systems," *Int. J. Control*, vol. 79, no. 12, pp. 1552–1564, 2006.

[125] X. Jing, Z. Lang, and S. A. Billings, "Mapping from parametric characteristics to generalized frequency response functions of non-linear systems," *Int. J. Control*, vol. 81, no. 7, pp. 1071–1088, 2008.

[126] D. A. George, *Continuous nonlinear systems.* Massachusetts Institute of Technology. Research Laboratory of Electronics, 1959.

[127] Z. Xiao and X. Jing, "Frequency-domain analysis and design of linear feedback of nonlinear systems and applications in vehicle suspensions," *IEEE/ASME Trans. Mechatronics*, vol. 21, no. 1, pp. 506–517, Feb. 2016.

[128] W. Sun, H. Gao, and O. Kaynak, "Finite frequency H_∞ control for vehicle active suspension systems," *IEEE Trans. Control Syst. Technol.*, vol. 19, no. 2, pp. 416–422, Mar. 2011.

[129] Y. Chen, W. Zhang, and H. Gao, "Finite frequency H_∞ control for building under earthquake excitation," *Mechatronics*, vol. 20, no. 1, pp. 128 – 142, 2010.

[130] H. Zhang, R. Wang, J. Wang, and Y. Shi, "Robust finite frequency H_∞ static-output-feedback control with application to vibration active control of structural systems," *Mechatronics*, vol. 24, no. 4, pp. 354 – 366, 2014.

[131] G. Wang, C. Chen, and S. Yu, "Robust non-fragile finite-frequency H_∞ static output-feedback control for active suspension systems," *Mechanical Systems and Signal Processing*, vol. 91, pp. 41 – 56, 2017.

[132] A. Kazemy, J. Lam, and X. Li, "Finite-frequency H_∞ control for offshore platforms subject to parametric model uncertainty and practical hard constraints," *ISA Transactions*, vol. 83, pp. 53 – 65, 2018.

[133] M. Wang, J. Qiu, and G. Feng, "Finite frequency memory output feedback controller design for T–S fuzzy dynamical systems," *IEEE Trans. Fuzzy. Syst.*, vol. 26, no. 6, pp. 3301–3313, Dec. 2018.

[134] Z. Xiao and X. Jing, "A novel characteristic parameter approach for analysis and design of linear components in nonlinear systems," *IEEE Transactions on Signal Processing*, vol. 64, no. 10, pp. 2528–2540, May 2016.

[135] B. Ren, S. Ge, K. Tee, and T. Lee, "Adaptive neural control for output feedback nonlinear systems using a barrier lyapunov function," *IEEE Trans. Neural Networks*, vol. 21, no. 8, pp. 1339–1345, Aug. 2010.

[136] K. Ahn, D. Nam, and M. Jin, "Adaptive backstepping control of an electro-hydraulic actuator," *IEEE/ASME Trans. Mechatronics*, vol. 19, no. 3, pp. 987–995, Jun. 2014.

[137] C. Yin, Z. Yao, H. Li, and S. Wen, "Research on suspension system based on genetic algorithm and neural network control," in *Intelligent Computation Technology and Automation, 2009. ICICTA'09. Second International Conference on*, vol. 1. IEEE, 2009, pp. 468–471.

[138] J. Sun, G. P. Liu, and J. Chen, "Delay-dependent stability and stabilization

of neutral time-delay systems," *Int. J. Robust & Nonlinear Control*, vol. 19, no. 12, pp. 1364–1375, 2009.

[139] B. Brogliato, R. Lozano, B. Maschke, and O. Egeland, *Dissipative Systems Analysis and Control: Theory and Applications, 2nd ed.* Springer-Verlag London, 2007.

[140] H. Li, H. Liu, H. Gao, and P. Shi, "Reliable fuzzy control for active suspension systems with actuator delay and fault," *Fuzzy Sets Syst.*, vol. 20, no. 2, pp. 342–357, Apr. 2012.

[141] J. F. Sturm, "Using sedumi 1.02, a matlab toolbox for optimization over symmetric cones," *Optimization Methods and Software*, vol. 11, no. 1-4, pp. 625–653, 1999.

[142] J. Lofberg, "Yalmip : a toolbox for modeling and optimization in matlab," in *2004 IEEE International Conference on Robotics and Automation (IEEE Cat. No.04CH37508)*, Sept 2004, pp. 284–289.

[143] P. Park, J. W. Ko, and C. Jeong, "Reciprocally convex approach to stability of systems with time-varying delays," *Automatica*, vol. 47, no. 1, pp. 235–238, Jan. 2011.

[144] A. Seuret and F. Gouaisbaut, "Jensen's and Wirtinger's inequalities for time-delay systems," in *11th IFAC Workshop on Time-Delay Systems*, Grenoble, France, Feb. 2013, p. 6p.

[145] Z. Li, J. Wang, and H. Shao, "Delay-dependent dissipative control for linear time-delay systems," *Journal of the Franklin Institute*, vol. 339, no. 6-7, pp. 529 – 542, 2002.

[146] Z. Feng, J. Lam, and H. Gao, "α-dissipativity analysis of singular time-delay systems," *Automatica*, vol. 47, no. 11, pp. 2548 – 2552, 2011.

[147] K. M. Grigoriadis and J. T. Watson, "Reduced-order H_∞ and $L_2 - L_\infty$ filtering via linear matrix inequalities," *IEEE Trans. Aerospace and Electronic Systems*, vol. 33, no. 4, pp. 1326–1338, Oct. 1997.

[148] Y. Zhang, P. Shi, R. K. Agarwal, and Y. Shi, "Dissipativity analysis for discrete time-delay fuzzy neural networks with Markovian jumps," *IEEE Trans. Fuzzy Syst.*, vol. 24, no. 2, pp. 432–443, Apr. 2016.

[149] J. Zhang and C. Peng, "Event-triggered H_∞ filtering for networked Takagi-Sugeno fuzzy systems with asynchronous constraints," *IET Signal Processing*, vol. 9, no. 5, pp. 403–411, Jun. 2015.

[150] B. Zhang, W. X. Zheng, and S. Xu, "Passivity analysis and passive control of fuzzy systems with time-varying delays," *Fuzzy Sets Syst.*, vol. 174, no. 1, pp. 83–98, Jul. 2011.

[151] P. Selvaraj, R. Sakthivel, S. Marshal Anthoni, M. Rathika, and M. Yong-Cheol, "Dissipative sampled-data control of uncertain nonlinear systems with time-varying delays," *Complexity*, pp. 142–154, 2016.

[152] J. Zhang, Y. Xia, and R. Tao, "New results on H_∞ filtering for fuzzy time-delay systems," *IEEE Trans. Fuzzy Syst.*, vol. 17, no. 1, pp. 128–137, Feb. 2009.

[153] Y. Su, Q. Zhou, and F. Gao, "A new delay-range-dependent H_∞ filter design for T-S nonlinear systems," *Journal of the Franklin Institute*, vol. 351, no. 6, pp. 3305–3321, Jun. 2014.

[154] J. Yoneyama, "H_∞ filtering for fuzzy systems with immeasurable premise variables: An uncertain system approach," *Fuzzy Sets and Systems*, vol. 160, no. 12, pp. 1738 – 1748, 2009.

[155] X. J. Li and G. H. Yang, "Switching-type H_∞ filter design for T-S fuzzy systems with unknown or partially unknown membership functions," *IEEE Trans. Fuzzy Syst.*, vol. 21, no. 2, pp. 385–392, Apr. 2013.

[156] Y.-C. Lin and J.-C. Lo, "Robust mixed H_2/H_∞ filtering for time-delay fuzzy systems," *IEEE Trans. Signal Process.*, vol. 54, no. 8, pp. 2897–2909, Aug. 2006.

[157] W. Chang, C. Kuo, and C. C. Ku, "Intelligent fuzzy control with imperfect premise matching concept for complex nonlinear multiplicative noised systems," *Neurocomputing*, vol. 154, pp. 276 – 283, 2015.

[158] P. Apkarian, Hoang Duong Tuan, and J. Bernussou, "Continuous-time analysis, eigenstructure assignment, and H_∞ synthesis with enhanced linear matrix inequalities (LMI) characterizations," *IEEE Trans. Automat. Control*, vol. 46, no. 12, pp. 1941–1946, Dec. 2001.

[159] G. C. Goodwin, S. F. Graebe, M. E. Salgado *et al.*, *Control system design.* Upper Saddle River, NJ: Prentice Hall,, 2001.

[160] X. Jing, "Truncation order and its effect in a class of nonlinear systems," *Automatica*, vol. 48, no. 11, pp. 2978 – 2985, 2012.

[161] Z. Xiao and X. Jing, "Frequency domain analysis of exponential-type nonlinearity," in *2016 American Control Conference (ACC)*, Jul. 2016, pp. 7466–7471.

[162] K. Tanaka, T. Ikeda, and H. O. Wang, "Robust stabilization of a class of uncertain nonlinear systems via fuzzy control: quadratic stabilizability, H_∞ control theory, and linear matrix inequalities," *IEEE Trans. Fuzzy. Syst.*, vol. 4, no. 1, pp. 1–13, Feb. 1996.

[163] J. Li, X. Jing, Z. Li, and X. Huang, "Fuzzy adaptive control for nonlinear suspension systems based on a bio-inspired reference model with deliberately designed nonlinear damping," *IEEE Trans. Ind. Electron.*, pp. 1–1, 2018.

[164] X. J. Jing, Z. Q. Lang, and S. A. Billings, "Parametric characteristic analysis for generalized frequency response functions of nonlinear systems," *Circuits, Systems & Signal Processing*, vol. 28, no. 5, pp. 699–733, Oct 2009.

[165] J. Li, X. Jing, Z. Li, and X. Huang, "Fuzzy adaptive control for nonlinear suspension systems based on a bioinspired reference model with deliberately designed nonlinear damping," *IEEE Transactions on Industrial Electronics*, vol. 66, no. 11, pp. 8713–8723, Nov. 2019.

[166] H. Pan, X. Jing, W. Sun, and H. Gao, "A bioinspired dynamics-based adaptive tracking control for nonlinear suspension systems," *IEEE Trans. Control Syst. Technol.*, vol. PP, no. 99, pp. 1–12, 2017.

[167] Z. Li, X. Zhao, and J. Yu, "On robust control of continuous-time systems with state-dependent uncertainties and its application to mechanical systems," *ISA Transactions*, vol. 60, 11 2015.

[168] Z. Li and X. Zhao, "New results on robust control for a class of uncertain systems and its applications to chua's oscillator," *Nonlinear Dynamics*, vol. 84, 01 2016.

[169] W. J. Rugh, *Nonlinear system theory.* Johns Hopkins University Press Baltimore, MD, 1981.

[170] X. J. Jing, Z. Q. Lang, and S. A. Billings, "Mapping from parametric characteristics to generalized frequency response functions of non-linear systems," *International Journal of Control*, vol. 81, no. 7, pp. 1071–1088, 2008.

[171] J. Li, X. Huang, and Z. Li, "Exponential stabilization for fuzzy sampled-data system based on a unified framework and its application," *Journal of the Franklin Institute*, vol. 354, no. 13, pp. 5302 – 5327, 2017.